

**REGULATION OF NUCLEOCYTOPLASMIC SHUTTLING OF THE
TRANSCRIPTIONAL REGULATOR HUMAN MESODERM INDUCTION
EARLY RESPONSE 1 α IN BREAST CARCINOMA CELLS**

By

© Shengnan Li

A Thesis submitted to the

School of Graduate Studies

In partial fulfillment of the requirements for the degree of

Doctor of Philosophy

Division of Biomedical Sciences

Faculty of Medicine

Memorial University of Newfoundland

(May 2018)

St. John's

Newfoundland and Labrador

Abstract

Temporal and spatial regulation of the subcellular distribution of transcriptional regulators is important to ensure their proper functioning in a cell. Mesoderm induction early response 1 α (MIER1 α) has been implicated as a tumour suppressor in breast cancer. Analysis of MIER1 α subcellular localization in breast samples revealed a stepwise translocation from the nucleus to the cytoplasm during progression to invasive carcinoma (McCarthy et al., 2008). Therefore, an investigation of MIER1 α nucleocytoplasmic shuttling is critical to unraveling its role in breast cancer progression.

Structurally, MIER1 α has conserved domains found in a number of other transcriptional regulators, including N-terminal acidic stretches, ELM2 and SANT domains. However, none of these domains contain the predicted nuclear import or export signals. In this thesis, I show that MIER1 α localizes in the nucleus in breast carcinoma MCF7 cells without an intrinsic nuclear localization signal (NLS). Although MIER1 α has been shown to bind to ER α , active nuclear import of MIER1 α is not through interaction with ER α ; instead, it depends on interaction and co-transport with HDAC1/2 through a “piggyback” mechanism. Deletion analysis demonstrated that the entire ELM2 (aa164-283) is required and sufficient for nuclear targeting of MIER1 α and that a simple mutation, ²¹⁴W→A in the ELM2 domain abolishes both the interaction between MIER1 α and HDAC1/2 and its nuclear localization.

Further investigation revealed that MIER1 α is exported out of the nucleus when cells are treated with insulin, IGF-1, EGF or FGF, but not with 17 β -estradiol, and this export out of the nucleus is mediated by CRM1. HDAC1 & 2 nuclear localization were not affected by MIER1 α export, suggesting they are only involved in MIER1 α nuclear import. Both Mitogen-activated protein kinase (MAPK) and phosphoinositide 3-kinase B/Akt (PI3'K/AKT) pathways are activated upon treatment with growth factors, and it was further confirmed MIER1 α nuclear export is triggered by the MAPK pathway, but not the PI3'K/AKT pathway. However, the mutation of predicted ERK1/2 consensus phosphorylation sites S¹⁰-P and/or S³⁷⁷-P motifs in the MIER1 α sequence had no effect on its localization. MIER1 α returns to the nucleus when activation of MAPK pathway diminishes, suggesting this process is transient and reversible. Deletion analysis narrowed the required sequence for export to the N-terminal region, aa1-163, containing acidic stretches. Overall, these results provide details of the mechanism responsible for MIER1 α nucleocytoplasmic shuttling in a breast cancer carcinoma cell line; a similar mechanism may be operating during breast cancer progression.

Acknowledgements

I would like to express my deepest gratitude and respect to my supervisor, Dr. Laura L. Gillespie for her supervision, support, and encouragement throughout the entire study. I am also very grateful to Dr. Gary Paterno for his constant guidance and help. Additionally, I would like to express my thanks to my committee members Dr. Ann Dorward and Dr. Ken Kao for their expertise and invaluable comments.

I would like to extend my thanks to the present and past lab members, Corinne, Roya, Amy, Leena, Julia, Satoko, Phil, Paula, and Youlian for the friendship and for providing a great working environment. Also sincere thanks to the Faculty of Medicine and the School of Graduate Studies for their cordial administrative help and support through this program.

My love and appreciation go to my parents, who instilled strong beliefs in me to pursue my dreams and took care of my daughter while I stayed abroad. My appreciation is also due to my dearest husband and sisters, who encouraged me and supported me throughout this journey. My apologies go to my daughter for my absence during her infancy.

Table of Contents

Abstract	i
Acknowledgements	III
Table of Contents.....	IV
List of Tables	VIII
List of Figures	IX
List of Abbreviations and Symbols	XII
List of Appendices	XVI
Chapter 1 General Introduction	1
1.1 Cancer overview	1
1.1.1 Types of cancer.....	1
1.1.2 The development of cancer	6
1.1.3 Hallmarks of cancer.....	7
1.1.4 Breast cancer	10
1.2 Transcriptional regulation.....	13
1.2.1 Transcription factors recognize specific DNA sequences.....	13
1.2.2 Transcription factor regulation	14
1.2.3 Transcriptional repression and activation	16
1.2.4 Roles of transcription regulators in cancer	18
1.3 Growth factors and their function.....	19
1.3.1 Growth factors and their receptors	20
1.3.2 Growth factor function	22
1.4 Nuclear-cytoplasm exchange system	24
1.4.1 Nuclear pore complexes.....	25
1.4.2 Transport machinery.....	29
1.4.3 Cargoes and signals	30
1.4.4 Nucleocytoplasmic exchange system aberration and cancer	36
1.5 Mesoderm early response gene 1 (<i>MIER1</i>).....	37
1.5.1 Immediate early response genes	37

1.5.2 <i>Xenopus</i> mesoderm induction early-response gene (<i>xmier1</i>)	38
1.5.3 <i>hMIER1</i> isolation, genomic structure and isoforms.....	39
1.5.4 <i>hMIER1</i> protein domains and their possible function	42
1.5.5 <i>hMIER1</i> expression and subcellular localization	50
1.5.6 <i>hMIER1</i> in breast cancer	51
1.6 Aims of this study.....	55
Chapter 2 Nuclear localization of the transcriptional regulator MIER1α requires interaction with HDAC1/2 in breast cancer cells	57
2.1 Introduction.....	58
2.2 Methods and materials	58
2.2.1 Plasmids and constructs	58
2.2.2 Cell lines and culture conditions.....	65
2.2.3 Transient transfection	66
2.2.4 Antibodies.....	67
2.2.5 Co-immunoprecipitation (co-IP)	69
2.2.6 Western blot	69
2.2.7 Immunofluorescence, Confocal microscopy and statistical analysis	70
2.3 Results	71
2.3.1 Nuclear localization of MIER1 α is not dependent on its interaction with ER α	71
2.3.2 The ELM2 domain of MIER1 α is required and sufficient for targeting to the nucleus.....	78
2.3.3 Interaction with HDAC1/2 is required for nuclear localization of MIER1 α	90
2.3.4 HDAC1 and 2 depletion causes MIER1 α nuclear loss.....	98
2.4 Discussion	104
Chapter 3 Peptide growth factors and insulin, but not 17β-estradiol, alter the subcellular localization of MIER1α in MCF7 breast carcinoma cells	108
3.1 Introduction.....	109
3.2 Methods and Materials	110
3.2.1 Plasmid.....	110
3.2.2 Cell line and culture condition	110
3.2.3 Transient transfection	111

3.2.4 Growth factors	111
3.2.5 Antibodies	111
3.2.6 Leptomycin B treatment	112
3.2.7 Immunofluorescence, confocal microscopy and statistical analysis	112
3.3 Results	113
3.3.1 Insulin and peptide growth factors cause nucleocytoplasmic shuttling of MIER1 α	113
3.3.2 HDAC1/2 nuclear localization does not change during incubation with insulin, peptide growth factors or E2	129
3.3.3 MIER1 α nucleocytoplasmic translocation is CRM1-dependent ...	140
3.4 Discussion	147
Chapter 4 The growth factor-dependent MAPK pathway regulates MIER1α nucleocytoplasmic shuttling	150
4.1 Introduction	151
4.2 Methods and Materials	158
4.2.1 Plasmids	158
4.2.2 Primer synthesis and site-directed mutagenesis	161
4.2.3 Cell line and culture condition	161
4.2.4 Transient transfection	162
4.2.5 Growth factors	162
4.2.6 Antibodies	163
4.2.7 Inhibitors	163
4.2.8 Western blot	164
4.2.9 Stripping buffer	165
4.2.10 Immunofluorescence, confocal microscopy and statistical analysis	165
4.3 Results	166
4.3.1 AKT activation by growth factor stimulation	167
4.3.2 MAPK activation by growth factor stimulation	171
4.3.3 Growth factor-dependent activation of MAPK causes MIER1 α nuclear loss	174
4.3.4 The mechanism responsible for growth factor directed nuclear export does not involve direct phosphorylation of MIER1 α on consensus motifs by pERK1/2	184

4.3.5 The N-terminal region of MIER1 α is required for nuclear export	195
4.3.6 MIER1 α nuclear loss is transient and reversible	201
4.4 Discussion	205
Chapter 5 Summary	208
5.1 “Piggyback” mechanism of MIER1 α nuclear localization	212
5.2 Possible mechanisms responsible for MIER1 α nuclear export	214
5.3 Possible mechanisms responsible for MIER1 α nuclear loss during breast cancer progression	217
5.4 Functional implication of MIER1 α nuclear loss.....	219
5.5 The potential role of MIER1 in breast cancer subtype development..	221
5.6 Conclusion	223
REFERENCES.....	225
APPENDICES.....	242

List of Tables

Table 1.1 Highlights of genomic, clinical and proteomic features of breast tumour subtypes	12
Table 2.1 List of cell lines used in this study	66
Table 2.2 Antibodies used for immunofluorescence (IF) and western blot (WB)	68
Table 2.3 ELM2 domain does not contain cNLS	85
Table 4.1 Primer sequences for site-directed mutagenesis of SP motifs on MIER1 α	161
Table 4.2 SP motifs within the MIER1 α sequence.....	187
Table 4.3 MIER1 post-transcriptional modification reported in research papers...	187

List of Figures

Figure 1.1 Incidence of cancers in 2017 in Canada.....	4
Figure 1.2 Schematic representation of the NPC.....	27
Figure 1.3 Ran directs nucleocytoplasmic transport.....	34
Figure 1.4 Structure of the human <i>MIER1</i> gene and splice variants.....	40
Figure 1.5 Protein domains and motifs in hMIER1 isoforms.....	48
Figure 1.6 Loss of nuclear MIER1 α during breast cancer progression.....	53
Figure 2.1 MIER1 α amino acid sequence.....	59
Figure 2.2 Amino Acid sequences of all plasmids used.....	61
Figure 2.3 Knockdown of ER α does not affect nuclear localization of MIER1 α in MCF7 cells.....	73
Figure 2.4 MIER1 α is localized in the nucleus in ER- breast carcinoma cells.....	76
Figure 2.5 The ELM2 domain directs nuclear localization of MIER1 α	80
Figure 2.6 The ELM2 domain is sufficient for nuclear localization of MIER1 α	82
Figure 2.7 Nuclear localization requires an intact ELM2 domain.....	86
Figure 2.8 Statistical data demonstrate the necessity of intact ELM2 domain for MIER1 α nuclear localization.....	88
Figure 2.9 Western blot showing that ELM2 mutant (²¹⁴ W \rightarrow A) does not interact with HDAC1 or HDAC2.....	92
Figure 2.10 Interaction with HDAC1/2 is required for nuclear localization of MIER1 α	94

Figure 2.11 ²¹⁴ W→A mutation abolishes MIER1α nuclear localization.....	96
Figure 2.12 Individual and double knockdown of HDAC1 and 2 in MCF7 cells using shRNA.....	100
Figure 2.13 HDAC1 and 2 knockdown reduces nuclear localization of MIER1α	102
Figure 3.1 Insulin treatment reduces nuclear localization of MIER1α	115
Figure 3.2 IGF-1 treatment reduces nuclear localization of MIER1α	118
Figure 3.3 EGF treatment reduces nuclear localization of MIER1α	121
Figure 3.4 FGF treatment reduces nuclear localization of MIER1α.....	124
Figure 3.5 E2 has no effect on subcellular localization of MIER1α.....	127
Figure 3.6 HDAC1 and 2 localization are not affected by insulin	130
Figure 3.7 HDAC1 and 2 localization are not affected by IGF-1	132
Figure 3.8 HDAC1 and 2 localization are not affected by EGF	134
Figure 3.9 HDAC1 and 2 localization are not affected by FGF.....	136
Figure 3.10 HDAC1 and 2 localization are not affected by E2.....	138
Figure 3.11 LMB abolishes MIER1α nuclear export caused by insulin.....	143
Figure 3.12 LMB rescues MIER1α nuclear loss caused by insulin and growth factors	145
Figure 4.1 The mammalian MAPK cascade	154
Figure 4.2 Schematic diagram depicting the most representative signaling of the PI3K/AKT pathway	156
Figure 4.3 MIER1α amino acid sequence and plasmids used in the study	159

Figure 4.4 AKT VIII inhibits growth factor-dependent AKT activation	169
Figure 4.5 U0126 inhibits growth factor-dependent MAPK activation	172
Figure 4.6 AKT inhibition has no effect on MIER1 α subcellular distribution.....	175
Figure 4.7 U0126 inhibits growth factor dependent nuclear loss of MIER1 α in MCF7 cells	178
Figure 4.8 ERK1/2 is not activated by E2	182
Figure 4.9 Substitution of S ¹⁰ to A has no effect on the subcellular distribution of MIER1 α in MCF7 cells	188
Figure 4.10 Substitution of S ³⁷⁷ to A has no effect on the subcellular distribution of MIER1 α in MCF7 cells	190
Figure 4.11 Double mutations of ¹⁰ S and ³⁷⁷ S to A has no effect on the subcellular distribution of MIER1 α in MCF7 cells	193
Figure 4.12 The N-terminus containing 4 acidic stretches is required for MIER1 α nuclear export	197
Figure 4.13 The N-terminus containing 4 acidic stretches is required for MIER1 α nuclear export	199
Figure 4.14 MIER1 α nuclear loss caused by ERK1/2 activation is transient and reversible.....	203
 Figure 5.1 Model of MIER1 α nucleocytoplasmic shuttling mechanism	 210

List of Abbreviations and Symbols

α	alpha
β	beta
aa	amino acid
Ada2	adaptor 2
AF-2	activation function-2
AID	activation-induced deaminase
ALK	Anaplastic Lymphoma Kinase
amp	ampicillin
ANOVA	analysis of variance
ARM	armadillo
ATCC	American Tissue Culture Collection
BAHD1	Bromo-Adjacent-Homology domain-containing 1
bp	base pair
BRCA1	breast cancer susceptibility gene 1
BSA	bovine serum albumin
CAT	chloramphenicol acetyltransferase
CBP	CREB-binding protein
CCL2	chemokine (C-C) motif ligand 2
CDKN1A	cyclin-dependent kinase inhibitor 1A
CDKN1B	CDK inhibitor 1B
CDKs	cyclin-dependent protein kinases
CDYL	chromodomain-containing protein
co-IP	co-immunoprecipitation
co-REST	REST co-repressor
CREB	cAMP response element binding protein
CRM1	Chromosomal Maintenance 1
DAD	deacetylase activating domain
$^{\circ}\text{C}$	degrees Celsius
DBD	DNA binding helix-turn-helix domain
DCIS	ductal carcinoma in situ
DMEM	Dulbecco's Modified Eagle's Medium
DMSO	dimethyl sulfoxide
DNA	deoxyribonucleic acid
E2	17- β -estradiol
<i>E. coli</i>	<i>Escherichia coli</i>
EGF	epidermal growth factor
EGFR	epidermal growth factor receptor
EHMT2	Euchromatic histone-lysine N-methyltransferase 2
Elf-1	ETS transcription factor
ELM2	<u>EGL</u> -27 and <u>MTA</u> 1 homology domain <u>2</u>

EMT	epithelial-mesenchymal transition
ER	estrogen receptor
ER α	estrogen receptor α
ERK1	extracellular signal-regulated kinase-1
ERK2	extracellular signal-regulated kinase-2
ETS	E-twenty six family transcription factor
FGFs	fibroblast growth factors
FGFR	fibroblast growth factor receptor
FG-repeats	phenylalanine-glycine repeats
G9a	histone methyltransferase
GCN5	general control of amino-acid synthesis
GSK-3	glycogen synthase kinase-3
h	hour
HATs	histone acetyltransferases
HDACs	histone deacetylases
HEK	human embryonic kidney
HER2	human epidermal growth factor receptor 2
HER2E	human epidermal growth factor receptor 2 enriched
HGF	hepatocyte growth factor
HGFR	hepatocyte Growth Factor Receptor
HOX	Homeobox
hTERT	human telomerase reverse transcriptase
IBB	importin- β binding
IDC	invasive ductal carcinoma
IEGs	Immediate early response genes
IHC	immunohistochemistry
IGF	Insulin-like growth factor
IMTs	inflammatory myofibroblastic tumours
IP	immunoprecipitation
JNKs	Jun N-terminal protein kinases
kDa	kilodalton
KLK3	prostate-specific antigen Kallikrein 3
LEF-1	lymphocyte enhancer factor 1
LMB	Leptomycin B
LPL	Lipoprotein Lipase
LXXLL	Leu-Xaa-Xaa-Leu-Leu
M	molar
MAPK	mitogen-activated protein kinase
MC2	MDA-MB-231 derived ER α + stable clone cell line
MEK1	mitogen-activated protein kinase kinase 1
MEK2	mitogen-activated protein kinase kinase 2
<i>MIER1</i>	mesoderm induction early response 1 (gene)
MIER1	mesoderm induction early response 1 (protein)

<i>MIER2</i>	mesoderm induction early response 2 (gene)
<i>MIER3</i>	mesoderm induction early response 3 (gene)
min	minute
miRNA	microRNA
ml	millitres
MTA-1	metastasis-associated protein
<i>mta1</i>	metastasis-associated gene 1
mRNA	messenger RNA
N-CoR	nuclear receptor co-repressor
NES	nuclear export signal
ng	nanogram
NLS	Nuclear localization signal
nM	nanomole
NGF	nerve growth factor
NPC	nuclear pore complex
NTF	nuclear transport factor 2
NTRK1	Neurotrophic tyrosine receptor kinase 1
Nups	nucleoporins
NuRD	nucleosome remodeling deacetylase
PAGE	polyacrylamide gel electrophoresis
PAS	polyadenylation signal
PBS	phosphate buffered saline
PDGF	Platelet derived growth factor
PDK1	phosphoinositide-dependent kinase 1
PH	pleckstrin-homology
PI3K	phosphoinositide 3-kinase B
PIP ₃	phosphatidylinositol (3,4,5)-trisphosphate
PKB	protein kinase B
PP2A	protein phosphatase 2A
PPAR- γ	peroxisome proliferator-activated receptor- γ
PR	progesterone receptor
PTGS2	Prostaglandin-endoperoxide synthase 2
PTMs	post-translational modifications
RanBP1	Ran-binding protein-1
RB	retinoblastoma
RCC1	chromosome condensation
RNPs	ribonucleoproteins
RTK	receptor tyrosine kinase
rRNA	ribosomal RNA
SANT	<u>S</u> wi13, <u>A</u> da2, <u>N</u> -CoR, <u>T</u> FIIB
SDS-PAGE	sodium dodecyl sulfate-polyacrylamide gel electrophoresis
SH3	SRC Homology 3
SMRT	silencing mediator of retinoic acid

SPP1	secreted phosphoprotein 1
STAT1	signal transducer and activator of transcription 1
S/T-P	Ser/Thr-Pro motif
STATs	Signal Transducers and Activators of Transcription
Swi3	switching-defective protein 3
T	thymidine
T-ALL	T-cell acute lymphoblastic leukemia
TFs	transcription factors
TGF β	transforming growth factor β
TMAS	tissues microarrays
TNBC	Triple-negative breast cancers
TPR	translocated promoter region
TREX	transcriptional export
tRNA	transfer RNA
TSP	tumour suppressor proteins
μ g	micrograms
μ l	microliters
VEGF	vascular endothelial growth factor
VC5	MDA-MB-231 derived ER α - stable clone cell line
W	tryptophan
<i>xmierl</i>	<i>xenopus</i> mesoderm induction early-response 1 (gene)
<i>xmier1</i>	<i>xenopus</i> mesoderm induction early-response 1 (protein)

List of Appendices

Appendix 1: EndoFree® Plasmid Maxi Kit Protocol	242
Appendix 2: Immunofluorescence	244
Appendix 3: <i>In silico</i> analysis of MIER1 α amino acid sequence by NetNES 1.1	245

Chapter 1 General Introduction

1.1 Cancer overview

In mammals and other multi-cellular organisms, the activities of normal cells are tightly regulated by signals in their surroundings. The signals released through paracrine, autocrine or endocrine mechanisms ultimately dictate a cell's fate: to grow, to differentiate, to proliferate or to undergo apoptosis. The plethora of signalling networks and interconnecting factors ensure the functional homeostasis of our bodies. A healthy cell is in harmony with its environment by responding and integrating the external messages through a highly regulated signal transduction network. This balance, however, can be destroyed and can result in the development of cancer.

Cancer cells are characterized by uncontrolled proliferation (Hanahan & Weinberg, 2011). Rather than responding to the signals that control normal cell behaviour, cancer cells proliferate in an uncontrolled manner, eventually resulting in accumulated abnormalities in several aspects of cell behaviour which distinguish cancer cells from normal cells.

1.1.1 Types of cancer

Types of cancer are usually named for the organs or tissues from which the cancers arise; they may be also further described by the subtypes of cancer initiating cells, and how they are characterized histologically. But in brief, one of the

most important issues in cancer pathology is the distinction between benign and malignant tumours. A benign tumour remains in its original location and does not invade the surrounding normal tissue or spread to distant body sites, while malignant tumours can invade normal tissue and spread through the body via blood circulatory or lymphatic systems, in a process called metastasis. Loss of primary organ function or distant organ function as a result of cancer metastasis threatens physiological homeostasis, leading to death of the patient.

Malignant tumours can arise in virtually any part of the body but fall into one of six main groups, including: carcinomas, sarcomas, myeloma, lymphomas, leukemia and mixed types. The most common cancers are carcinomas, accounting for 80 to 90 % of all cancer cases (Canadian Cancer Society, 2017). Carcinomas originate from epithelial cells, which either cover surfaces or line internal organs such as skin, breast, prostate or lung. Sarcomas are solid tumours appearing in connective tissues, such as muscle, bone or fibrous tissue; while only accounting for less than 1% of all adult solid malignant cancers (Burningham, Hashibe, Spector, & Schiffman, 2012), they are often fatal. Unlike solid tumours, leukemias are cancers arising from the blood-forming cells or immune system cells. They manifest as the overproduction of white blood cells and account for approximately 8% of human malignancies (Canadian Cancer Society, 2015).

Cancer is an age-related disease (Fig. 1.1A) and 70% of new cancer cases will occur in Canadians aged 50 years or older (Statistics Canada, 2014). Cancers occurring in ten different body sites account for more than 75% of total cancer

incidence; among these breast, prostate, lung and colon/rectum are the four most common cancer sites, accounting for more than half of all cancer cases in men and women (Fig. 1.1B). Fig. 1.1 is the cancer incidence in Canada reported by Canadian Cancer Society (Canadian Cancer Society, 2017).

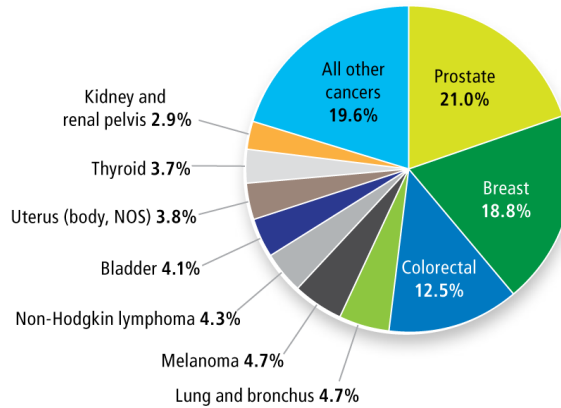
Figure 1.1 Incidence of cancers in 2017 in Canada.

(Modified from **(Canadian Cancer Society, 2017)** with permission) **(A)**

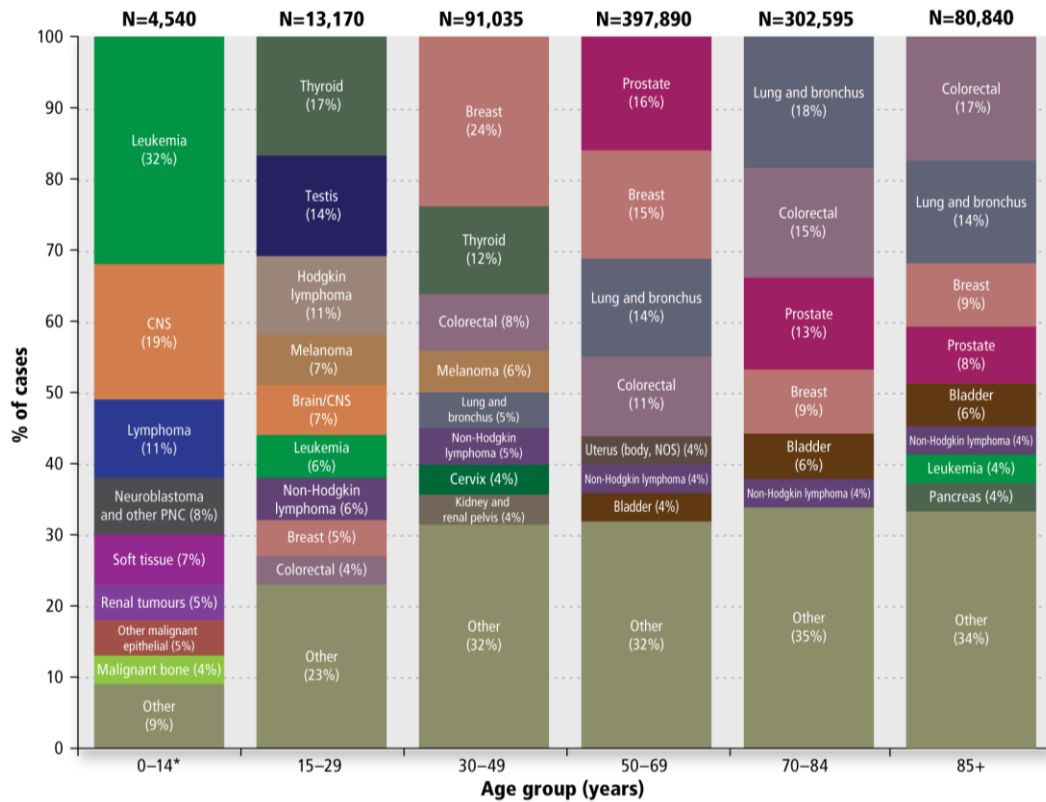
Distribution of 10-year tumour-based prevalence for selected cancers, Canada,
January, 1, 2009;

(B) Distribution of new cancer cases for selected cancers by age group, Canada,
2009–2013.

A



B



Analysis by: Surveillance and Epidemiology Division, CCDP, Public Health Agency of Canada and Health Statistics Division, Statistics Canada
Data source: Canadian Cancer Registry database at Statistics Canada

N is the total number of cases over 5 years: 2009–2013 for each age group except ages 0–14 for which cases are over 2006–2010; CNS=central nervous system; PNC=peripheral nervous cell tumours; NOS=not otherwise specified
 * Cancers in children (ages 0–14 years) are classified according to ICCO Recode ICD-O-3/WHO 2008.

1.1.2 The development of cancer

The molecular view of cancer today is that cancer develops over time rather than all at once, as a result of the cumulative effect of genetic changes (Podlaha, Riester, De, & Michor, 2012). Each change causes the cells to acquire some traits and the accumulation of these changes altogether promotes the malignant growth of cancer cells. There is clear evidence that the control of cell cycle, cell survival and the elimination of unnecessary or damaged cells in normal cellular programs are altered during tumourigenesis.

A single point mutation is not sufficient to generate a cancer cell from a preexisting normal cell. Two main types of genes play a major role in triggering normal mouse cells to be transformed: proto-oncogenes and tumour-suppressor genes (Alberts, 2008). Proto-oncogenes usually regulate cellular growth. On the other hand, tumour-suppressor genes inhibit cell division, promote apoptosis, or both. Proto-oncogenes and tumour-suppressor genes coordinate to regulate the growth of each tissue and organ in the body. In rat models, the disturbance of cell growth control and cell morphology can transform normal rat cells into cancerous cells (Alberts, 2008). For example, the co-introduction of *myc*, a gene that helps cells to become immortalized, and *ras* oncogene, which changes the morphology of cells to rat embryo fibroblasts, yields a foci of transformants (Wang, Lisanti, & Liao, 2011). The separate existence of *myc* or *ras*, would not result in these transformants in human cells (Wang et al., 2011); transformation of human cells usually requires the collaboration of more than one mutated gene. Experimental results imply that five

distinct cellular regulatory circuits need to be altered for normal human cells to develop into tumour cells (Alberts, 2008). The first change is the the induction of the human telomerase reverse transcriptase (*hTERT*) gene, as this gene is necessary to maintain the telomere. The other four changes involve: (1) the mitogenic signalling pathway controlled by Ras-like genes; (2) the cell cycle checkpoint controlled by pRb; (3) the guarding pathway controlled by p53; and (4) the signalling controlled by protein phosphatase 2A (PP2A). However, the necessity of these five changes was determined by *in vitro* experiment; it is still unclear whether the steps needed *in vitro* reflects the changes that occur *in vivo* and lead to cancer in humans.

1.1.3 Hallmarks of cancer

The traits that cancerous cells acquire are called the “Hallmarks of Cancer.” These traits are the characteristics that distinguish cancer cells from normal cells. When cell division and the cell death are both interrupted by external factors, normal cells can then overwhelm the body’s defenses and become cancerous. The hallmarks of cancer are described in two landmark scientific papers by Douglas Hanahan of the University of California and Robert Weinberg of the Massachusetts Institute of Technology (Hanahan & Weinberg, 2000, 2011).

1. Self-sufficient cell division The most fundamental trait of cancer cells is that they are able to sustain proliferation. Growth-promoting signals in normal tissues are carefully controlled and released to maintain a homeostasis of cell number and thus normal tissue architecture. Cancer cells, on the contrary, control their own

proliferation by producing growth signals themselves or by elevating signal receptors.

2. Resistance to anti-growth signals Cell proliferation is stimulated by signals; also, some signals “put the brakes” on cell growth and proliferation. Once growth inhibition is interrupted or ignored, cancer cells can have unlimited proliferation. Unlimited proliferation is usually a result of mutations or alterations of tumour suppressor genes and proto-oncogenes.

3. Evading programmed cell death Cells are programmed to die in the event they become damaged, a mechanism called apoptosis to prevent the propagation of DNA errors. On the other hand, the apoptosis signals of cancer cells can be disrupted when tumour suppressor genes suffer mutations or other damage.

4. Limitless replicative ability A solid tumour may be composed of billions of cells, an indication of uncontrolled cell division. The telomere is a small portion located at the end of each chromosome. In normal cell division, the telomere is shortened every time DNA is replicated because the end of the telomere cannot be covered by the Okazaki fragment and therefore, get copied. Ultimately, telomeres reach a critical point and the cell can no longer divide. Telomerase is an enzyme which can maintain telomere length and when it is activated in a cancer cell, telomerase will allow it to replicate indefinitely compared to normal non-cancerous cells with self-limited replication.

5. Sustained angiogenesis The development of new blood vessels is called angiogenesis. Angiogenesis is a multi-step process and begins with local degradation of the basement membrane. In order to grow, a tumour needs a vast blood supply for oxygen and nutrients. It is equally important for blood to supply oxygen and nutrients to both normal and tumour cells. Pro-angiogenic factors such as vascular endothelial growth factor (VEGF) and fibroblast growth factors (FGFs) are upregulated during angiogenesis, while anti-angiogenic factors are down-regulated. These signals can stimulate endothelial cells to construct capillaries within a tumour.

6. Ability to invade and metastasize Metastases are the cause of 90% of human cancer deaths. Metastasis is the spread of cancer cells to new areas of the body and is defined as the formation of secondary tumour foci. The classical simplification of metastasis steps includes: local invasion, intravasation, survival in the circulation, extravasation and colonization (Nguyen, Bos, & Massagué, 2009). In order to invade and metastasize to other parts of the body, the related gene expression level involved in the regulation of cell-cell and cell-matrix interactions will be altered and cells undergo a process called epithelial-mesenchymal transition (EMT). For example, loss of E-cadherin and acquisition of vimentin are two critical steps during EMT (Myong, 2012).

7. Ability to survive with hypoxia Even with angiogenesis, cells in the interior of a tumour may be in an oxygen-deprived situation called hypoxia. Hypoxia is detrimental to normal cells as aerobic metabolism requires oxygen to convert glucose to energy. Cancer cells can switch from aerobic to anaerobic glucose

metabolism to allow cancer cells to produce energy and survive in oxygen-deprived conditions.

8. Escaping from the immune system The body's immune system detects and destroys abnormal cells to protect the human body when they are functioning properly. Cancer cells are able to evade destruction by the body's immune defenses, proliferate and eventually invade other tissues.

1.1.4 Breast cancer

Breast cancer is the most common cancer in women and 1 in 8 Canadian women is expected to develop breast cancer during their lifetime (Canadian Cancer Society, 2015). Breast cancer is not a single disease, but is comprised of many biological subtypes with distinct pathological features and clinical implications (Iwamoto & Pusztai, 2010; Tang, Wang, & Bourne, 2008). According to different histopathological and biological features demonstrated in breast cancer subtypes, the relevant therapeutic strategies may vary as well (Blows et al., 2010). Thus, it is clinically important to accurately group breast cancers into subtypes for therapeutic decision-making. Clinically, this heterogeneous disease is categorized into three therapeutic groups (The Cancer Genome Atlas Network, 2012): The estrogen receptor (ER) positive group is the most numerous and patients with ER⁺ status receive endocrine therapy. The human epidermal growth factor receptor 2 (HER2) Enriched (HER2E) group is a major improvement because of effective therapeutic targeting of HER2 with Herceptin. Triple-negative breast cancers (TNBCs, lacking

expression of ER, progesterone receptor (PR) and HER2) are a group with only chemotherapy as an option for treatment.

Gene expression profiling is a potentially powerful tool aimed at identifying the “molecular portrait” of invasive breast cancer, and breast tumours were accordingly classified into four intrinsic subtypes with distinct clinical outcomes (Table 1.1) (The Cancer Genome Atlas Network, 2012). The rationale for this classification lies in the distinct gene expression patterns in each subtype and reflects the precise molecular level differences. Based on the recent development of high information content assays including DNA methylation, microRNA (miRNA) expression and protein expression, The Cancer Genome Atlas Network characterizes more completely the molecular architecture of breast cancer using six different technology platforms. The integrated molecular analyses of breast carcinomas significantly extend the knowledge base to produce a comprehensive catalogue of what is likely the genomic drivers of the most common invasive breast cancer subtypes (Table 1.1). The biological outcome of the four main breast cancer subtypes caused by genetic and epigenetic abnormalities may indicate that plasticity and heterogeneity observed in clinic occurs within these major biological subtypes of breast cancer.

Table 1.1 Highlights of genomic, clinical and proteomic features of invasive breast tumour subtypes

(Modified from (The Cancer Genome Atlas Network, 2012) with permission).

Subtype	Luminal A	Luminal B	Basal-like	HER2E
ER ⁺ /HER2 ⁻ (%)	87	82	10	20
HER2 ⁺ (%)	7	15	2	68
TNBCs(+)	2	1	80	9
TP53 pathway	TP53 mut (12%); gain of MDM2 (14%)	TP53 mut (32%); gain of MDM2 (31%)	TP53 mut (84%); gain of MDM2 (14%)	TP53 mut (75%); gain of MDM2 (30%)
PIK3CA/PTEN pathway	PIK3CA mut (49%); PTEN mut/loss (13%); INPP4B loss (9%)	PIK3CA mut (32%); PTEN mut/loss (24%); INPP4B loss (16%)	PIK3CA mut (7%); PTEN mut/loss (35%); INPP4B loss (30%)	PIK3CA mut (42%); PTEN mut/loss (19%); INPP4B loss (30%)
RB1 pathway	Cyclin D1 amp (29%); CDK4 gain (14%); low expression of CDKN2C; high expression of RB1	Cyclin D1 amp (58%); CDK4 gain (25%)	RB1 mut/loss (20%); cyclin E1 amp (9%); high expression of CDKN2A; low expression of RB1	Cyclin D1 amp (38%); CDK4 gain (24%)
mRNA expression	High ER cluster; low proliferation	Lower ER cluster; high proliferation	Basal signature; high proliferation	HER2 amplicon signature; high proliferation
Copy number	Most diploid; many with quiet genomes; 1q, 8q, 8p11 gain; 8p, 16q loss; 11q13.3 amp (24%)	Most aneuploid; many with focal amp; 1q, 8q, 8p11 gain; 8p, 16q loss; 11q13.3 amp (51%); 8p11.23 amp (28%)	Most aneuploid; high genomic instability; 1q, 10p gain; 8p, 5q loss; MYC focal gain (40%)	Most aneuploid; high genomic instability; 1q, 8q gain; 8p loss; 17q12 focal ERB2 amp (71%)
DNA mutations	PIK3CA (49%); TP53 (12%); GATA3 (14%); MAP3K1 (14%)	TP53 (32%); PIK3CA (32%); MAP3K1 (5%)	TP53 (84%); PIK3CA (7%)	TP53 (75%); PIK3CA (42%); PIK3R1 (8%)
DNA methylation	-	Hypermethylated phenotype for subset	Hypomethylated	-
Protein expression	High oestrogen signalling; high MYB; RPPA reactive subtypes	Less oestrogen signalling; high FOXM1 and MYC; RPPA reactive subtypes	High expression of DNA repair proteins, PTEN and INPP4B loss signature (pAKT)	High protein and phosphoprotein expression of EGFR and HER2

Percentages are based on 466 tumour. Amp, amplification; mut, mutation.

In summary, the hallmark characteristics distinguish cancer cells from normal ones. The transformation of a normal cell into a cancerous one requires deregulation of multiple cellular activities regulated by gene expression patterns. Gene expression is mainly controlled by transcription regulation and post-translational regulation (see section 1.2).

1.2 Transcriptional regulation

Transcription is the process of RNA synthesis. The DNA code is transcribed into a sequence of messenger RNAs (mRNA), which are then translated to proteins. Transcription factors (TFs) are sequence-specific DNA-binding factors involved in the process of transcription and are key cellular components that control gene expression. Thus, their activities determine how cells function and respond to the environment. Currently, there is keen interest in research into human transcriptional regulation, but much remains to be explored.

1.2.1 Transcription factors recognize specific DNA sequences

Research in recent decades has contributed to the understanding of how TFs recognize their cognate binding sites in the genome and then initiate gene regulatory functions. Structural analysis of protein-DNA recognition motif and sequence-dependent DNA recognition have revealed why many TFs preferentially bind to a specific DNA sequence (Rohs et al., 2010). The physical interactions between the amino acid side chains of the TFs and the accessible chemical and conformational signature of the base pairs determine the preference of TFs for a

given nucleotide at a typical position. These two recognition types are so-called base- and shape-readout, respectively. Furthermore, high-throughput datasets have revealed that TFs have distinct DNA-binding profiles, even when they exhibit a high degree of similarity in their DNA-binding domains. This means that they can precisely regulate gene expression through temporal and spatial regulation (Noyes et al., 2008; Sibly et al., 2012).

The full picture of the assembly of multi-protein complexes on transcriptional regulation cannot be entirely provided by the high-throughput *in vitro* technology about specific individual TFs. Sequence-based computational models for describing the DNA-binding specificities of TFs are generated for predicting the binding specificity to any new site (Zhou et al., 2015). These sequence-based DNA motif methods have the benefit of easily visualizing DNA sequence motif. However, these models only describe the DNA base readout by a TF and do not include the binding affinity. Recently, probabilistic models incorporating DNA structure-derived features perform better than DNA-sequence based models (Sharon, Lubliner, & Segal, 2008). Hence, the integrated genomic and structural information about protein-DNA binding models is taken into both base- and shape-readout mechanisms.

1.2.2 Transcription factor regulation

The expression and or the activity of TFs themselves can be regulated. For example, the so-called “guardian of genome” *p53*'s gene expression is regulated by directing binding of several types of TFs (Saldaña-Meyer & Recillas-Targa, 2011).

Post-translational modifications (PTMs) is another way that can rapidly and reversibly regulate TF functions, including subcellular localization, stability and interactions with cofactors (Tootle & Rebay, 2005). Phosphorylation of E-twenty-six (ETS) family members, for example, at Serine/Threonine (S/T) residues in response to a variety of upstream signals, exerts broad spectrum effects on their activity. In addition, it has been shown that TFs activity may be regulated by glycosylation and some TFs are included in this cadre of targets including ETS transcription factor Elf-1 is *O*-GlcNAc glycosylated (Juang, Tenbrock, Nambiar, Gourley, & Tsokos, 2002) and nuclear factor I (NFI) isoform which undergo N-glycosylation (Kane et al., 2002). Other potential PTMs, such as acetylation and sumoylation are also involved in the activity regulation of TFs (Zhou et al., 2015).

Regulation of subcellular localization is another means to control the activities of TFs or other proteins with nuclear targets. Active nuclear import and export of transcriptional regulators are based on the recognition of specific signals in the protein sequence. A nuclear localization signal (NLS) in the protein sequence can direct it to the nucleus, while a nuclear export signal (NES) can lead the molecule to be transported out of the nucleus (Nardozzi, Lott, & Cingolani, 2010). Alternatively, subcellular localization can be regulated through a piggyback mechanism by binding to another molecule, transport signal masking, or by cytoplasmic retention (Cautain, Hill, Pedro, & Link, 2015). For example, activation-induced deaminase (AID), functioning as a mutator by deaminating cytosine and thus converting it into uracil, is unable to diffuse into the nucleus despite its small

size and its nuclear entry requires active import mediated by a conformational nuclear localization signal. In contrast, its C-terminus is a determinant for AID cytoplasmic retention (Patenaude et al., 2009). Another example is the cytoplasmic retention of hormone nuclear receptors. For instance, nuclear hormone receptor estrogen receptor α (ER α) is sequestered by metastasis-associated protein (MTA-1) in the cytoplasm and executes its non-genomic activity (Kumar et al., 2002).

Therefore, the subcellular distribution of TFs can determine their biological effect on the cell: genomic effects when they localize to the nucleus, and non-genomic effects in the cytoplasm.

1.2.3 Transcriptional repression and activation

The first and most fundamental order on gene regulation is achieved by the preferential binding of a TF to specific DNA sequence in promoters or enhancers. Higher orders of regulation are accomplished by PTMs on TFs domains and recruiting chromatin-modifying enzymes to induce chromatin structural changes (Geertz & Maerkl, 2010). TFs bind to sequence-specific binding sites in the context of free DNA. However, when the recognition sites are buried in chromatin, TFs need to achieve proper binding by exploiting various strategies (Hahn, 2005) through their cofactors to regulate gene expression (Stampfel et al., 2015). Gene expression is not only regulated by TFs but also by epigenetic modifications.

Epigenetic modifications include DNA methylation and histone modifications. DNA methylation is a post-replication modification predominantly found in

cytosines of the dinucleotide sequence CpG. Specifically, DNA methylation contributes to a silent chromatin state together with proteins that modify nucleosomes (Jaenisch & Bird, 2003). The nucleosome is the fundamental unit of chromatin, and it is composed of an octamer of the four core histones (H3, H4, H2A and H2B). The histones N-terminal “tails” are unstructured and possess a large number of amino acid residues that are targets for PTMs, particularly lysine and arginine. There are at least eight distinct types of modifications found on histones, including acetylation, methylation (lysines, arginines), phosphorylation, ubiquitylation, sumoylation and crotonylation. The extra complexity lies in that methylation at lysines or arginines could have three different forms: mono-, di-, or tri-methylation. Of all the known modifications, acetylation has the most potential to unfold chromatin. This vast array of epigenetic modifications allows an organism to respond to the environment through changes in gene expression.

In order to initiate transcription, nucleosomal DNA has to disassemble first. The cooperative TFs binding, chromatin-remodeling complexes and actively transcribing Pol II can all mediate histone displacement. The cofactors of TFs can act as activators or repressors on gene regulation. For example, histone acetyltransferases (HATs) and histone deacetylases (HDACs) are two counteracting enzyme families controlling the acetylation state of the lysine residues of the core histones. The acetylation of lysine residue removes the positive charge on the histones and thereby the interaction of the N termini of histones with the negatively charged DNA decreases. As a consequence of acetylation, the condensed chromatin

is transformed into a relaxed structure which facilitates gene transcription. But this relaxed state can be reversed by deacetylation, which is performed by HDACs. Once the lysine is deacetylated, the chromatin is back to the condensed state. Acetylation or deacetylation cannot be done by HATs or HDACs alone and is always coupled by other molecules to complete this reaction. For example, the deacetylase activity of HDAC3 strictly requires interaction with its transcriptional co-repressor nuclear receptor co-repressor (N-CoR) (Zhou et al., 2015).

1.2.4 Roles of transcription regulators in cancer

Many TFs are inactive under normal physiological conditions and their expression and activity are tightly regulated. A high proportion of oncogenes and tumour suppressor genes encode TFs. Many human cancers are dependent on the inappropriate expression or activation and inactivation of TFs as well as mutation. For instance, somatic mutations in the p53 gene are some of the most frequent alterations in human cancers (Olivier, Hollstein, & Hainaut, 2010). Hence, TFs represent highly desirable and logical points of therapeutic interference.

Cellular signal transduction induced by the genetic and epigenetic changes is dysregulated in cancer cells. In each pathway, the extracellular signal is received by a receptor and conveyed into the nucleus. TFs and their cofactors are at the end of the signalling pathway, which can regulate gene expression or repression (Nebert, 2002). In clinical trials, progression-free survival of patients with cancers who were previously regarded as untreatable, were improved by drugs that target intracellular

signalling pathways. However, alternate signalling pathways that are not targeted by drugs or a downstream mutation within the kinase-mediated signalling cascades has curtailed the benefit (Gonda & Ramsay, 2015). The cancer phenotype is not only defined by the misregulation of key transcriptional regulators but the misregulation is also critical for cancer development and maintenance. It can therefore be proposed that when these transcriptional regulators act as therapeutic targets, they are less prone to be bypassed by an alternative pathway (Gonda & Ramsay, 2015). Some transcriptional regulators are already under-investigation as potential therapeutic targets (Berg et al., 2002; Yardley et al., 2013). For example, a vector-based DNA Myb vaccine showed some antitumour efficiency against the metastatic spread in a model of mammary cancer (Carpinteri, 2012).

Multicellular organisms are strictly ordered and require extensive coordination and communication between cells; many TFs and cofactors are involved in this hierarchical communication. In response to external stimuli, TFs and cofactors turn on/off appropriate gene expression. Growth factors act as one of the external stimuli which can activate multiple pathways and lead to pleiotropic effect on cell biology.

1.3 Growth factors and their function

Cellular phenomena—proliferation, differentiation, migration and survival/death are not autonomous; much of this is regulated by extracellular proteins (growth factors) that positively and negatively regulate these actions.

Regulation is achieved via transmembrane receptors that growth factors bind on the extracellular surface of cells in order to transduce cellular signalling events in the cytoplasmic compartment (Lemmon & Schlessinger, 2011). Once the ligand binds to the respective receptors, it will trigger intracellular signalling events in both transcription-dependent and independent pathways in the target cells (Brunet, Datta, & Greenberg, 2001). Briefly, growth factors are divided into cytokines, and polypeptide growth factors (Vlasova & Bohjanen, 2016), both of which affect nearly every biological process (Vlasova & Bohjanen, 2016). Cytokines, often compared with growth factors, are a class of signalling molecules that primarily affect the cells of the immune system (An, 2009). From here on, we will mainly focus on polypeptide growth factors that affect most cells of the body.

1.3.1 Growth factors and their receptors

Polypeptide growth factors types: Polypeptide growth factors can act by multiple means paracrine, endocrine and autocrine systems (Hull & Harvey, 2014). There are multiple “superfamilies” of peptide growth factors that contain subfamilies of proteins, with related primary sequences. For example, fibroblast growth factor (FGF) superfamily contains at least 22 distinct members (Zhang et al., 2006).

Growth factors are ligands for transmembrane receptors. Each growth factor superfamily has a corresponding family of related receptors with high specificity. Family members can bind to a single receptor and there are also ones that bind to multiple receptors. For instance, the aforementioned FGF family of 22 structurally-

related molecules can bind to four high affinity, ligand-dependent FGF receptor tyrosine kinase molecules (FGFR1-4) (Zhang et al., 2006). The activation of FGFR results in the stimulation of various signal transduction cascades implicated in multiple aspects of embryonic development, tumour growth, angiogenesis, wound healing, and physiology (Ornitz & Itoh, 2001; Powers, McLeskey, & Wellstein, 2000).

Growth factor receptors: Growth factor receptors are plasma membrane-spanning proteins that bind with a specific growth factor on the external surface of a cell and transduce a signal that regulates cell division. They contain an intracellular domain with enzymatic function that is activated by growth factor binding. For example, epidermal growth factor (EGF) is an approximately 6 kDa molecule and binds to a 170 kDa plasma membrane receptor (EGFR) resulting in receptor dimerization, autophosphorylation (in *trans*) and activation of various downstream signalling pathways (Zhang et al., 2006). Growth factor receptors also define cancer hierarchies (Venere, Lathia, & Rich, 2013) and increased expression or activation of receptor tyrosine kinases occur frequently in human breast carcinomas. For example, breast cancers are classified into different subtypes depending on the expression of ER, PR or Her2 (refer to Table 1.1). Epithelial breast cancer cells are well recognized as commonly over-expressing the Insulin-like Growth Factor-1 (IGF-I) receptor (Christopoulos, Msaouel, & Koutsilieris, 2015), which is a high-affinity receptor for both insulin and IGF-I (Belfiore & Frasca, 2008). EGFR is frequently over-expressed in TNBC (Nakai, Hung, & Yamaguchi, 2016) and an over-expression

of EGFR is correlated with poor prognosis of colon cancers as well (Sasaki, Hiroki, & Yamashita, 2013).

1.3.2 Growth factor function

A. Growth factors can regulate proliferation: Few cells can proliferate without the stimulus of growth factors. Thus, in this regard, growth factors play a significant role during development. The presence of IGF-1 dramatically enhanced early stage proliferation of EGF/FGF-responsive neural stem cells in vitro (Supeno et al., 2013). In other cases, growth factors (i.e. transforming growth factor β (TGF β)) can inhibit cell proliferation (Zermati et al., 2000).

B. Positive and negative regulation in development by GFs: The complexity of embryogenesis is reflected in the presence of complex interactions between growth factor signalling pathways. Recent studies have demonstrated that growth factor receptors are expressed by pre-implantation embryos and growth factor deprivation can result in suboptimal growth as well as developmental abnormalities (Richter, 2008). Pre-implantation embryos also express many growth factors of their own, including EGF, insulin-like growth factor1 (IGF-1), IGF-2, VEGF, platelet-derived growth factor (PDGF) and fibronectin (Richter, 2008). These autocrine growth factors are believed to be the primary reason for embryonic development (Richter, 2008). In some cases, growth factors and their receptors can act as development inhibitors. An example of that is Met, the receptor of Hepatocyte growth factor (HGF), which regulates skeletal muscle differentiation; a novel spliced isoform

Δ 13Met has been found, which can inhibit muscle cell differentiation (Park et al., 2015).

C. Growth factors regulate transcription: Many different types of stimuli can cause the activation of protein kinases, which can further affect gene expression. Growth factor-dependent MAPK and PI3K/AKT pathway activation can phosphorylate many downstream transcription factors. These phosphorylated transcription factors (TFs) are activated and will further up-regulate or down-regulate gene expression (including other transcriptional factors' gene expression).

D. Growth factors and wound healing: Wound sites release several growth factors, including IGF, EGF, FGF, PDGF, TGF and so on. The clinical application of growth factors to stimulate the healing of wounds is currently being investigated (Grazul-Bilska et al., 2003).

Taken together, a cell receives extracellular signals through ligand-receptor interaction and the signal is sensed through activation of related pathways in the cytosol. The signals then have to be transduced into the nucleus, where signals eventually reflect on the genomic level of gene expression/repression. The signal, from the external to cytosol to nucleus, is through tiers of activation and translocation of molecules.

1.4 Nuclear-cytoplasm exchange system

A cell consists of different cellular compartments, which are associated with a diverse range of biochemical processes (Sprenger et al., 2008). Protein function is always related to its subcellular localization and proteins must be targeted to the appropriate compartment to ensure proper function. Therefore, a protein's cellular role may be inferred by localizing to distinct compartments (Rezácová, Borek, Moy, Joachimiak, & Otwinowski, 2008). Understanding protein subcellular localization is not only important for elucidating its function in cells, but also for the organization of the cell as a whole (Scott, Calafell, Thomas, & Hallett, 2005).

The nuclear membrane separates nuclear and cytoplasmic compartments in eukaryotic cells and supports as a structural frame of the nucleus. The nuclear membrane, acting as a barrier between cytosol and nucleus, prevents the free nuclear to cytoplasmic diffusion of molecules; such movement is directed by signals to translocate (Cooper & Hausman, 2000). Nuclear pore complexes (NPC) penetrate through the nuclear membrane and serve as a transporting channel for macromolecules between the two compartments. Many essential regulatory molecules are shuttled between compartments; as example, histones and TFs are imported into the nuclear compartment, while transfer RNA (tRNA), ribosomal RNA (rRNA), and messenger RNAs (mRNA) are transcribed in the nucleus and exported out to the cytoplasm where they function in translation (Beck & Hurt, 2016).

1.4.1 Nuclear pore complexes

Macromolecules can transiently dock and interact with nucleoporins during the transportation process. NPCs create an aqueous channel through which macromolecules are transported (Adam, 2001). The NPC is a large protein complex that can be easily detected by electron microscopy and acts as a molecular transportation gate between cytoplasm and nucleus (Appen & Beck, 2016). The mass of NPCs in higher eukaryotes is about 125 MDa and the proteins that comprise the complex are called nucleoporins (Nups) (Adam, 2001). Each NPC is composed of about 50-100 different Nups. Morphologically, NPCs contain a membrane-embedded central core structure, cytoplasmic and nuclear extensions which form cytoplasmic filaments and nuclear baskets, respectively, which act as cargo docking sites (Beck & Hurt, 2016) (Fig. 1.2). The membrane-embedded central core contains three stacked rings. The middle ring spans and crosses the fused inner and outer nuclear membranes and is sandwiched by the cytoplasmic and nucleoplasmic rings from both distal ends (Beck & Hurt, 2016). The cytoplasmic ring constitutes of eight 50 nm filaments and the nuclear ring is connected to a basket-like assembly of eight thin terminal rings (Fig. 1.2). Macromolecules bearing transport signals translocate through the center of an NPC gate.

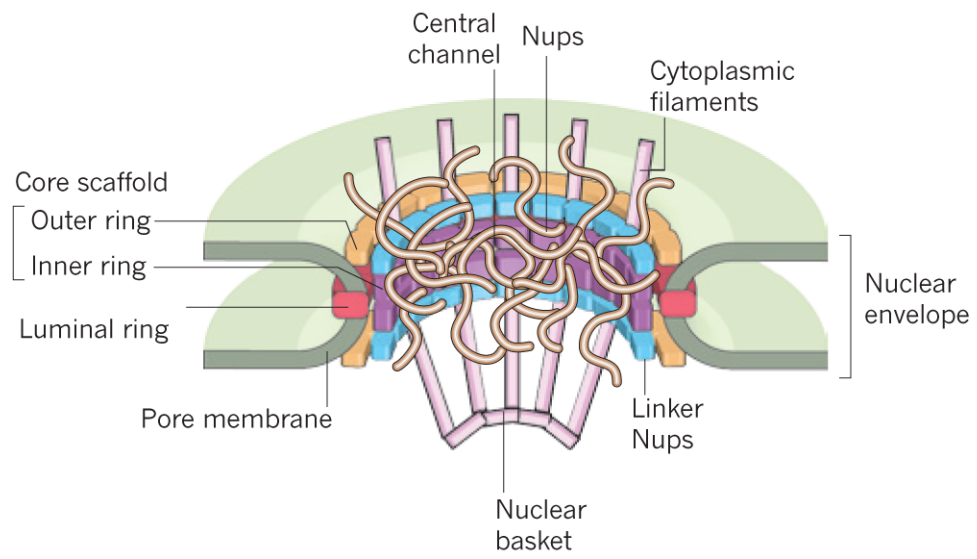
The number of NPCs depends on the demands of cells for nucleocytoplasmic exchange and varies dramatically with cell size and the demands of cellular activities, such as proliferation. For example, there are about 3000-5000 NPCs in a proliferating human cell (Kabachinski & Schwartz, 2015). The commonly used

human cell line, HeLa, contain on average 3000 NPCs in each nucleus (Kabachinski & Schwartz, 2015).

As the sole gateway for the exchange of material between nucleus and cytoplasm, NPCs support two modes of transport: passive diffusion and receptor-facilitated translocation (Naim et al., 2007). Small molecules such as metabolites can passively diffuse through the pore without assistance, but it becomes increasingly slow as the size of the particle approaches ~10 nm in diameter, which corresponds to a protein with a molecular weight of about 45 kDa (Naim et al., 2007). Passive diffusion is only reasonably fast for proteins smaller than 20-30 kDa. In contrast, larger proteins, RNAs, and their complexes require active transport into the nucleus. But not all molecules whose molecular weight is less than 20-30 kDa will diffuse passively in the cells. For example, histones and tRNAs enter the nucleus through carrier-mediated transport, even though their molecular weight is less than 20-30 kDa (Suntharalingam & Wenthe, 2003).

Figure 1.2 Schematic representation of the NPC

(Modified from (Grünwald, Singer, & Rout, 2011) with permission) Cytoplasmic and nuclear extensions of the NPC's periphery are indicated on the cytoplasmic and the nuclear surface.



1.4.2 Transport machinery

Facilitated transport requires specific interactions between the molecule being translocated and the NPC. This nucleocytoplasmic transport is mainly mediated by transport receptors belonging to the superfamily of importin- β -like proteins called karyopherins. Based on the direction to which these receptors carry their cargo, they are classified as importins or exportins which can directly interact with the proteins on the surface of NPCs. As the name implies, importins are accountable for directing the cargo to the nucleus, whereas exportins shuttle the molecules from nucleus to cytoplasm (Yuh & Blobel, 2001).

Nucleoporins (Nups) are often grouped into three types: (i) transmembrane Nups which anchor the NPCs in the nuclear envelope; (ii) phenylalanine-glycine repeats (FG-repeats), and (iii) structural Nups, which act as a scaffold to interact with transmembrane Nups and FG-Nups. Amongst them, FG-Nups play dual roles in nucleocytoplasmic exchange: first, they function as a permeability barrier of the NPCs; second, karyopherins can transiently interact with FG-Nups and transport the cargo through NPCs, which the FG-Nups support as an anchor (Wälde & Kehlenbach, 2010).

Another part of the machinery is Ran(Ras-related nuclear protein), a member of the Ras family of small G proteins, which is essential for the translocation of proteins and RNA through NPCs (Sazer & Dasso, 2000). The prime function of Ran is

to regulate the binding of cargo molecules and will be further discussed in section 1.4.3.2.

1.4.3 Cargoes and signals

Eukaryotic cells must accomplish the rapid and receptor-mediated transport of thousands of proteins and RNAs into and out of the nucleus and karyopherins are taking care of this bidirectional transport (Pemberton & Paschal, 2005). This parcel-like delivery model raises the question of how karyopherin: cargo recognition occurs. Many studies have shown proteins that undergo nuclear import or export generally contain a NLS or NES, respectively (Lange et al., 2007; Weis, 2003).

1.4.3.1 NLS-dependent and independent nuclear import

In 1984, a NLS was first characterized from SV40 Large T antigen and consisted of a short sequence of basic amino acids (Dingwall & Laskey, 1991). The NLS region in SV40 Large T antigen had a stretch of five basic amino acids ¹²⁷PKKKRKV¹³³ and was defined as monopartite NLS (Kalderon, Richardson, Markham, & Smith, 1984). Subsequently, a related signal of two basic clusters separated by about ten residues was identified in *Xenopus* nucleoplasmin and defined as bipartite (Dingwall, Robbins, Dilworth, Roberts, & Richardson, 1988). The sequences identified in SV40 T-Ag and *Xenopus* nucleoplasmin are now referred to as classical NLSs (cNLSs) and require the karyopherins importin- α and importin- β for nuclear transport (Lange et al., 2007).

Consecutive residues from the N-terminal lysine of monopartite NLS are referred to as P1, P2 and a lysine in P1 position is mandatory for monopartite cNLS (Conti & Kuriyan, 2000; Fontes, Teh, & Kobe, 2000; Hodel, Corbett, & Hodel, 2001), followed by basic residues in positions P2 and P4 to yield a consensus sequence of K-K/R-X-K/R, where X stands for any amino acid. Quantitative analyses of the accumulation percentage of nuclear import of eGFP fused with different NLSs demonstrated that a monopartite NLS is more efficient than a bipartite NLS (Ray, Tang, Jiang, & Rotello, 2015). Since the discovery of the NLSs in SV40 T antigen and nucleoplasmin, many other NLSs have been described, as well.

The formation of the import complex is mediated by specific sites on importin- α by recognizing the NLS in the molecules to be imported (Conti, Uy, Leighton, Blobel, & Kuriyan, 1998). Importin- α is composed of a tandem series of Armadillo (ARM) repeats which form a banana-like molecule, producing a curving structure with two NLS-binding sites (Stewart, 2007). Classically, the adaptor protein importin- α recognizes the NLS present in the cargo and forms a dimer with importin- β . Importin- α binds to importin- β through a domain known as the importin- β binding (IBB) domain, which is located in the N-terminus. IBB can compete with NLS and replace the NLS-binding sites, leading to the release of cargo proteins (Lott & Cingolani, 2011). The cargo:importin- α :importin- β complex is transported through NPC and dissociated by the binding of RanGTPase.

The import of many nuclear proteins is thought to be mediated by the classical NLS. However, it is now accepted that import signals unrelated to the

classical NLS exist (Freitas & Cunha, 2009). These NLS-independent molecules could be imported through interaction with other proteins that contain a functional NLS, called a piggyback mechanism, or rely on importin- β -related molecules. For instance, β -catenin, which mediates a late step of the Wnt/Wingless pathway, is imported into the nucleus by binding directly to importin- β or β -like import factors (Fagotto, Gluck, & Gumbiner, 1998).

1.4.3.2 NES-dependent and independent nuclear export

Typically, basic residues (e.g. K, R) are enriched in NLSs. In contrast, a leucine-rich nuclear export signal (NES) is present in cargos exported to the cytoplasm. NES also contain critical hydrophobic residues, which are necessary for recognition by the nuclear export receptor CRM1 (Fung, Fu, Brautigam, & Chook, 2015). The most conserved NES pattern is the LXXXLXXLXL motif where “L” is a hydrophobic residue (Leucine) and “X” is any other amino acid. The spacing between the hydrophobic amino acid residues varies, although the most conserved pattern is LXXLXL, while some fit the LXXXLXL pattern. However, it has been determined that approximately 15% of protein NESs do not conform to either of the LXXLXL or LXXXLXL patterns, indicating a significant degree of flexibility in the export signal (L. Cour et al., 2004).

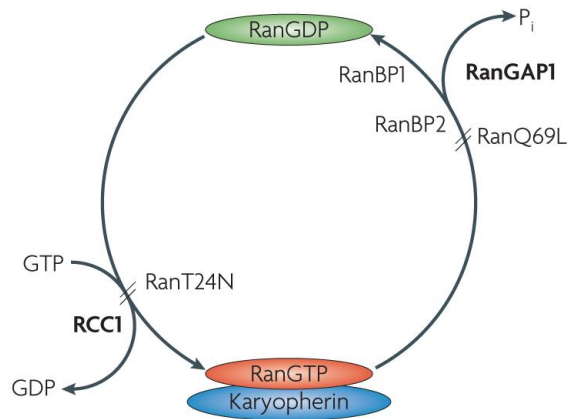
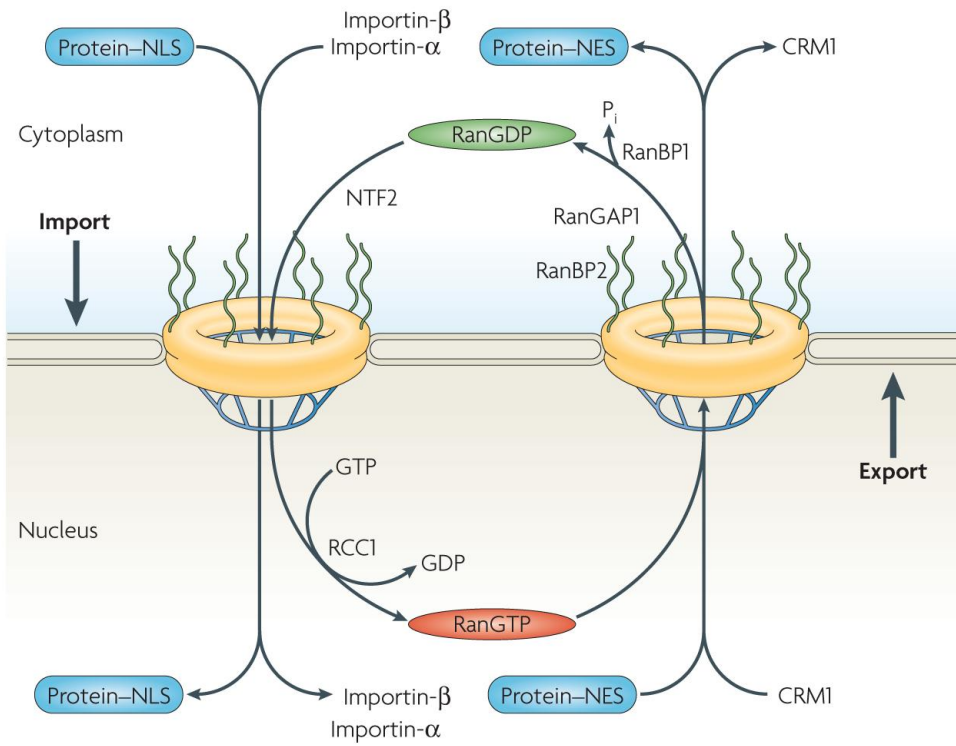
CRM1 is an essential exportin utilized in all types of cells, and it exports numerous cargos including proteins and RNAs (Cullen, 2003; Delaleau & Borden, 2015). NESs bind weakly to CRM1, which ensures that once transport is completed,

these cargos are easily released (Fischer et al., 2015). The way molecules bind to CRM1 through NESs for exportation is called the canonical pathway; also, a non-canonical CRM1 export mechanism exists as well.

During the whole cycle of nucleocytoplasmic shuttling, Ran plays a major role in assisting loading or discharging cargo. For nuclear import, the cargo molecule with an accessible NLS binds to an importin molecule and this complex transports into the nucleus through NPC (Cingolani, Petosa, Weis, & Müller, 1999; Conti et al., 1998). RanGTP can then bind to importin and cause the dissociation of imported complexes by direct or indirect competition (Chook & Blobel, 1999; Cautain et al., 2015). Subsequently, the RanGTP-importin complex is recycled to the cytoplasm. Conversely, RanGTP binds to CRM1 and promotes the tight assembly of exported complexes in the nucleus (Cassar et al., 2007). Once the complex is exported to the cytoplasm, RanGTP is hydrolyzed to RanGDP by RanGAP. RanGDP weakens the affinity between NES and exportin, causing the dissociation of cargoes (Koyama & Matsuura, 2010). RanGDP is then recycled in the cytoplasm by Nuclear Transport Factor 2 (NTF2) back to the nucleus where Ran is loaded with GTP by the guanine nucleotide-exchange factor regulator of chromosome condensation (RCC1). The import and export cycle is illustrated in Fig. 1.3.

Figure 1.3 Ran directs nucleocytoplasmic transport

(Modified from (Clarke & Zhang, 2008) with permission) **(A)** The GTP–GDP cycle of Ran. Ran is loaded with GTP by the guanine nucleotide-exchange factor RCC1. RanGTP adopts a distinct conformation that allows it to interact with a transport factor from the importin- β superfamily, also known as the karyopherins. Hydrolysis of GTP to GDP by Ran requires the interaction of a Ran GTPase-activating protein, RanGAP1, and is stimulated by Ran-binding protein-1 (RanBP1) or RanBP2. RanGDP has a different conformation that does not interact strongly with karyopherin and can be considered inactive. Mutants of Ran block the GTP–GDP cycle: RanT24N has a reduced affinity for nucleotides and forms a stable complex with RCC1, thereby blocking RanGTP formation, whereas RanQ69L cannot hydrolyse GTP and is locked in the GTP-bound conformation. **(B)** Ran shuttles across the nuclear envelope through nuclear pores, but is concentrated in the nucleus because of nuclear transport factor-2 (NTF2)-mediated active import. In the nucleus, a high concentration of RanGTP is generated by nucleotide exchange. This is catalysed by chromatin-bound RCC1 and might be promoted by the nucleotide dissociation factor MOG1 and the accessory factor RanBP3 (not shown). RanGTP causes the dissociation of imported complexes, which contain proteins that carry a nuclear localization signal (NLS), by binding to importin- β and ejecting the cargo. Conversely, binding of RanGTP to chromosome-region maintenance protein-1 (CRM1) promotes the assembly of export complexes containing proteins with a nuclear export signal (NES). In the cytoplasm, RanGTP meets RanGAP1 and RanBP1 or RanBP2, which stimulates GTP hydrolysis and the export complexes dissociate. The importins and exportins are recycled by transport back across the pore.

A**B**

1.4.4 Nucleocytoplasmic exchange system aberration and cancer

The dynamic distribution of molecules between nucleus and cytoplasm is tightly modulated in normal cells. The mislocalization of molecules may alter their usual biological function, thus disturbing the homeostasis of cells and causing diseases such as cancer (Conforti et al., 2015). For example, the cyclin-dependent kinase inhibitor 1A (CDKN1A) and CDK inhibitor 1B (CDKN1B) act as tumour suppressors in the nucleus but they acquire oncogenic properties when mislocalized in the cytoplasm, which leads to increased cell migration and invasion (Besson, Dowdy, & Roberts, 2008; Conforti et al., 2015). Growing evidence illustrates that misregulation of nucleocytoplasmic shuttling is involved in many aspects of the cancer cell phenotype, including promotion of cell survival, carcinogenesis, tumour progression, and drug resistance (Hung & Link, 2011).

Given that tumour suppressor proteins (TSP) execute the antineoplastic functions within the nucleus, mechanisms that misregulate their nuclear export or cytoplasmic ratio effectively will result in their functional inactivation (Gravina et al., 2014). This can result from alterations in the shuttling machinery, which is frequently detected in cancer. For instance, in the breast cancer cell line ZR-75-1, a substantial amount of p53 was localized in the cytoplasm and a truncated form of importin- α was identified. This truncated importin- α is not functional for nuclear localization and p53 accumulates in the cytoplasm in this truncated overexpressing cells (Kim et al., 2000). Another example is elevated expression of CRM1 that is

detected in many tumours, such as cervical and pancreatic cancers, and its high expression level is related to poor outcome (Huang et al., 2009; Shen et al., 2009).

1.5 Mesoderm early response gene 1 (*MIER1*)

1.5.1 Immediate early response genes

Gene transcription is regulated through many complementary processes and one of them is the timing of induced gene expression when responding to an external signal. Immediate early response genes (IEGs) are a particular group of genes activated directly by intracellular signalling in response to growth factors (e.g. PDGF; EGF; FGF), mitogens, developmental and immunological signals, and stress (i.e. ultraviolet) (Healy, Khan, & Davie, 2012; O'Donnell, Odrowaz, & Sharrocks, 2012). By definition, activation of these genes does not require prior protein synthesis. Many IEGs encode TFs, which in turn regulate delayed primary response genes (Bahrami & Drabløs, 2016). IEG expression does not require *de novo* protein synthesis which supports a rapid cellular response. Hence, their expression can lead to the initiation or termination of transcription for other genes, which ultimately carry out the functions relayed by the original signal. Thus, isolation and characterization of IEGs may help to identify the pivotal points in the signal transduction cascade that are critical for determining the response of the target cell.

1.5.2 *Xenopus* mesoderm induction early-response gene (*xmier1*)

Embryos from the amphibian *Xenopus laevis* were used as a model system to study early response genes in FGF signalling transduction in the laboratory of Drs. Paterno and Gillespie (Ryan, Gillespie, 1994; Ryan, Paterno, & Gillespie, 1998; Paterno *et al.*, 1997; Teplitsky, *et al.*, 2003). FGF contributes to the induction/maintenance of mesoderm and in an effort to elucidate the particular early response genes that are active in the FGF signalling cascade, the prospective ectoderm of a blastula stage embryo was incubated with FGF-2 and differentially expressed genes identified by the differential display technique. This led to a novel, developmentally regulated gene discovered in *Xenopus* that was designated mesoderm induction early response 1 (*mier1*), since it is expressed during mesoderm induction (Paterno *et al.*, 1997).

In response to FGF-2 treatment, *xmier1* steady-state levels were shown to increase 3-4 fold and the increase did not require *de novo* protein synthesis, demonstrating that *xmier1* is one of the IEGs. FGF is highly implicated in cell differentiation, mitogenesis, motility and angiogenesis (Grose & Dickson, 2005). It is capable of inducing embryonic cells to differentiate into mesodermal tissues. Therefore, the FGF responding genes, such as *xmier1*, serve to propagate the growth factor's signal at different time points in development. Later, a human homolog of *xmier1*, *hMIER1*, was discovered (Paterno *et al.*, 1997, 1998).

1.5.3 *hMIER1* isolation, genomic structure and isoforms

A human orthologue of *xmier1* was cloned from human testis cDNA library in our laboratory and designated as *hMIER1 α* (Paterno et al., 1998, 2002). *hMIER1* is a single copy gene located on Chromosome 1p31.2 and spans 63 kb (Fig. 1.4A).

Seventeen exons encode this gene in humans; the size of most exons is smaller than 160bp and most introns range 630 bp to 11.7 kb in size. As shown in Fig. 1.4B, alternative splicing, alternative promoter usage or polyadenylation signal (PAS) usage generates 12 distinct *hMIER1* transcripts (Paterno et al., 2002).

Alternate 5' ends result from alternate promoter usage or alternate inclusion of exon 3A to generate three distinct amino terminal regions, N1, N2 and N3. The four variant 3' ends --a, bi, bii and biii --result from alternative splicing or alternate PAS usage; while bi, bii and biii give rise to the same 102aa C-terminal of β isoform. The three distinct N-terminal domains, in combination with two C-terminal regions, gives six distinct *hMIER1* proteins: N1 α (457aaa), N1 β (536 aa), N2 α (432 aa), N2 β (511 aa), N3 α (433 aa), and N3 β (512 aa).

Figure 1.4 Structure of the human *MIER1* gene and splice variants

(Modified from (Paterno et al., 2002) with permission) Schematics illustrating the organization of the *hMIER1* gene and the various *hMIER1* transcripts. **(A)**

Exon/intron organization of the *hMIER1* gene. *hMIER1* is a single copy gene located at 1p31.2 (adapted from <http://genome->

www.stanford.edu/cgi-bin/genecards/carddish?MI-ER1). The two alternate starts of

translation, ML- and MAE- are indicated. Exon numbers are indicated below each

schematic. **(B)** Schematics illustrating the variants 5' and 3' ends of *hMIER1*

transcripts. Alternate promoter usage or alternate inclusion of exon 3A generates

three distinct 5 ends. Activation of MLP-P1 promoter produces N-terminal ends "N1"

and "N2", and MAEP-P2 promoter activation will generate N-terminal end "N3". The

difference between N1 and N2 lies at N1 includes the skipped exon 3A (74bp in

length) which is inserted after the first two amino acid residues, while N2 does not

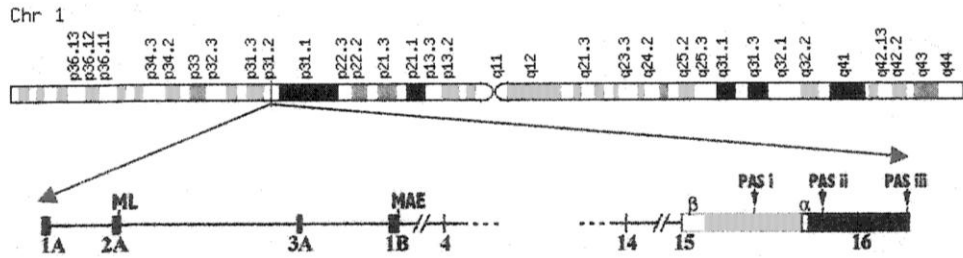
(Paterno et al., 2002). The four variants at 3' ends, a, bi, bii and biii, result from

alternative splicing or alternate PAS usage. The 3' alpha-end portion of *hMIER1*

encodes the 23 aa C-terminal and is named α isoform; while the bi, bii and biii 3'

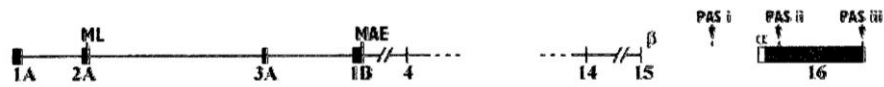
portions all encode the same 102 aa C-terminal, comprising the β isoform.

A

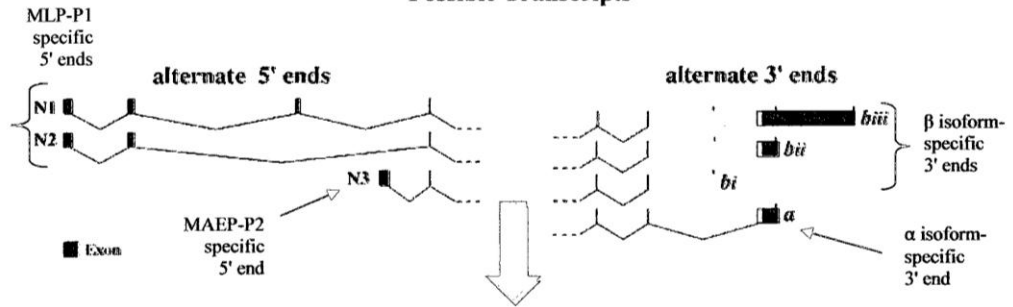


B

Gene Structure



Possible Transcripts



Possible Protein Isoforms

N1 β (536aa), N1 α (457aa)
 N2 β (511aa), N2 α (432aa)
 N3 β (512aa), N3 α (433aa)

1.5.4 hMIER1 protein domains and their possible function

Fig. 1.5 shows a schematic of putative functional domains and motifs contained in hMIER1 as determined by *in silico* analysis. These domains have predicted functions based on investigation of other well-characterized proteins:

The acidic activation domain: The acidic activation domain was first described in the yeast transcriptional activator GAL4 (Ptashne, 2003). In this paper, GAL4 transcriptional activation is mediated by acidic amino acid residues and transcriptional activation correlates with the net negative charge, indicating that acidic amino acids are crucial for GAL4 transactivation. Likewise, acidic amino acid rich regions in the N-terminus of xmier1 are important for transcriptional activation function (Paterno et al., 1997). The N-terminal region which contains the first 98 amino acids of xmier1, stimulated transcription 80 fold, while full-length xmier1 did not activate transcription in NIH 3T3 cells. Fusion with other parts did not demonstrate transcription activity either. These data implied that in isolation, the acidic activation domains in the N-terminal region of xmier1 can function as a transcription activator (Paterno et al., 1997).

The ELM2 domain: All MIER1 isoforms contain an ELM2 domain, as shown in Fig. 1.6. ELM2 stands for EGL-27 and MTA1 homology domain 2 and is also contained in metastasis-associated protein (MTA1) which is part of the nucleosome remodeling deacetylase (NuRD) complex (Solari, Bateman, & Ahringer, 1999). The ELM2 domain was initially identified in the EGL-27 protein, a *Caenorhabditis elegans* protein

similar to human MTA1 (Solari et al., 1999). Together with EGR-1 (*egr-1* is *egl-27* related gene in *C. elegans*), EGL-27 is required for the proper organization in all parts of the embryo and plays a critical role in Wnt signalling, possibly by regulating Homeobox (HOX) gene expression (Hettenbach & Herman, 1999; Solari et al., 1999). As part of NuRD, MTA1 regulates the transcription of its targets by modifying the acetylation status of the target chromatin and cofactors' accessibility to the target DNA (Millard, Fairall, & Schwabe, 2014).

MIER1 functions as a transcriptional repressor by recruiting HDAC1 (Ding, Gillespie, & Paterno, 2003). Depending on the sequence of the C-terminus, MIER1 exists as two isoforms: α and β , which is illustrated in detail in section 1.5.3. Overexpression of MIER1 isoforms α and β respectively can both function equally well as transcriptional repressors through the recruitment of HDAC1 and an intact ELM2 domain is required for these activities (Ding et al., 2003). Blackmore *et al.* 2008 found that MIER1 β interacted with CREB-binding protein (CBP), a known histone acetyltransferase (HAT). The interaction involves the ELM2 and acidic activation domains which are located in the N-terminal half of the protein. Moreover, overexpression of MIER1 β with CBP in HEK 293 cells shows MIER1 β inhibits CBP activity (Blackmore, Mercer, Paterno, & Gillespie, 2008). Taken all the evidence together, MIER1 acts as a transcriptional repressor.

The SANT domain: All MIER1 isoforms contain a SANT domain C-terminal to the ELM2 domain (Fig. 1.5). It was identified in nuclear receptor co-repressors and named after Switching-defective protein 3 (Swi3), Adaptor 2 (Ada2), Nuclear

receptor co-repressor (N-CoR) and Transcription factor (TF)IIIB (Aasland, Stewart, & Gibson, 1996). The SANT domain consists of ~50 amino acid residues and shows remarkable structural similarity to the DNA binding helix-turn-helix domain (DBD) of the MYB oncoprotein (Aasland et al., 1996). However, instead of DNA binding function, SANT domains are protein-protein interaction modules and some can bind to histone tails (e.g. in Ada2 and Silencing Mediator of Retinoic acid and Thyroid hormone receptor (SMRT)). For example, the ADA2 SANT domain is essential for HAT activity to assist general control of amino-acid synthesis (GCN5) to bind to histones in *S. cerevisiae* (Sterner, Wang, Bloom, Simon, & Berger, 2002). The corepressor CoREST has two SANT domains, and the first domain is important for its co-repression function by interaction with HDAC1/2 (You, Tong, Grozinger, & Schreiber, 2001). The SANT domain was also found in N-COR and the silencing mediator of retinoic acid and SMRT, and was shown to bind and activate HDAC3 (Guenther et al., 2000). After SMRT/N-CoR recruits HDAC3 to specific chromatin loci, one of the two closely spaced SANT motifs in the N terminus of SMRT and N-CoR can strongly potentiate HDAC3 enzymatic activity, acting as deacetylase activating domain (DAD) (Guenther et al., 2000; Wen et al., 2000; Zhang et al., 2005). The cumulative evidence for the SANT domain supports its function as a histone-interaction module that couples histone-tail binding to enzyme catalysis for the remodeling of nucleosomes (Grüne et al., 2003).

The SANT domain was demonstrated the repressive regulatory potential in the context of MIER1 function (Ding, Gillespie, Mercer, & Paterno, 2004). This study

showed that MIER1 could form a complex with Sp1 *in vitro* and *in vivo*, and an intact SANT domain was required. This was necessary and sufficient to prevent Sp1 binding to its cognate sites on DNA. Specifically, both isoforms of MIER1 (α & β), through the SANT domain-mediated interaction with Sp1, displace Sp1 from its cognate binding sites and repress Sp1-activated transcription.

The proline rich motif: A proline rich motif is contained in all MIER1 isoforms at the C-terminal of SANT domain. The canonical proline (P) rich motif consensus sequence is PXXP tetrapeptide, in which P stands for proline, and X represents any amino acid residue which can be recognized by SRC Homology 3 (SH3) domain, (Alexandropoulos & Baltimore, 1996). The SH3 domain containing proteins interact with adaptor proteins and tyrosine kinases, mediating assembly of specific protein complexes (Kurochkina & Guha, 2013). The proline rich sequence on MIER1 is PSPPP which also fits the consensus for an SH3 recognition motif (Cesareni, Panni, Nardelli, & Castagnoli, 2002). Also, the consensus of S/T-P motif serves as a proline-directed phosphorylation site (Suzuki et al., 2015). Proline-directed protein kinases for such phosphorylation include cyclin-dependent protein kinases (CDKs), Jun N-terminal protein kinases (JNKs) and glycogen synthase kinase-3 (GSK-3)(Lu, Liou, & Zhou, 2002). Therefore, the proline rich motif on MIER1 not only has potential to function as an SH3 recognition motif, but also as a proline-directed phosphorylation site. Mutation of the proline-rich region of xmier1 (³⁶⁵P³⁶⁶SPPP) showed that only ³⁶⁵P in the proline-rich region was required for the xmier1 effect on embryonic development and mesoderm induction (Teplitzky et al., 2003).

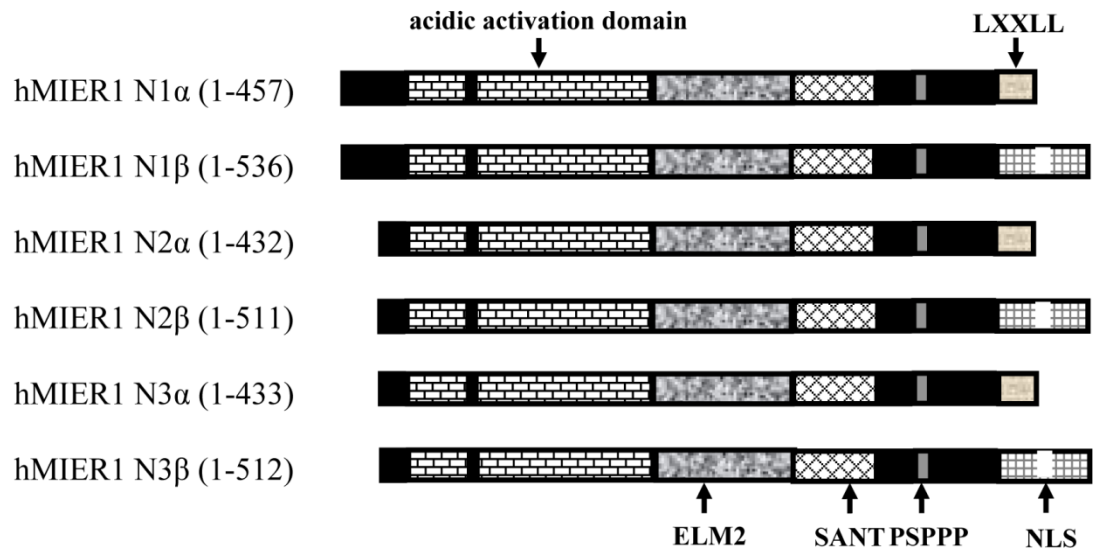
The LXXLL motif: The LXXLL motif was originally identified in proteins that bind the activation function-2 (AF-2) region of nuclear-receptor ligand-binding domains (LBDs) (Garber, Vidanes, & Toczyski, 2005). The LXXLL sequence is a protein-protein interaction motif used in transcriptional regulation and this motif also presents in other proteins; it is reported that the LXXLL motif present in RIP-140, SRC-1 and CBP is necessary and sufficient to mediate the binding of these proteins to ligand-bound nuclear receptors (Heery, Kalkhoven, Hoare, & Parker, 1997). For example, SRC-1 binds the ER and enhances its transcriptional activity dependent on the integrity of the LXXLL motif. The amino acid sequences flanking LXXLL motif have an effect on the selective affinity for hormone receptors. A hydrophobic residue at position -1 relative to the first conserved L and a non-hydrophobic residue at position +2 has a high affinity for steroid and retinoid receptors (Heery, Hoare, Hussain, Parker, & Sheppard, 2001).

The α isoform of MIER1 contains an LXXLL motif at the C-terminal while β isoforms do not. The core LXXLL motif in α isoforms is embedded in an amphipathic helix; both the -1 I and +2 V positions in this domain within α isoforms are hydrophobic amino acid. It was further confirmed that MIER1 α physically interacted with endogenous ER α . ER α and MIER1 α can interact both in the presence and absence of 17- β estradiol (E2) and the interaction was stronger in the absence of ligand, implying the interaction was ligand-independent (McCarthy et al., 2008). The increased expression of MIER1 α greatly inhibited breast carcinoma cell growth in

response to E2 stimulus, indicating that MIER1 α as a possible corepressor of ER α (McCarthy et al., 2008).

Figure 1.5 Protein domains and motifs in hMIER1 isoforms

Schematics illustrating the protein motifs common and unique to the hMIER1 isoforms. The acidic activation domain, the ELM2 domain, the SANT domain, and the proline rich motif PSPPP are common to the hMIER1 isoforms. The nuclear localization signal (NLS) is localized on the C-terminal region of hMIER1 β . The LXXLL motif is localized in the C-terminal region of hMIER1 α .



1.5.5 hMIER1 expression and subcellular localization

Expression pattern: An investigation of the *MIER1* expression pattern revealed that MIER1 β is ubiquitously expressed at very low levels in most human tissues (Paterno et al., 1998, 2002). Of the 23 tissues tested, β isoform displays above average expression levels in the heart, placenta, liver, testis, ovary, colon, peripheral blood leukocyte, stomach, thyroid, spinal cord, lymph node and adrenal gland, while the testis exhibited the highest degree of expression in both studies (Paterno et al., 1998, 2002). MIER1 α isoform-specific transcript expression revealed its expression is restricted to endocrine and endocrine-responsive tissues, relative to the ubiquitous expression noted for the β isoform.

MIER1 splice variants vary in specific tissues. For example, the lung and skeletal muscle produced MIER1 β isoform harboring the N3 N-terminal domain but not the α isoform. Moreover, splice variant transcripts harboring exon 3A display tissue-specific expression patterns and it is not expressed in the lungs. These studies imply that regulation of *MIER1* splice variants transcription undergoes different promoter usage in particular tissues.

In virtually all cell lines examined, endogenous MIER1 α protein was not detectable by western blot. However, its transcript could be detected by qPCR, albeit at low levels. One exception was in 3T3-L1 cells, induced to differentiate into adipocytes. During differentiation, MIER1 α protein expression increased such that it

was detectable on a western blot. The low levels of MIER1 α in cell lines is consistent with its ability to inhibit proliferation (described in section 1.5.6).

Subcellular localization: Originally, it was presumed only MIER1 β isoform localized in the nucleus as it contains an NLS (Post, Gillespie, & Paterno, 2001; Ding et al., 2003; Clements, Mercer, Paterno, & Gillespie, 2012), delineated in Fig. 1.5. This NLS resides in the MIER1 β -specific stretch of 102 amino acids at the C-terminal end and MIER1 β isoforms do localize in the nucleus. However, MIER1 α also localizes in the nucleus in the MCF7 breast carcinoma cell line (Clements et al., 2012). The cassette exon 3A encodes a consensus Leu-rich nuclear export signal (NES) and alternative splicing to include exon 3A produces an N-terminal variant MIER1-3A α with altered subcellular distribution in MCF7 cells. MIER1 α demonstrates 81% nuclear localization while only 2% MIER1-3A α localizes in the nucleus (Clements et al., 2012). In contrast, the inclusion of exon 3A in MIER1 β to produce MIER1-3A β had little effect on the nuclear targeting of this isoform, which implies that the NES contained in exon 3A cannot compete with the NLS contained in C-terminal β isoform (Clements et al., 2012).

1.5.6 hMIER1 in breast cancer

MIER1 α overexpression in T47D human breast carcinoma cells, in conjunction with E2 treatment, significantly reduces the anchorage-independent growth of these cells (McCarthy et al., 2008). These results suggest MIER1 α may inhibit breast carcinoma cell's ability to proliferate without adhering to a

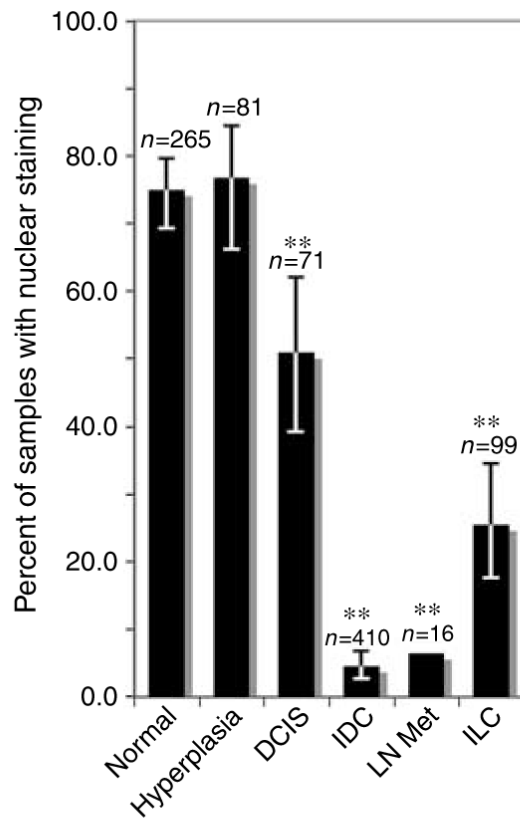
substratum, a distinct indicator of cell tumourigenicity. ER α is a receptor whose misregulation plays a fundamental role in breast cancer development and tumourigenesis (Roy & Vadlamudi, 2012). Therefore, MIER1 α corepressor functions and its potential to interact with ER α strongly imply that MIER1 plays a role in the regulation ER α activity.

Furthermore, MIER1 α protein expression is strongly associated with breast cancer staging based on immunohistochemistry (IHC) (Fig. 1.6). It was determined that 96% invasive ductal carcinoma (IDC) samples have lost nuclear MIER1 α , while only half of DCIS samples showed this shift in subcellular localization and 75% of normal breast samples show nuclear staining. This may be due to ductal carcinoma *in situ* consists of heterogeneous group of pre-invasion lesions which may or may not develop to IDC (McCarthy et al., 2008).

Figure 1.6 Loss of nuclear MIER1 α during breast cancer progression

(Modified from (McCarthy et al., 2008) with permission). Values are from the tissues microarrays (TMAs) and whole tissue sections. The percentage and 95% confidence intervals are shown. The number of samples (n) in each category is listed above the bar; **indicates $P \leq 0.001$. Nuclear MIER1 α was detectable in 75% of normal breast samples and in 77% of hyperplasia, but in breast carcinoma, only 51% of DCIS, 25% of ILC and 4% of IDC contained nuclear staining.

(DCIS: ductal carcinoma in situ; IDC: invasive ductal carcinoma; ILC: invasive lobular carcinoma.)



1.6 Aims of this study

Precise control of transcriptional regulators is critical to ensure a proper cellular response in normal cells. One key variable is the correct subcellular distribution of transcription regulators in cellular compartments in order to execute their proper function. Misregulation of this cellular distribution may lead to aberrant gene expression/repression, which results in the abnormal physiological responses of cells to growth factor or hormonal stimulation. Therefore, it is pivotal to uncover the mechanism that regulates nucleocytoplasmic shuttling of transcription regulators.

The regulation of nucleocytoplasmic transport can be modulated by PTMs, NLSs masking, cytoplasmic retention and/or modulation of the import machinery. In the context of MIER1 α , it has been demonstrated that MIER1 α acts as a transcriptional repressor when localized in the nucleus and breast cancer development is coupled with decreased MIER1 α nuclear localization. The aim of this study is to investigate the regulation of nuclear import and export of the human transcription regulator MIER1 α in breast carcinoma cell lines, which can assist in understanding the mechanism of MIER1 α nuclear loss during breast cancer progression.

Objective 1: Investigating the mechanism of MIER1 α nuclear localization

Analysis of MIER1 α reveals it does not contain a predicted NLS; however, it still localizes in the nucleus in MCF7 cells (Clements et al., 2012). Since the α isoform

of MIER1 showed a stepwise loss of nuclear localization during breast cancer progression (McCarthy et al., 2008), we proposed that controlling nuclear localization of MIER1 α might be a critical step for breast cancer development and/or progression. Therefore, our first goal was to unravel how MIER1 α gets into the nucleus in the MCF7 breast carcinoma cell line, in the absence of an intrinsic NLS.

Objective 2: Molecular mechanism responsible for MIER1 α nuclear loss

The factors responsible for MIER1 α shuttling from the nucleus to cytoplasm during breast cancer progression are not known. In this part, I investigated the role of various hormones and peptide growth factors in regulating MIER1 α nuclear export.

Objective 3: Identification of the signalling pathway responsible for shuttling MIER1 α out of the nucleus

During the course of tumour progression, cancer cells acquire a number of characteristic alterations through changes in the cellular signalling pathways. Cell signalling is dominated by response to stimuli through ligand binding to its receptor that transmits the signal inside the cell. Hormones and growth factors cause pleiotropic effects in cells through the activation of multiple signalling pathways. In this section, I continued my investigation of hormone and growth factor-dependent activation of pathways that caused MIER1 α nuclear export in a human breast carcinoma cell line and my goal was to investigate the molecular mechanism.

**Chapter 2 Nuclear localization of the transcriptional regulator
MIER1 α requires interaction with HDAC1/2 in breast cancer cells**

This chapter is a version of the paper: Li S, Paterno GD, Gillespie LL (2013) Nuclear Localization of the Transcriptional Regulator MIER1 α Requires Interaction with HDAC1/2 in Breast Cancer Cells. PLoS ONE 8(12): e84046.
<https://doi.org/10.1371/journal.pone.0084046>

Author contributions to the published manuscript: Conceived and designed the experiments: LLG GDP SL. Performed the experiments: SL. Analyzed the data: LLG GDP SL. Contributed reagents/materials/analysis tools: LLG GDP. Wrote the paper: LLG.

Candidate contributions to Chapter 2: Elaboration on the introductory material, expanded description.

2.1 Introduction

Previous research in the Gillespie laboratory revealed that MIER1 α localizes in the nucleus even though it does not contain a classic NLS (Clements et al., 2012). Deletion analysis had demonstrated that the MIER1 β C-terminus contains the only functional NLS, leading to the question of how MIER1 α is transported to the nucleus (Post et al., 2001). The MIER1 α sequence contains a classic LXXLL motif for interaction with nuclear receptors and indeed, MIER1 α interacts with ER α in breast carcinoma cells (McCarthy et al., 2008). Furthermore, regulated overexpression of MIER1 α was shown to inhibit estrogen-stimulated growth in these cells (McCarthy et al., 2008). This led us to hypothesize that MIER1 α nuclear localization occurs via a piggyback mechanism, through its interaction with ER α . In this chapter, we demonstrated that nuclear targeting of MIER1 α was not through its association with ER α as expected; instead, it is transported to the nucleus through a piggyback mechanism with HDAC1/2. We also demonstrated that an intact ELM2 domain is required for nuclear localization of MIER1 α .

2.2 Methods and materials

2.2.1 Plasmids and constructs

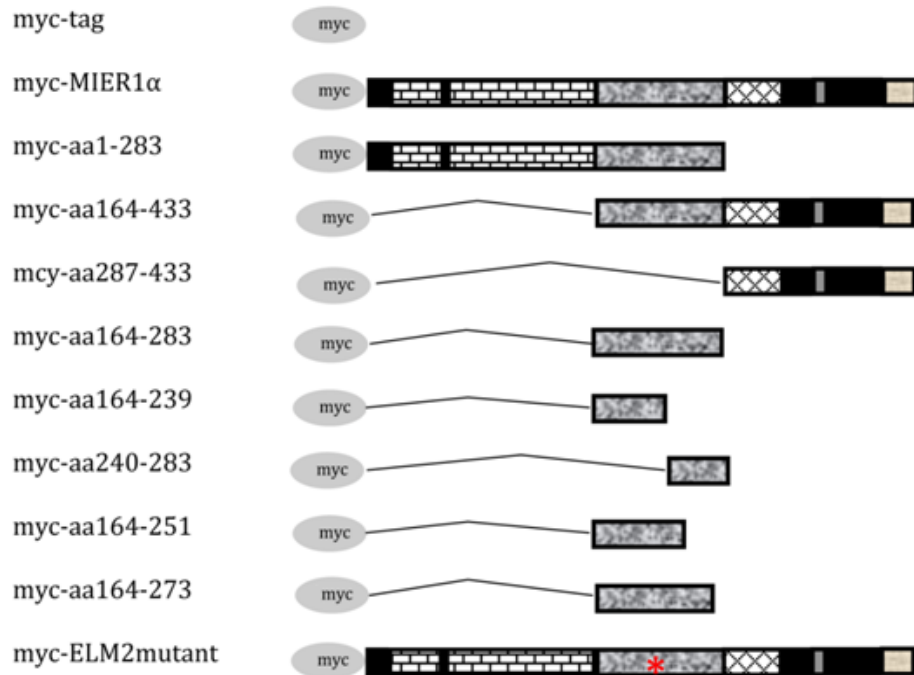
MIER1 α amino acid residues are numbered from the start of translation (1) to the stop codon (433), as shown in Fig. 2.1. Constructs were generated for use in cell culture.

Figure 2.1 MIER1 α amino acid sequence

10	20	30	40	50
MAEPSVESSS	PGGSATSDDH	efdpsadmlv	HDFDDERTLE	EEEMMEGETN
60	70	80	90	100
FSSEIEDLAR	EGDMPIHELL	SLYGYGSTVR	LPEEDEEEEEE	EEEEGEDDED
110	120	130	140	150
ADNDDNSGCS	GENKEENIKD	SSGQEDETQS	SNDDPSQSV	SQDAQEIIRP
160	170	180	190	200
RRCKYFDTNS	EVEEESSEDE	DYIPSEDWKK	EIMVGSMFQA	EIPVGICRYK
210	220	230	240	250
ENEKVYENDD	QLLWDPEYLP	EDKVIIIFLKD	ASRRTGDEKG	VEAIPEGSHI
260	270	280	290	300
KDNEQALYEL	VKCNFDTEEA	LRRLRFNVKA	AREELSVWTE	EECRNFEQGL
310	320	330	340	350
KAYGKDFHLI	QANKVRTRSV	GECVAFYYMW	KKSERYDFFA	QOTRFGKKKY
360	370	380	390	400
NLHPGVTDYM	DRLLDESESA	ASSRAPSPPP	TASNSSNSQS	EKEDGTVSTA
410	420	430		
NQNGVSSNGP	GILQMLLPVH	FSAISSRANA	FLK*	

Figure 2.2 Amino Acid sequences of all plasmids used

Constructs



 : N-terminal acidic stretches;

 : ELM2 domain

 : SANT+ α C-terminus

* : 214W \rightarrow A

2.2.1.1 Generation of myc-tag fusion constructs

2.2.1.1.1 Ligation of *MIER1* α insert into myc-tagged plasmid

Human *MIER1* gene structure, the sequence of its transcripts and the myc-tag vector, pCS3+MT, (a kind gift of Dr. David Turner, University of Michigan; http://sitemaker.umich.edu/dltturner.vectors/cs2_polylinker_descriptions) containing full-length *MIER1* α have been described (Paterno et al., 2002). Specific primers incorporating 5' and 3' BamHI sites were used to amplify the entire coding sequence of hMIER1 α and the amplified sequence was inserted into the BglII site of CS3+MT plasmid. For the *MIER1* α deletion constructs, previously described constructs representing amino acids (aa)1-283, aa164-433, aa287-433 or aa164-283 of *MIER1* α in the Clontech pM vector (Ding et al., 2003) were digested with EcoRI and the *MIER1* α insert was ligated into the EcoRI site of a pCS3+MT vector that had been modified to maintain the *MIER1* sequence in-frame with the myc-tag. This modified pCS3+MT, renamed pCS4+MT, contains a thymidine (T) inserted upstream of the EcoRI site.

Plasmids containing ER α shRNA (Cat. No. TR320346), HDAC1 shRNA (Cat. No. TR312496), HDAC2 shRNA (Cat. No. TR312495) or a control scrambled shRNA (Cat. No. TR20003) were purchased from Origene Technologies, Inc.

2.2.1.1.2 Digestion and purification of inserts from pM and pCR3.1vector

pCR3.1 vector containing the desired insert aa287-433 was digested with restriction enzyme EcoRI and incorporated in the myc-tagged vector CS4+MT,

generating myc-aa 287-433. pM vector containing the desired insert (aa164-239, aa240-283, aa164-251, aa164-273) were digested with restriction enzyme EcoRI and incorporated in the myc-tagged vector CS4+MT, generating myc-aa164-239, myc-aa240-283, myc-aa164-251 and myc-aa164-273. The digested inserts were gel purified from a 1% agarose gel in 1xTris/Borate/EDTA (TBE) buffer.

2.2.1.2 Site-direct mutagenesis

Myc-tagged MIER1 α containing a point mutation ²¹⁴W→A in the ELM2 domain (ELM2 mutant) was produced using the QuikChange site-directed mutagenesis kit (Stratagene) according to the manufacturer's instructions along with the following primers: 5'GAT CAG CTC CTG GCG GAC GCT GAG TAC TTA GC-3' (forward); 5'-GGT AAG TAC TCA GGG TCC GCC AGG AGC TGA TC-3' (reverse).

2.2.1.3 Sequencing

The sequences/mutations were confirmed by automated dideoxynucleotide sequencing of both strands (DNA Sequencing Facility, The Center for Applied Genomics, The Hospital for Sick Children, Toronto, Canada).

2.2.1.4 Plasmid isolation and purification

For transfection, transformed *XL1-Blue* cells were grown o/n in 200 ml LB containing 50 μ g/ml ampicillin. All plasmids were prepared using the EndoFree[®] Plasmid Maxi Kit (QIAGEN, Cat. No. 12362), according to the manufacturer's instructions, which is listed in detail in Appendices 1.

2.2.2 Cell lines and culture conditions

The human breast adenocarcinoma cell line, MCF7, was obtained from the American Tissue Culture Collection (ATCC) and cultured in DMEM (GIBCO, REF 11965-092) containing 10% serum (7.5% calf serum (CS) (GIBCO Cat. No. 16010-159) plus 2.5% fetal bovine serum (FBS) (GIBCO, REF 1884253)) and 1 mM sodium pyruvate (GIBCO, REF 11360-070). The MC2 and VC5 cell lines were produced by Dr. V.C. Jordan (Georgetown University Medical Center, Washington, DC) and derived by stably transfecting the ER-negative MDA-MB-231 breast carcinoma cell line with wild-type *era* or empty vector (pSG5), respectively, as described (Liu, Lee, Reyes, Zapf, & Jordan, 2001; Pearce, Liu, & Jordan, 2003). MC2 and VC5 cells were maintained in phenol red-free MEM (GIBCO, REF 31053-028) containing 5% charcoal-dextran treated FBS (HyClone, Cat. No. SH30068.03), 1% L-glutamine (GIBCO, Cat. No. 25030081), 6 ng/ml insulin (Gibco, REF 12585-014) and 200 µg/ml Geneticin (Invitrogen, Cat. No. 10131035). All cells were grown in a humidified 37 °C incubator with 5% CO₂. These three different cell lines were used in this study, as depicted in the following Table 2.1.

All cells were grown in 100 mm plates (Corning) containing 10 ml of respective media as described above. The optimal confluency is different for every cell line and depends on their respective growth patterns and cellular structure. Cells were subcultured at various dilutions depending on the cell line once they reached the optimal confluency. Briefly, cells were trypsinized in 0.025% trypsin in 1×PBS/1 mM EDTA and diluted into a fresh 100 mm tissue culture dish. Stocks of

cells were frozen at -70°C in CS containing 10% DMSO and 1×10^6 /ml cells were frozen in one freezing vial (Nalge Nunc International).

Table 2.1 List of cell lines used in this study

Cell line	Description	Supplier
MCF7	Mammary gland, adenocarcinoma, ER positive	ATCC: ATCC®#: HTB-126™
MC2	Mammary gland, adenocarcinoma, ER positive	Georgetown University Medical Center, Washington, DC
VC5	Mammary gland, adenocarcinoma, ER negative	Georgetown University Medical Center, Washington, DC

2.2.3 Transient transfection

2.2.3.1 Neon® electroporation

Cells were transfected by electroporation using the Neon® electroporation device (Invitrogen Corp.) and the following settings: 1000 V, 30 ms, 2 pulses for MCF7 or 1400 V, 10 ms, 4 pulses for MC2 and VC5 cell lines. 3×10^5 (MCF7) or 2.6×10^5 (MC2 and VC5) cells were mixed with 0.5 µg myc-tagged plasmid and loaded into a 10 µl tip for electroporation. For the ERα shRNA knockdown experiments, 1.0 µg shRNA and 0.5 µg myc-tagged plasmid were mixed together with 3×10^5 MCF7 cells, and then loaded into a 10 µl tip for electroporation. After transfection, cells were plated at a density of 4×10^4 /well in Falcon 8-well culture slides (BD

BioSciences, Cat. No. 0877426) for confocal analysis or 3×10^5 /well in 6-well dish for Western blot analysis. For HDAC1 and 2 double knockdown experiments, 0.8 μ g of each HDAC shRNA plasmid was used for electroporation; for single knockdowns, the total amount of plasmid transfected was kept constant by adding 0.8 μ g of scrambled shRNA plasmid. Electroporation and plating was performed as above.

2.2.3.2 Mirus TransIT-LT1

Sixteen hours after electroporation, cells were transfected with 0.5 μ g plasmid encoding myc-tagged MIER1 α using Mirus TransIT-LT1 (Mirus[®], Cat. No. MIR 2300) transfection reagent (Medicorp, Inc.) in a 3:1 ratio of reagent: DNA (v/w), according to the manufactures' protocol. Transfected cells were cultured for a total of 48h, then either fixed with 4% paraformaldehyde/PBS for confocal analysis, or solubilized in 400 μ l of SDS sample buffer (50 mM Tris-Cl pH6.8, 2% SDS, 5% β -mercaptoethanol, 10% glycerol, 0.1% bromophenol blue) for western analysis.

2.2.4 Antibodies

The 9E10 anti-myc tag mouse monoclonal antibody was prepared as described in Blackmore *et al.* (Blackmore et al., 2008). The anti-ER α antibody (HC-20), anti-HDAC1 antibody (H-51) and anti-HDAC2 antibody (H-54) were purchased from Santa Cruz Biotechnology Inc. For confocal analysis, Alexa Fluor-488 labeled donkey anti-mouse (Cat. No. 715-545-150) and Alexa Fluor-647 labeled donkey anti-rabbit (Cat. No. 715-606-150) were purchased from Jackson ImmunoResearch Laboratories Inc. HRP-labeled sheep anti-mouse (Cat. No. SLBM8280V) and donkey

anti-rabbit antibodies (Cat. No. SLBL4004V) were purchased from GE Healthcare Corp. Anti- β -actin (A5441) was purchased from Sigma-Aldrich Co.

Table 2.2 Antibodies used for immunofluorescence (IF) and western blot (WB)

Name	Usage	Source	Dilution	Incubation
9E10	Anti-myc	Developmental Studies Hybridoma Bank	1:200 in IF; 1:2000 in WB	o/n in IF; o/n in WB
HC-20	Anti-ER α	Santa Cruz Biotechnology Inc.	1:200 in IF; 1:2000 in WB	o/n in IF; o/n in WB
H-51	Anti-HDAC1	Santa Cruz Biotechnology Inc.	1:200 in IF; 1:2000 in WB	o/n in IF; o/n in WB
H-54	Anti-HDAC2	Santa Cruz Biotechnology Inc.	1:200 in IF; 1:2000 in WB	o/n in IF; o/n in WB
DAM-AlexaFluor-488	Donkey-anti-mouse	Jackson ImmunoResearch Laboratories Inc.	1:300 in IF	1h in IF
DAR-AlexaFluor-647	Donkey-anti-rabbit	Jackson ImmunoResearch Laboratories Inc.	1:300 in IF	1h in IF
HRP-SAM	Sheep-anti-mouse	GE Healthcare Corp.	1:3000 in WB	1h in WB
HRP-DAR	Donkey-anti-rabbit	GE Healthcare Corp.	1:3000 in WB	1h in WB
A5441	Anti- β -actin	Sigma-Aldrich Co.	1:5000 in WB	1h in WB

2.2.5 Co-immunoprecipitation (co-IP)

Forty-eight hours post-transfection, cells were washed once with 1×PBS and lysed on ice for 30 min in 1×IP buffer (1% Triton X-100, 150 mM NaCl, 10 mM Tris-Cl pH7.4, 10 mM EDTA, 0.02% Sodium Azide, 1 mM PMSF, 1% protease inhibitor cocktail). Cell lysates were passed several times through a 26-gauge needle then centrifuged at 12,000×g for 15 min at 4°C. The supernatants were incubated overnight at 4°C with anti-HDAC1 or anti-HDAC2 antibody pre-bound to Protein A-agarose beads (Pierce Biotechnology). After incubation, the beads were washed six times with ice-cold 1×IP buffer and bound proteins were solubilised in 30 µl of 1.5× SDS sample buffer and analyzed by SDS-PAGE-Western.

2.2.6 Western blot

2.2.6.1 Western blot materials

The 0.2 µm PVDF membranes (Trans-Blot Turbo™ transfer Pack) and Trans-blot Turbo™ system were purchased from Bio-Rad Laboratories. Prestained high and low molecular weight markers (GeneDireX®), Amersham's ECL Plus Western Blotting System purchased from GE Healthcare Corp. were used for the detection.

2.2.6.2 Western blot methods

Western blot analysis was performed using 7.5% SDS-PAGE gels. After transfer of the proteins to the PVDF membranes, the membrane was incubated in 5% blocking powder (skim milk powder) in TBS-T (20 mM Tris, 137 mM NaCl, 1% (v/v) Tween-20, pH7.6) for 1 h at RT. The membrane was then incubated overnight in

TBS-T containing a primary antibody (see Table 2.2 for list of antibodies used, dilution and incubation time for each antibody) at 4°C. After incubation with the first antibody, the membrane was washed in large volumes of TBS-T for 1 h and then the secondary antibody (see Table 2.2) was added in TBS-T and incubated for 1h. After incubation with secondary antibody, the membrane was washed in TBS-T for another 1 h before detection of the protein with Amersham's ECL Plus Western Blotting System.

2.2.6.3 Cell lysis for direct western blot

MCF7 cells were plated at 3×10^5 cells/well in 6-well dish and left to grow in incubator. Cells were collected at 48 h post-transfection in ER α knockdown experiment. After washing in cold $1 \times$ PBS on ice, cells were then solubilized in $400 \mu\text{l}$ $1 \times$ SDS sample buffer (50 mM Tris-Cl pH6.8, 2% SDS, 5% β -mercaptoethanol, 10% glycerol, 0.1% bromophenol blue) for western blot. $1/20^{\text{th}}$ of the cell lysate was separated on a 7.5% SDS-PAGE acrylamide gel and the separated proteins were transferred to PVDF membranes by Trans-blot Turbo™ system.

2.2.7 Immunofluorescence, Confocal microscopy and statistical analysis

2.2.7.1 Immunofluorescence

Immunofluorescence was performed as listed in Appendix 2.

2.2.7.2 Confocal microscopy

Cells were examined under an Olympus FluoView FV1000 confocal microscope. Fluorescence images were obtained by sequential z-stage scanning in

two or three channels (DAPI, Alexa Fluor-488 and/or Alexa Fluor-647); z-stacks were compiled into individual images.

2.2.7.3 Statistical analysis

Quantitative analysis of confocal z-stacks was performed using Image J software v1.48 (Bankhead, 2014), as described in (Clements et al., 2012). Briefly, cell outlines were traced and the sum of the pixel values within the outlines for all slices was determined. After subtracting the background, this value was used as the corrected whole cell MIER1 fluorescence. The sum of the pixel values for nuclei was determined in the same way and used as corrected nuclear MIER1 fluorescence. The nuclear value was subtracted from the whole cell value to obtain cytoplasmic MIER1 fluorescence and the corrected fluorescence value in each compartment was plotted as a proportion of the total. 20-30 cells were measured for each sample from 3 independent experiments.

Statistical analysis was performed using a two-sided Fisher's exact test with the InStat v3.0 software program (Graphpad Software, San Diego, CA, USA).

2.3 Results

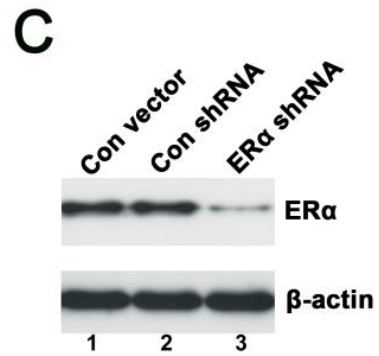
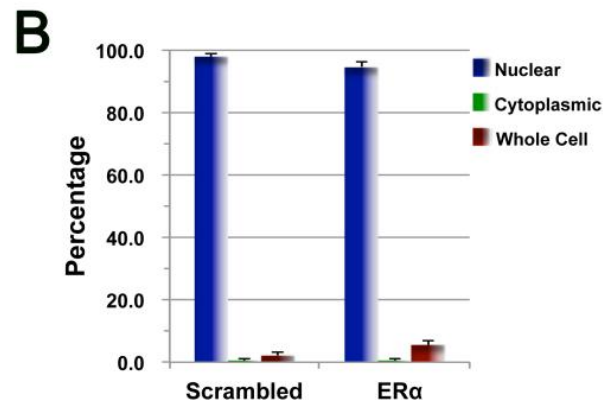
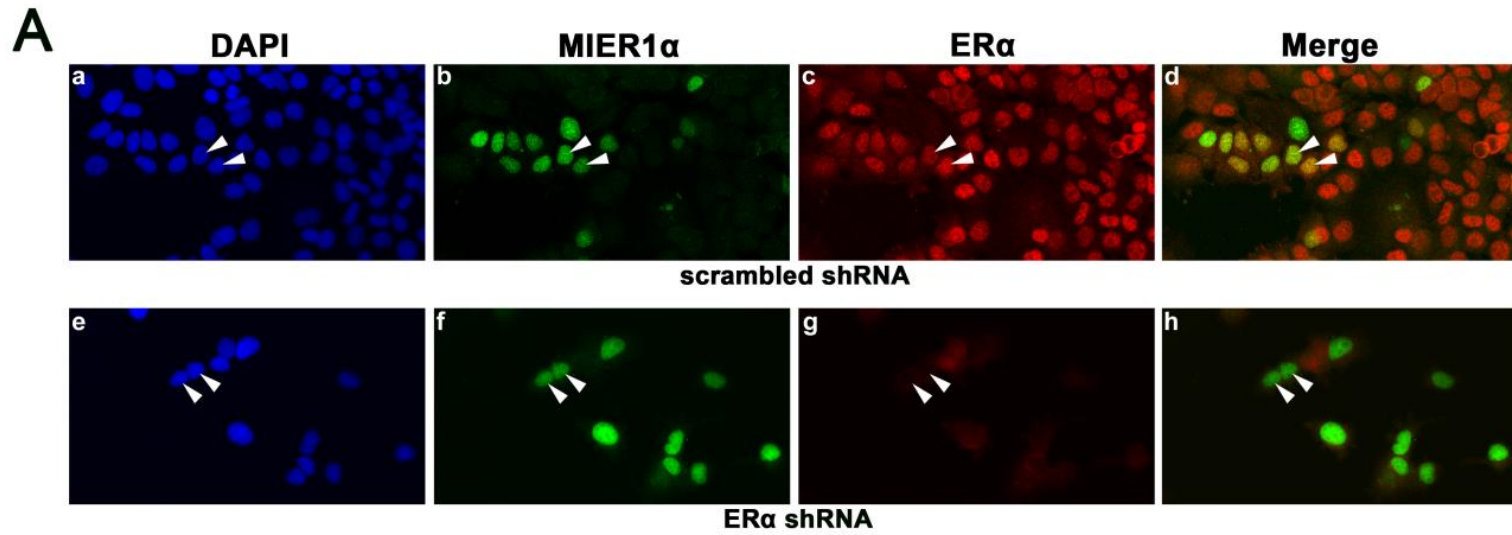
2.3.1 Nuclear localization of MIER1 α is not dependent on its interaction with ER α

In the original characterization of human MIER1 α and MIER1 β , it was determined that α isoform localized in the cytoplasm of NIH3T3, while the β isoform was exclusively nuclear (Paterno et al., 1998). Subsequently, MIER1 α was

demonstrated that it is localized in the nucleus of MCF7 breast carcinoma cells (Clements et al., 2012). Given that MIER1 α does not contain NLS and interacts with ER α (McCarthy et al., 2008), we investigated whether MIER1 α is carried into the nucleus of MCF7 cells by binding to ER α , in a “piggyback” fashion. Cells were transfected with plasmids encoding a myc-tagged MIER1 α along with either an ER α shRNA or a scrambled, control shRNA and localization was determined by confocal microscopy. Subcellular localization was scored as: 1) NUCLEAR; if the nucleus was intensely stained, with little or no cytoplasmic staining; 2) CYTOPLASMIC; if staining was primarily in the cytoplasm, with little or no staining in the nucleus; 3) WHOLE CELL; if both the nucleus and cytoplasm were stained. The shRNA was effective at knocking down endogenous ER α expression levels, as determined by Western blot and confocal microscopy, while the scrambled shRNA had no effect (Fig. 2.3A, compare panels c & g; Fig. 2.3C, compare lanes 2 & 3). ImageJ analysis of the Western blot in Fig. 2.3C, determined that ER α expression was knocked down to 22% of control. In cells expressing the scrambled shRNA, 98% displayed nuclear MIER1 α (Fig. 2.3A panels a-d, & Fig 2.3B) and this pattern did not change when ER α expression was knocked down. The cells expressing ER α shRNA displayed 95% nuclear MIER1 α (Fig. 2.3A panels e-h, & Fig. 2.3B), even cells with no detectable ER α (see arrowheads in Fig. 2.3A, panes f&g).

Figure 2.3 Knockdown of ER α does not affect nuclear localization of MIER1 α in MCF7 cells

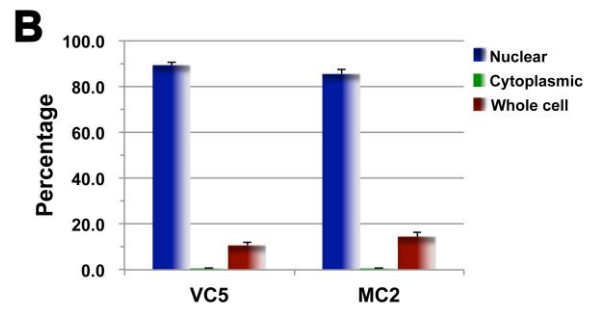
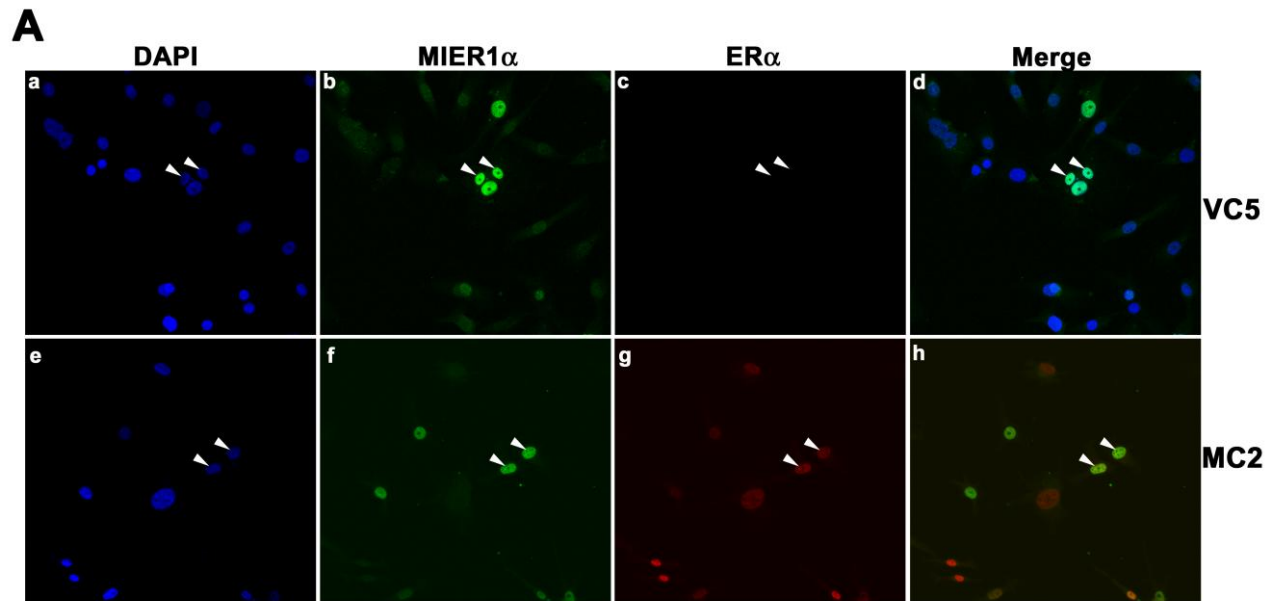
MCF7 cells were transfected with myc-tagged MIER1 α plus either a control, scrambled shRNA or an ER α shRNA and analysed by confocal microscopy **(A, B)** or immunoblotting **(C)**. **(A)** Illustrative examples of cells showing stained nuclei (DAPI; panels a, e), MIER1 α localization (9E10 anti-myc tag and an AlexaFluor-488 secondary antibody; panels b, f) and ER α localization (HC-20 antibody and an AlexaFluor-647 secondary antibody, panels c, g). Panels d, h show merged 488 and 647 channels. Arrowheads indicate nuclei. Note that MIER1 α is nuclear even in cells that lack detectable ER α (arrowheads in panels f & g). **(B)** Histogram showing the results of 3 independent experiments; random fields were selected and the stained pattern of each cell within the field was scored visually according to the categories described in the RESULTS. 180-190 cells were scored for each shRNA. Plotted is the percentage of cells in each category \pm S.D; there is no significant difference between the percent nuclear for the two samples ($p > 0.05$). **(C)** Western blot to confirm knockdown of ER α . Extracts from MCF7 cells transfected with myc-tagged MIER1 α and either empty vector (lane 1), control scrambled shRNA (lane 2) or ER α shRNA (lane 3). The blot was stained with anti- β -actin (lower panel) to verify equal loading or with anti-ER α (upper panel).



To confirm that ER α is not required for targeting MIER1 α to the nucleus, we examined localization in two clonal lines of MDA-MB-231 (ER-), MC2 and VC5, stably expressing ER α or empty vector, respectively (Liu et al., 2001; Pearce et al., 2003). MC2 and VC5 cells were transfected with myc-tagged MIER1 α and localization was determined by confocal microscopy (Fig. 2.4). Similar localization patterns were seen in the 2 cell lines: most cells exhibited nuclear MIER1 α (Fig. 2.4 B; 89% for VC5 and 86% for MC2), regardless of whether ER α was present or not (Fig. 2.4 A, panels b-c & f-g). Taken together, these data demonstrate that ER α is not involved in transporting MIER1 α to the nucleus.

Figure 2.4 MIER1 α is localized in the nucleus in ER- breast carcinoma cells

(A) MDA231-derived cell lines, VC5 (vector) and MC2 (stably expressing ER α), were transfected with myc-tagged MIER1 α and analyzed by confocal microscopy using DAPI (a,e), 9E10 anti-myc tag (b,f), anti-ER α (c,g) and the secondary antibodies described in the legend to Fig. 2.2. Panel d shows merged MIER1 α and DAPI staining while panel h shows merged MIER1 α and ER α staining. Note that MIER1 α is localized in the nucleus in VC5 cells, even in the absence of ER α (arrowheads in panels a-d). **(B)** Histogram showing the results of 3 independent experiments; random fields were selected and the staining pattern of each cell within the field was scored visually. 170-380 cells were scored for each cell line. Plotted is the percentage of cells in each category \pm S.D; there is no significant difference between the percent nuclear for the two cell lines ($p>0.05$).



2.3.2 The ELM2 domain of MIER1 α is required and sufficient for targeting to the nucleus

Identifying the region of MIER1 α that is required for nuclear targeting might provide insight into the mechanism involved. Therefore, we performed a deletion analysis of myc-tagged MIER1 α . MCF7 cells were transfected with plasmids encoding full-length MIER1 α (aa1-433) or with a deletion construct containing the following regions: 1) the N-terminal acidic stretches + the ELM2 domain (aa1-283), 2) the ELM2 + SANT + α C-terminus (aa164-433), 3) the SANT + α C-terminus (aa287-433) or 4) the ELM2 domain alone (aa164-283) (Fig. 2.5). Localization was determined by confocal microscopy and compared to the myc-tag alone and to full-length MIER1 α . The myc-tag alone displays whole cell staining (Fig. 2.5, panels a-c; Fig. 2.5 A-B), as expected of a macromolecule that is sufficiently small (<40 kDa) to undergo passive diffusion through the nuclear pore (reviewed in (Marfori et al., 2011)). Myc-tagged full-length MIER1 α , on the other hand, is almost exclusively nuclear (97%; Fig. 2.5, panels d-f; Figs. 2.5 A-B). Constructs 1 & 2 localized in the nucleus, similar to full-length MIER1 α (94% and 98% nuclear; Fig. 2.5, panels g-l; Figs. 2.5 A-B), while construct 3 showed a distribution pattern similar to the myc tag alone, i.e. whole cell (0% exclusively nuclear; Fig. 2.5, panels m-o; Fig. 2.6 A-B). Thus, only constructs containing the ELM2 domain were targeted to the nucleus and indeed, the ELM2 domain in isolation was localized in the nucleus (85% nuclear; Fig. 2.5, panels p-r, & Figs. 2.6 A-B). To obtain a quantitative measure of MIER1 α localization within the cell, we performed an analysis of confocal z-stacks for each

construct, using the ImageJ software program (Bankhead, 2014) and determined the fluorescence in the nuclear and cytoplasmic compartments (Fig. 2.6 B). The results of this analysis show that 93% of full-length MIER1 α and 83-84% of constructs 1, 2 & 4 are in the nuclear compartment, while only 37% of construct 3 was nuclear. Together these results demonstrate that the ELM2 domain is necessary and sufficient to target MIER1 α to the nucleus.

Figure 2.5 The ELM2 domain directs nuclear localization of MIER1 α

MCF7 cells were transfected with myc-tag empty vector (panels a-c), myc-tagged full-length MIER1 α (d-f) or a myc-tagged MIER1 α deletion construct containing either the acidic + ELM2 domains (g-i), the ELM2 + SANT + α C-terminus (j-l), the SANT domain + α C-terminus (m-o) or the ELM2 domain alone (p-r). Localization was analyzed by confocal microscopy using DAPI and 9E10 anti-myc tag antibody. Illustrative examples of cells showing stained nuclei and MIER1 α localization; arrowheads show examples of nuclei. A schematic, drawn to scale and illustrating the MIER1 α domains and constructs used, is shown on the right; the acidic stretches are shown as black bars, the ELM2 domain is in yellow, the SANT domain in purple, the α C-terminus in pink and all remaining sequence in blue. The amino acids (aa) encoded by each construct are indicated. The myc epitope tag is shown in green.

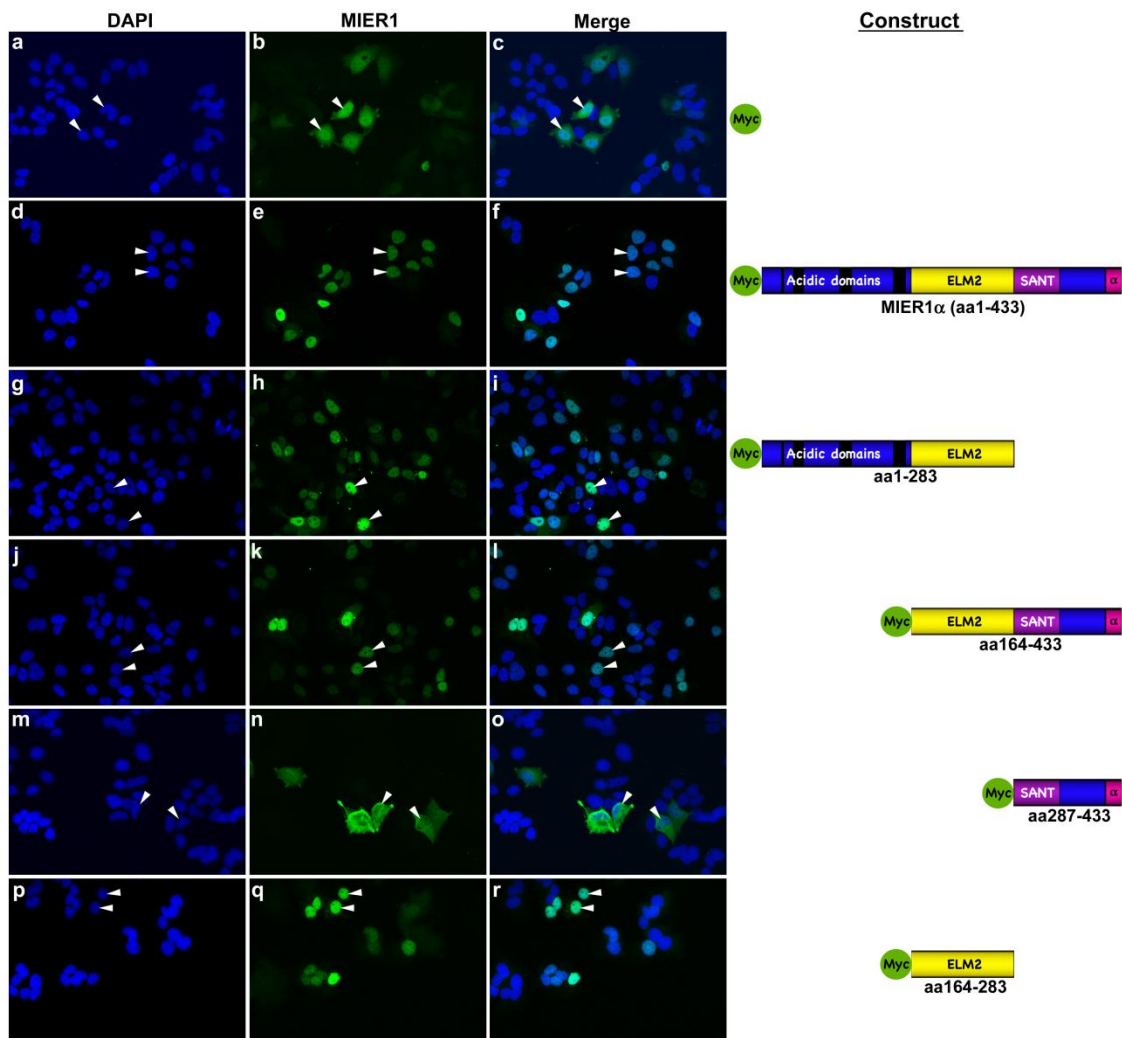
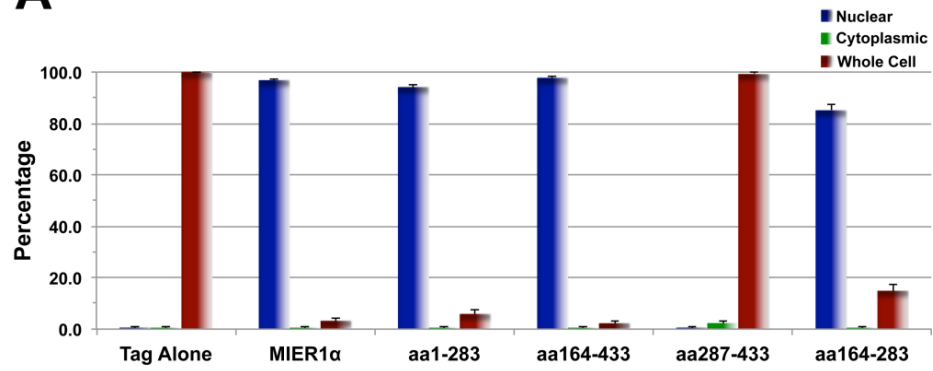
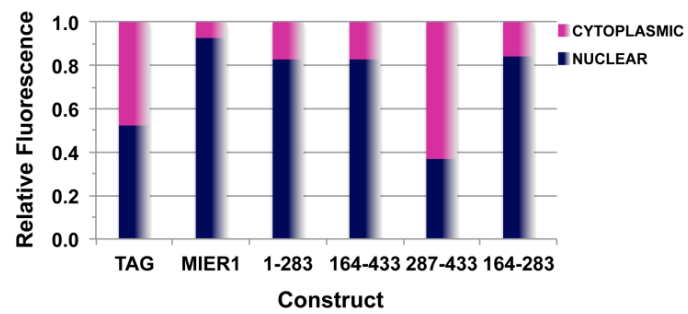


Figure 2.6 The ELM2 domain is sufficient for nuclear localization of MIER1 α

(A) Histogram showing the results of 3 independent experiments; random fields were selected and the staining pattern of each cell within the field was scored visually. 220-970 cells were scored for each construct. Plotted is the percentage of cells in each category \pm S.D; the percent nuclear for the SANT domain + α C-terminus (aa287-433) construct is significantly less than that for full-length MIER1 α ($p < 0.05$).

(B) Bar graph showing the intracellular distribution of MIER1 α . Pixel values for the nuclear and the cytoplasmic compartments were measured in confocal z-stacks using Image J v1.38; plotted is the proportion of the total signal in each compartment, using measurements from 20-30 cells for each construct. The proportion of the SANT domain + α C-terminus (aa287-433) construct in the nuclear compartment is significantly less than that of full-length MIER1 α ($p < 0.05$).

A**B**

Non-canonical NLSs contained in cargo proteins can be recognized and directed into the nucleus by importin- β . Since the ELM2 domain of MER1 α does not contain a classical NLS, we investigated whether it contains non-canonical NLS that was yet to be described.

First, we aimed to define the sequence required for nuclear targeting by producing six myc-tagged deletion constructs of the ELM2 domain for analysis. The first two were designed to divide the 120aa ELM2 domain into an N-terminal 76aa and a C-terminal 44aa portion (Fig. 2.7, panels d-i). In contrast to the intact ELM2 construct (Fig. 2.5, panels a-c, & Fig. 2.6), neither portion was targeted to the nucleus (Fig. 2.7, panels d-l). To verify that the critical sequence was not bisected in these 2 constructs, we produced 2 additional constructs that maintained the integrity of this region. C-terminal deletions were designed to remove either the last 10aa or the last 32aa. As can be seen in Fig. 2.7, panels j-o, and Fig. 2.8, neither construct was localized in the nucleus. Thus, removal of as little as 10aa from the C-terminus of the ELM2 domain abolished nuclear targeting. These data led us to conclude that an intact ELM2 domain is required for nuclear targeting of MER1 α .

Table 2.3 ELM2 domain does not contain cNLS

ELM2 domain sequence (aa164-283):

EESEDEDYIPSEDWKKEIMVGSMFQAEIPVGICRYKENEKVVYENDDQLLWDPEYLP
EDKVIIFLKDASRRRTGDEKGV EAIPEGSHIKDNEQALYELVKCNFDTEEALRRLRFNVKA
ARE

Classical NLS:

Monopartite NLSs: K(K/R)X*(K/R)

Bipartite NLSs : (K/R)(K/R)X*10-12(K/R)3/5

*: X stands for any amino acid.

Figure 2.7 Nuclear localization requires an intact ELM2 domain

MCF7 cells were transfected with a myc-tagged intact ELM2 domain (aa164-283) (panels a-c) or a myc-tagged ELM2 deletion construct containing aa 164-239 (panels d-f), aa240-283 (panels g-i), aa 164-251 (panels j-i), aa164-273 (panels m-o).

Localization was analyzed by confocal microscopy using DAPI and the 9E10 anti-myc tag antibody. Illustrative examples of stained cells showing MIER1 α localization.

Note that nuclear localization was only detected with an intact ELM2 domain (a-c); arrowheads indicate examples of stained nuclei. The rest of constructs displayed whole cell staining (arrows in d-o). A schematic drawn to scale and illustrating the constructs used, is shown on the right as are the amino acids (aa) encoded by each construct. The myc epitope tag is shown in green.

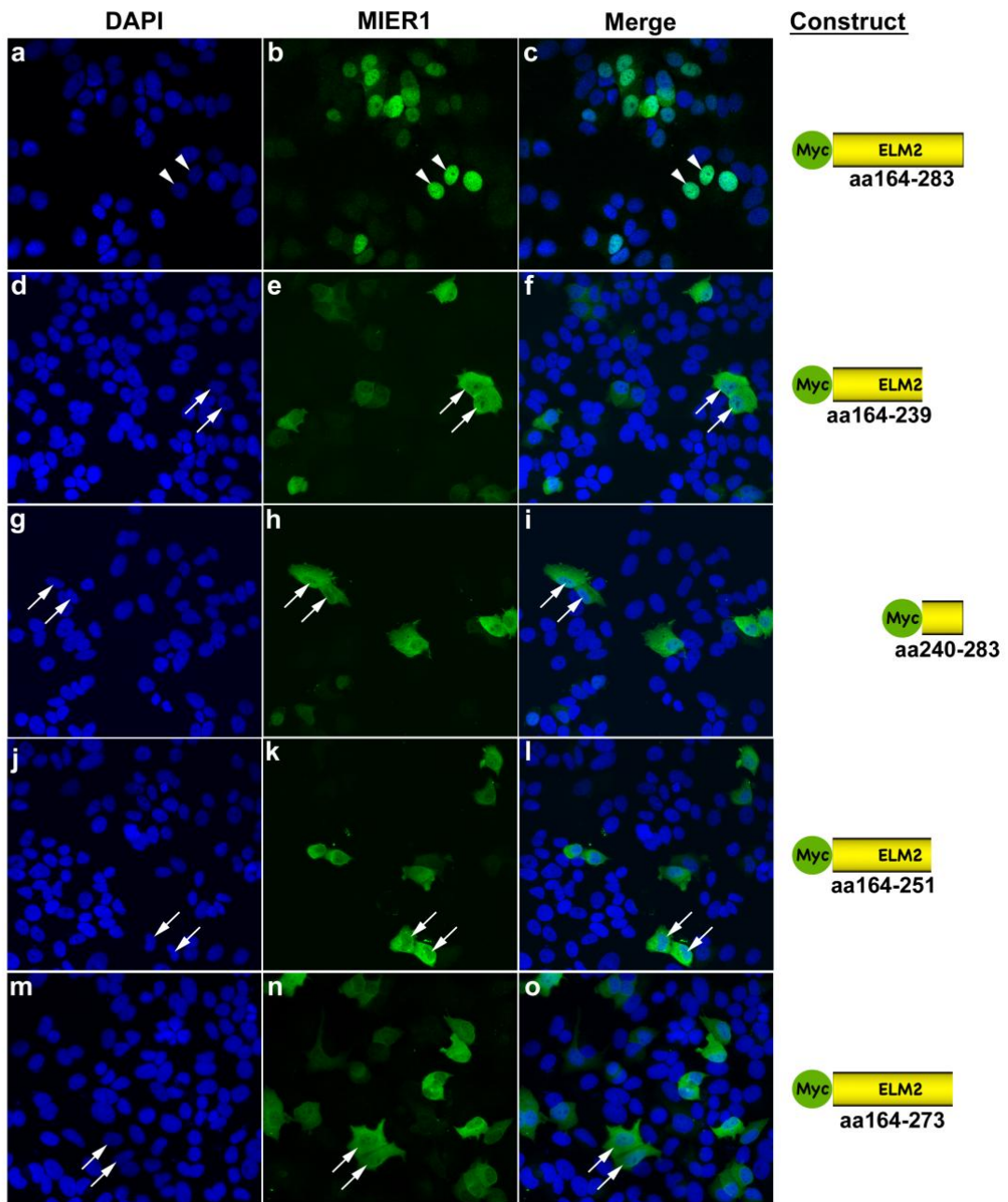
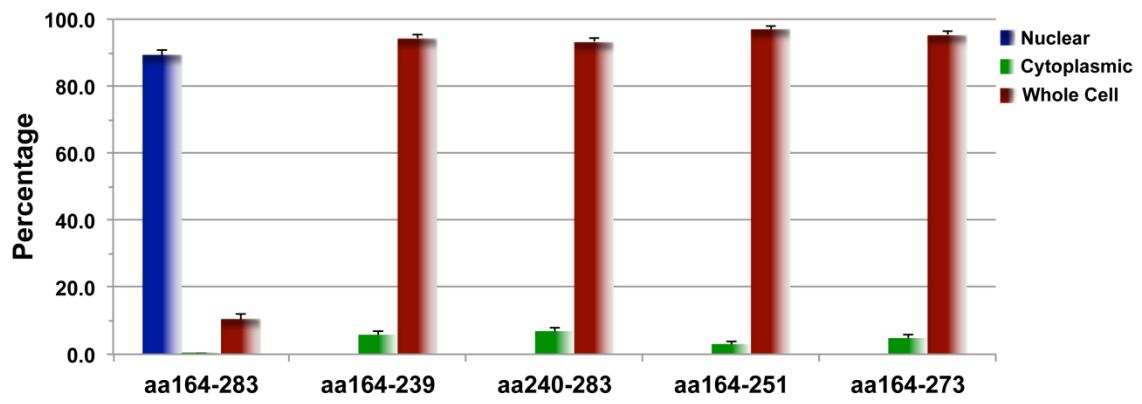


Figure 2.8 Statistical data demonstrate the necessity of intact ELM2 domain for MIER1 α nuclear localization

Histogram showing the results of 3 independent experiments; random fields were selected and the staining pattern of each cell within the field was scored visually. 465-565 cells were scored for each construct. Plotted is the percentage of cells in each category \pm S.D; the percent nuclear of all deletion constructs are significantly less than that of the intact ELM2 domain ($p < 0.05$).



2.3.3 Interaction with HDAC1/2 is required for nuclear localization of MIER1 α

The results presented in Figs. 2.9 and 2.10 are reminiscent of a previous study characterizing the interaction of MIER1 α with HDAC1 (Ding et al., 2003). Utilizing a similar deletion analysis, this interaction was shown to require an intact ELM2 domain. In fact, a single point mutation of a highly conserved tryptophan (W) at position 214 in the ELM2 domain abolished interaction between MIER1 and HDAC1. MIER1 also interacts with the highly related HDAC2 by ²¹⁴W, but not with any of the other class I, IIa, IIb or IV HDACs (Bantscheff et al., 2011; Joshi et al., 2013) and HDAC1/2 are the only proteins known to interact with the ELM2 domain of MIER1 α . Therefore, we investigated whether interaction with HDAC1/2 plays a role in nuclear localization of MIER1 α . MCF7 cells were transfected with either a myc-tagged, full-length wild-type MIER1 α (WT-MIER1 α) or a myc-tagged full-length mutant containing the point mutation ²¹⁴W \rightarrow A (ELM2 mutant) and analyzed by co-IP for interaction with endogenous HDAC1 or HDAC2. Subcellular localization was determined by confocal microscopy in parallel samples. Our co-IP results confirm WT-MIER1 α interaction with both HDAC1 and HDAC2 (Fig. 2.9, lane 2, upper and lower panels) and demonstrate that the ELM2 mutant does not interact with either HDAC1 or HDAC2 (Fig. 2.9, lane 3, upper and lower panels). Confocal analysis revealed that HDAC1 and 2 expression levels were not affected by expression of the ELM2 mutant (Fig. 2.10 A&B, compare panels b&f); however, nuclear targeting is lost with this ELM2 point mutation (Fig. 2.10 A&B, compare panels c and g; Fig. 2.11), with only 10% of cells now showing nuclear staining. Quantitative analysis of

the fluorescence in the nuclear and cytoplasmic compartments using ImageJ shows that 90% of wild-type MIER1 α is in the nucleus but that there was significantly less (44%) of the ELM2 mutant located in the nuclear compartment (Fig. 2.11B; $p < 0.05$). These data suggest that interaction with HDAC1/2 is required to target MIER1 α to the nucleus.

Figure 2.9 Western blot showing that ELM2 mutant (²¹⁴W→A) does not interact with HDAC1 or HDAC2

MCF7 cells were transfected myc-tag empty vector (lane 1, 6), myc-tagged full-length wild-type MIER1α (lanes 2, 4) or myc-tagged full-length ELM2 mutant (lanes 3, 5). Cells extracts were either subjected to immunoprecipitation (lanes 1-3) with anti-HDAC1 (upper panel) or anti-HDAC2 (lower panel) or loaded directly on the gel (lanes 4-6). Blots were stained with the 9E10 anti-myc tag antibody.

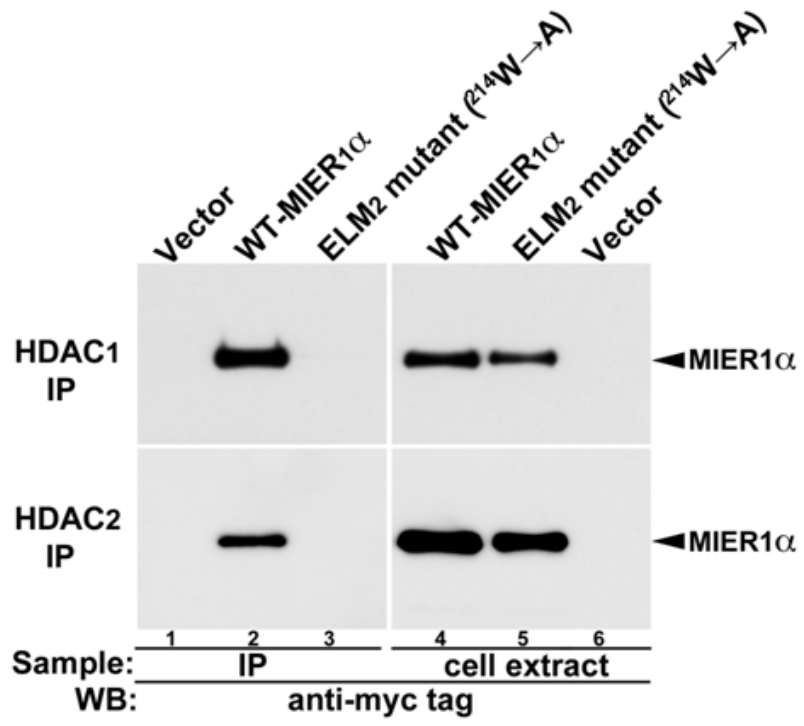


Figure 2.10 Interaction with HDAC1/2 is required for nuclear localization of MIER1 α

MCF7 cells were transfected with myc-tagged, full-length, wild-type MIER1 α (a-d) or a full-length, mutant MIER1 α (e-h) containing a single point mutation (²¹⁴W \rightarrow A) in the ELM2 domain (ELM2 mutant) known to abrogate its ability to interact with HDAC1/2. Localization was analyzed by confocal microscopy using DAPI, 9E10 anti-myc tag (AlexaFluor-488) and anti-HDAC1 (panel A) or anti-HDAC2 (panel B) (AlexaFluor-647). **(A-B)** Illustrative examples of cells showing HDAC and MIER1 α localization. Note that ELM2 mutant loses the exclusively nuclear staining seen with wild-type MIER1 α (arrowheads in c) and shows predominantly whole cell staining (arrows in g).

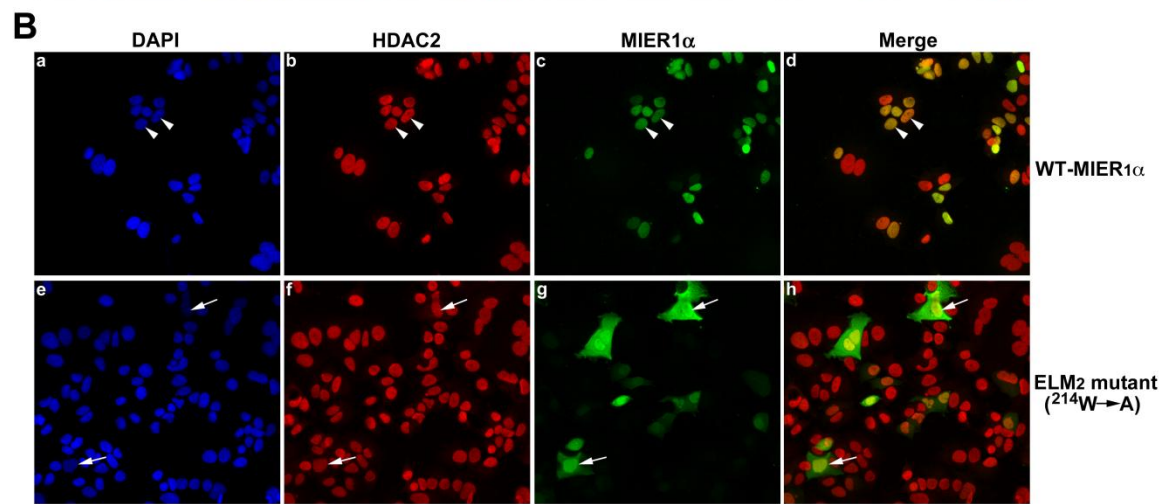
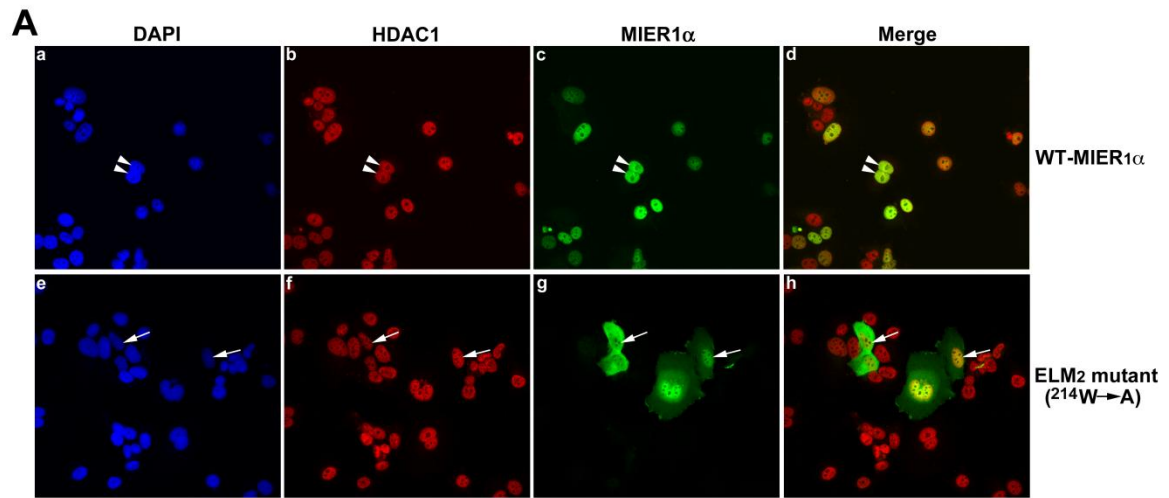
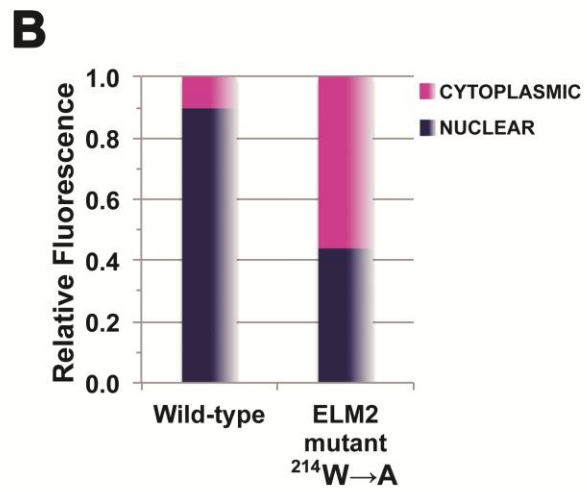
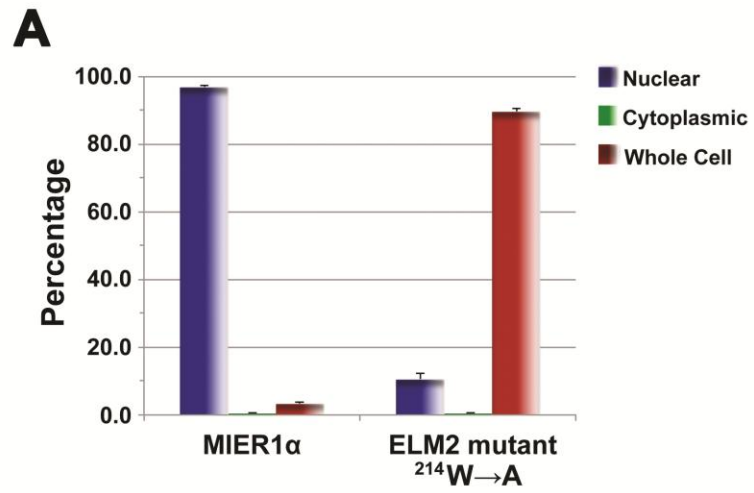


Figure 2.11 ²¹⁴W→A mutation reduces MIER1α nuclear localization

(A) Histogram showing the results of 3 independent experiments; random fields were selected and the staining pattern of each cell within the field was scored visually; >275 cells were scored for each construct. Plotted is the percentage of cells in each category ± S.D; the percent nuclear for the ELM2 mutant is significantly less than that of wild-type MIER1α ($p<0.05$). **(B)** Bar graph showing the intracellular distribution of MIER1α Pixel values for the nuclear and the cytoplasmic compartments were measured in confocal z-stacks using Image J v1.38; plotted in the proportion of the total signal in each compartment, using measurements from 30 cells for each construct. The proportion of the ELM2 mutant in the nucleus is significantly less than that of WT-MIER1α ($p<0.05$).



2.3.4 HDAC1 and 2 depletion causes MIER1 α nuclear loss

To confirm the role of HDAC1/2 in nuclear localization of MIER1 α , we investigated the effect of depleting HDAC1 and 2 using shRNA. MCF7 cells were co-transfected with a plasmid encoding a myc-tagged MIER1 α along with either a control shRNA, an HDAC1 shRNA, an HDAC2 shRNA or both HDAC1&2 shRNAs. Localization was determined by confocal microscopy and quantified by ImageJ analysis of confocal z-stacks (Fig. 2.12); HDAC1 and 2 knockdown was verified in parallel samples by Western Blot (Fig. 2.11). Individual knockdowns of HDAC1 and HDAC2 help confirm that each shRNAs used in this analysis is specific for its target and allow us to determine the requirement of each for nuclear localization of MIER1 α . HDAC1 shRNA was effective in knocking down endogenous HDAC1 to 27% of control while having little effect on HDAC2 expression (Fig. 2.11A, lanes 2 & 6; Fig. 2.12B). Likewise, HDAC2 shRNA reduced endogenous HDAC2 levels to 45% of control without affecting HDAC1 (Fig. 2.11A, lanes 7 & 3; Fig. 2.12B). In cells transfected with both shRNAs, HDAC1 and 2 were reduced to 26% and 44% respectively (Fig. 2.11A, lanes 4 & 8; Fig. 2.12B). These data confirm the specificity and effectiveness of the shRNAs used in this set of experiments.

Confocal analysis of cells depleted for HDAC1, HDAC2 or for both revealed a significant reduction in the percentage of cells with nuclear MIER1 α when compared to controls ($p < 0.05$; Fig. 2.12A & C). Exclusively nuclear MIER1 α was detected in 86% of control cells, but reduced to 58% of those depleted for HDAC1,

51% of those depleted for HDAC2 and 44% of those depleted for both (Fig. 2.12A). Quantitative analysis of confocal z-stack revealed a similar pattern: in the control, 88% of MIER1 α was in the nuclear compartment and this was reduced to 59%, 55% and 52% in HDAC1, HDAC2 and both HDAC1 and 2 depleted cells, respectively (Fig. 2.12B). These data confirm that depletion of HDAC1 or HDAC2 or both results in a significant reduction of MIER1 α in the nucleus ($p < 0.05$). Together, these results demonstrate that both HDAC1 and 2 are involved in targeting MIER1 α to the nucleus.

Figure 2.12 Individual and double knockdown of HDAC1 and 2 in MCF7 cells using shRNA

MCF7 cells were transfected with myc-tagged MIER1 α and either control shRNA or HDAC shRNA(s), then analyzed by immunoblotting. **(A)** Western blot analysis to confirm HDAC knockdown and specificity of each shRNA. Extracts from MCF7 cells were transfected with myc-tagged MIER1 α and either control scrambled shRNA (Con; lane 1, 5), HDAC1 shRNA (Hd1; lane 2, 6), HDAC2 shRNA (Hd2, lane 3, 7) or both HDAC1 and 2 shRNAs (Hd1+Hd2; lanes 4, 8). Duplicate samples were stained with anti-HDAC1 (lanes 1-4) or anti-HDAC2 (lanes 5-8). The blots were restained with anti- β -actin (lower panels) to verify equal loading. **(B)** The HDAC protein bands shown in (A) were quantified using ImageJ, normalized to β -actin and plotted as a proportion of the HDAC level in control cells. Note that each shRNA is specific for its target.

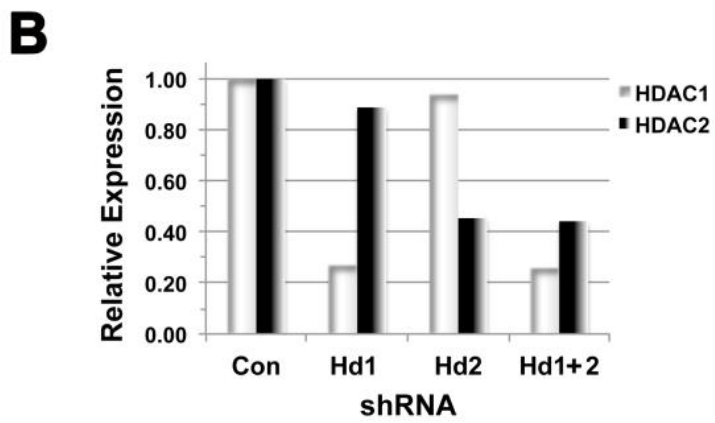
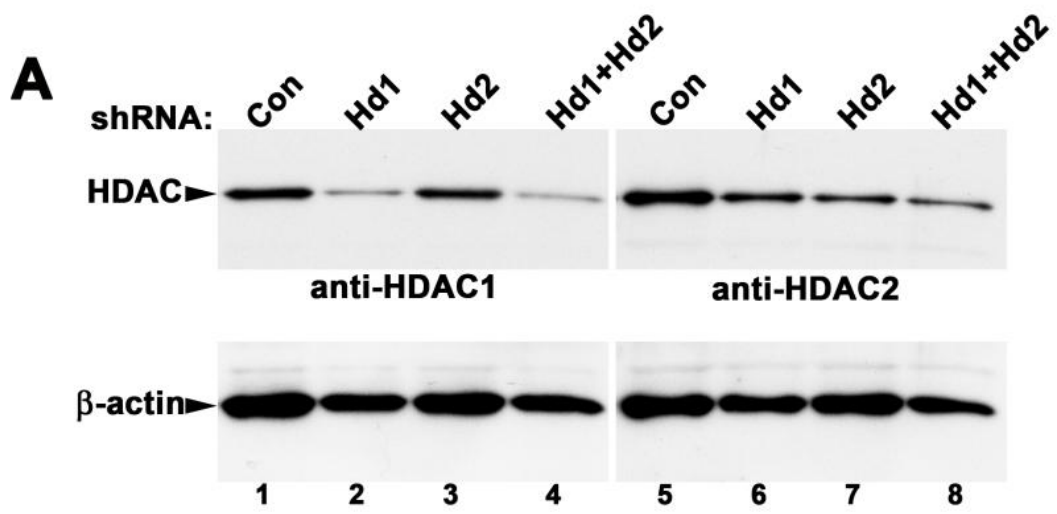
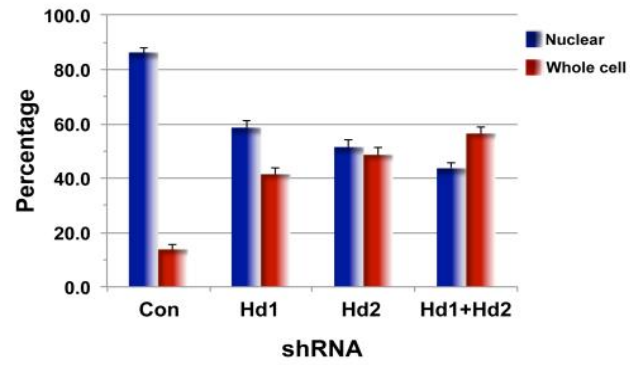
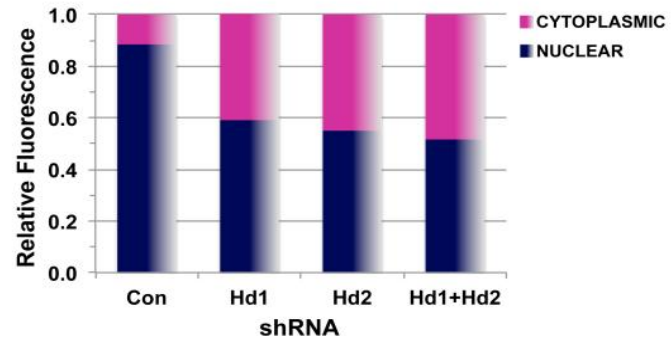
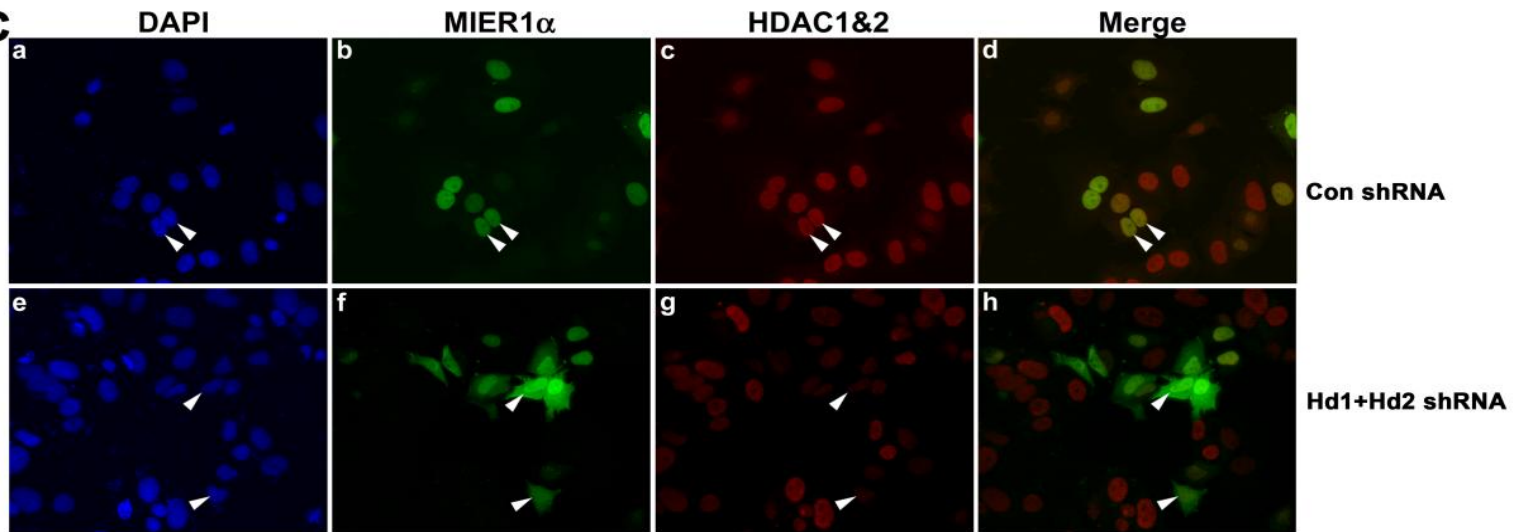


Figure 2.13 HDAC1 and 2 knockdown reduces nuclear localization of MIER1 α

(A) Localization was analyzed in parallel samples by confocal. Histogram showing the results of 2 independent experiments; random fields were selected and the staining pattern of each cell within the field was scored visually; 400-600 cells were scored for each shRNA. Plotted is the percentage of cells in each category \pm S.D; the percent nuclear of HDAC1, HDAC2 or HDAC1&2 depleted cells were significantly less than that of controls ($p < 0.05$). **(B)** Bar graph showing the intracellular distribution of MIER1 α . Pixel values for the nuclear and the cytoplasmic compartments were measured in confocal z-stacks using Image J v1.38; plotted is the proportion of the total signal in each compartment, using measurements from 20-25 cells for each shRNA. The proportion of MIER1 α in the nucleus is significantly less in depleted cells than in controls ($p < 0.05$ for each). **(C)** Illustrative examples of cells depleted for both HDAC1 and 2, stained as described in the legend to Fig. 2.11 for MIER1 α (panels b, f) and with combined anti-HDAC1 and 2 antibodies (panels c, g), using MCF7 cells co-transfected with myc-tagged MIER1 α and either control shRNA (panels a-d) or HDAC1+HDAC2 shRNAs (panels e-h). Note that MIER1 α staining is nuclear in control cells (arrowheads in a-d) but predominantly “whole cell” in cells with reduced HDAC1&2 staining (arrowheads in e-h).

A**B****C**

2.4 Discussion

Although small proteins can passively diffuse through the nuclear pore, the majority of proteins with nuclear functions undergo active transport into the nucleus (reviewed in (Wagstaff & Jans, 2009)). The most common transport mechanism involves recognition of a classic NLS within the cargo protein by the importins, which then mediate interaction with the NPC and translocation into the nucleus. However, other mechanisms have been described, including direct binding to nucleoporins in the NPC, e.g. β -catenin (Fagotto et al., 1998), piggybacks through the interaction with another nuclear protein, lymphocyte enhancer factor 1 (LEF-1) (Asally & Yoneda, 2005); breast cancer susceptibility gene 1 (BRCA1) can enter the nucleus piggybacked by BRCA1-associated RING domain protein 1 (BARD1) (reviewed in (Thompson, 2010)). Therefore, it is not surprising that MIER1 α can be localized in the nucleus even though it does not contain a recognizable, functional NLS. However, it was unexpected to discover that even though MIER1 α binds to ER α and inhibits its growth stimulating activity, this interaction is not involved in transporting MIER1 α to the nucleus. This leads us to conclude that MIER1 α only interacts with ER α once it is in the nucleus.

HDAC1 and 2 are widely expressed (Wen-ming, Yao, Sun, Davie, & Seto, 1997; de Ruijter, van Gennip, Caron, Kemp, & van Kuilenburg, 2003) and frequently located together in three major multi-protein corepressor complexes: Sin3, NuRD, and CoREST (Haberland, Montgomery, & Olson, 2009; Joshi et al., 2013; Yang & Seto, 2003). Interestingly, MIER1 is not contained in any of these complexes, but rather

forms part of a unique corepressor complex with HDAC 1&2, CDYL and G9a (Bantscheff et al., 2011; Joshi et al., 2013). HDAC1 and HDAC2 are nearly identical (Gregorette, Lee, & Goodson, 2004; Haberland et al., 2009), with an overall sequence identity of 82% and both belong to the class I HDACs along with HDAC3 and 8 (reviewed in de Ruijter et al., 2003). They contain a C-terminal NLS and, unlike other classes, members of this class are found almost exclusively in the nucleus. HDAC1 can associate with itself as well as heterodimerize with HDAC2 and this interaction is mediated through an N-terminal region that includes part of the conserved HDAC domains (Ruijter et al., 2003). While HDAC's primary role is in chromatin remodeling, HDAC2 has been shown to interact with the endosomal protein APPL1 (adaptor protein containing PH (pleckstrin homology) domain, PTB (phosphotyrosine binding) domain and leucine zipper motif) and carry it to the nucleus, enabling APPL1 to associate with the active NuRD complex (Banach-Orlowska, Pilecka, Torun, Pyrzynska, & Miaczynska, 2009). Our results provide additional evidence that HDACs can play a role in nuclear localization.

Our results provide additional evidence that HDACs can play a role in the nuclear localization of proteins. Depletion of either HDAC1 or HDAC2 reduces nuclear localization of MIER1 α , demonstrating that both are involved in this process. It was interesting to note that the reduction in nuclear localization was similar whether HDAC1 or 2 or both were knocked down. This finding, combined with the fact that 80-90% of HDAC1 and 2 exist as heterodimers in MCF7 cells (Mains, Sulston, & Wood, 1990), suggest that it is the heterodimer that is required for targeting MIER1 α to the nucleus.

In a recent report, we showed that alternative splicing of MIER1 α to include an additional exon encoding a functional NES resulted in shuttling of this α isoform to the cytoplasm (Clements et al., 2012). Thus RNA splicing may represent a primary mechanism for regulating the nucleo-cytoplasmic distribution of the α isoform. However, we cannot rule out the possibility that the MIER1 α isoform is also shuttled out of the nucleus through interaction with a NES-containing protein. MIER1 α has been shown to interact with several molecules in addition to ER α (McCarthy et al., 2008) and HDAC1/2 (Ding et al., 2003); these include the histone methyltransferase G9a (Wang, Charroux, Kerridge, & Tsai, 2008), the chromodomain-containing protein CDYL (Mulligan et al., 2008) and the histone acetyltransferase CBP (Blackmore et al., 2008). However, none of these has been reported to contain a NES.

Current evidence suggests that MIER1 α functions as a tumour suppressor (McCarthy et al., 2008), possibly through its interaction with ER α . Our previous analysis of the normal breast tissue and breast cancer tumours using an antibody that specifically recognizes the α C-terminus, showed that the α isoform(s) is localized in the nucleus in normal tissue and in hyperplasia; however, the percentage of cells with nuclear staining decreased to 51% in DCIS and to 4% in IDC (McCarthy et al., 2008). This suggests that loss of nuclear MIER1 α might represent a critical event in breast cancer progression since shuttling to the cytoplasm would interfere with its nuclear function as a transcriptional repressor. It is also possible that MIER1 α has additional, as yet undescribed, activity in the cytoplasm. Several instances of dual roles have been reported for other transcriptional regulators (reviewed in (Boonyaratanakornkit & Edwards, 2007; Ordóñez-Morán & Muñoz,

2009)). For example, ER α functions in the nucleus to regulate transcription of target genes but also has non-genomic functions (reviewed in (Moriarty, Kim, & Bender, 2006)). Most of these involve activation of various signalling cascades in a tissue-specific manner, including activation of ERK, PI3'K and Akt pathways as well as signalling through GPCR and growth factor receptors. Whether or not MIER1 α also has non-genomic functions awaits further investigation.

**Chapter 3 Peptide growth factors and insulin, but not 17 β -estradiol,
alter the subcellular localization of MIER1 α in MCF7 breast
carcinoma cells**

This chapter is a version of the paper: Li S, Paterno GD, Gillespie LL (2015) Insulin and IGF-1, but not 17 β -estradiol, alter the subcellular localization of MIER1 α in MCF7 breast carcinoma cells. BMC Research Notes 8: 356.
<https://doi.org/10.1186/s13104-015-1336-0>.

Author contributions to the published manuscript: SL performed the experiments. LLG analysed the data, prepared the Figures and wrote the manuscript. LLG and GDP participated in the design of the experiments and interpretation of the data. All authors were involved in the revisions. All authors read and approved the final manuscript.

Candidate contributions to Chapter 3: Elaboration on the introductory material, expanded description of the published paper by SL. New experimental sections incorporated to this chapter were designed, performed, analyzed and written by SL with the supervision of LLG.

3.1 Introduction

MIER1 α was originally reported to be localized in the cytoplasm in NIH 3T3 cells (Paterno et al., 2002); however, it is exclusively in the nucleus of the MCF7 human breast carcinoma cell line. Analysis of patient breast biopsies revealed a dramatic reduction in nuclear MIER1 α during breast cancer progression, from 75% nuclear MIER1 α in normal samples to 51% nuclear in ductal carcinoma in situ (DCIS) to 4% nuclear in invasive ductal carcinoma (IDC) (McCarthy et al., 2008). We noticed that inclusion of 10 μ g/ml insulin in the MCF7 growth medium, as is routine when culturing MCF7 cells by the American Tissue Culture Collection (ATCC) protocol (ATCC, n.d.), resulted in a significant loss of nuclear MIER1 α .

MIER1 represses transcription through several distinct mechanisms (Blackmore et al., 2008; Ding et al., 2004, 2003) and all of these functions are dependent on the localization of MIER1 α in the nucleus, yet it does not contain a functional NLS (Post et al., 2001). Therefore, nuclear loss of MIER1 α induced by insulin addition to the growth medium suggests that insulin could attenuate MIER1 α 's transcriptional repressor/chromatin modifying functions in MCF7 cells. Insulin is a peptide hormone; under general culture conditions, hormones and growth factors are more rapidly depleted than other media components (Goustin, Leof, Shipley, & Moses, 1986). Insulin-like growth factor-1 (IGF-1) is very closely related to insulin; IGF-1 can bind to insulin receptor, also vice versa for insulin. EGFR is expressed in MCF7 cells; also, MIER1 was originally discovered in response to fibroblast growth factor (FGF) stimulation (Xing, Hung, Bonfiglio, Hicks, & Tang, 2010; Paterno et al., 1997). Therefore, to further investigate the effect of growth

factors on MIER1 α subcellular distribution, we included another three growth factors: IGF-1, epidermal growth factor (EGF) & FGF, together with insulin to study the MIER1 α subcellular pattern with growth factors stimulation.

3.2 Methods and Materials

3.2.1 Plasmid

Human *mier1* gene structure, the sequence of its transcripts and the myc-tag vector, pCS3+MT, (a kind gift of Dr. David Turner, University of Michigan; http://sitemaker.umich.edu/dlturner.vectors/cs2_polylinker_descriptions) containing full-length MIER1 α have been described in (Paterno et al., 2002). Full-length human MIER1 α (GenBank: AY124188) was amplified by specific primers incorporating 5' and 3' BamHI sites and inserted into the BglII site of the CS3+MT plasmid (Paterno et al., 2002).

3.2.2 Cell line and culture condition

MCF7 human breast adenocarcinoma cell line was obtained from the ATCC and cultured in DMEM (GIBCO, REF 11965-092) containing 10% serum (7.5% calf serum (CS) (GIBCO, Cat. No. 16010-159) plus 2.5% fetal bovine serum (FBS) (GIBCO, REF 1884253)) and 1 mM sodium pyruvate (GIBCO, REF 11360-070). Charcoal-dextran treated FBS (Hyclone, Cat. No SH30068.03) contains reduced levels of many hormones and growth factors. Before electroporation transfection was performed, the cell growth medium was changed to DMEM (GIBCO) supplemented with 10% charcoal-dextran treated FBS plus 1 mM sodium pyruvate to remove the effect generated by growth factors contained in the serum; the transfected cells were

cultured in this medium until cell collection. In the experiments using 17 β -estradiol (E2), cells were cultured in phenol red-free DMEM (GIBCO, REF 31053-028) supplemented with 10% charcoal-dextran treated FBS.

3.2.3 Transient transfection

Neon[®] transient transfection was performed with the following settings: 1000 V, 30 ms, 2 pulses for MCF7 cells. 3x10⁵ MCF7 cells were mixed with 0.5 μ g myc-tagged plasmid and loaded into a 10 μ l tip for electroporation. Transfected cells were plated at a density of 4x10⁴/well in Falcon 8-well culture slides (BD BioSciences, Cat. No. 0877426) for confocal analysis and 3x10⁵/well in 6-well dish for western blot analysis.

3.2.4 Growth factors

Human recombinant insulin (REF 12585-014) was purchased from GIBCO[®] and used at a concentration of 10 μ g/ml. Recombinant human IGF-1 (Cat. No. 100-11), recombinant human EGF (Cat. No. AF-100-15) and recombinant human FGF acidic (Cat. No. 100-17A) were purchased from PEPROTECH and used at a concentration of 10 ng/ml. E2 (Cat. No. E125) was purchased from Sigma-Aldrich and used at a concentration of 10nM. At 24 h after transfection, cells were incubated with insulin, IGF-1, EGF, FGF or E2 for another 4 h prior to fixation.

3.2.5 Antibodies

The 9E10 anti-myc tag mouse monoclonal antibody was prepared as described in Blackmore *et al.* (Blackmore et al., 2008) and used at a dilution of 1:200 for immunofluorescence. Anti-HDAC1 H-51 (Cat. No. SC-81598) and anti-HDAC2 H-

54 (Cat. No. SC-7899) obtained from Santa Cruz Biotechnology Inc. were used at the dilution 1:200 in immunofluorescence. Alexa Fluor-488 labeled donkey anti- mouse (Cat. No. 715-606-150) and Alexa Fluor-647 (Cat. No. 715-606-150) labeled donkey anti-rabbit were purchased from Jackson ImmunoResearch Laboratories Inc. and used at the dilution 1:200 in immunofluorescence.

3.2.6 Leptomycin B treatment

Leptomycin B (LMB, Cat. No. 431050) purchased from Sigma Aldrich was added to MCF7 cells at the final concentration of 5 ng/ml in the medium at 23 h after *MIER1 α* transfection to inhibit nuclear export caused by growth factors. The LMB vehicle, 0.1% ethanol, was added in equal volume in transfected MCF7 cells as a negative control.

3.2.7 Immunofluorescence, confocal microscopy and statistical analysis

3.2.7.1 Immunofluorescence

Immunofluorescence was performed as listed in Appendix 2.

3.2.7.2 Confocal microscopy

Cells were examined under an Olympus FluoView FV1000 confocal microscope. Fluorescence images were obtained by sequential z-stage scanning in two or three channels (DAPI, Alexa Fluor-488 and/or Alexa Fluor-647); z-stacks were compiled into individual images.

The cells were classified into three categories according to the *MIER1 α* distribution. Subcellular localization was scored as “nuclear” if the nucleus was

intensely stained, with little or no cytoplasmic staining; “cytoplasmic” if staining was primarily in the cytoplasm, with little or no staining in the nucleus; and “whole cell” if both the nucleus and cytoplasm were stained.

3.2.7.3 Statistical analysis

Each experiment was repeated at least three times if not specified, and the results are expressed as means \pm standard deviations ($M \pm SD$). All the graphs and statistical analysis were performed using GraphPad Prism 7.0 for Windows (GraphPad Software, San Diego, California, USA); $p < 0.05$ was considered to indicate a statistically significant result. One-way ANOVA (analysis of variance) was used for the comparison of quantitative data between different groups when only nuclear localization percentage was shown in the graph. Two-way ANOVA was utilized to evaluate the data when more than one factor has to be assessed in one group.

3.3 Results

3.3.1 Insulin and peptide growth factors cause nucleocytoplasmic shuttling of MIER1 α

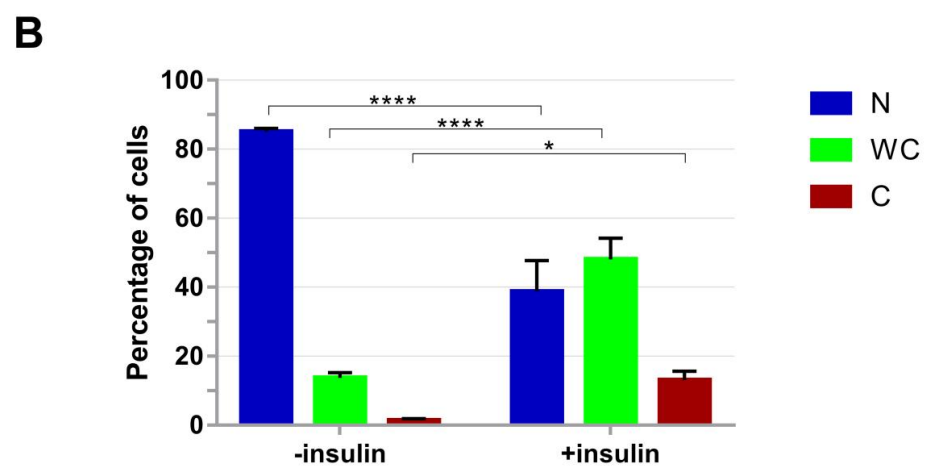
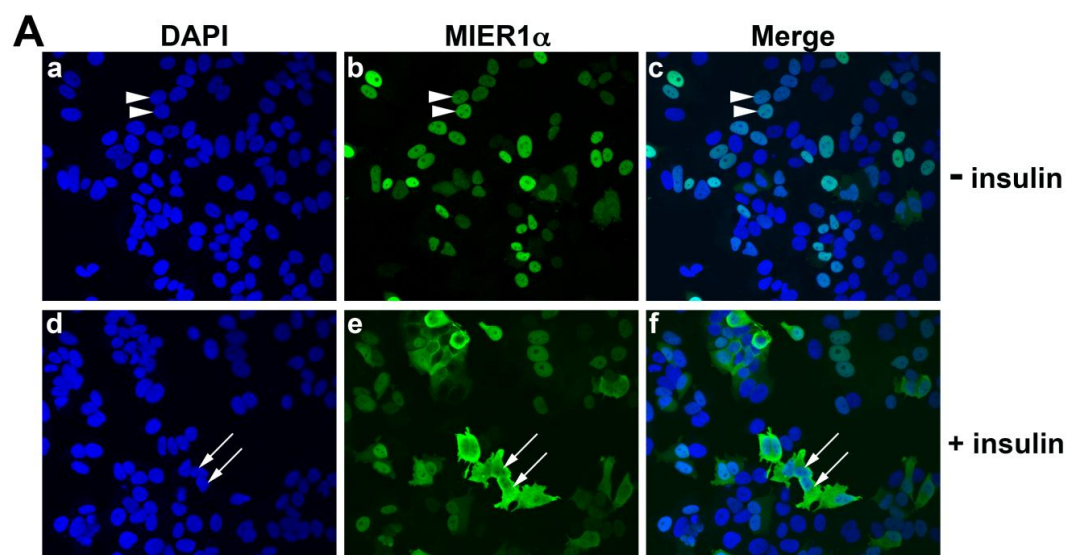
3.3.1.1 Insulin alters nuclear localization of MIER1 α in MCF7 cells

It was previously shown that MIER1 α is targeted to the nucleus in MCF7 cells despite the lack of an intrinsic NLS (Li et al., 2013; Clements et al., 2012). In those studies, cells were cultured in DMEM containing 10% CS/FBS. ATCC suggests adding 10 μ g/ml insulin to the MCF7 culture media; however, when we added insulin, we noticed a change in the subcellular localization pattern of MIER1 α . To investigate this effect more thoroughly, we analyzed *MIER1 α* -transfected MCF7 cells by confocal

microscopy. In the presence of insulin, only 41% of cells had exclusively nuclear MIER1 α (Fig. 3.1Ad-f, B), compared to 81% of cells in the absence of insulin (Fig. 3.1Aa-c, B). The percentage of cells with MIER1 α in both the nucleus and cytoplasm (whole cell staining) increased in the presence of insulin, from 18 to 42% (Fig. 3.1B). Likewise, the proportion of cells with exclusively cytoplasmic MIER1 α increased over tenfold, from 1 to 17% (Fig. 3.1B). These results demonstrate that in the presence of insulin, the localization of MIER1 α in MCF7 cells is shifted from the nucleus to the cytoplasm.

Figure 3.1 Insulin treatment reduces nuclear localization of MIER1 α

MCF7 cells were transfected with myc-tagged *MIER1 α* and treated 24 h later with either vehicle (*panels a-c*) or 10 μ g/ml insulin (*panel d-f*). Cells were fixed 4 h after the addition of insulin and localization was analyzed by confocal microscopy. Random fields were selected and the staining pattern of each cell within the field was scored as 'nuclear,' 'whole cell' or 'cytoplasmic' using sequential z-stage scanning. **(A)** Shown are z-stacks compiled into individual images, illustrating stained nuclei (DAPI; *panels a, d*), MIER1 α localization (9E10 anti-myc tag antibody and an AlexaFluor-488 secondary antibody; *panels b, e*) and merged channels (*panels c, f*); arrowheads show examples of nuclear staining and arrows show whole cell staining. **(B)** Histogram showing the results of 3 independent experiments; the MIER1 α localization pattern of >1000 cells was scored. Two-way analysis of variance (ANOVA) was utilized for statistical analysis. Plotted is the percentage of cells in each category \pm SD; an asterisk indicates the difference was statistically significant, * p <0.05, **** p <0.0001 (Sidak's multiple comparisons test).

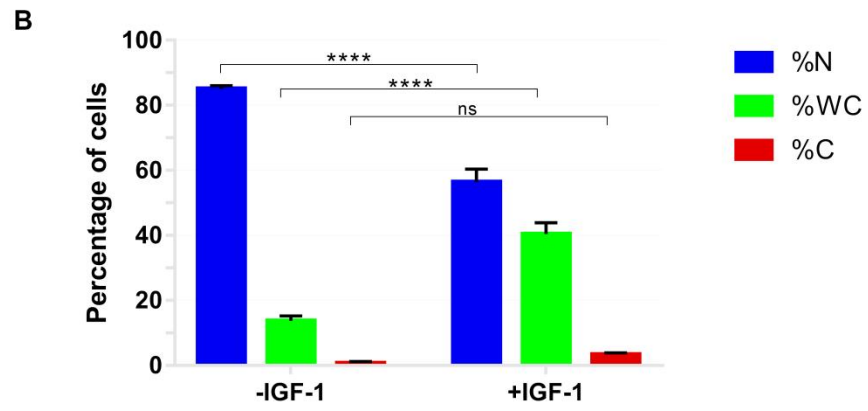
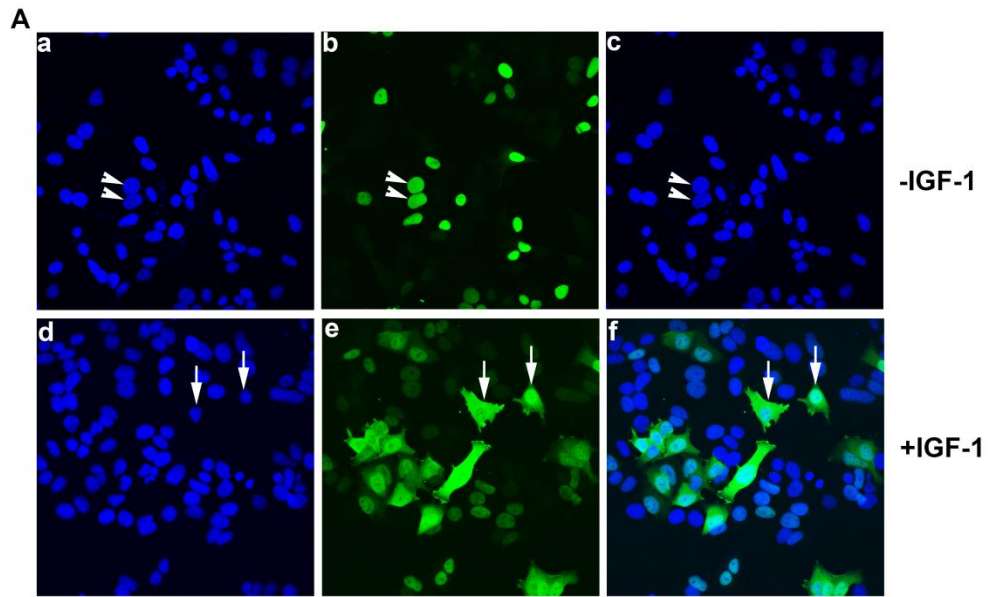


3.3.1.2 IGF-1 alters nuclear localization of MIER1 α in MCF7 cells

IGF-1 is closely related to insulin and both can interact with insulin and IGF receptors, albeit with differing affinities (Werner, Weinstein, & Bentov, 2008). Also, there is a wealth of evidence implicating IGF-1 in breast cancer development and progression (reviewed in (Christopoulos et al., 2015)) and it has been shown to increase the invasiveness of MCF7 cells (Walsh & Damjanovski, 2011). Since MCF7 cells express receptors for both insulin and IGFs (Mukohara et al., 2009), we explored the possibility that IGF-1 also affects the localization of MIER1 α . As expected, confocal analysis demonstrated that IGF-1 had a similar effect on the nuclear accumulation of MIER1 α (Fig. 3.2Ad-f, B). IGF-1 reduced the percentage of cells with nuclear MIER1 α from 89 to 56% and increased the percentage with “whole cell” staining from 10 to 40%. The percent with “cytoplasmic” MIER1 α was also increased from 0.3 to 4%. Thus, both insulin and IGF-1 have similar effects on the subcellular localization of MIER1 α in MCF7.

Figure 3.2 IGF-1 treatment reduces nuclear localization of MIER1 α

MCF7 cells were transfected with myc-tagged *MIER1 α* and treated 24 h later with either vehicle (*panels a-c*) or 10 ng/ml IGF-1 (*panel d-f*). Cells were fixed 4h after the addition of IGF-1 and localization was analyzed by confocal microscopy. Random fields were selected and the staining pattern of each cell within the field was scored as 'nuclear,' 'whole cell' or 'cytoplasmic,' using sequential z-stage scanning. **(A)** Shown are z-stacks compiled into individual images, illustrating stained nuclei (DAPI; *panels a, d*), MIER1 α localization (9E10 anti-myc tag antibody and an AlexaFluor-488 secondary antibody; *panels b, e*) and merged channels (*panels c, f*); arrowheads show examples of nuclear staining and arrows show whole cell staining. **(B)** Histogram showing the results of 3 independent experiments; the MIER1 α localization pattern of >1000 cells was scored. Plotted is the percentage of cells in each category \pm SD; an asterisk indicates the difference was statistically significant, ns: not significant, **** $p < 0.0001$ (Sidak's multiple comparisons test).



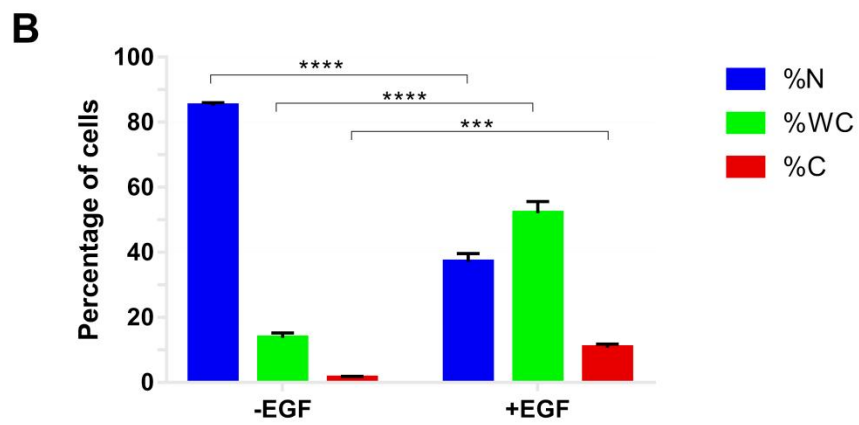
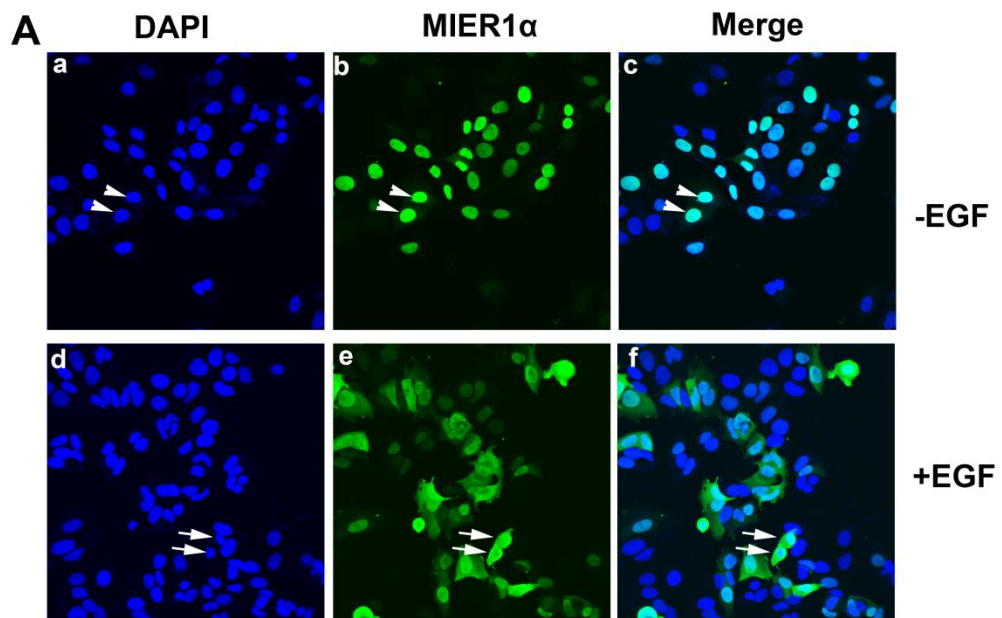
3.3.1.3 EGF alters nuclear localization of MIER1 α in MCF7 cells

EGF is another growth factor that regulates cell growth, proliferation and differentiation through binding to its receptor EGFR on the cell surface. The EGF receptor family are frequently expressed at high levels in human carcinomas and over-expressed EGFR is associated with more aggressive clinical behaviour (Mendelsohn, Mendelsohn, Baselga, & Baselga, 2000). EGF and EGFR were found to contribute to the unregulated proliferation of cancer cells through an autocrine growth-promoting mechanism (Nahta, Hortobagyi, & Esteva, 2003).

MCF7 cells not only express receptors for insulin and IGF-1, but they also express the EGF receptor (Xing et al., 2010); hence, we investigated the effect of EGF on MIER1 α nuclear localization. MCF7 cells were transfected with *MIER1 α* and 24 h post-transfection, cells were treated with 10ng/ml EGF for 4h before fixation. Statistical analysis demonstrated that EGF had a significant effect on MIER1 α subcellular distribution (Fig 3.3 Ad-f, B). In the EGF-treated group, the percentage of cells with nuclear MIER1 α drops from 89 to 37% and “whole cell” staining increased to 52%, compared with 14% in the control group. Also, “cytoplasmic” MIER1 α increased from 1.3 to 11%. These data demonstrate that EGF also regulates MIER1 α nuclear accumulation, similar to what we observed with insulin and IGF-1.

Figure 3.3 EGF treatment reduces nuclear localization of MIER1 α

MCF7 cells were transfected with myc-tagged *MIER1 α* and treated 24 h later with either vehicle (*panels a-c*) or 10 ng/ml EGF (*panel d-f*). Cells were fixed 4h after the addition of EGF and localization was analyzed by confocal microscopy. Random fields were selected and the staining pattern of each cell within the field was scored as 'nuclear,' 'whole cell' or 'cytoplasmic,' using sequential z-stage scanning. **(A)** Shown are z-stacks compiled into individual images, illustrating stained nuclei (DAPI; *panels a, d*), MIER1 α localization (9E10 anti-myc tag antibody and an AlexaFluor-488 secondary antibody; *panels b, e*) and merged channels (*panels c, f*); arrowheads show examples of nuclear staining and arrows show whole cell staining. **(B)** Histogram showing the results of 3 independent experiments; the MIER1 α localization pattern of >1000 cells was scored. Plotted is the percentage of cells in each category \pm SD; an asterisk indicates that the difference was statistically significant, *** $p < 0.001$, **** $p < 0.0001$ (Sidak's multiple comparisons test).



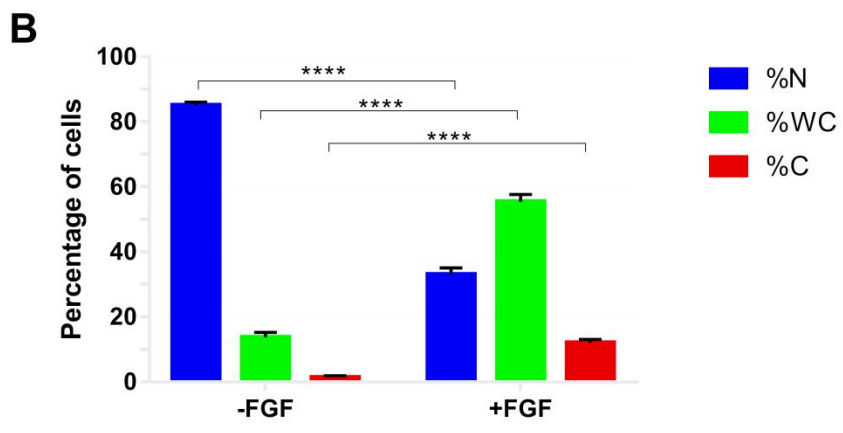
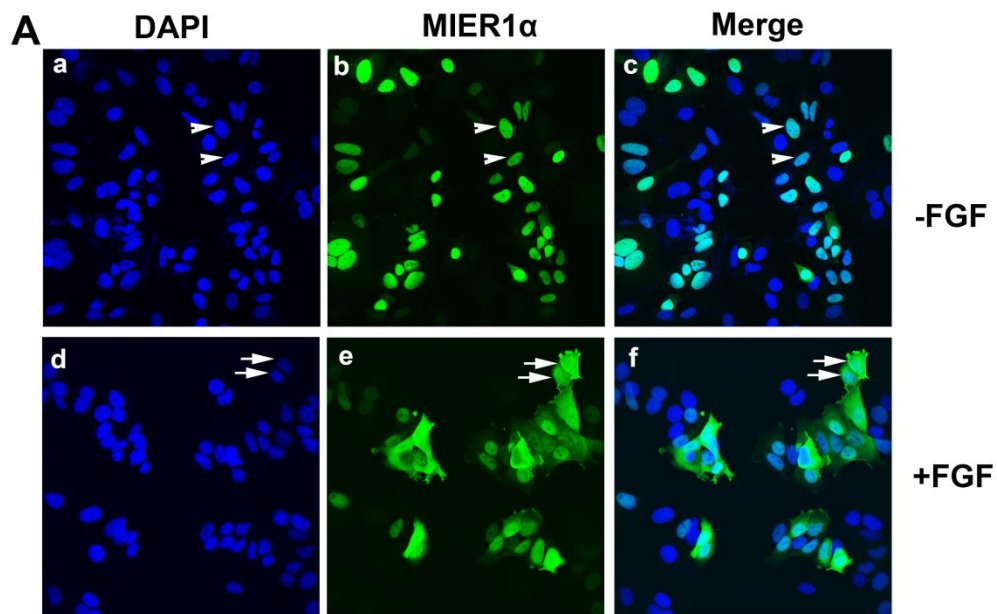
3.3.1.4 FGF alters nuclear localization of MIER1 α in MCF7 cells

The FGFs family regulates a plethora of developmental processes (Beenken & Mohammadi, 2009). The *mier1* gene was originally isolated as a novel FGF-regulated immediate-early gene from *Xenopus* embryonic cells induced to differentiate into the mesoderm (Paterno et al., 1997). FGF imposes its effect by mediating FGF receptor dimerization and this dimerization can activate FGFR (Mukohara et al., 2009). FGFR signalling is a vital component not only in embryonic development but also in postnatal mammary gland development. Furthermore, deregulated FGFR signalling occurs in breast cancer (Brady, Chuntova, Bade, & Schwertfeger, 2013).

Both FGFR1 and 2 are expressed in MCF7 cells (Luqmani, Graham, & Coombes, 1992); therefore, we investigated whether MIER1 α subcellular localization in MCF7 cells would also be affected by FGF. As expected, FGF also had a dramatic effect on MIER1 α subcellular distribution. The percentage of cells with nuclear MIER1 α drops from 86% in the control group to 33% in the FGF-treated group (Fig. 3.4 Ad-f, B), which means MIER1 α whole cell and cytoplasmic staining increases up to 67% compared with 14% in the control group.

Figure 3.4 FGF treatment reduces nuclear localization of MIER1 α

MCF7 cells were transfected with myc-tagged *MIER1 α* and treated 24 h later with either vehicle (*panels a-c*) or 10 ng/ml FGF (*panels d-f*). Cells were fixed 4h after the addition of FGF and localization was analyzed by confocal microscopy. Random fields were selected and the staining pattern of each cell within the field was scored as 'nuclear,' 'whole cell' or 'cytoplasmic,' using sequential z-stage scanning. **(A)** Shown are z-stacks compiled into individual images, illustrating stained nuclei (DAPI; *panels a, d*), MIER1 α localization (9E10 anti-myc tag antibody and an AlexaFluor-488 secondary antibody; *panels b, e*) and merged channels (*panels c, f*); arrowheads show examples of nuclear staining and arrows show whole cell staining. **(B)** Histogram showing the results of 3 independent experiments; the MIER1 α localization pattern of >1000 cells was scored. Plotted is the percentage of cells in each category \pm SD; an asterisk indicates that the difference was statistically significant, **** $p < 0.0001$ (Sidak's multiple comparisons test).



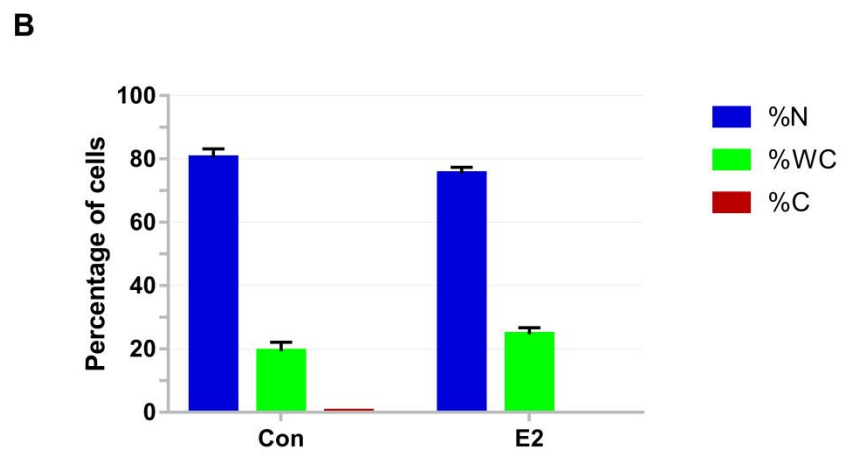
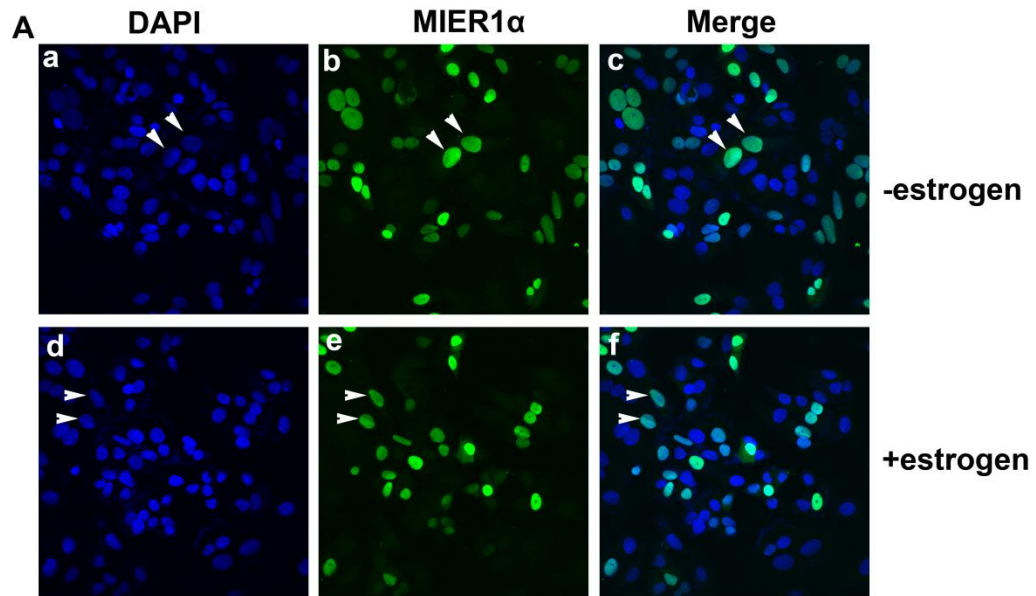
3.3.1.5 17- β -estradiol does not affect MIER1 α subcellular localization

Insulin, IGF-1, EGF and FGF are all potent mitogens for MCF7 cells (Bentel et al., 1995), leading to the question of whether changes in the nuclear localization of MIER1 α are related to the fact that the cells are proliferating. We therefore examined MIER1 α localization in cells treated with 10 nM E2, a classic mitogen for ER+ breast carcinoma cells. Unlike insulin and the growth factors IGF-1, EGF and FGF, E2 had no significant effect on the subcellular distribution of MIER1 α (Fig. 3.5Ad-f, B). In the presence of 10 nM E2, 77% of cells displayed nuclear MIER1 α (Fig. 3.5Af B) compared to 80% of untreated cells (Fig. 3.5Ab, B). Likewise, there was no significant difference ($p>0.05$) in the percentage of cells with “whole cell” or “cytoplasmic” staining (Fig. 3.5B).

Our data indicates insulin and the peptide growth factors, IGF-1, EGF and FGF can each cause nuclear loss of MIER1 α when MCF7 cells are incubated in their presence (Figs 3.1-3.4). Even though the percentage of nuclear loss varies slightly, the trend caused by these 4 molecules is the same, suggesting that the molecular mechanism that causes MIER1 α nuclear loss is shared by these factors, but not by E2.

Figure 3.5 E2 has no effect on subcellular localization of MIER1 α

MCF7 cells were transfected with myc-tagged *MIER1 α* and 24 h later, either vehicle (*panels a-c*) or 10 nM E2 (*panels d-f*) was added. Cells were fixed 4h later and localization was analyzed by confocal microscopy. **(A)** Compiled z-stacks showing nuclei (DAPI; *panels a, d*), MIER1 α (AlexaFluor-488, *panels b, e*), merged DAPI and 488 channels (*panels c, f*). **(B)** Histogram showing the results of two independent experiments; the MIER1 α localization pattern of >500 cells was scored. Plotted is the percentage of cells in each category \pm S.D; there was no statistically significant difference between the percentage of control and E2 treated cells in each of the three categories, $p>0.05$ (Sidak's multiple comparisons test).



3.3.2 HDAC1/2 nuclear localization does not change during incubation with insulin, peptide growth factors or E2

Our previous research outlined in Chapter 2 demonstrated that MIER1 α localizes to the nucleus through interaction and co-transport with HDAC1/2. Therefore, we investigated whether insulin would also affect the localization of HDAC1/2. Confocal analysis demonstrated that while insulin reduces the nuclear accumulation of MIER1 α (Fig. 3.6Ab, f, j), it does not affect the localization of HDAC1 or 2 (Fig. 3.6A, c, g, k) and both were 100% nuclear (Fig. 3.6B). The same was observed with IGF-1, EGF & FGF; they do not have an effect on HDAC1 or 2 nuclear localization (Figs. 3.7, 3.8 and 3.9).

The addition of E2 has no statistical effect on MIER1 α subcellular distribution as depicted above (Fig 3.5). Also, confocal microscopy analysis demonstrates that HDAC1/2 nuclear localization is not affected either, the same as observed above (Fig 3.10).

Figure 3.6 HDAC1 and 2 localization are not affected by insulin

Cells were transfected, treated with insulin and prepared for confocal microscopy as described in Chapter 1, section 2.2.7. **(A)** Compiled z-stacks showing nuclei (DAPI; *panels a, e, i*), MIER1 α (AlexaFluor-488, *panels b, f, j*), HDAC1 (AlexaFluor-647, *panels c, g*), HDAC2 (AlexaFluor-647, *panel k*) and merged 488 and 647 channels (*panels d, h l*); arrowheads show examples of nuclei and arrows show whole cell staining. **(B)** Histogram showing the localization of HDAC1 and HDAC2 in untreated (Con) and in insulin-treated MCF7 cells; plotted is the percentage of cells in each category \pm SD from three independent experiments. $p > 0.05$ (Sidak's multiple comparisons test).

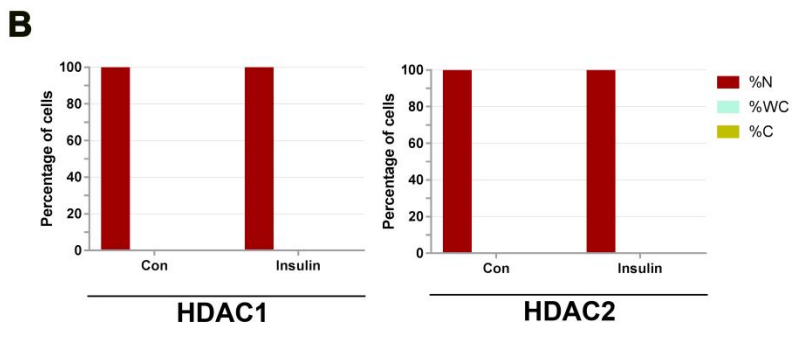
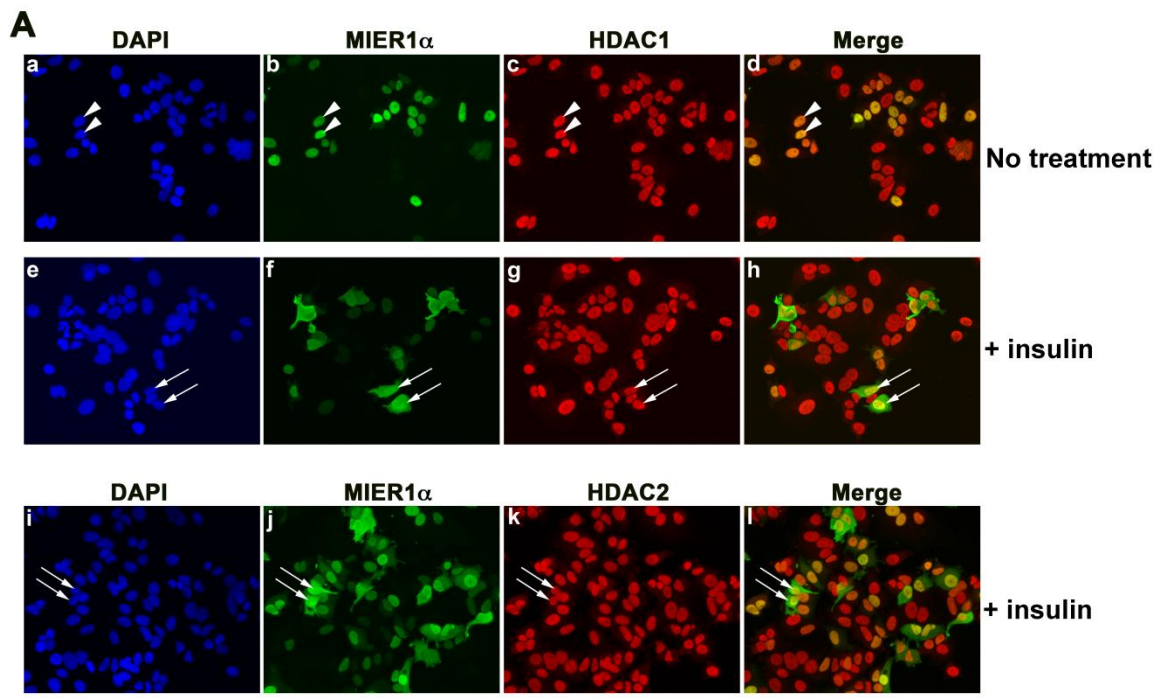
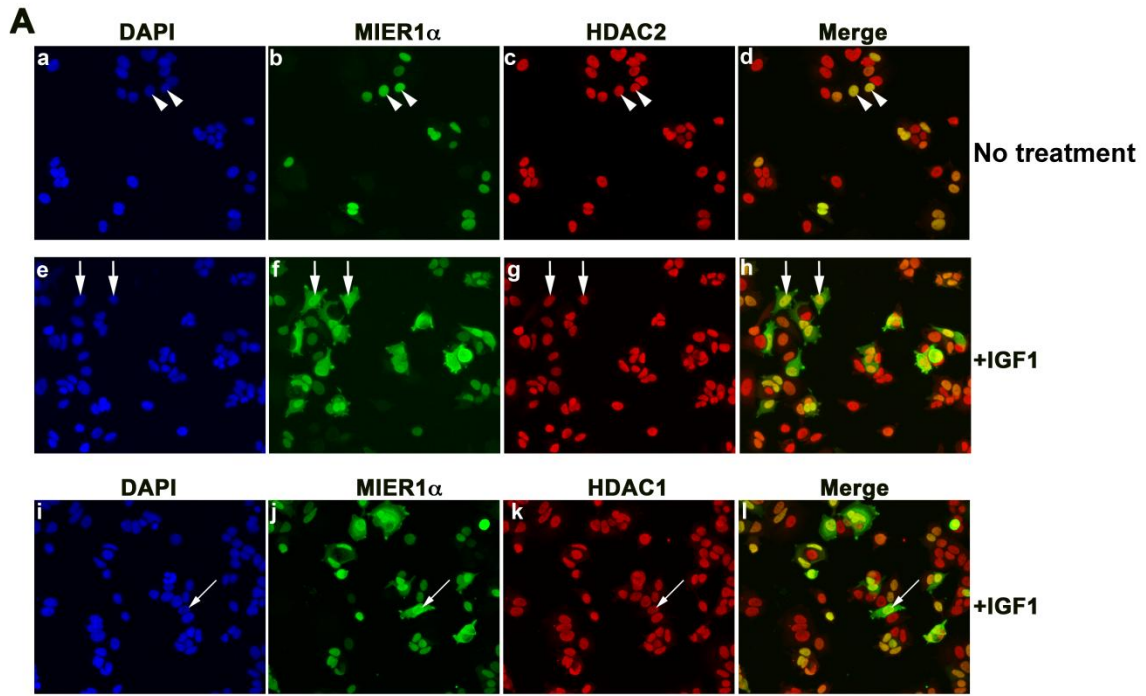


Figure 3.7 HDAC1 and 2 localization are not affected by IGF-1

Cells were transfected, treated with IGF-1 and prepared for confocal microscopy as described in Chapter 1, section 2.2.7. **(A)** Compiled z-stacks showing nuclei (DAPI; *panels a, e, i*), MIER1 α (AlexaFluor-488, *panels b, f, j*), HDAC1 (AlexaFluor-647, *panels c, g*), HDAC2 (AlexaFluor-647, *panel k*) and merged 488 and 647 channels (*panels d, h l*); arrowheads show examples of nuclei and arrows show whole cell staining. **(B)** Histogram showing the localization of HDAC1 and HDAC2 in untreated (Con) and in IGF-1-treated MCF7 cells; plotted is the percentage of cells in each category \pm SD from three independent experiments. $p > 0.05$ (Sidak's multiple comparisons test).



B

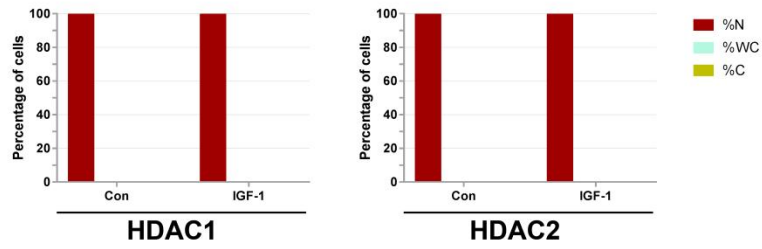


Figure 3.8 HDAC1 and 2 localization are not affected by EGF

Cells were transfected, treated with EGF and prepared for confocal microscopy as described in Chapter 1, section 2.2.7. **(A)** Compiled z-stacks showing nuclei (DAPI; *panels a, e, i*), MIER1 α (AlexaFluor-488, *panels b, f, j*), HDAC1 (AlexaFluor-647, *panels c, g*), HDAC2 (AlexaFluor-647, *panel k*) and merged 488 and 647 channels (*panels d, h l*); arrowheads show examples of nuclei and arrows show whole cell staining. **(B)** Histogram showing the localization of HDAC1 and HDAC2 in untreated (Con) and in EGF treated MCF7 cells; plotted is the percentage of cells in each category \pm SD from three independent experiments. $p > 0.05$ (Sidak's multiple comparisons test).

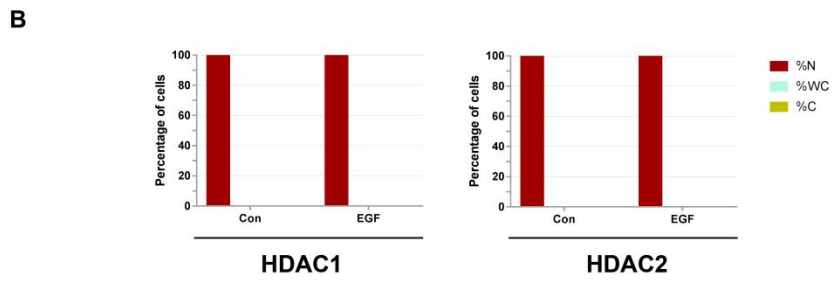
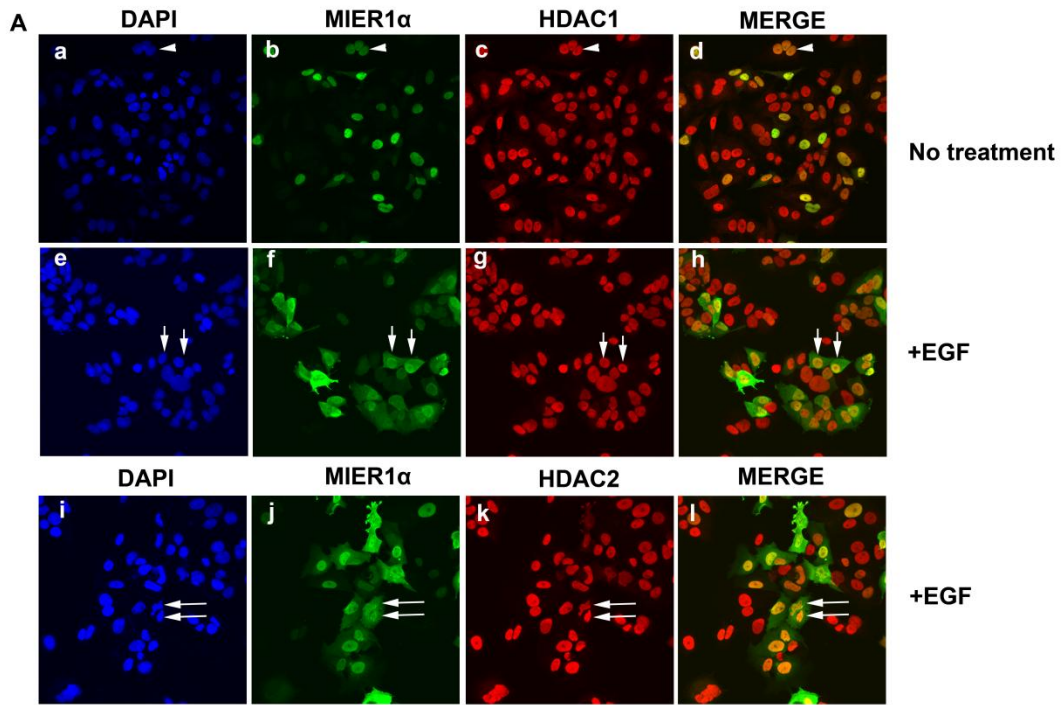


Figure 3.9 HDAC1 and 2 localization are not affected by FGF

Cells were transfected, treated with FGF and prepared for confocal microscopy as described in Chapter 1, section 2.2.7. **(A)** Compiled z-stacks showing nuclei (DAPI; *panels a, e, i*), MIER1 α (AlexaFluor-488, *panels b, f, j*), HDAC1 (AlexaFluor-647, *panels c, g*), HDAC2 (AlexaFluor-647, *panel k*) and merged 488 and 647 channels (*panels d, h l*); arrowheads show examples of nuclei and arrows show whole cell staining. **(B)** Histogram showing the localization of HDAC1 and HDAC2 in untreated (Con) and in FGF treated MCF7 cells; plotted is the percentage of cells in each category \pm SD from three independent experiments. $p > 0.05$ (Sidak's multiple comparisons test).

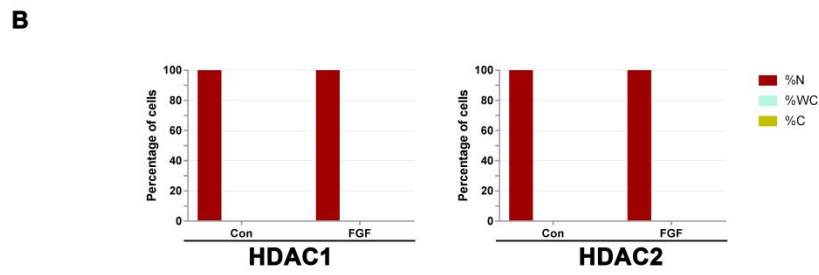
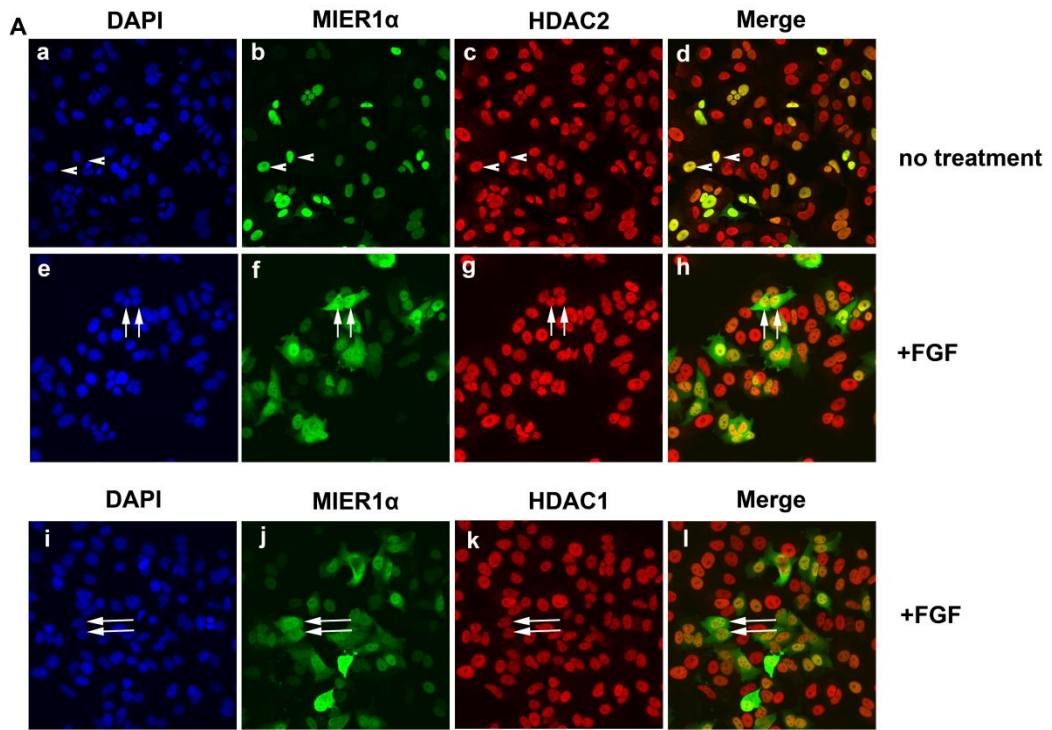
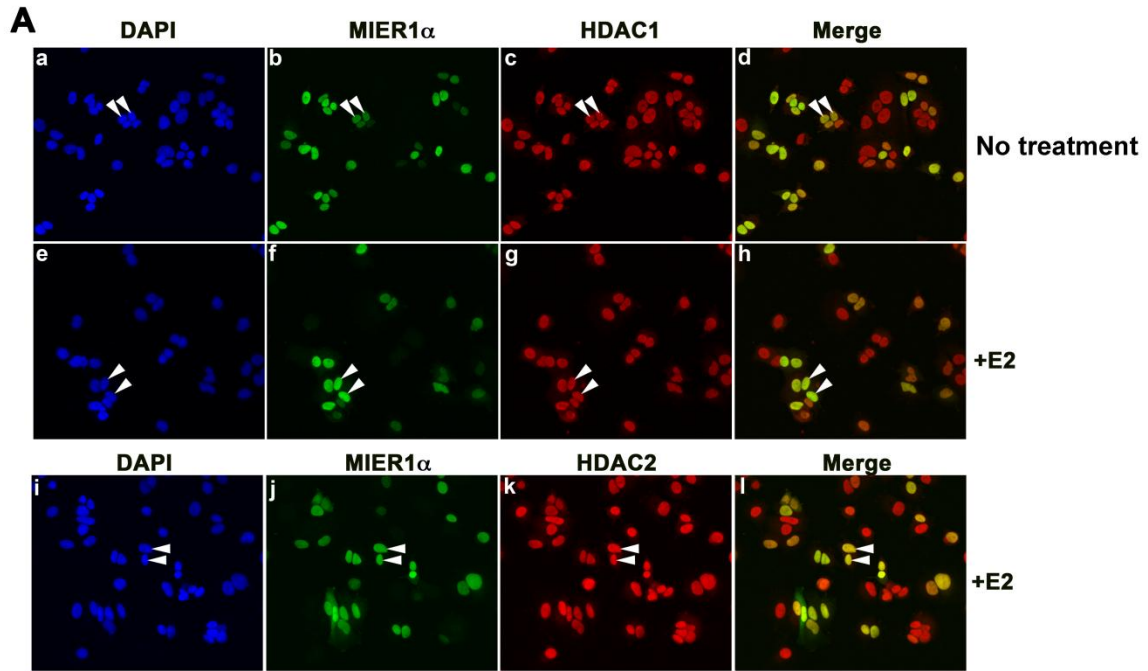
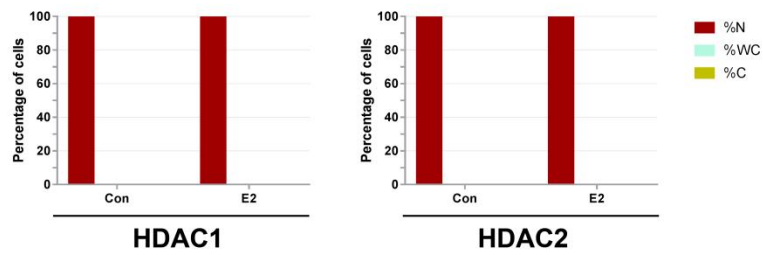


Figure 3.10 HDAC1 and 2 localization are not affected by E2

MCF7 cells were transfected with myc-tagged *MIER1 α* and 24 h later, either vehicle (panels a-d) or 10 nM E2 (panels e-l) was added. Cells were fixed 4 h later and localization was analyzed by confocal microscopy, as described in Chapter 1, section 2.2.7. **(A)** Compiled z-stacks showing nuclei (DAPI; *panels a, e, i*), *MIER1 α* (AlexaFluor-488, *panels b, f, j*), HDAC1 (AlexaFluor-647, *panels c, g*) HDAC2 (AlexaFluor-647, *panel k*) and merged 488 and 647 channels (*panels d, h, l*). **(B)** Histogram showing the results of two independent experiments; the *MIER1 α* localization pattern of >500 cells was scored. Plotted is the percentage of cells in each category \pm SD; there was no statistical difference between the percentage of control and E2-treated cells in each of the three categories, $p > 0.05$ (Sidak's multiple comparisons test).



B



3.3.3 MIER1 α nucleocytoplasmic translocation is CRM1-dependent

Although HDAC1 and 2 transport MIER1 α into the nucleus (Chapter 1), they are not involved in nuclear loss of MIER1 α as they still localize in the nucleus in the presence of these 4 molecules- insulin, IGF-1, EGF and FGF. Cytoplasmic localization can be caused either by nuclear export or cytoplasmic retention. CRM1 is the major karyopherin protein and LMB is its inhibitor (Sun et al., 2013). Hence, if MIER1 α is exported out of the nucleus by CRM1, one would expect to see the accumulation of MIER1 α in the nucleus in LMB-treated cells. However, if MIER1 α nuclear loss is caused by cytoplasmic retention, LMB would not have any effect on MIER1 α subcellular distribution. Therefore, to distinguish what determines MIER1 α nuclear loss, we examined the effect of LMB on the localization pattern of MIER1 α in the presence of insulin or the other three growth factors.

As a control, I first determined if LMB has any effect on MIER1 α in the absence of hormone or growth factor. When MCF7 cells were fixed at 24h post-transfection, approximately 15-20% of cells still display whole cell staining for MIER1 α (Fig. 3.11 A (MIER1 α group)). This 15-20% might represent proteins in the cytosol that have been: 1) just *de novo* synthesized and are waiting to be imported into the nucleus, 2) retained in the cytoplasm through binding to a cytoplasmic protein, or 3) exported out of the nucleus. To investigate these possibilities, we treated MCF7 cells only with LMB for 5 h before collection, staining and imaging. Compared with the control, MIER1 α subcellular localization demonstrates a similar pattern in the LMB-treated group, and nuclear localization percentage is ~85%,

which is not a statistically significantly different compared with the non-treated MIER1 α group ($P>0.05$) (Fig 3.11 A). The result of this control experiment excludes the possibility that LMB has an effect on cytoplasmic MIER1 α localization in the absence of growth factors. Therefore, I proceeded with the experiment to determine MIER1 α subcellular distribution pattern with LMB+growth factor combinations compared with the pattern in the presence of growth factor alone, to determine whether MIER1 α nuclear loss is mediated through CRM1. If MIER1 α localization is not affected by the combined treatment of “LMB+growth factor,” that would imply MIER1 α cytoplasmic localization occurs by a growth factor-mediated cytoplasmic retention mechanism. Conversely, if the anticipated increase in cytoplasmic localization of MIER1 α is not observed under the conditions of “LMB+growth factor” treatment, we would conclude CRM1 is involved to actively export MIER1 α out of the nucleus in the presence of growth factors.

MCF7 cells were transfected with *MIER1 α* and pre-treated with LMB 1h before adding insulin or vehicle. In the experimental group “+LMB + insulin,” MIER1 α nuclear localization is 82%. The nuclear percentage is 40% in “+insulin” group and 85% in non-treated control group, which implies LMB reversed MIER1 α nuclear loss caused by insulin (Fig. 3.11 Bg-i). The same trend occurred with IGF-1, EGF and FGF treatment groups (Fig 3.12 A-D). LMB can bind directly to CRM1 and abolish CRM-dependent nuclear export. Our results indicate that MIER1 α nuclear localization is restored when MCF7 cells are pre-treated with LMB, to demonstrate that MIER1 α growth factor induced nuclear loss is CRM1-dependent, indicating the

overall influence of growth factors involves nuclear export rather than cytoplasmic retention.

Figure 3.11 LMB abolishes MIER1 α nuclear export caused by insulin

(A) The effect of LMB on MIER1 α localization. Cells were transfected with myc-tagged *MIER1 α* and 23 h later, cells were treated with either vehicle or 5 ng/ml LMB for 5 h and analyzed by confocal microscopy. Random fields were selected and the staining pattern of each cell within the field was scored as 'nuclear,' 'whole cell' or 'cytoplasmic,' using sequential z-stage scanning. Histogram showing the results of 2 independent experiments; plotted is the percentage of cells in each category \pm S.D. Two-way analysis of variance (ANOVA) was utilized for statistical analysis. The asterisk indicates that the difference was not statistically significant, $P > 0.05$ (Sidak's multiple comparisons test). **(B)** Illustrative examples of cells when expressing MIER1 α and treated with insulin or + LMB + insulin. Z-stage scanning was utilized. Note that the nuclear accumulation of MIER1 α in the group "+ LMB + insulin."

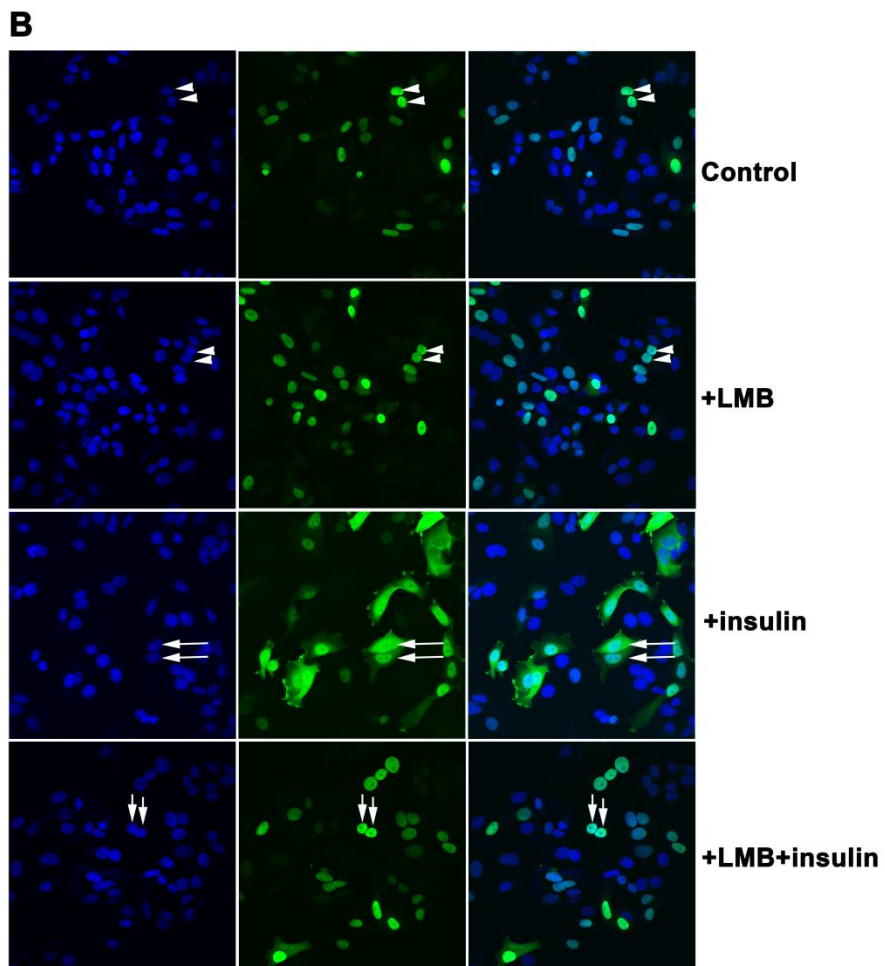
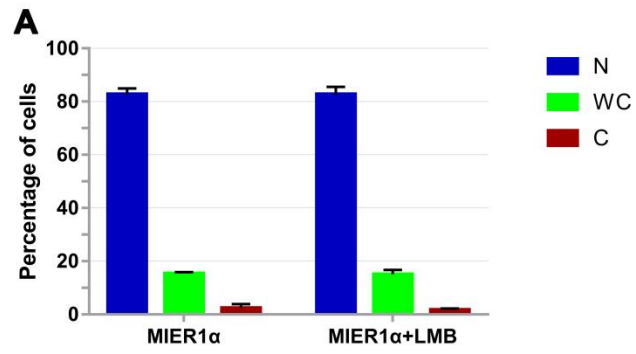
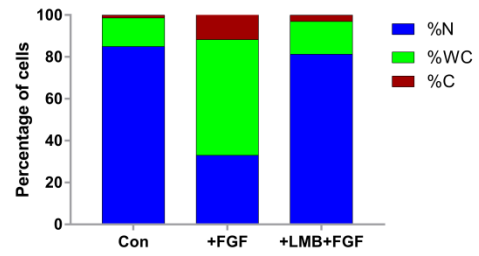
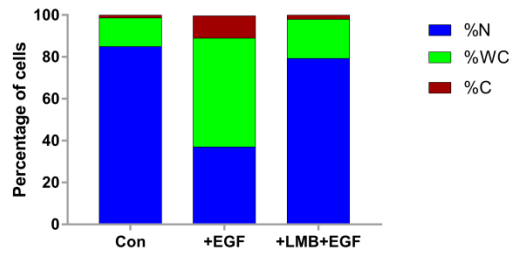
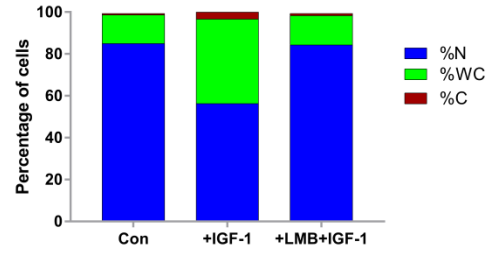
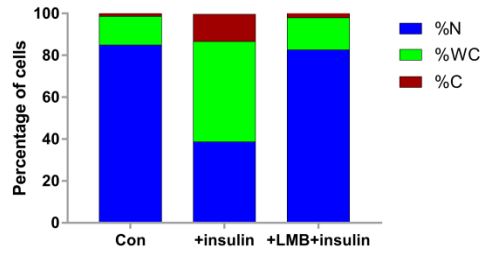


Figure 3.12 LMB rescues MIER1 α nuclear loss caused by insulin and growth factors

MCF7 cells were transfected with myc-tagged *MIER1 α* and 23 h later pre-treated with either vehicle or 5 ng/ml LMB for 1 h. Cells were then treated with either vehicle or growth factors again. Cells were fixed 4 h after the addition of growth factors and localization was analyzed by confocal microscopy. Random fields were selected and the staining pattern of each cell within the field was scored as 'nuclear,' 'whole cell' or 'cytoplasmic,' using sequential z-stage scanning. Bar graphs **(A-D)** are the results of 3 independent experiments and show the intracellular distribution of MIER1 α . More than 151 cells were counted for each group.



3.4 Discussion

My investigation showed that HDAC1/2 localization is 100% nuclear during MIER1 α nuclear export triggered by growth factors, implying that the cytoplasmic MIER1 α is physically dissociated from HDAC1/2. Therefore, MIER1 α loses its interaction with HDAC1/2 during the event of being exported when cells are stimulated by growth factors. This leads us to conclude that the presence of any of these 4 molecules might cause MIER1 α to lose its transcriptional repression function by losing its interaction with HDAC1/2.

It was also demonstrated that all 4 growth factors -insulin, IGF-1, EGF and FGF- caused MIER1 α nuclear export is through CRM1. However, *in silico* analysis of the MIER1 α sequence shows that it does not contain any NES (see Appendix 3) (T. la Cour et al., 2003). Since CRM1 has to bind to the NES on its cargo in order to transport the cargo molecule out of the nucleus, the evidence suggests that there could be an NES-containing bridging molecule connecting MIER1 α and CRM1. Once dissociated from HDAC1/2, I hypothesize MIER1 α associates with an NES-containing adaptor molecule to be exported, but this theory remains to be tested. At present, the triggers for MIER1 α disassociation with HDAC1/2 and association with CRM1 are not clear.

Proteins that are exported by CRM1 in cancer cells are often tumour suppressor and oncoproteins, such as p53, BRCA1, NPM and APC (Hill, Cautain, de Pedro, & Link, 2014). An imbalance in the cytosolic level of these proteins can result in either inactivation (tumour suppressor) or anti-apoptotic over-activity

(oncoprotein). As a tumour suppressor, MIER1 α nuclear export caused by insulin or peptide growth factors leads to its cytoplasmic localization instead of nuclear accumulation. This shuttling out of the nucleus would result in loss of nuclear activity and possibly a gain of function in the cytosol.

MIER1 α is a transcriptional repressor when localized in the nucleus, therefore, compartmentalization is a mechanism that can regulate its function. The change of MIER1 α subcellular localization caused by insulin or peptide growth factors has also been observed for other molecules. For example, FOXO is relocalized from the nucleus to the cytoplasm in the presence of insulin as well as other growth factors (Greer & Brunet, 2005) and by Src signalling (Bülow, Bülow, Hoch, Pankratz, & Jünger, 2014). In *C. elegans*, the activation of DAF-2, the nematode ortholog of the IGF-1 receptor, prevents nuclear accumulation of the DAF-16 (FOXO) transcription factor (Lin, Hsin, Libina, & Kenyon, 2001). FOXO factors are associated with a variety of biological processes, including cell cycle, cell death and DNA repair; its shuttling mechanism contributes to the understanding of the FOXO function in terms of signalling and gene regulation (Van Der Heide, Hoekman, & Smidt, 2004). Therefore, elucidation of MIER1 α nucleocytoplasmic shuttling mechanism will shed light on its biological function in breast cancer progression as well.

Most of the transcription factors and tumour suppressor proteins require nuclear retention to induce transcriptional regulation of targeted genes. Nuclear export is a critical aspect in the view of biology because mislocalization of any protein causes functional inactivation. Ample evidence shows that cancer cells

harbor an unusually higher expression of CRM1, which makes it an attractive therapeutic target to restore the proper localization of tumour suppressor proteins. Maintaining tumour suppressors in the nucleus is becoming a strategy to treat patients. Our data suggest that breast cancer progression is coupled with MIER1 α nuclear loss and therefore, MIER1 α is a putative target for breast cancer treatment.

**Chapter 4 The growth factor-dependent MAPK pathway regulates
MIER1 α nucleocytoplasmic shuttling**

Candidate contributions to Chapter 4: the research in this chapter was designed, performed, analyzed and written by SL with the supervision of LLG.

A version of this chapter is currently being prepared as a manuscript.

4.1 Introduction

Signalling pathways in mammalian cells consist of a series of biochemical events that are precisely controlled. The initial extracellular signals are sensed at the cell surface by a receptor, which then transduces the signal into the cytosol of the cell (Cyert, 2001). The transduced signal can cause pleiotropic effects, including modification of transcriptional regulators and alteration of gene expression, eventually leading to specific cellular responses (Witsch, Sela, & Yarden, 2011).

In response to peptide growth factor binding to its membrane receptor, two main pathways are activated: mitogen-activated protein kinase (MAPK) and phosphoinositide 3-kinase B/Akt (PI3'K/AKT) pathways. There are four major mammalian MAPKKK-MAPKK-MAPK protein kinase cascades (Fig. 4.1) and the MAPK pathway can be activated by many stimuli, such as growth factors, UltraViolet (UV) and stress. At least three MAPK families have been characterized: extracellular signal-regulated kinase (ERK), Jun kinase (JNK/SAPK) and p38 MAPK, while growth factors mainly activate ERK1/2 (as shown in Fig. 4.1) and are of particular relevance to cancer (Dhillon, Hagan, Rath, & Kolch, 2007).

ERK signalling is associated with cell proliferation in development and it is now clear that the tumour phenotype is linked with deregulation of this pathway (Dhillon et al., 2007). In the MAPK cascade, MEK activation depends on phosphorylation by Raf (Raf-1, B-Raf and A-Raf) and ERK is activated upon phosphorylation by MEK. Phosphorylated ERK1/2 will then translocate into the nucleus within minutes, where pERK1/2 can then phosphorylate hundreds of

substrates including regulatory molecules and transcription factors (Fowler, Sen, & Roy, 2011; Roskoski, 2012) on “P-X-S/T-P” or “S/T-P” motifs, leading to functional or localization changes, which further regulate gene expression.

The activation of a cell surface receptor initiated by growth factors can also cause phosphorylation of PI3’K (Fig. 4.2). Activated PI3’K then phosphorylates lipids which form the second messenger phosphatidylinositol (3,4,5)-trisphosphate (PIP₃). PIP₃ serves as a plasma membrane docking site for proteins that harbor pleckstrin-homology (PH) domains, including AKT and its upstream activator phosphoinositide-dependent kinase 1 (PDK1). Upon recruitment to the cell membrane, AKT is phosphorylated by PDK1, a reaction triggered by PIP₃ binding to the PH domains of both molecules. Activated AKT regulates diverse cellular processes, including cell survival (anti-apoptotic), proliferation, cell migration and angiogenesis, all by phosphorylating a range of intracellular proteins (Crowell, Steele, & Fay, 2007). For example, activated AKT can phosphorylate and inactivate the proapoptotic factors BAD and procaspase-9. FOXO can also be phosphorylated and inactivated by AKT, which leads to the expression of genes critical for apoptosis (Altomare & Testa, 2005).

In Chapter 3, I demonstrated that insulin and peptide growth factors (IGF-1, EGF and FGF) can cause changes in the subcellular distribution of MIER1 α in MCF7 cells. However, the mechanism that leads to the change is unknown. I propose that the activation of a signalling pathway common to these four molecules: insulin, IGF-1, EGF and FGF is most likely responsible for the altered MIER1 α distribution in

MCF7. In this chapter, I show that growth factor-dependent activation of MAPK causes MIER1 α nuclear export, while activation of PI3K/AKT pathway has no effect. Mutation of 2 activated ERK1/2 consensus phosphorylation motifs within the MIER1 α protein sequence had no effect on MIER1 α subcellular distribution, indicating that the mechanism responsible for MIER1 α nuclear export either does not involve direct phosphorylation by pERK1/2 or involves phosphorylation on sites other than ERK1/2 consensus phosphorylation motifs. Further investigation with deletion constructs revealed the N-terminal region containing acidic stretches is required for MIER1 α nuclear export by the MAPK pathway. In addition, MIER1 α nuclear loss caused by growth factors is transient and reversible; when the effect of growth factors on the activation of MAPK diminishes, MIER1 α returns to the nucleus.

Figure 4.1 The mammalian MAPK cascade

(Modified from “MAPK-pathway-mammalian, Wikimedia commons” with permission) There are four major mammalian MAPKKK-MAPKK-MAPK protein kinase cascades. Whereas the ERK pathway is commonly activated by growth factors, the JNK, p38 and ERK5 pathways are activated by environmental stress, including osmotic shock, and ionizing radiation. Many of the substrates for MAPKs are nuclear transcription factors. Interactions and substrates were compiled from information from STKE (<http://stke.sciencemag.org/index.dtl>).

Simplified overview of mammalian MAPK cascades

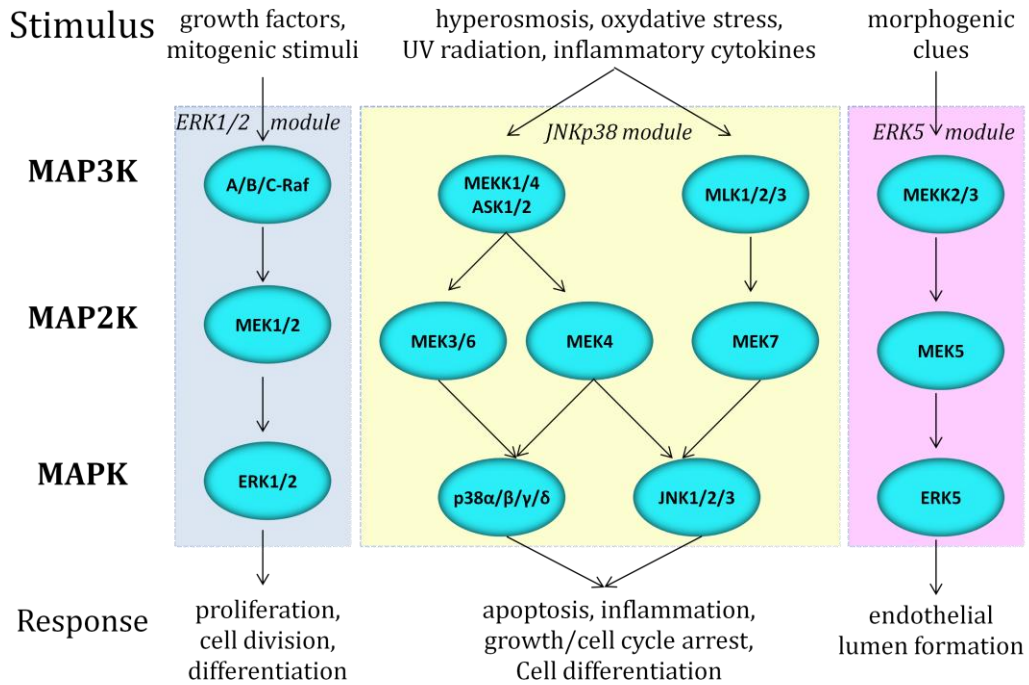
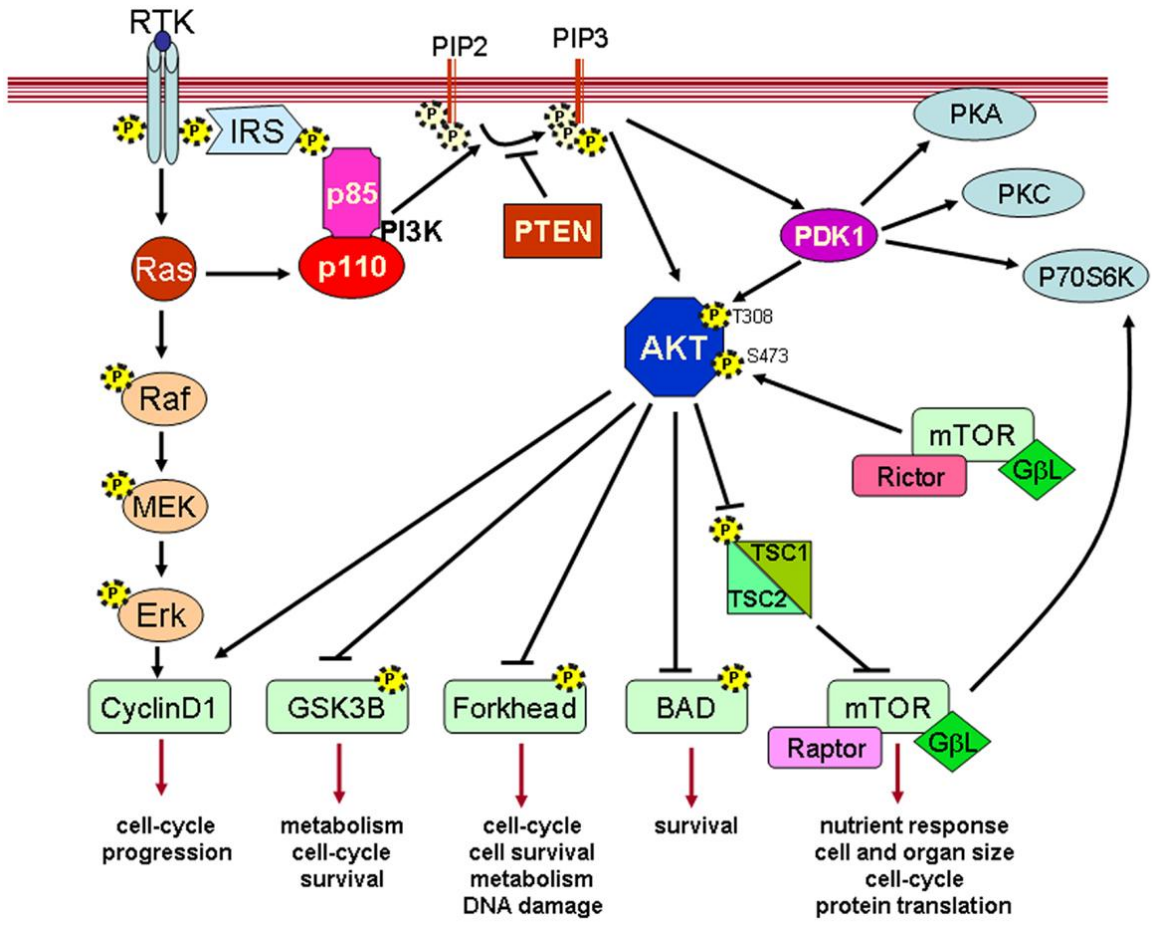


Figure 4.2 Schematic diagram depicting the most representative signaling of the PI3K/AKT pathway

(Modified from (Carnero & Paramio, 2014)) PI3'K is activated by receptor tyrosine kinases and RAS and, in turn, activates downstream effectors by generating PIP₃ at the membrane. PIP₃ binds to the pleckstrin homology domain of AKT, localizing it to the membrane. AKT is then phosphorylated on T³⁰⁸ and S⁴⁷³. AKT regulates metabolism cell-cycle survival, cell survival, proliferation and intermediary metabolism by phosphorylating an array of substrates. The tumour suppressor PTEN is a negative regulator of AKT. PTEN catalyzes dephosphorylation of PIP₃; this prevents recruitment of AKT to the plasma membrane and inhibits activation.



4.2 Methods and Materials

4.2.1 Plasmids

Human *MIER1* gene structure, the sequence of its transcripts and the myc-tag vector, pCS3+MT, (a kind gift of Dr. David Turner, University of Michigan; http://sitemaker.umich.edu/dlturner.vectors/cs2_polylinker_descriptions) containing full-length *MIER1* α have been described in (Paterno et al., 2002). Full-length human *MIER1* α (GenBank: AY124188) was amplified by specific primers incorporating 5' and 3' BamHI sites and inserted into the BglII site of the CS3+MT plasmid (Paterno et al., 2002). For the *MIER1* α deletion constructs, previously described constructs containing amino acids (aa)1-283, aa164-433, or aa164-283 of *MIER1* α in the Clontech pM vector (Ding et al., 2003) were digested with EcoRI and inserted into the EcoRI site of a pCS3+MT vector that had been modified to maintain the *MIER1* sequence in-frame with the myc-tag. This modified pCS3+MT, renamed pCS4+MT, contains a thymidine (T) inserted upstream of the EcoRI site.

Figure 4.3 MIER1 α amino acid sequence and plasmids used in the study

(A) MIER1 α amino acid sequence; (B) The diagram illustrates the deletion domains of MIER1 α fused to myc-tag in CS3+MT vector. The individual domains are identified in the legend below the diagram, and MIER1 α amino acid residues encoded by each construct are listed on the left.

A:

10	20	30	40	50
MAEPSVSSSS	PGGSATSDDH	EFDPSADMLV	HDFDDERTLE	EEEMMEGETN
60	70	80	90	100
FSSEIEDLAR	EGDMPIHELL	SLYGYGSTVR	LPEEDEEEEE	EEEEGEDDED
110	120	130	140	150
ADNDDNSGCS	GENKEENIKD	SSGQEDETQS	SNDDPSQSVA	SQDAQEIIRP
160	170	180	190	200
RRCKYFDTNS	EVEEESSEDE	DYIPSEDWKK	EIMVGSMFQA	EIPVGICRYK
210	220	230	240	250
ENEKVYENDD	QLLWDPEYLP	EDKVIIIFLKD	ASRRTGDEKG	VEAIPGSHI
260	270	280	290	300
KDNEQALYEL	VKCNFDTEEA	LRRLRFNVKA	AREELSVWTE	EECRNFEQGL
310	320	330	340	350
KAYGKDFHLI	QANKVTRTSV	GECVAFYYMW	KKSERYDFFA	QQTRFGKKKY
360	370	380	390	400
NLHPGVTDYM	DRLLDESESA	ASSRAPSPPP	TASNSSNSQS	EKEDGTVSTA
410	420	430		
NQNGVSSNGP	GILQMLLPVH	FSAISSRANA	FLK*	

B:

Constructs

myc-MIER1 α



myc-aa1-283



myc-aa164-433



myc-aa164-283



 : N-terminal acidic stretches;
  : ELM2 domain
 : SANT domain+ α C-terminus;

4.2.2 Primer synthesis and site-directed mutagenesis

Primers used for site-directed mutagenesis were designed online: www.agilent.com/home and synthesized by Integrated DNA Technologies. The sequences of the primers are listed in Table 4.1.

S¹⁰→A α and S³⁷⁷→A α were generated, separately; S³⁷⁷→A α primers were used to mutate the S¹⁰→A α mutant construct in order to produce the double mutation S¹⁰→A/S³⁷⁷→A α . Mutations were produced by the QuikChange site-directed mutagenesis kit (Stratagene), performed according to the manufacturer's instructions. The mutations were confirmed by automated dideoxynucleotide sequencing of both strands (DNA Sequencing Facility, The Center for Applied Genomics, The Hospital for Sick Children, Toronto, Canada).

Table 4.1 Primer sequences for site-directed mutagenesis of SP motifs on MIER1 α

S ¹⁰ →A α sense primer:	5'-cggagccatctgttgaatcttcagctccaggagggttc-3'
S ¹⁰ →A α anti-sense primer:	5'-gaacctcctggagctgaagattcaacagatggctccg-3'
S ³⁷⁷ →A α sense primer:	5'-catctagtcgagcaccagcccctcccc-3'
S ³⁷⁷ →A α anti-sense primer:	5'-ggggaggggctggtgctcgactagatg-3'

4.2.3 Cell line and culture condition

The MCF7 human breast adenocarcinoma cell line was obtained from the American Tissue Culture Collection (ATCC) and cultured in DMEM (GIBCO, REF 11965-092) containing 10% serum (7.5% calf serum (CS) (GIBCO, Cat. No. 16010-159) plus 2.5% fetal bovine serum (FBS) (GIBCO, REF 1884253)) and 1 mM sodium

pyruvate (GIBCO, REF 31053-028). Before electroporation transfection was performed, the cell growth medium was changed to DMEM (GIBCO) supplemented with 10% charcoal-dextran treated fetal bovine serum (Hyclone, Cat. No. SH30068.03) plus 1 mM sodium pyruvate (GIBCO, REF 11360-070) to eliminate any effect generated by growth factors contained in the serum; the transfected cells were cultured in this medium until cell collection. In the experiments using 17 β -estradiol (E2), cells were cultured in phenol red-free DMEM (GIBCO, REF 31053-028) supplemented with 10% charcoal-dextran treated fetal bovine serum after transfection.

4.2.4 Transient transfection

Neon[®] transient transfection was performed with the following settings: 1000 V, 30 ms, 2 pulses for MCF7 cells. 3x10⁵ MCF7 cells were mixed with 0.5 μ g myc-tagged plasmid and loaded into a 10 μ l tip for electroporation. Transfected cells were plated at a density of 4x10⁴/well in Falcon 8-well culture slides (BD BioSciences, Cat. No. 0877426) for confocal analysis and 3x10⁵/well in 6-well dish for western blot analysis.

4.2.5 Growth factors

Human recombinant insulin (REF 12585-014) was purchased from GIBCO[®] and used at a concentration of 10 μ g/ml. Recombinant human IGF-1 (Cat. No. 100-11), recombinant human EGF (Cat. No. AF-100-15) and recombinant human FGF acidic (Cat. No. 100-17A) were purchased from PEPROTECH and used at a concentration of 10 ng/ml. E2 (Cat. No. E125) was purchased from Sigma-Aldrich

and used at a concentration of 10nM. At 24 h after transfection, cells were incubated with insulin, IGF-1, EGF, FGF or E2 for another 4 h prior to fixation or cell collection.

4.2.6 Antibodies

The 9E10 anti-myc tag mouse monoclonal antibody was prepared as described in Blackmore *et al.* (Blackmore et al., 2008) and used at a dilution of 1:200 for immunofluorescence. Alexa Fluor-488 labeled donkey anti- mouse (Cat. No. 715-606-150) was purchased from Jackson ImmunoResearch Laboratories Inc. and used at the dilution 1:200 in immunofluorescence.

For western blot, anti-pERK1/2 (Cat#9101), anti-AKT (C67E7) and anti-pAKT (D9E) were purchased from Cell Signaling Technology® and used at the dilution 1:2000. Anti-ERK 1/2 (K-23) and anti-Lamin A (H-102) were purchased from Santa Cruz Biotechnology Inc and used at a dilution of 1:2000. Anti-GAPDH (G8795) was purchased from Sigma-Aldrich and used at a dilution of 1:2000. HRP-labeled sheep anti-mouse (NA934V) and donkey anti-rabbit (NA931V) antibodies were purchased from GE Healthcare Corp and used at a dilution of 1:5000. All antibodies used in western blot were diluted in 5% skim milk in 1xTBST.

4.2.7 Inhibitors

AKT inhibitor AKT VIII (Cat. No. 124018) was purchased from EMD Millipore and used at a concentration of 10 μ M diluted in DMSO. MEK1/2 inhibitor U0126 (Cat. No. 1144/5) was purchased from Tocris Bioscience and used at a concentration of 10 μ M diluted in DMSO. Growth factors were added directly to the medium pretreated with DMSO or inhibitor for 1 h and cells were left in “DMSO+

growth factor-treatment” or “inhibitor+ growth factor-treatment” medium for another 4 h before fixation.

4.2.8 Western blot

4.2.8.1 Western blot materials

The 0.2 μm PVDF membranes (Trans-Blot Turbo™ transfer Pack) and Trans-blot Turbo™ system were purchased from Bio-Rad Laboratories. Prestained high and low molecular weight markers (GeneDireX®), Amersham’s ECL Plus Western Blotting System, purchased from GE Healthcare Corp. were used for the detection.

4.2.8.2 Western blot methods

Western blot analysis was performed using 7.5% SDS-PAGE gels. After transfer of the proteins to the PVDF membranes, the membrane was incubated in 5% blocking powder (skim milk powder) in TBS-T (20 mM Tris, 137 mM NaCl, 1% (v/v) Tween-20, pH7.6) for 1 h at RT. The membrane was then incubated overnight in 5% blocking powder/1xTBS-T containing a primary antibody at 4°C. After the first antibody incubation, the membrane was washed in large volumes of TBS-T for 1 h and then the secondary antibody was added in 5% blocking powder/1xTBS-T and incubated for 1 h. After incubation with secondary antibody, the membrane was washed in TBS-T for another 1 h before detection of the protein with Amersham’s ECL Plus Western Blotting System.

4.2.8.3 Cell lysis for direct western blot

MCF7 cells were plated at 3×10^5 cells/well in 6-well dish and left to grow for 28 h. After washing in cold 1×PBS on ice, cells were then solubilized in 400 μ l 1×SDS sample buffer (50mM Tris-Cl pH6.8, 2% SDS, 5% β -mercaptoethanol, 10% glycerol, 0.1% bromophenol blue) for western blot. 1/20th of the cell lysate was separated on a 7.5% SDS-PAGE acrylamide gel and the separated proteins were transferred to PVDF membranes by Trans-blot Turbo™ system.

4.2.9 Stripping buffer

The protocol used is from Abcam-Stripping for reprobing. Stripping buffer, 1 liter composition: 15 g glycine, 1 g SDS, 10 ml Tween20, Adjust pH to 2.2 and volume to 1 L with ultrapure water.

Membrane incubation: The membrane was washed with the stripping buffer for 5-10 minutes, twice. The buffer was discarded and the membrane was washed 2X with PBS for 10 minutes. It was then washed 2X with TBST for 5 minutes. The membrane was then ready for the blocking stage. All the steps were performed at room temperature.

4.2.10 Immunofluorescence, confocal microscopy and statistical analysis

4.2.10.1 Immunofluorescence

Immunofluorescence was performed as listed in Appendix 2.

4.2.10.2 Confocal microscopy

Cells were examined under an Olympus FluoView FV1000 confocal microscope. Fluorescence images were obtained by sequential z-stage scanning in two channels (DAPI and/or Alexa Fluor-488); z-stacks were compiled into individual images.

The cells were classified into three categories according to the MIER1 α distribution. Subcellular localization was scored as “nuclear” if the nucleus was intensely stained, with little or no cytoplasmic staining; “cytoplasmic” if staining was primarily in the cytoplasm, with little or no staining in the nucleus; and “whole cell” if both the nucleus and cytoplasm were stained.

4.2.10.3 Statistical analysis

Each experiment was repeated at least three times if not specified, and the results are expressed as mean \pm standard deviation ($M \pm SD$). All the graphs and statistical analysis were performed using GraphPad Prism 7.0 for Windows (GraphPad Software, San Diego, California, USA); $p < 0.05$ was considered to indicate a statistically significant result. One-way ANOVA (analysis of variance) was used for the comparison of quantitative data between different groups when only the nuclear localization percentage was shown in the graph. Two-way ANOVA was utilized to evaluate the data when more than one factor had to be assessed.

4.3 Results

MIER1 α nuclear loss is growth factor-dependent and the result of CRM1-dependent export (discussed in Chapter 3, $p < 0.05$); therefore, I postulated that a

signalling pathway(s) commonly activated by these four molecules (insulin, IGF-1, EGF and FGF) is involved in MIER1 α subcellular distribution alteration. Growth factors cause pleiotropic cellular effects and regulate diverse pathways in both normal and cancer cells (Esther Witsch, Michael Sela, 2010) by binding to their receptors (McInnes & Sykes, 1997). Insulin, IGF-1, EGF and FGF were originally considered to manifest their mitogenic actions through separate pathways. However, there is a growing body of evidence suggesting that these growth factor signalling pathways are intertwined, and amongst these pathways, mitogen-activated protein kinase (MAPK) and phosphoinositide 3-kinase B/Akt (PI3K/AKT) pathways can both be activated by insulin, IGF-1, EGF and FGF (Hemmings & Restuccia, 2012; Roberts & Der, 2007).

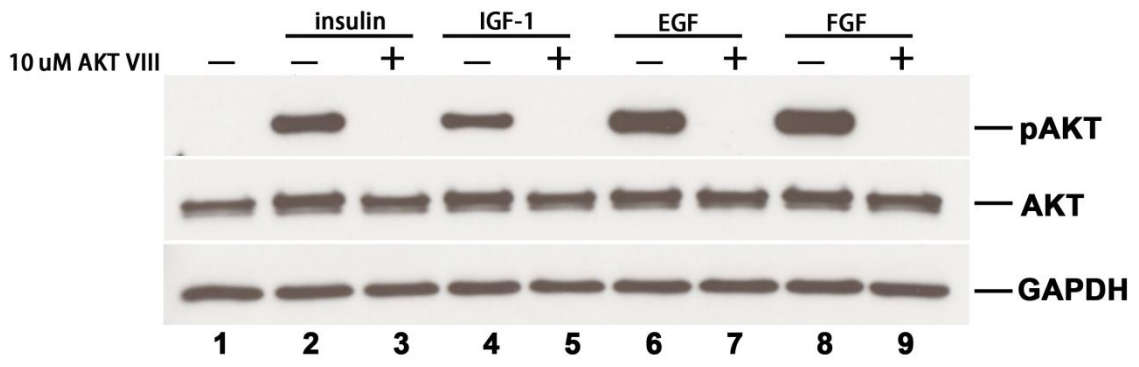
4.3.1 AKT activation by growth factor stimulation

Receptor tyrosine kinase and PI3K/AKT pathway analysis began in the early 1980s through characterization of insulin receptor signalling (Brazil & Hemmings, 2001) and led to the identification of the components and mechanisms (Hemmings & Restuccia, 2012). AKT is a serine/threonine-specific protein and contains a pleckstrin homology (PH) domain through which AKT is recruited to PIP₃ first and then phosphorylated by PDK1 at the ³⁰⁸T residue (Fig. 4.2). AKT inhibitor VIII is PH domain-dependent and inhibits AKT phosphorylation in vivo. First, I confirmed that under the conditions used here, AKT is activated by growth factors and that AKT VIII can inhibit this activation 4 h after growth factor treatment.

MIER1 α expressing cells were pre-treated with either vehicle (DMSO) or 10 μ M AKT VIII for 1 h, and then incubated for 4 h with growth factors before cell extraction. Compared with the DMSO treated control (Fig. 4.4 lane1), insulin, IGF-1, EGF and FGF can all trigger AKT phosphorylation (lanes 2, 4, 6, 8); when the AKT inhibitor VIII is present, phosphorylation of AKT is completely inhibited (lanes 3, 5, 7, 9). This result confirms that PI3K/AKT pathway can be activated by growth factors and that AKTVIII inhibits this activation.

Figure 4.4 AKT VIII inhibits growth factor-dependent AKT activation

MCF7 cells were transfected with *MIER1* α and seeded at 3×10^5 /well in a six-well dish. At 24 h post-transfection, cells were treated either with DMSO (in the control group), DMSO+growth factor, or 10 μ M AKT VIII+growth factor, and incubated for 4h. Cells were collected and 1/20th of the cell lysate was loaded per lane and resolved by western blotting. The blot was probed for either phospho-AKT (pAKT, top blot), or GAPDH as a loading control (bottom blot). The top blot was stripped once and reprobed for AKT to show the AKT protein level. The western blot in this figure demonstrates AKT is activated when cells were treated with growth factors (lanes 2, 4, 6, 8). In contrast, AKT activation is completely inhibited by AKT VIII (lanes 3, 5, 7 & 9).

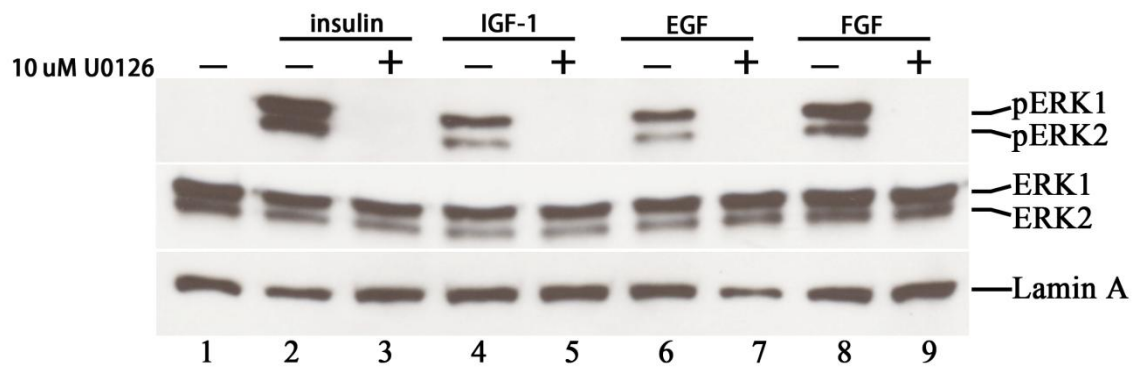


4.3.2 MAPK activation by growth factor stimulation

U0126 is a selective inhibitor of the MAP kinase kinases, MEK1 and MEK2 (Favata et al., 1998); it inhibits their kinase activity thus preventing activation of the MAP kinases, ERK1 and ERK2. To confirm that under the conditions used here, ERK1/2 can be activated by growth factors and U0126 inhibits growth factor stimulated phosphorylation of ERK1/2, *MIER1 α* transfected cells were pre-treated with either vehicle (DMSO) or 10 μ M U0126 for 1 h, and then incubated for 4 h with growth factors before cell extraction. Compared with the DMSO treated control (Fig. 4.5, lane1), insulin, IGF-1, EGF and FGF can all trigger ERK1/2 phosphorylation (lanes 2, 4, 6, 8); when the MEK1/2 inhibitor U0126 is present, ERK1/2 phosphorylation is completely inhibited (lanes 3, 5, 7, 9). This result confirms MAPK pathway can be activated by growth factors and U0126 can prevent this activation.

Figure 4.5 U0126 inhibits growth factor-dependent MAPK activation

MCF7 cells were transfected with myc-tagged *MIER1* α and seeded at 3×10^5 /well in a six-well dish. At 24 h post-transfection, cells were treated either with DMSO (in the control group), DMSO+growth factor, or 10 μ M U0126+growth factor, and incubated for 4h. Cells were collected and 1/20th of the cell lysate was loaded per lane and resolved by western blotting. The blot was probed for either phospho-ERK1/2 (pERK; top blot), or Lamin A (bottom blot) as a loading control. The top blot was stripped once and reprobed for ERK1/2 (middle blot) to demonstrate equivalent amounts of ERK1/2 protein in each lane. The western blot in this figure demonstrates ERK1/2 is activated when cells were treated with growth factors (lanes 2, 4, 6, 8). In contrast, pERK1/2 activation by growth factors is completely inhibited by U0126 (lanes 3, 5, 7 & 9).



4.3.3 Growth factor-dependent activation of MAPK causes MIER1 α nuclear loss

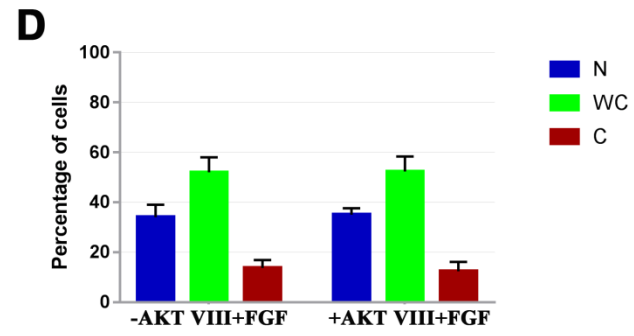
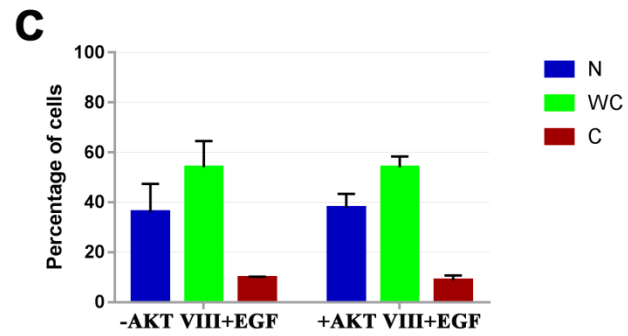
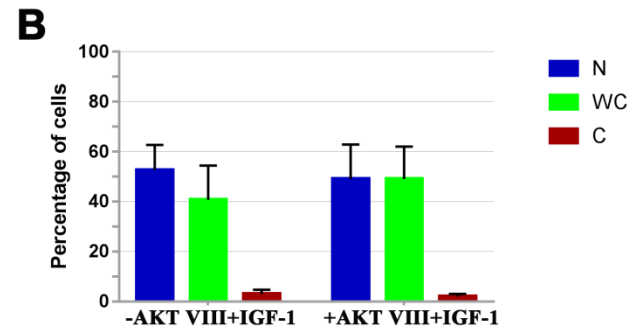
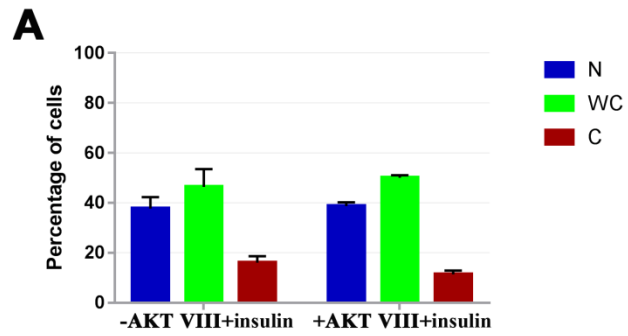
Growth factor-induced tyrosine kinase receptor activation catalyzes inactive GDP-bound Ras into active GTP-bound Ras; active RasGTP hereafter stimulates multiple downstream effectors, including PI3Ks and MAPK. This creates one point of cross-talk between the PI3K and Ras/MAPK pathway. As discussed in Section 3.3.1, Chapter 3, MCF7 expresses receptors for all four growth factors. As shown in section 4.3.1 & 4.3.2, both PI3K/AKT and MAPK pathways can be activated by growth factors. In order to distinguish whether one or both are responsible for MIER1 α nuclear loss, MIER1 α subcellular distribution was analyzed in the presence of the respective pathway inhibitors AKTVIII and U0126.

4.3.3.1 PI3K/AKT pathway activation is not involved in MIER1 α nuclear export

PI3K/AKT pathway was shown to be activated in section 4.3.1 and AKT VIII can inhibit this activation. Here, we transfected MCF7 cells with the myc-tagged MIER1 α and 23 h after transfection, cells were pre-incubated with DMSO or 10 μ M AKT VIII for 1 h. Cells were then incubated with growth factors for another 4 h and fixed. The results demonstrate that there is no statistical difference between the groups “-AKT VIII+growth factor” and “+AKT VIII+growth factor” (Fig. 4.6), the nuclear percentage in the (-AKT VIII+ growth factor-treated) group: (+AKTVIII+ growth factor-treated) group is 38%:39% with insulin, 53%:49% with IGF-1, 36%:38% with EGF and 34%:35% with FGF. Overall, MIER1 α nuclear loss was not rescued when the AKT inhibitor AKTVIII was added into the cells. The data in Fig 4.6 demonstrate that the inhibition of AKT activity has no effect on MIER1 α nuclear loss.

Figure 4.6 AKT inhibition has no effect on MIER1 α subcellular distribution

MCF7 cells were transfected with myc-tagged *MIER1 α* , and 23 h after transfection cells were pretreated with DMSO or 10 μ M AKTVIII for 1 h. Growth factors were added to the cells and incubated for another 4 h before fixation. >160 cells were scored for each type. **(A-D)** MIER1 α subcellular distribution with AKT VIII treated with insulin (panel A), IGF-1 (panel B), EGF (panel C) & FGF (panel D); the histograms shown the combined results of 3 independent experiments and data are expressed as mean \pm standard deviation (SD). $p > 0.05$, (Sidak's multiple comparisons test).



4.3.3.2 U0126 inhibits growth factor dependent nuclear loss of MIER1 α in MCF7 cells

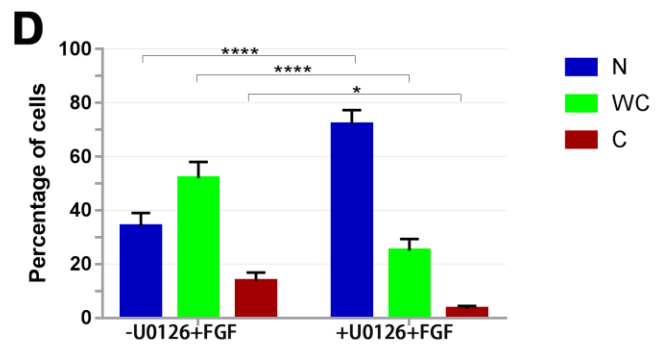
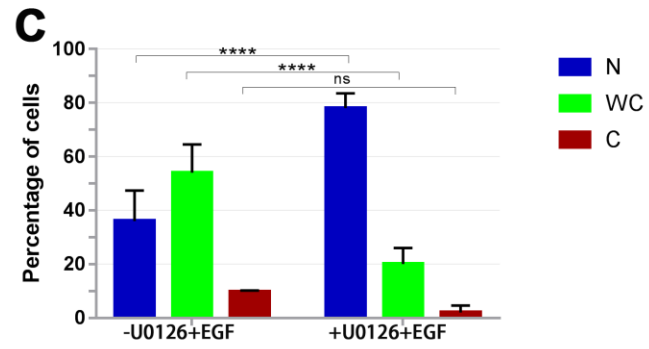
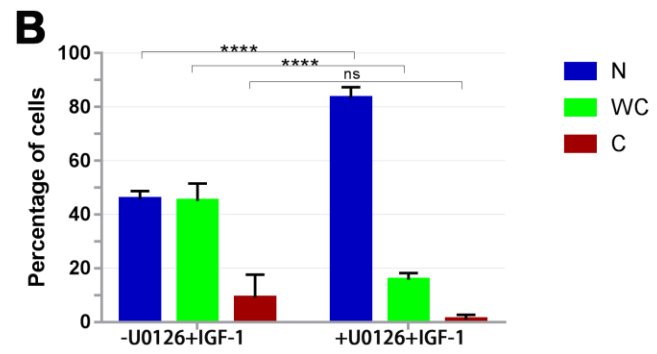
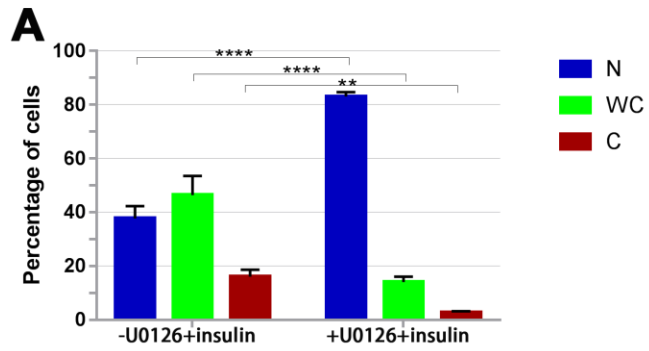
To investigate whether the MAPK pathway was involved in MIER1 α nuclear loss, MCF7 cells were transfected with myc-tagged *MIER1 α* and 23 h later, cells were pretreated with DMSO or 10 μ M U0126 first for 1 h and then growth factors were added for another 4 h to the medium that contains DMSO or U0126 before fixation.

The results demonstrate a statistical difference between the groups “-U0126+growth factor” and “+U0126+growth factor” (Fig. 4.7), the nuclear percentage in the (-U0126+ growth factor-treated) group: (+U0126+ growth factor-treated) group is 37%:83% with insulin, 46%:83% with IGF-1, 36%:78% with EGF and 34%:72% with FGF (Fig. 4.7A-D). Correspondingly, the percentage of whole cell and cytoplasmic staining dropped in each group (Fig. 4.7A-D). These data confirm that the growth factor-dependent activation of MAPK is required for MIER1 α nuclear export. When U0126 inhibits MEK1/2 to phosphorylate ERK1/2, MIER1 α remains in the nucleus in MCF7 cells.

Figure 4.7 U0126 inhibits growth factor dependent nuclear loss of MIER1 α in MCF7 cells

MCF7 cells were transfected with myc-tagged *MIER1 α* and 23 h after transfection, cells were treated with DMSO or 10 μ M U0126 for 1 h. Then, growth factors were added to the cells and incubated for another 4h before the cells were fixed and processed for confocal analysis. More than 160 cells were scored for each type.

(A-D) MIER1 α subcellular distribution with U0126 treated with insulin (panel A), IGF-1 (panel B), EGF (panel C) & FGF (panel D). Shown are the average and standard deviations (S.D.) of 3 independent experiments. ns: not significant; *, $p < 0.05$; **, $p < 0.01$, ***, $p < 0.0001$, (Sidak's multiple comparisons test).



Taken together, the results shown in sections 4.3.1-4.3.3 demonstrate that both PI3K/AKT and MAPK pathways can be activated by insulin, IGF-1, EGF and FGF (Figs. 4.4&4.5), however, MIER1 α nuclear loss is only rescued by MEK1/2 inhibitor U0126 & not by the AKT inhibitor VIII (Figs. 4.6&4.7), implying that activation of the MAPK pathway regulates MIER1 α nuclear export.

4.3.3.3 Estrogen does not activate MAPK pathway

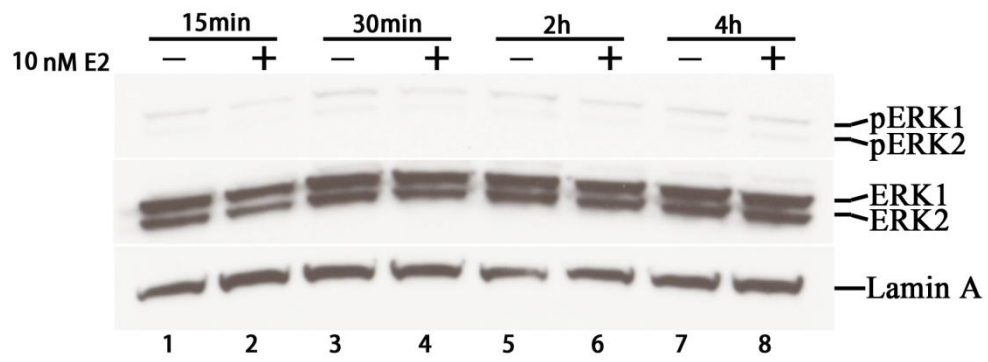
The above experiments demonstrated that the MAPK pathway is involved in MIER1 α nuclear export (Figs. 4.5 & 4.7), while in the previous study (see section 3.3.1.5), E2 treatment did not affect the MIER1 α subcellular distribution pattern in MCF7 (Fig. 3.5); therefore, one would predict that this pathway is not activated by E2 stimulation. However, one report showed that the pERK1/2 level in MCF7 cells was slightly increased in the first 30 min after treatment with 10 nM E2 (Wang et al., 2013). Hence, I examined MCF7 cells treated with either vehicle or 10 nM of E2 at 15 min, 30 min, 2 h or 4 h. The collected samples were analyzed by western blot. As shown in Fig. 4.8, ERK1/2 is not activated during the first four hours of E2 treatment, suggesting that E2 does not cause MIER1 α nuclear export because its intracellular signalling pathways in MCF7 do not include activation of ERK1/2.

It was reported that ERK1/2 activation is initiated by a membrane-initiated (non-genomic) estrogen signalling pathway through the isoform estrogen receptor alpha 36 (ER α 36) when cells were treated with 10nM E2 (Wang et al., 2006). ER α 36, which predominantly localizes on the plasma membrane, lacks the transcriptional activation domains of the classical ER α and its expression level is low in MCF7 cells

(Wang et al., 2006). Therefore, the inactivation status of ERK1/2 in our study is probably due to a low level of ER α 36 and consequently, E2 mainly binds to ER α and exerts its effect through genomic action.

Figure 4.8 ERK1/2 is not activated by E2

MCF7 cells were transfected with myc-tagged *MIER1α* and 3×10^5 cells were seeded in each well in a six-well dish. At 24 h post-transfection, cells were treated either with vehicle or 10 nM E2. Cells were collected at 15 min, 30 min, 2 h and 4 h after treatment. $1/20^{\text{th}}$ of the cell lysate was loaded per lane and the proteins resolved by western blotting. The blot was probed for either phospho-ERK1/2 (pERK1/2; top blot) or Lamin A (bottom blot) as a loading control. The blot was stripped once and reprobed for ERK1/2 (middle blot) to determine the amount of ERK1/2 protein in each lane. The western blot in this figure demonstrates ERK1/2 is not activated when MCF7 cells were treated with E2.



4.3.4 The mechanism responsible for growth factor directed nuclear export does not involve direct phosphorylation of MIER1 α on consensus motifs by pERK1/2

Phosphorylation is a common modification in biology, leading to pleiotropic effects and playing a vital role in regulating a multitude of biological pathways. Transport across the nuclear envelope is an essential cellular function and therefore phosphorylation of cargos trafficking between the cytoplasm and nucleus is emerging as an important step. Shuttling of cargoes regulates nuclear availability, which directly affects gene expression (Nardozzi et al., 2010). Phosphorylation can regulate nucleocytoplasmic shuttling in either direction (Nardozzi et al., 2010). For example, Signal Transducers and Activators of Transcription (STATs) are an important family of transcription factors that regulate cellular viability, immune response and development. Upon stimulation of extracellular receptors, STAT1, which mediates the innate immune response (Jr, 1997), is activated through tyrosine phosphorylation at position Y⁷⁰¹ (Nardozzi et al., 2010). The phosphorylation of STAT1 induces homodimerization and leads to a structural rearrangement of STATs and a dimer-specific NLS becomes exposed (Nardozzi et al., 2010). This unconventional dsNLS can only function as a nuclear import signal within the context of phosphorylated STAT1. On the other hand, the nuclear factor of activated T-cells (NFAT) is a well-characterized example of cargo localized to the cytoplasm due to phosphorylation of its serine-rich region (Ortega-pe, Cano, Were, Villar, & Redondo, 2005).

Activated ERK1/2 are “Proline-directed” protein kinases, which means they phosphorylate S or T residues adjacent to P residues (Wortzel & Seger, 2011). P-X-S/T-P serves as the most common sequence for ERK1/2 substrate recognition but the S/T-P motif can also serve as a substrate (Gonzalez, Raden, & Davis, 1991). The MIER1 α amino acid sequence contains two S-P motifs (Table 4.2): S¹⁰-P¹¹ & S³⁷⁷-P³⁷⁸ and studies by other groups revealed that S¹⁰ and S³⁷⁷ can be phosphorylated (Table 4.3). In sections 4.3.1-4.3.3, it was confirmed that the activated MAPK pathway regulates MIER1 α nuclear export; therefore, my proposal here is if MIER1 α nuclear loss is due to direct phosphorylation S-P motifs by pERK1/2, then mutation of S¹⁰ and S³⁷⁷ to A should abolish phosphorylation and block nuclear export stimulated by growth factors. Hence, I investigated the subcellular distribution of S-P motif mutant MIER1 α . I began by constructing single point mutations of these two S-P motifs to A residues and named the mutants S¹⁰→A- α , S³⁷⁷→A- α , respectively. WT-MIER1 α or S¹⁰→A- α or S³⁷⁷→A- α were transfected into MCF7 cells. The transfected MCF7 cells were incubated with or without growth factors 24 h post-transfection and cells were collected 4 h later. 76% of S¹⁰→A- α and 83% of S³⁷⁷→A- α localize in the nucleus compared to 81% of WT-MIER1 α , demonstrating that mutagenesis of the individual S-P motifs had no effect on nuclear targeting (Figs. 4.9A & 4.10A). When incubated with growth factors, each mutant shows an altered subcellular distribution, similar to WT-MIER1 α . A comparison of the percent nuclear for S¹⁰→A- α : WT-MIER1 α shows 39%: 41% with insulin, 46%: 43.5% with IGF-1, 39.5%:37.5% with EGF and 32.5%: 33% with FGF (Fig. 4.9B-C). Likewise, the percent nuclear for S³⁷⁷→A- α : WT-MIER1 α is 56%: 41% with insulin, 51.5 %: 43.5% with IGF-1,

41%:37.5% with EGF and 40%: 33% with FGF (Fig. 4.10B-C). Although the percent nuclear for the latter mutation was consistently higher, this difference was not statistically significant as determined by Sidak's multiple comparisons test.

Table 4.2 SP motifs within the MIER1 α sequence

MAEPSVESS¹⁰SPGGSATSDDHEFDPSADMLVHDFDDERTLEEEEMMEGETNFSSEIEDLAR
EGDMPIHELLSLYGYGSTVRLPEEDEEEEEEEEEEGEDDEDADNDNSGCSGENKEENIKD
SSGQEDETQSSNDDPSQSVASQDAQEIIRPRRCKYFDTNSEVEEESEEDYIPSEDWKKEI
MVGSMFQAEIPVGICRYKENEKVYENDDQLLWDPEYLPEDKVIIFLKDASRRTGDEKGV
AIEGSHIKDNEQALYELVKCNFDTEEALRRLRFNVKAAREELSVWTEEECRNFEQGLKA
YGKDFHLIQANKVRTRSVGECVAFYMWKKSERYDFFAQQTRFGKKKYNLHPGVTDYM
DRLLDESESAASSRAP³⁷⁷SPPTASNSSNSQSEKEDGTVSTANQNGVSSNGPGILQMLLPVHF
SAISSRANAFLK*

Table 4.3 MIER1 post-transcriptional modification reported in research papers

Sites:	Cell lines/tissue:	Reference:	Types of modification
S10	C57 mice liver	(Bian et al., 2014)	Phosphorylation
S141,367, 369, 377, 448, 491	Hela	(Zhou et al., 2012)	Phosphorylation
S160, 166, 483	Hela	(Dephoure et al., 2008)	Phosphorylation
S488	Hela	(Olsen et al., 2006)	Phosphorylation
H420	HeLa and U2-OS cells	(Hendriks et al, 2015)	SUMOylation

Figure 4.9 Substitution of S¹⁰ to A has no effect on the subcellular distribution of MIER1 α in MCF7 cells

MCF7 cells were transfected with myc-tagged *MIER1* α or S¹⁰→A- α . At 24 h after transfection, cells were either treated with vehicle or insulin, IGF-1, EGF or FGF and incubated for 4 h. Cells were then fixed and processed for confocal analysis. **(A)** Mutation of S¹⁰→A does not affect nuclear localization of MIER1 α . Histogram showing the results of two independent experiments; the localization pattern of >250 cells were scored. S¹⁰→A- α shows a similar pattern as wild type MIER1 α . **(B)** Percentage of cells showing nuclear localization for S¹⁰→A- α compared to wild type MIER1 α after growth factor treatment. The dot chart typically demonstrates there is no statistical significance of the percent nuclear localization between the wild type MIER1 α and the S¹⁰→A- α mutant (Sidak's multiple comparisons test). **(C)** Subcellular distribution of S¹⁰→A- α compared with WT-MIER1 α . $p > 0.05$.

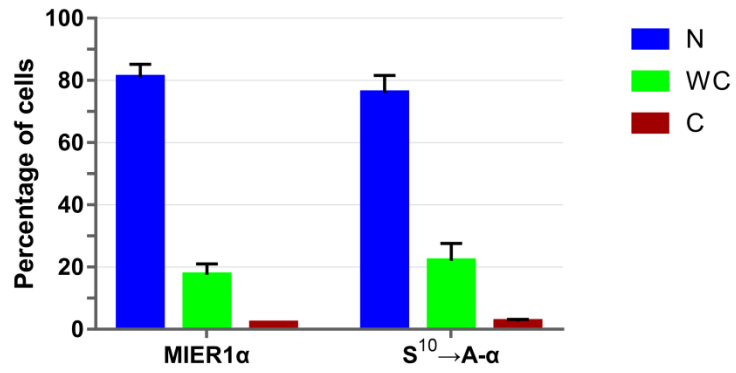
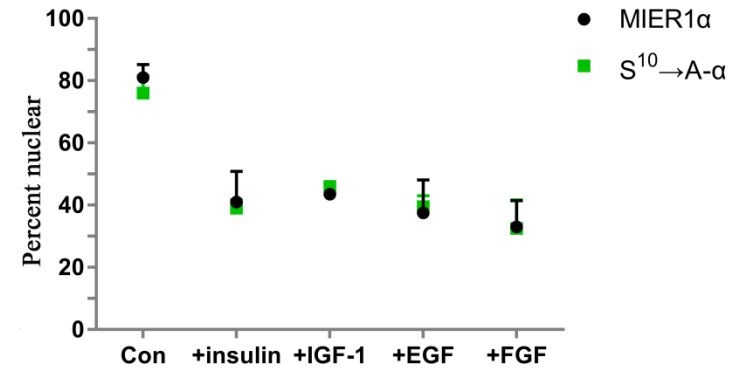
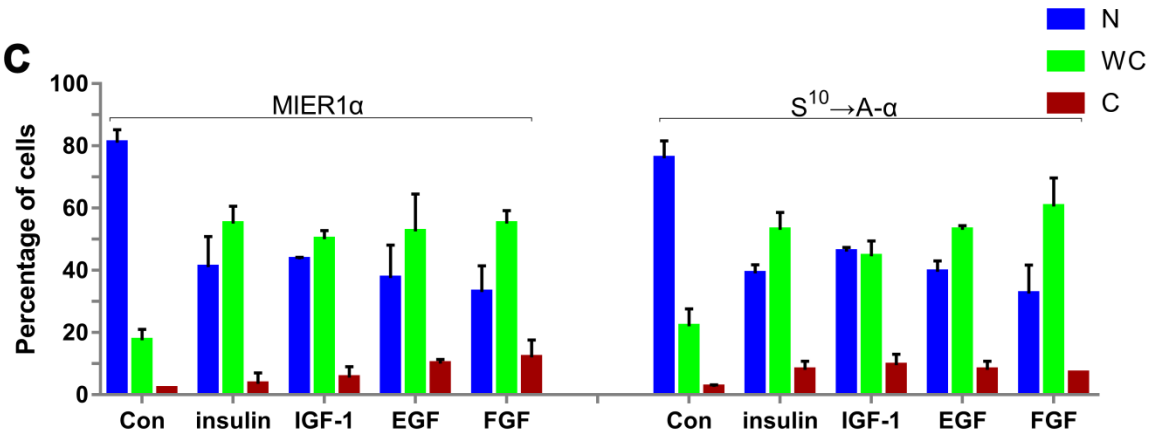
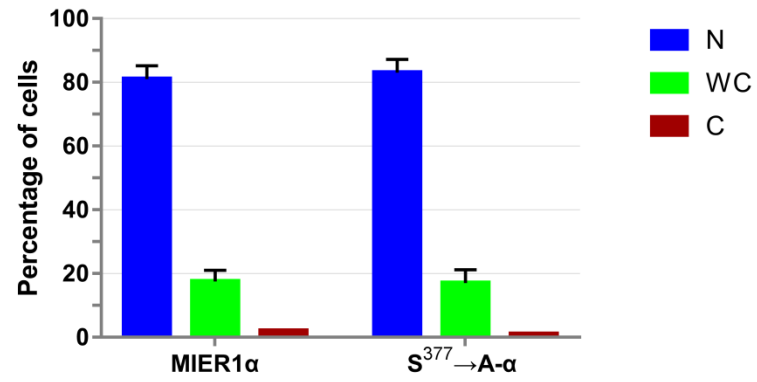
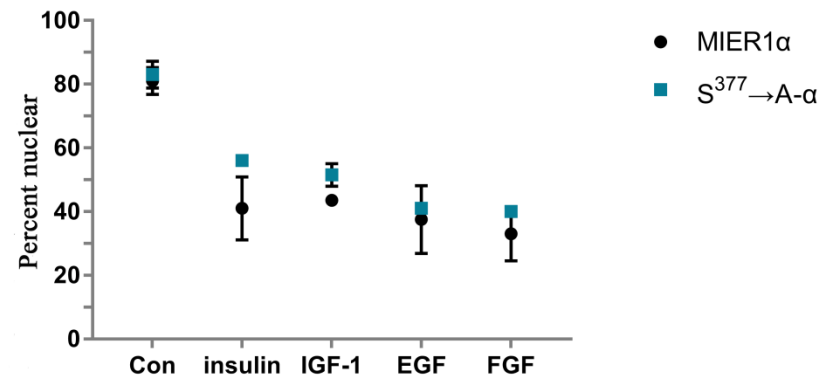
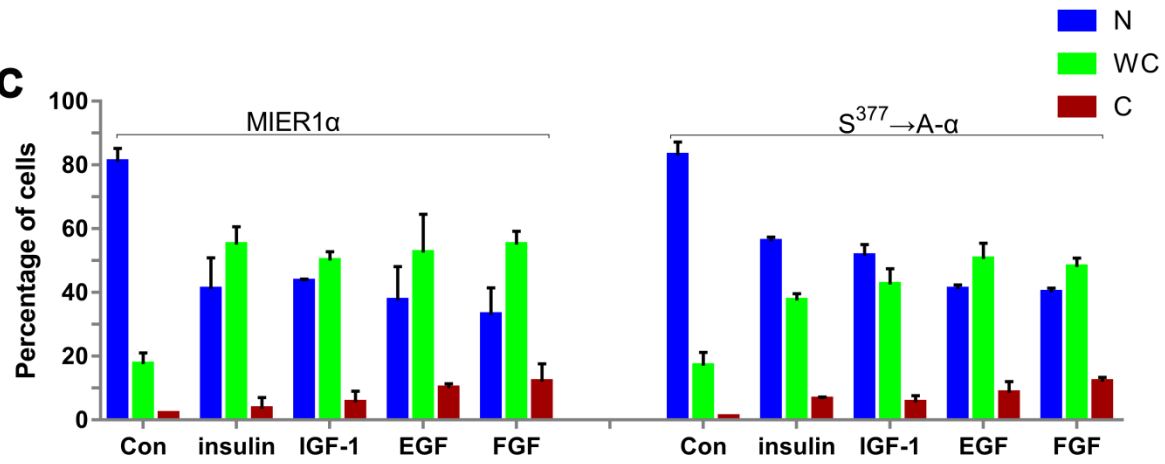
A**B****C**

Figure 4.10 Substitution of S³⁷⁷ to A has no effect on the subcellular distribution of MIER1 α in MCF7 cells

MCF7 cells were transfected with myc-tagged MIER1 α or S³⁷⁷→A- α . At 24 h after transfection, cells were either treated with vehicle or insulin, IGF-1, EGF or FGF and incubated for 4 h. Cells were then fixed and processed for confocal analysis. **(A)** Mutation of S³⁷⁷→A does not affect nuclear localization of MIER1 α . Histogram showing the results of two independent experiments; the localization pattern of >250 cells were scored. S³⁷⁷→A- α shows a similar pattern as wild type MIER1 α . **(B)** Percentage of cells showing nuclear localization for S³⁷⁷→A- α compared to wild type MIER1 α after growth factor treatment. The dot chart typically demonstrates there is no statistical significance of the percent nuclear localization between the wild type MIER1 α and the S¹⁰→A- α mutant (Sidak's multiple comparisons). **(C)** Subcellular distribution of S¹⁰→A- α compared with WT-MIER1 α . $p > 0.05$.

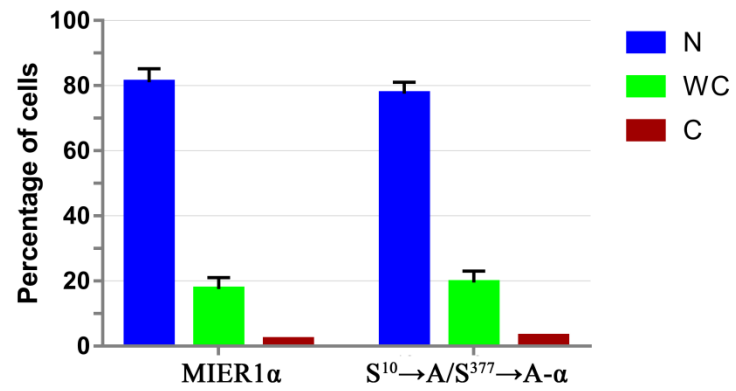
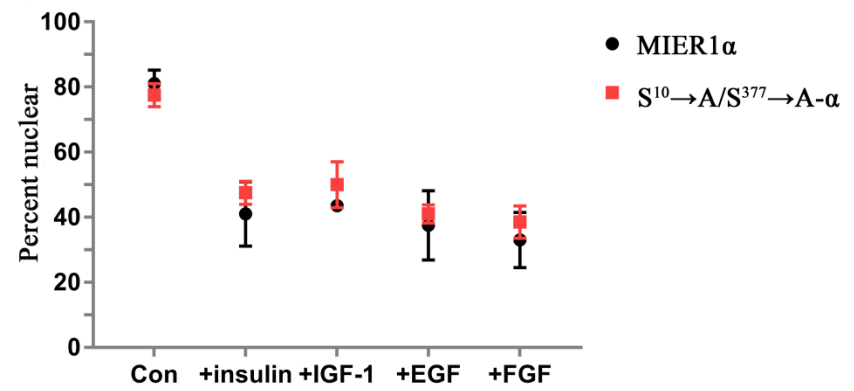
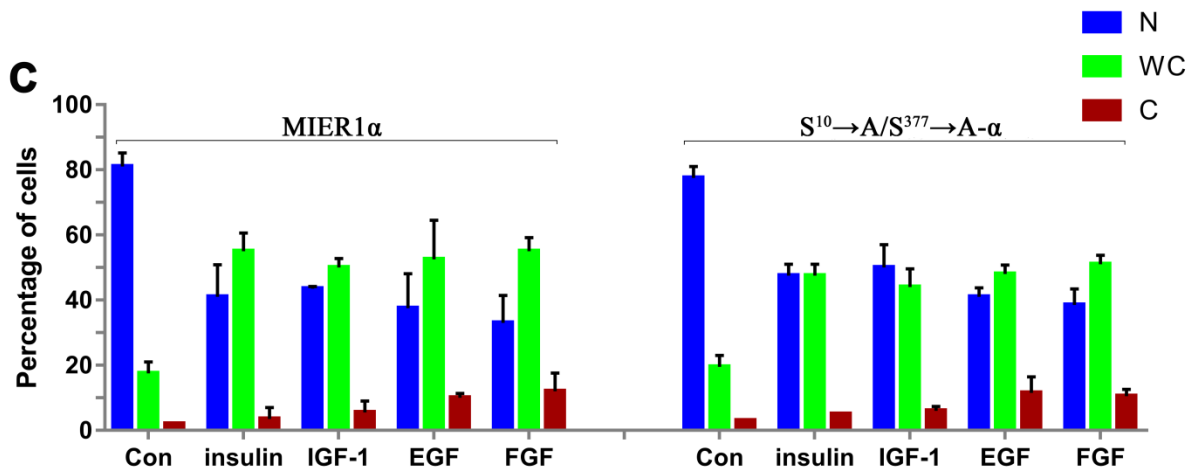
A**B****C**

The single mutation of S-P motifs did not show a statistical difference between WT-MIER1 α and mutant- α . This leads us to propose that MIER1 α nuclear loss may require both S-P motifs. Therefore, a double mutant, containing both S¹⁰→A and S³⁷⁷→A was generated and named S¹⁰→A/S³⁷⁷→A- α . Compared to 81% nuclear with WT-MIER1 α , 77.5% of S¹⁰→A/S³⁷⁷→A- α were nuclear, demonstrating that the double mutation still mainly localizes in the nucleus (Fig. 4.11A). When treated with growth factors, S¹⁰→A/S³⁷⁷→A- α showed an altered subcellular distribution, similar to WT-MIER1 α . Comparison of the percent nuclear for S¹⁰→A/S³⁷⁷→A- α : WT-MIER1 α is 47.5%: 41% with insulin, 50%: 43.5% with IGF-1, 41%:37.5% with EGF and 38.5%: 33% with FGF (Fig. 4.11B-C). Once again, the percent nuclear was consistently high with the mutant but this difference was not statistically significant (Sidak's multiple comparisons test).

Taken together, the subcellular distribution of the single mutants of S¹⁰→A- α or S³⁷⁷→A- α did not block nuclear loss of MIER1 α , nor did the double mutant S¹⁰→A/S³⁷⁷→A- α , indicating that phosphorylation of these residues is not the mechanism responsible for nuclear export of MIER1 α by growth factor signalling.

Figure 4.11 Double mutations of ¹⁰S and ³⁷⁷S to A has no effect on the subcellular distribution of MIER1 α in MCF7 cells

MCF7 cells were transfected with myc-tagged *MIER1* α or double mutant $S^{10}\rightarrow A/S^{377}\rightarrow A$ - α . At 24 h after transfection, cells were either treated with vehicle or with insulin, IGF-1, EGF or FGF and incubated for 4 h. Cells were then fixed and processed for confocal analysis. **(A)** Double mutations of $^{10}S\rightarrow A$ and $^{377}S\rightarrow A$ do not affect nuclear localization of MIER1 α . Histogram showing the results of two independent experiments; the localization pattern of >250 cells were scored. $S^{10}\rightarrow A/S^{377}\rightarrow A$ - α shows a similar pattern as wild type MIER1 α . **(B)** Percentage of cells showing nuclear localization for of $S^{10}\rightarrow A/S^{377}\rightarrow A$ - α compared to wild type MIER1 α after growth factor treatment. The dot chart typically demonstrates there is no statistical significance of the percent nuclear localization between the wild type MIER1 α and the $S^{10}\rightarrow A/S^{377}\rightarrow A$ - α mutant (Sidak's multiple comparisons test). **(C)** Subcellular distribution of $S^{10}\rightarrow A/S^{377}\rightarrow A$ - α compared with WT-MIER1 α . $p>0.05$.

A**B****C**

4.3.5 The N-terminal region of MIER1 α is required for nuclear export

My data have excluded the possibility that direct phosphorylation on S-P motifs by pERK1/2 is responsible for MIER1 α nuclear loss (as discussed in section 4.3.4). To further investigate the mechanism by which ERK1/2 causes nuclear export, I decided to begin by identifying which region of MIER1 α is required for nuclear export during growth factor treatment.

MIER1 α contains 4 N-terminal acidic stretches, an ELM2 domain, a SANT domain and α C-terminus (Fig. 4.3B). I transfected MCF7 cells with myc-tagged constructs containing either the full-length MIER1 α (aa1-433) or a deletion series. Each of the deletion constructs needed to include the ELM2 domain, since this sequence is required for nuclear targeting. Plasmids containing the following regions were constructed: 1) aa1-283(the N-terminal acidic stretches+ELM2 domain), 2) aa164-433 (ELM2 +SANT + α C-terminus), 3) aa164-283 (the ELM2 domain alone). Transfected MCF7 cells were treated with insulin or IGF-1, EGF, FGF, respectively. Localization was determined by confocal microscopy and compared to full-length MIER1 α in each group.

In the control group, myc-tagged full-length MIER1 α is mainly nuclear (80%; Fig. 4.12 panels a-c, Fig. 4.13 A). All constructs localized in the nucleus, similar to full-length MIER1 α : construct 1 is 79% and construct 3 is 80% nuclear (Fig. 4.12, panels g-i, s-u; Fig. 4.13 B&D), surprisingly, construct 2 is almost exclusively nuclear (98% nuclear, Fig. 4.12, panels m-o; Fig. 4.13 C), demonstrating a statistic difference when compared with full-length MIER1 α ($p<0.05$). All these data further confirmed

ELM2 domain is required for MIER1 α nuclear localization, which is consistent with the data presented in section 2.3.2. After all of these groups were treated without/with insulin, IGF-1, EGF or FGF, construct 2 and 3 remained nuclear. The percent nuclear for each was: construct 2: 97% with insulin, 96% with IGF-1; 96% with EGF and 94% with FGF (Fig. 4.13C); construct 3: 76% with insulin, 79% with IGF-1, 77% with EGF and 76% with FGF (Fig. 4.13D). None of these distribution patterns gave a statistically significant difference after treating with growth factors ($p>0.05$). The subcellular distribution of construct 1, on the other hand, changes dramatically after growth factor treatment: the nuclear localization of construct 1 is 30% with insulin, 29% with IGF-1, 26% with EGF and 25% with FGF (Fig. 4.13B). Together, these results demonstrate that the N-terminal sequence containing acidic stretches is required for MIER1 α nuclear export triggered by growth factors insulin, IGF-1, EGF and FGF.

Figure 4.12 The N-terminus containing 4 acidic stretches is required for MIER1 α nuclear export

MCF7 cells were transfected with myc-tagged full-length MIER1 α (a-f) or a myc-tagged MIER1 α deletion construct containing either the acidic + ELM2 domains (construct 1; panels g-l), the ELM2 + SANT + α C-terminus (construct 2; panels m-r) or the ELM2 domain alone (construct 3; panels s-x). And 24 h later, transfected cells were either treated with vehicle or 10 μ g/ml insulin for 4 h before fixation.

Localization was analyzed by confocal microscopy using DAPI and 9E10 anti-myc tag antibody. Illustrative examples of cells showing stained nuclei and MIER1 α localization; arrowheads indicate nuclear staining and arrows indicate whole cell staining. The amino acids (aa) encoded by each construct are indicated on the right.

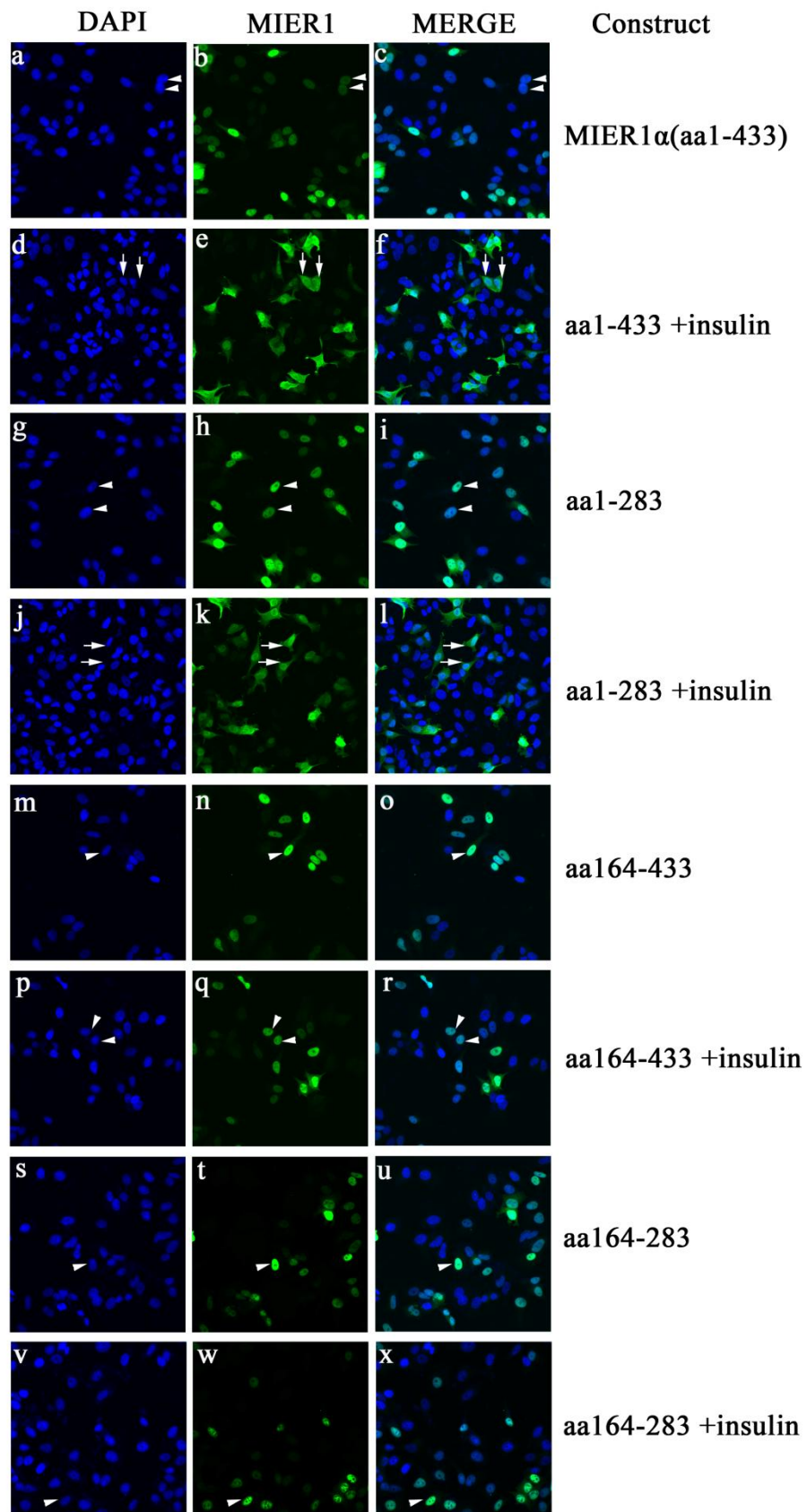
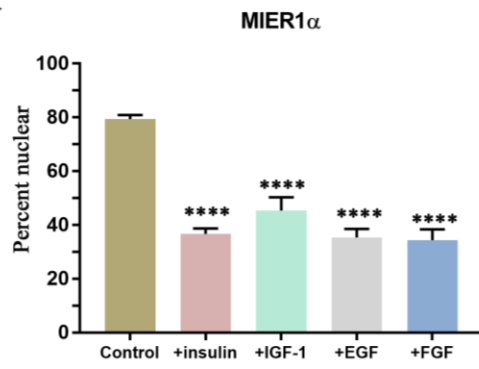
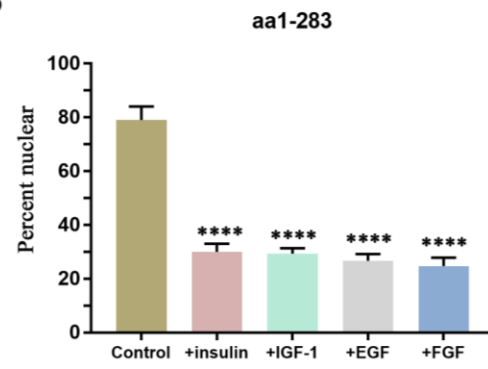
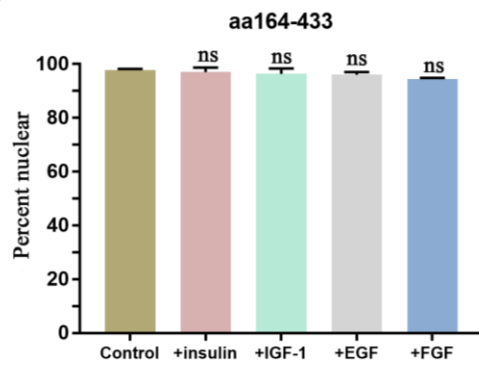
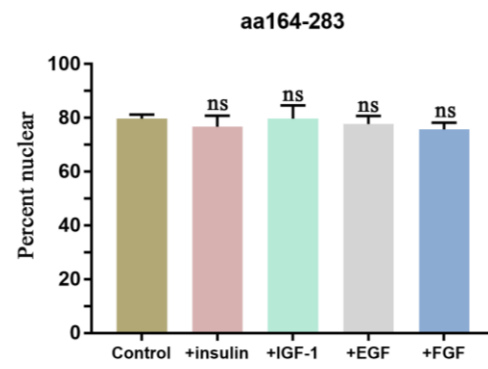


Figure 4.13 The N-terminus containing 4 acidic stretches is required for MIER1 α nuclear export

MIER1 α or deletion constructs transfected MCF7 cells were treated with vehicle (Control) or growth factors 24 h after transfection and incubated for 4 h before fixation. The amino acids (aa) encoded by each construct are indicated above each histogram. (A-D) Histogram showing the results of 3 independent experiments; random fields were selected and the staining pattern of each cell within the field was scored visually. Plotted is the percentage of cells in each category \pm S.D; the percent nuclear for the N-terminal acidic stretches + ELM2 domain(aa1-283) construct with growth factor is significantly less than control(B, **** $p < 0.0001$).

A**B****C****D**

4.3.6 MIER1 α nuclear loss is transient and reversible

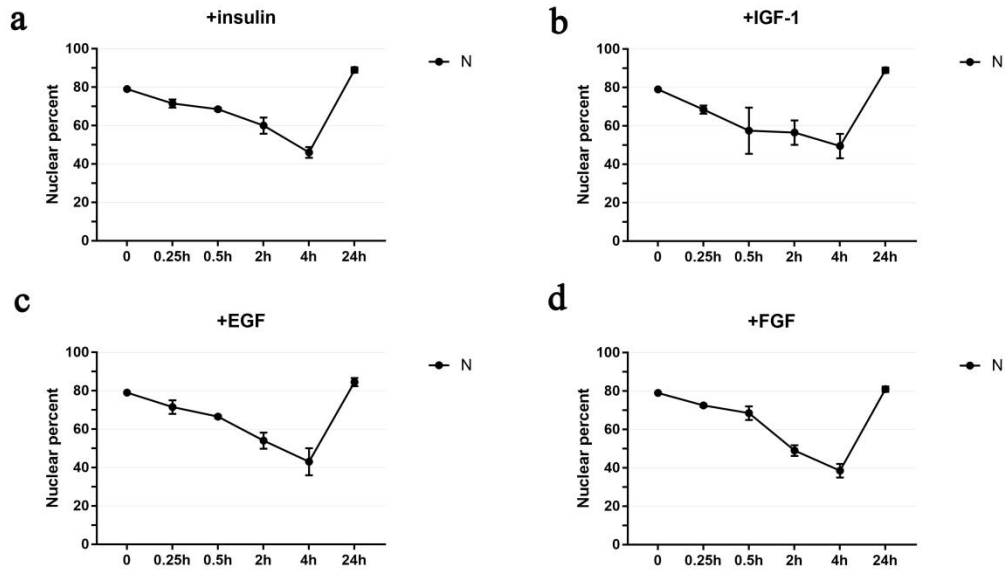
Growth factors are depleted faster compared to other components in the culture media (Yu et al., 2015). Once growth factors are depleted in the medium, the signal for ERK1/2 activation is gone, and events will return to the basal level naturally. Hence, to investigate whether MIER1 α nuclear loss was sustained beyond 4 h incubation period, we analyzed the cells at several time points after growth factor treatment. MCF7 cells were transfected with myc-tagged MIER1 α and 24 h later treated either with vehicle or growth factors. Then, the cells were fixed at different time points after growth factor addition. In the vehicle-treated groups, MIER1 α nuclear percentage is 80% before treating with growth factors. Then MIER1 α nuclear localization decreases gradually in all groups at 0.25 h, 0.5 h, 2 h and 4 h after growth factor incubation. MIER1 α nuclear percentage is 71.5% at 0.25 h, 68.5% at 0.5 h, 60% at 2 h and 46% at 4 h after insulin treatment (Fig. 4.14 A a). The IGF-1, EGF & FGF groups demonstrate the same trend. However, in all of the groups fixed at 24h after growth factor addition, MIER1 α nuclear localization percentage returns to control level: 89% with insulin, 89.5% with IGF-1, 85.5% with EGF and 81% with FGF compared with 89% with MIER1 α (Fig. 4.14A a-d). At the same time, ERK1/2 phosphorylation level diminishes after 24h of growth factor treatment in all groups (Fig. 4.14B). Compared with the basal level, pERK1/2 is still slightly higher in EGF and FGF groups and this corresponds to a lower percentage of MIER1 α nuclear localization in EGF & FGF groups, which means EGF and FGF have a lasting effect on activation of pERK1/2 and the residue of this activation keeps pumping a small amount of MIER1 α out of the nucleus. This data implies that when

growth factor-dependent activation of pERK1/2 diminishes and the effect of growth factors on cells disappears, MIER1 α returns to the nucleus. In short, growth factor triggered MIER1 α nuclear loss is transient and reversible. Moreover, the duration and intensity of pERK1/2 activation can profoundly influence the subcellular distribution of MIER1 α .

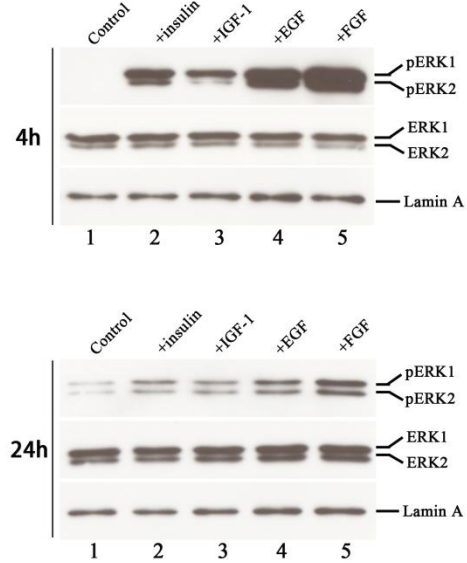
Figure 4.14 MIER1 α nuclear loss caused by ERK1/2 activation is transient and reversible

MCF7 cells were transfected with myc-tagged *MIER1 α* and seeded at 3×10^4 /well in 8-well chamber slide and 3×10^5 /well in a six-well dish. At 24 h after transfection, cells were either treated with vehicle (control) or growth factor. Cells seeded in chamber slides were fixed at 0.25 h, 0.5 h, 2 h, 4 h & 24 h after growth factor treatment; cells seeded in 6-well dish were collected at 24 h after growth factor treatment. **(A)** MIER1 α nuclear localization during-24 h of growth factor treatment; **(B)** Activation of pERK1/2 4 h & 24 h after growth factor treatment with insulin, IGF-1, EGF or FGF. 1/20th of cell lysate was loaded per lane and resolved by western blotting. The blot was probed for either phospho-ERK1/2 (pERK; top blot), or Lamin A (bottom blot) as a loading control. The top blot was stripped once and reprobed for ERK1/2 (middle blot) to demonstrate equivalent amounts of ERK1/2 protein in each lane.

A



B



4.4 Discussion

Phosphorylation is one mechanism utilized by molecules to regulate nucleocytoplasmic shuttling by triggering a conformational change which further causes nuclear import or export (Nardozzi et al., 2010). Quite a few articles report that ¹⁰S or ³⁷⁷S on MIER1 protein can be phosphorylated (Bian et al., 2014, Zhou et al., 2012) (Table 4.3). S-P motifs serve as the minimal phosphorylation motifs for pERK1/2; however, the single or double mutagenesis of S-P motifs on MIER1 α does not prevent its nuclear export, implying that direct phosphorylation of S-P motifs on MIER1 α is not involved in its nucleocytoplasmic shuttling. Although pERK1/2 is defined as Proline-directed protein kinase, some motifs lacking a Proline in the +1 position, herein referred to as non-S/T-P motifs, have been also reported to be phosphorylated by pERK1/2 (Carlson et al., 2011). Hence, phosphorylation on other sites due to MAPK pathway activation may be responsible for MIER1 α nuclear loss. It is worth investigating whether MIER1 α contains non-canonical S/T-P motifs that can be phosphorylated by pERK1/2 and lead to nuclear export. Since N-terminal acidic stretches (aa1-164) are required for MIER1 α nuclear export, further study should focus on residues of S141 and S160, all of which have been shown to be phosphorylated (Table 4.3).

Nuclear export mediated through binding to another adaptor molecule is a well-recognized export mechanism for some proteins. For example, the 60S ribosomal subunit does not bind directly to CRM1, but instead binds to an adaptor protein, Nmd3, which possesses a classical hydrophobic NES to be exported (Ho,

Kallstrom, & Johnson, 2000). MIER1 α nuclear loss may also be mediated by such a mechanism as discussed in section 3.4.

Although multiple polypeptide growth factors were included in MIER1 α localization study here, there are still some other growth factors or cytokines that were not investigated. For example, nerve growth factor (NGF) is widely expressed in all different kinds of breast cancer cell lines but not in normal breast epithelial cells; it activates downstream pathways by binding to its two cognate receptors, TrkA, a receptor tyrosine kinase and p75^{NTR}.(Dolle, Yazidi-Belkoura, EAdriaenssens, Nurcombe, & Hondermarck, 2003; Molloy, Read, & Gorman, 2011). How MIER1 α localization responds to other growth factors like NGF is unknown.

Cells receive fate-determining signals from the surrounding micro-environment under physiological conditions, mainly in the form of polypeptide growth factors (Witsch et al., 2011). Although tumour initiation is instigated by oncogenic mutations rather than by growth factors, the subsequent steps are mainly regulated by the latter, including clonal expansion, invasion and angiogenesis (Witsch et al., 2011). During breast cancer progression, MIER1 α is translocated from the nucleus in hyperplasia and DCIS stages to the cytoplasm in the IDC stage (McCarthy et al., 2008); through my investigations, I have confirmed that growth factor-induced activation of MAPK leads to MIER1 α nuclear loss in a breast carcinoma cell line, but this cytoplasmic shuttling is reversible once the growth signal has diminished. The transient activation of MAPK usually initiates immediate early genes (IEGs) activation/expression (Fowler et al., 2011) and usually, the

regulation of IEGs by transient activation of MAPK is always transient and reversible (Fowler et al., 2011). *MIER1* is defined as an IEG activated during FGF stimulation of embryonic cells. Therefore, it is not surprising that MIER1 α nuclear loss behaves in a transient and reversible pattern in response to growth factor induced activation of MAPK, followed by inactivation of the signalling cascade.

Our findings that MAPK activation influences MIER1 α nucleocytoplasmic shuttling in a breast cancer cell line may shed new light on the underlying mechanism responsible for altered MIER1 α cellular distribution during breast cancer progression. Thus, constitutive MAPK activation could explain the significant loss of MIER1 α in the nucleus of advanced stage breast cancer and this is further discussed in section 5.3.

Chapter 5 Summary

Over the past decade, *MIER1* was shown to encode a potent nuclear transcriptional regulator and play a role in the regulation of gene expression (Ding et al., 2004, 2003). In human breast cancer, the MIER1 α isoform physically interacts with ER α acting as a corepressor and breast cancer development is coupled with aberrant subcellular localization of MIER1 α (McCarthy et al., 2008). Tumour suppressors are frequently reported to have their function inactivated by nuclear export (Azmi & Mohammad, 2016). All this evidence supports the hypothesis that subcellular mislocalization of MIER1 α in breast cancer leads to functional loss. Therefore, investigation of MIER1 α 's dynamic subcellular translocation may help to uncover the specific role MIER1 α plays in breast cancer development.

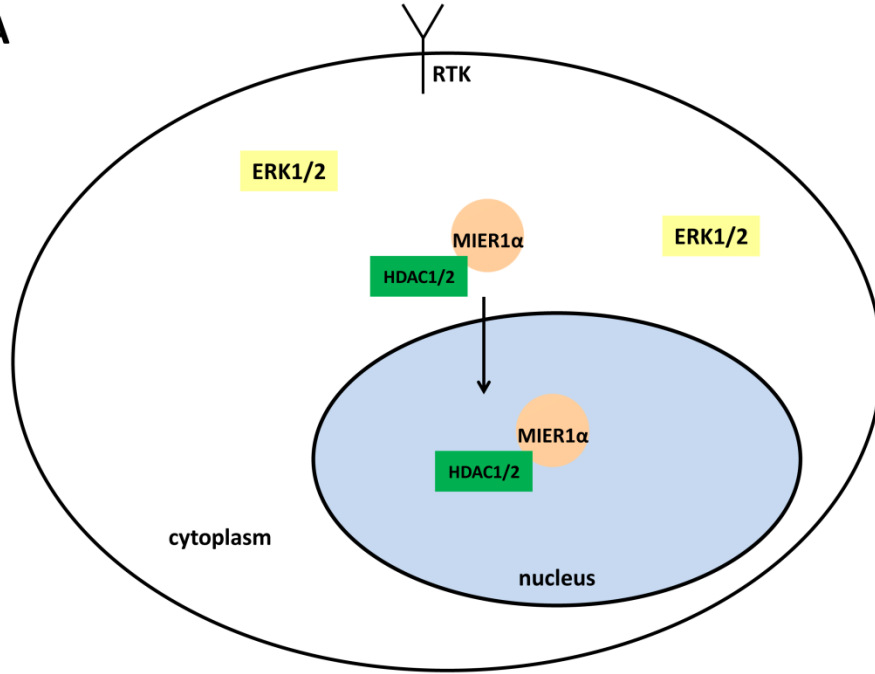
In this thesis, I investigated the MIER1 α nucleocytoplasmic shuttling mechanism in a breast carcinoma cell line. Although MIER1 α interacts with ER α and suppresses cell growth, MIER1 α nuclear localization is not dependent upon ER α . Instead, MIER1 α nuclear targeting is dependent on HDAC1/2 through a piggyback mechanism involving binding to HDAC1/2 via the ELM2 domain (Chapter 2). Further study revealed that ERK1/2 activation by insulin, IGF-1, EGF or FGF can cause MIER1 α nuclear loss and this export process does not involve the ELM2 or SANT domain of MIER1 α , but instead requires sequence within the N-terminal 163aa that contains 4 acidic stretches. HDAC1/2 nuclear localization is not affected during the nuclear export process, demonstrating that while HDAC1/2 are responsible for MIER1 α nuclear localization, they are not involved in nuclear loss. MIER1 α nuclear localization is not affected by E2 (Chapter 3) and consistent with

this is the fact that ERK1/2 is not activated by E2 (Chapter 4). ERK directed nuclear loss of MIER1 α is CRM-1-dependent and requires the sequence within the N-terminal 163aa. In addition, the nuclear loss of MIER1 α is transient and reversible. Together, my data lead me to propose the following model for nucleocytoplasmic shuttling of MIER1 α in the breast carcinoma cell line (Fig 5.1).

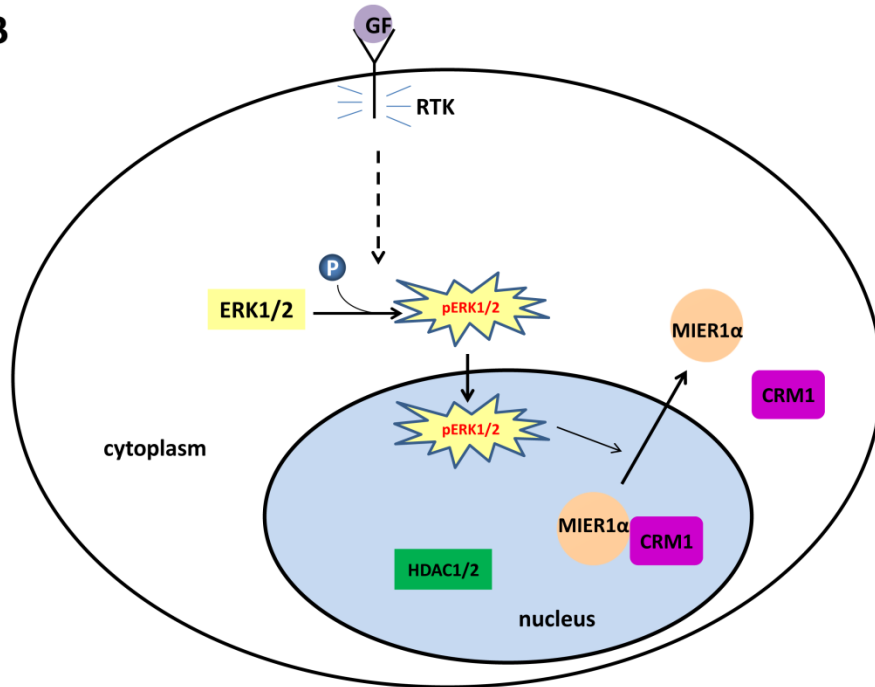
Figure 5.1 Model of MIER1 α nucleocytoplasmic shuttling mechanism

(A) MIER1 α nuclear import. In the environment in which extracellular stimuli are absent and the MAPK pathway is not activated, MIER1 α is targeted to the nucleus through binding to HDAC1/2 by a “piggyback” mechanism. (B) MIER1 α nuclear export. When the MAPK pathway is activated by growth factors binding to their respective receptor tyrosine kinase (RTK), active pERK1/2 causes MIER1 α nuclear export through CRM1.

A



B



5.1 “Piggyback” mechanism of MIER1 α nuclear localization

NLSs are stretches of residues in proteins that mediate their import into the nucleus. The nuclear translocation of proteins mainly depends on the presence of NLSs and most nuclear proteins contain one or more NLSs. Some nuclear proteins lacking an NLS can enter the nucleus by piggybacking as a preassembled complex with another protein containing an NLS. For example, the hetero-trimeric CCAAT-binding complex is evolutionarily conserved in eukaryotic organisms including fungi, plants and mammals. The three homolog subunits of this complex in Fungi are HapC and HapE, which associate with the NLS-containing protein HapB for nuclear import (Steidl et al., 2004). Based on computer analysis of MIER1 α , no classical NLS has been identified but it does localize in the nucleus of MCF7 cells. MIER1 α deletion analysis indicates that the nuclear translocation of MIER1 α is dependent on the presence of an intact ELM2 domain and that it piggybacks on HDAC1/2 to achieve nuclear localization. Previous research also reported that an intact ELM2 domain is necessary for recruiting HDAC1 activity and transcriptional repression activities of MIER1 (Ding et al., 2003).

Molecules that are smaller than 40-45 kDa can diffuse freely through NPC in the cells. The molecular mass of the myc-tagged ELM2 domain predicted by ExPASy is 21.5 kDa, and with this size, one would expect that it can easily diffuse in and out of the nucleus and the cellular distribution would be balanced between the cytoplasmic and nuclear compartments. However, instead of displaying whole cell

staining, the myc-fused ELM2 domain shows 85% nuclear localization (section 2.3.2), meaning that the ELM2 domain cannot diffuse freely through NPCs. This also suggests that ELM2 domain itself can form the correct structure to be translocated to the nucleus without the aid of the other domains in MIER1 α . Secondary-structure analysis of the ELM2 region by PREDICTPROTEIN (<https://www.predictprotein.org/>) revealed that the ELM2 domain has a propensity to form α -helix (aa221-235, aa254-262, aa267-276). The substitution of ²¹⁴W with A in MIER1 α does not result in any alteration of the predicted three α -helical structures in the ELM2 domain. Therefore, it is possible that ²¹⁴W is part of the binding site for HDAC1 or HDAC2; the substitution of this residue may not result in a structural conformation change in MIER1 α , but a loss of the binding site.

To date, 18 different HDACs have been identified in humans and divided into four classes based on sequence similarity to the *Saccharomyces cerevisiae* counterparts (Ruijter et al., 2003). Evidence confirms that different HDACs have unique temporal and spatial expression patterns contributing to tissue-specific regulation of chromatin and transcription-regulatory complexes (Delcuve, Khan, & Davie, 2012). The MIER1 isoform only interacts with HDAC1 and 2, which belong to class I HDACs and it has no interaction with other class I HDACs (Bantscheff et al., 2011; Joshi et al., 2014), suggesting the specific function of MIER1 is with class I HDAC activity. Previous findings showed that a point mutation of the highly conserved ²¹⁴W on the ELM2 domain eliminated MIER1's ability to recruit HDAC1 enzymatic activity (Ding et al., 2003). In our research, mutagenesis of ²¹⁴W abolishes the interaction between MIER1 α and HDAC1 & 2. Therefore, we conclude that the

²¹⁴W residue is not only critical for MIER1's ability to recruit HDAC activity, but also for its localization in the nucleus.

The dissociation between MIER1 α and HDAC1/2 may have a biological effect on cells. MIER1 α is well-known for acting as a transcriptional repressor through binding to HDAC1/2; the ²¹⁴W \rightarrow α mutant may lose its repressive function by dissociating with HDAC1/2. This also suggests a way to study the non-genomic function of MIER1 α since the ²¹⁴W \rightarrow A mutation does not cause a conformation change and nothing is known about possible cytoplasmic functions of MIER1 α under normal or pathological conditions. The α isoform was shown to be lost from the nucleus during breast cancer progression, but it may interact with some other cytoplasmic molecules based on its atypical presence and/or facilitate breast cancer progression by stimulating the growth of tumour cells. Overall, a functional study of the ²¹⁴W \rightarrow A mutant may help to elucidate the role MIER1 α plays in breast cancer.

5.2 Possible mechanisms responsible for MIER1 α nuclear export

The NPC mediates translocation of molecules across the nuclear envelope. The NPC is a large protein complex consisting of ~30 types of Nups (Wente & Rout, 2017). FG repeat regions on Nups are natively unfolded in the central tube of the NPC and act as a permeability barrier. Karyopherins are the carriers and pass through the barrier of the NPC by binding FG Nups. MIER1 α nuclear export was shown to be CRM1-mediated (section 3.3.3) and this excludes the possibility that it goes through the NPC without the assistance of Karyopherins. In addition, without an NES, MIER1 α cannot bind to CRM1 directly. Therefore, one possibility is that an

adaptor protein acts as a bridge between MIER1 α and CRM1. MIER1 α might go a post-translation modification in the presence of growth factors and the modified residue(s) of MIER1 α might offer a binding site for the adaptor protein. The complex of modified MIER1 α :adaptor protein:CRM1 might then be exported out of the nucleus.

One possible adaptor that could mediate CRM1-mediated MIER1 α export is the 14-3-3 protein. 14-3-3 is a well-known adaptor protein that acts by binding to a partner protein, and this binding often leads to the altered subcellular localization of the partner; specifically, 14-3-3 facilitates nuclear export of its target protein via a NES present on its carboxy-terminus and this NES is recognized by CRM1 for CRM1-dependent nuclear export (Lopez-Girona, Furnari, Mondesert, & Russell, 1999). Although the majority of 14-3-3 molecules are present in the cytoplasm, 14-3-3 translocates back to the nucleus when the bound ligands are absent (Brunet et al., 2002). For example, growth factor-stimulation first leads to the phosphorylation of the transcription factor FKHRL1 at its 14-3-3 binding site within the nucleus and then FKHRL1 is exported to the cytoplasm. Therefore, it is possible that a residue(s) in the MIER1 α N-terminal 163aa, other than S¹⁰-P (see section 4.3.4), are phosphorylated by pERK1/2 or another downstream kinase. This phosphorylation may facilitate MIER1 α binding to 14-3-3 and CRM1, causing the complex to be exported out of the nucleus. 14-3-3 siRNA or inhibitors are commercially available products and this would facilitate future research on whether this molecule plays a role as an adaptor protein between MIER1 α and CRM1. MIER1 α nuclear localization

can be studied in the presence of growth factors while 14-3-3 is knocked down or inhibited to elucidate its role in MIER1 α nuclear export.

Another possibility is that one of the IEGs regulated by the MAPK pathway is directing MIER1 α nuclear export. The first cellular response following exposure to growth factors is the induction of IEGs, representing the first major transcriptional program which leads to changes in a variety of cellular responses. The MAPK pathway is known to positively regulate IEGs, resulting in various cellular outcomes. Specifically, the MAPK signalling pathway directly activates IEG promoter-bound transcription factors (Whitmarsh, Shore, Sharrocks, & Davis, 1995), resulting in transient transcription of the IEGs (Greenberg, Greene, & Ziff, 1985) acting as the sensor of duration and strength of the input signals. For instance, Fos is one of the well known IEGs functioning as a sensor of ERK1 and ERK2 signals and its peak expression is 30 to 60 minutes after stimulation (Healy et al., 2012; O'Donnell et al., 2012). The phosphorylation of S374 and S362 of c-Fos by pERK1/2 prevents it from being degraded (Murphy, MacKeigan, & Blenis, 2004). This example suggests that there might be a NES-containing IEG product acting as a bridge molecule connecting MIER1 α to CRM1. Once growth factors are depleted in the medium and stimulation of ERK1/2 diminishes, the transiently expressed IEG would then be degraded, causing MIER1 α re-entry into the nucleus through interaction with HDAC1/2.

In summary, it is important to narrow down the molecules that can bind to N-terminal 163aa of MIER1 α and CRM1 at the same time, then test each through knock down or inhibitors to determine which one is responsible for bridging

MIER1 α and CRM1. One approach would be to analyze the CRM1-MIER1 α complex in the presence and absence of growth factors by mass spectrometry to narrow down the possible bridging molecules.

5.3 Possible mechanisms responsible for MIER1 α nuclear loss during breast cancer progression

Seven classes of MAPK intracellular signalling cascades exist and signalling through the ERK1/2 pathway has been implicated as being important in some forms of human breast cancer and breast cancer models. In our research, we included four different growth factors and they all can cause ERK1/2 activation. But ERK1/2 can be activated by a variety of stimuli, including cytokines and non-nuclear steroid hormone receptors. Up to 40% of inflammatory breast cancer over-express human Her2 which can cause the persistent activation of ERK1/2 in breast cancers (Zell, Tsang, Taylor, Mehta, & Anton-Culver, 2009).

In the IHC study in which the MIER1 α isoform showed an altered subcellular localization, the antibody used in that study could not distinguish between the MIER1 α and MIER1-3A α isoforms (McCarthy et al., 2008, Clements et al., 2012). The two alternate N-termini of MIER1 are distinct, in that one includes an additional exon (exon 3A) encoding a *bona fide* NES (Clements et al., 2012) and the other does not. The expression of MIER1 α or MIER1-3A α can result from alternative promoter usage and splicing. If MIER1 α is expressed and excluded from the nucleus during breast cancer progression, this implies that progression is coupled with the loss of MIER1 α 's nuclear function. But it could also be that MIER1 α is expressed during the

early stages of breast cancer (demonstrating nuclear localization) and that there is a switch to MIER1-3A α expression by P1 promoter usage (demonstrating non-nuclear staining) at later stages of breast cancer progression.

Alternative splicing is a mechanism which can increase protein diversity by excluding or including exons; alternatively spliced proteins may contribute to the etiology of cancer and are particularly relevant in oncology (Gardina et al., 2006). Thus, this demonstrates the importance of distinguishing the specific isoform of MIER1 α expressed during breast cancer, which might also provide a marker for different stages of breast cancer development. At the moment, there are no antibodies available that can distinguish between MIER1 α and MIER1-3A α .

DCIS is non-invasive cancer and defined as neoplastic proliferation of epithelial cells confined in the milk ducts in the breast. It is considered a non-obligate precursor of invasive breast cancer. MCF7, ER⁺ cell line, is epithelial-like adenocarcinoma breast cancer cell line and is a popular choice for research for ER positive breast cancer cell experiments (Comsa, Cimpean, & Raica, 2015). In my research, MIER1 α contains a LXXLL motif, which has the potential to interact with ER α to regulate cellular function. Combine with the previous finding that 51% of MIER1 α isoform localized in the nucleus in DCIS biopsies (McCarthy et al., 2008), MCF7 cell line supports as a good model to study the nucleocytoplasmic shuttling of MIER1 α .

5.4 Functional implication of MIER1 α nuclear loss

Tumour suppressors involved in cancer pathogenesis have been extensively investigated in past decades. Tumour suppressors can promote tumour formation through point mutation or deletion which abolishes their proper function in normal cells. Initially, Knudson proposed that the tumour suppressor retinoblastoma (RB) gene played a role in tumorigenesis when both alleles were impaired (Knudson, 1971). Later, data collected on non-hereditary tumours clearly demonstrated that the role of tumour suppressors in cancer is much more complicated (Berger, Knudson, & Pandolfi, 2011). The function of tumour suppressors can be modulated by subtle dosage variations at the protein expression level, proper cellular compartmentalization and PTMs (Correia, Gírio, Antunes, Martins, & Barata, 2014; Leslie & Foti, 2011). MIER1 α acts as a tumour suppressor in the nucleus, but when it is exported to the cytoplasm, it is not known whether the only effect is loss of its transcriptional repressor function because of the change of location or whether it gains a non-genomic function in the cytoplasm.

Many important tumour suppressors and transcription regulators regulate cell growth and apoptosis by localizing in the nucleus leading to uncontrolled growth and the onset of disease, while cytoplasmic localization can serve as an inactivation mechanism (Vousden & Woude, 2000). For instance, BCR-ABL promotes the sequestration and inactivation of p53 in the cytoplasm through I κ B α (Crivellaro et al., 2015). The mislocalization of p53 is associated with impaired function, which reflects on the markedly reduced expression of the p21 mRNA level (Crivellaro et al., 2015). Mislocalization of tumour suppressors not only makes them

lose their nuclear function, but they might gain function as an oncogene in the cytoplasm. For instance, p27 acts as a tumour suppressor promoting cell cycle regulation when localized in the nucleus, while cytoplasmic p27 increases oncogenicity in melanoma and breast cancer xenograft models acting as an oncogene (Agarwal, Mackenzie, & Deininger, 2014). Therefore, the aberrant localization of MIER1 α might also result in a non-genomic and oncogenic function in the cytosol.

One limit to investigating the non-genomic function of MIER1 α is that the transient activation of MAPK cannot be sustained and MIER1 α returns to the nucleus. Hormones and growth factors themselves have multiple effects in the cell; therefore, it would be difficult to determine which, if any, are due to mislocalization of MIER1 α . Hence, the inclusion of MIER1-3A α isoform in a future investigation may help to solve this problem. The biological effect caused by expressing MIER1-3A α might mimic the effect caused by MIER1 α when localized in the cytoplasm, as they only differ in the N-terminal 20aa. For example, it was shown that MIER1 α can suppress anchorage independent growth of T47D cells (McCarthy et al., 2008); hence, if MIER1-3A α expression can promote this growth, this effect would provide evidence for an oncogenic function of cytoplasmic MIER1 α . However, it has to be kept in mind that even a single amino acid mutation may cause dramatic functional change of a protein. Cytoplasmic MIER1-3A α may have a different function compared with cytoplasmic MIER1 α as the 3A exon encodes a 20 amino acid sequence. Except for the ⁷FTDCLWTLFL¹⁶ aa NES contained in this 20 amino acid sequence, the presence of other potentially functional domains in this 3A exon is not

known. An alternative way is to use a mutant MEK1 in which S218 and S222 are replaced by D (Aspartate), causing it to be constitutively active, as measured by phosphorylation and activation of pERK1/2 (Lemieux et al., 2009; Pages, Brunet, Allemain, & Pouyssegur, 1994). Theoretically, sustained expression of MEK1(S218D/S222D) would maintain MAPK pathway activation and in theory, MIER1 α would be continuously exported out of the nucleus. This provides an alternative means of studying non-genomic function of MIER1 α .

5.5 The potential role of MIER1 in breast cancer subtype development

In general, the MIER1 α isoform is expressed mainly in endocrine or endocrine-response human tissues, including ovary, breast tissue, testes and the pancreas but not the thyroid gland (McCarthy, Paterno, & Gillespie, 2013). The ovarian oocytes are stained in both the nucleus and cytoplasm, while only cytoplasm is stained in the follicular cells. Germinal epithelia ovarian cells show both cytoplasmic and nuclear staining. In breast tissue, the epithelial cells show exclusively nuclear staining of MIER1 α . The tissue-specific expression of α isoform implies that function of MIER1 α is mainly involved in endocrine-related organs.

ER⁺ breast cancers account for 70% of all types of breast cancers and are sensitive to estrogen as estrogen can fuel breast cancer growth. Estrogen mainly produced by the ovaries, affects the growth, differentiation, and function of the mammary gland. Bierne *et al.* (2016) showed that the combined knockdown of MIER1 and MIER3 increased ER α expression, which means MIER family members

may compensate for the functional loss of each other and suppress the expression of ER α .

In addition to estrogen, progesterone is another hormone that is released by the ovaries and is also involved in breast cancer development, by binding to its receptor. The role of estrogen as a potent breast mitogen is undisputed. The progesterone receptor (PR) is another driver of early breast cancer progression. The gene encoding the PR, contains a RNA PolII binding site at the promoter and two ER α binding site upstream of the gene and estrogen is usually required to induce the expression of PR in ER $^+$ cells (Carroll et al., 2006). As a consequence, PR expression is significantly increased in MIER1/3-knockdown cells; however, the expression of another hormone receptor, androgen receptor, was not affected (Lakisic et al., 2016).

ER α^+ and PR $^+$ breast cancer belong to the Luminal A or B types. One of the therapies for ER $^+$ breast cancers involves treatment with Tamoxifen. Therefore, it would be interesting to determine MIER1 α localization in the presence of Tamoxifen. The up-regulated expression of ER α and PR caused by knockdown MIER1/3 implies that the MIER family plays an important role in breast cancer subtype development. It is reported PR expression cannot be induced in response to estrogen unless EGF is present in mice mammary glands (Ankrapp, Bennett, & Haslam, 1998). In our research, the presence of EGF causes MIER1 α nuclear export through MAPK activation. To summarize, MIER1/3 knockdown causes ER α elevated expression; ER α elevated expression further up-regulates PR expression level when EGF is

present; and the presence of EGF activates MAPK directed MIER1 α nuclear export. Therefore, it is possible that MIER1&3 together may regulate the subtype development of breast cancer by regulating the expression of ER α and PR. Furthermore, growth factors may also have a role in this process as they regulate the subcellular distribution of MIER1 α . Further investigation could involve examination of MIER3 localization in the presence of growth factors. If both MIER1 and MIER3 can be exported out of the nucleus, the expression of ER α is proposed to be upregulated, as is PR expression. This provides information on how MIER1 and 3 might cooperate together to regulate breast cancer subtype development.

5.6 Conclusion

The study of MIER1 α nucleocytoplasmic shuttling mechanism has provided some new insights into how it may be involved in breast cancer development. Investigation into the regulation of the nuclear import of MIER1 α in breast carcinoma MCF7 cells shows that the ELM2 domain targets it to the nucleus through a piggyback mechanism by interacting with HDAC1/2. The highly conserved residue ²¹⁴W may provide as an import interaction site between MIER1 α and HDAC1/2. The growth factor-dependent activation of MAPK regulates MIER1 α nuclear export through the N-terminal sequence containing acidic stretches, which possibly inactivates MIER1 α function as a transcriptional repressor by altering subcellular localization. Thus, it is likely that MIER1 α links signal transduction and transcription. Although ER α does not regulate MIER1 α subcellular distribution, the role of MIER1 α regulation on breast cancer subtype development cannot be

neglected. MIER1 α nuclear loss may contribute to ER α and PR elevated expression, a consistent feature of some subtypes of breast cancer.

Eukaryotic cells are divided into various morphologically and functionally distinct compartments by the lipid bilayer membrane. This division not only ensures the morphology of organelles but also the proper functioning of proteins. To prevent aberrant expression of genes and assure their normal function in the cells, proteins must be targeted to the appropriate compartment to ensure functional cellular homeostasis. Proper localization secures the regulated pathways governing fundamental physiological processes that, when altered or dysregulated, promote survival, proliferation, and cellular growth. Therefore, understanding the mechanism of protein subcellular localization not only helps reveal the function of individual proteins but also the organization of the cell as a whole.

REFERENCES

- Aasland, R., Stewart, A. F., & Gibson, T. (1996). The SANT domain: A putative DNA binding domain in the SWI-SNF and ADA complexes, the transcriptional co-repressor N-CoR and TFIIB. *Trends in Biochemical Sciences*, 21(3), 87–88. [http://doi.org/10.1016/0968-0004\(96\)30009-1](http://doi.org/10.1016/0968-0004(96)30009-1)
- Adam, S. A. (2001). The nuclear pore complex. *The Journal of Cell Biology*, 2(9), 977–984. <http://doi.org/10.1146/annurev.bi.64.070195>
- Agarwal, A., Mackenzie, R. J., & Deininger, M. W. (2014). BCR-ABL1 promotes leukemia by converting p27 into a cytoplasmic oncoprotein Materials and methods Patient samples and cell lines Immunoblot analysis MEFs and retroviral infection Lentiviral infection In vitro transformation and BM transplantation assays R. *Blood*, 124, 1–13.
- Alberts. (2008). Tumor Suppressor Genes and Oncogenes : Genes that Prevent and Cause Cancer. *Molecular Biology of the Cell; 5th Edition, Garland Science*, Chapter 20; Cancer, pp.1230–1256.
- Alexandropoulos, K., & Baltimore, D. (1996). Coordinate activation of c-Src by SH3-and SH2-binding sites on a novel, p130(Cas)-related protein, Sin. *Genes and Development*, 10(11), 1341–1355. <http://doi.org/10.1101/gad.10.11.1341>
- Altomare, D. A., & Testa, J. R. (2005). Perturbations of the AKT signaling pathway in human cancer. *Oncogene*, 24(50), 7455–7464. <http://doi.org/10.1038/sj.onc.1209085>
- An, J.-M. Z. and J. (2009). Cytokines, Inflammation and Pain. *Int Anesthesiol Clin.*, 69(2), 482–489. <http://doi.org/10.1097/AIA.0b013e318034194e.Cytokines>
- Ankrapp, D. P., Bennett, J. M., & Haslam, S. Z. (1998). Role of epidermal growth factor in the acquisition of ovarian steroid hormone responsiveness in the normal mouse mammary gland. *Journal of Cellular Physiology*, 174(2), 251–260. [http://doi.org/10.1002/\(SICI\)1097-4652\(199802\)174:2<251::AID-JCP12>3.0.CO;2-F](http://doi.org/10.1002/(SICI)1097-4652(199802)174:2<251::AID-JCP12>3.0.CO;2-F) [pii]r10.1002/(SICI)1097-4652(199802)174:2<251::AID-JCP12>3.0.CO;2-F
- Appen, V., & Beck. (2016). Structure Determination of the Nuclear Pore Complex with Three-Dimensional Cryo electron Microscopy. *Journal of Molecular Biology*, 428(10), 2001–2010. <http://doi.org/10.1016/j.jmb.2016.01.004>
- Asally, M., & Yoneda, Y. (2005). beta-Catenin can act as a nuclear import receptor for its partner transcription factor, lymphocyte enhancer factor-1 (lef-1). *Experimental Cell Research*, 308(2), 357–363. <http://doi.org/10.1016/j.yexcr.2005.05.011>
- ATCC. (n.d.). Mcf7 (atcc ® htb 22™), 3–5.
- Azmi, A. S., & Mohammad, R. M. (2016). Targeting Cancer at the Nuclear Pore. *J. Clin. Oncol.*, 34(34), JCO.2016.67.5637. <http://doi.org/10.1200/JCO.2016.67.5637>
- Bahrami, S., & Drablø, F. (2016). Gene regulation in the immediate-early response process. *Advances in Biological Regulation*, 62(7491), 37–49. <http://doi.org/10.1016/j.jbior.2016.05.001>
- Banach-Orlowska, M., Pilecka, I., Torun, A., Pyrzynska, B., & Miaczynska, M. (2009). Functional characterization of the interactions between endosomal adaptor protein APPL1 and the NuRD co-repressor complex. *The Biochemical Journal*, 423(3), 389–400. <http://doi.org/10.1042/BJ20090086>

- Bankhead, P. (2014). Analyzing fluorescence microscopy images with ImageJ. *ImageJ*, (May), 1–195. <http://doi.org/10.1109/NER.2015.7146654>
- Bantscheff, M., Hopf, C., Savitski, M. M., Dittmann, A., Grandi, P., Michon, A. M., ... Drewes, G. (2011). Chemoproteomics profiling of HDAC inhibitors reveals selective targeting of HDAC complexes. *Nat Biotechnol*, 29(3), 255–265. <http://doi.org/10.1038/nbt.1759>
- Beck, M., & Hurt, and E. (2016). The nuclear pore complex: understanding its function through structural insight. *Nature Reviews Molecular Cell Biology*, 18(2), 73–89. <http://doi.org/10.1038/nrm.2016.147>
- Beenken, A., & Mohammadi, M. (2009). The FGF family: biology, pathophysiology and therapy. *Nature Reviews. Drug Discovery*, 8(3), 235–53. <http://doi.org/10.1038/nrd2792>
- Belfiore, A., & Frasca, F. (2008). IGF and insulin receptor signaling in breast cancer. *Journal of Mammary Gland Biology and Neoplasia*, 13(4), 381–406. <http://doi.org/10.1007/s10911-008-9099-z>
- Bentel, J. M., Lebowitz, D. E., Cullen, K. J., Rubin, M. S., Rosen, N., Mendelsohn, J., & Miller Jr., W. H. (1995). Insulin-like growth factors modulate the growth inhibitory effects of retinoic acid on MCF-7 breast cancer cells. *Journal of Cellular Physiology*, 165(0021–9541; 0021–9541; 1), 212–221. <http://doi.org/10.1002/jcp.1041650124>
- Berg, T., Cohen, S. B., Desharnais, J., Sonderegger, C., Maslyar, D. J., Goldberg, J., ... Vogt, P. K. (2002). Small-molecule antagonists of Myc/Max dimerization inhibit Myc-induced transformation of chicken embryo fibroblasts. *Proceedings of the National Academy of Sciences of the United States of America*, 99, 3830–3835. <http://doi.org/10.1073/pnas.062036999>
- Berger, Knudson, & Pandolfi. (2011). A Continuum Model for Tumour Suppression. *Nature*, 144(5), 724–732. <http://doi.org/10.1038/jid.2014.371>
- Besson, A., Dowdy, S. F., & Roberts, J. M. (2008). CDK Inhibitors: Cell Cycle Regulators and Beyond. *Developmental Cell*, 14(2), 159–169. <http://doi.org/10.1016/j.devcel.2008.01.013>
- Bian, Y., Song, C., Cheng, K., Dong, M., Wang, F., Huang, J., ... Zou, H. (2014). An enzyme assisted RP-RPLC approach for in-depth analysis of human liver phosphoproteome. *Journal of Proteomics*, 96, 253–262. <http://doi.org/10.1016/j.jprot.2013.11.014>
- Blackmore, Mercer, Paterno, & Gillespie. (2008). The transcriptional cofactor MIER1-beta negatively regulates histone acetyltransferase activity of the CREB-binding protein. *BMC Research Notes*, 1, 68. <http://doi.org/10.1186/1756-0500-1-68>
- Blows, F. M., Driver, K. E., Schmidt, M. K., Broeks, A., van Leeuwen, F. E., Wesseling, J., ... Huntsman, D. (2010). Subtyping of breast cancer by immunohistochemistry to investigate a relationship between subtype and short and long term survival: A collaborative analysis of data for 10,159 cases from 12 studies. *PLoS Medicine*, 7(5). <http://doi.org/10.1371/journal.pmed.1000279>
- Boonyaratanakornkit, V., & Edwards, D. P. (2007). Receptor mechanisms mediating non-genomic actions of sex steroids. *Seminars in Reproductive Medicine*.
- Brady, N., Chuntova, P., Bade, L. K., & Schwertfeger, K. L. (2013). The FGF/FGFR axis as a therapeutic target in breast cancer. *Expert Review of Endocrinology & Metabolism*, 8(4), 391–402. <http://doi.org/10.1586/17446651.2013.811910>

- Brazil, D. P., & Hemmings, B. A. (2001). Ten years of protein kinase B signalling: A hard Akt to follow. *Trends in Biochemical Sciences*, 26(11), 657–664. [http://doi.org/10.1016/S0968-0004\(01\)01958-2](http://doi.org/10.1016/S0968-0004(01)01958-2)
- Brunet, A., Datta, S. R., & Greenberg, M. E. (2001). Transcription-dependent and -independent control of neuronal survival by the PI3K-Akt signaling pathway. *Current Opinion in Neurobiology*, 11(3), 297–305. [http://doi.org/10.1016/S0959-4388\(00\)00211-7](http://doi.org/10.1016/S0959-4388(00)00211-7)
- Brunet, A., Kanai, F., Stehn, J., Xu, J., Sarbassova, D., Frangioni, J. V., ... Yaffe, M. B. (2002). 14-3-3 Transits To the Nucleus and Participates in Dynamic Nucleocytoplasmic Transport. *Journal of Cell Biology*, 156(5), 817–828. <http://doi.org/10.1083/jcb.200112059>
- Bülow, M. H., Bülow, T. R., Hoch, M., Pankratz, M. J., & Jünger, M. a. (2014). Src tyrosine kinase signaling antagonizes nuclear localization of FOXO and inhibits its transcription factor activity. *Scientific Reports*, 4, 4048. <http://doi.org/10.1038/srep04048>
- Burningham, Hashibe, Spector, & Schiffman. (2012). The Epidemiology of Sarcoma. *Clinical Sarcoma Research*, 2(1), 14. <http://doi.org/10.1186/2045-3329-2-14>
- Canadian Cancer Society. (2015). Canadian Cancer Statistics Special topic : Predictions of the future burden of cancer in Canada. *Public Health Agency of Canada*, 1–151. <http://doi.org/Canadian Cancer Society>
- Canadian Cancer Society. (2017). Canadian Cancer Statistics 2017. *Canadian Cancer Society, 2017*, 1–132. <http://doi.org/0835-2976>
- Carlson, S. M., Chouinard, C. R., Labadorf, A., Lam, C. J., Schmelzle, K., Fraenkel, E., & White, F. M. (2011). Large-Scale Discovery of ERK2 Substrates Identifies ERK-Mediated Transcriptional Regulation by ETV3. *Science Signaling*, 4(196), rs11-rs11. Retrieved from <http://www.pubmedcentral.nih.gov/articlerender.fcgi?artid=3779841&tool=pmcentrez&rendertype=abstract>
- Carnero, A., & Paramio, J. M. (2014). The PTEN/PI3K/AKT Pathway in vivo, Cancer Mouse Models. *Frontiers in Oncology*, 4(October). <http://doi.org/10.3389/fonc.2014.00252>
- Carpinteri, S. (2012). Optimizing DNA Vaccines Against Nuclear Oncogenes. *ImmunoGastroenterology*, 1(2), 108. <http://doi.org/10.7178/ig.19>
- Carroll, J. S., Meyer, C. A., Song, J., Li, W., Geistlinger, T. R., Eeckhoute, J., ... Brown, M. (2006). Genome-wide analysis of estrogen receptor binding sites. *Nat Genet*, 38(11), 1289–1297. <http://doi.org/10.1038/ng1901>
- Cassar, N., Bender, M. L., Barnett, B. A., Fan, S., Moxim, W. J., Ii, H. L., & Tilbrook, B. (2007). Reports 10., 219(2005), 2005–2008.
- Cautain, Hill, Pedro, & Link. (2015). Components and regulation of nuclear transport processes. *FEBS Journal*, 282(3), 445–462. <http://doi.org/10.1111/febs.13163>
- Cesareni, G., Panni, S., Nardelli, G., & Castagnoli, L. (2002). Can we infer peptide recognition specificity mediated by SH3 domains? *FEBS Letters*, 513(1), 38–44. [http://doi.org/10.1016/S0014-5793\(01\)03307-5](http://doi.org/10.1016/S0014-5793(01)03307-5)
- Chook, Y. M., & Blobel, G. (1999). Structure of the nuclear transport complex karyopherin-beta2-Ran x GppNHp. *Nature*, 399(6733), 230–7. <http://doi.org/10.1038/20375>

- Christopoulos, P. F., Msaouel, P., & Koutsilieris, M. (2015). The role of the insulin-like growth factor-1 system in breast cancer. *Molecular Cancer*, *14*, 43. <http://doi.org/10.1186/s12943-015-0291-7>
- Cingolani, G., Petosa, C., Weis, K., & Müller, C. W. (1999). Structure of importin-beta bound to the IBB domain of importin-alpha. *Nature*, *399*, 221–229. <http://doi.org/10.1038/20367>
- Clements, Mercer, Paterno, & Gillespie. (2012). Differential splicing alters subcellular localization of the alpha but not beta isoform of the mier1 transcriptional regulator in breast cancer cells. *PLoS ONE*, *7*(2). <http://doi.org/10.1371/journal.pone.0032499>
- Comsa, Cimpean, & Raica. (2015). The story of MCF-7 breast cancer cell line: 40 Years of experience in research. *Anticancer Research*, *35*(6), 3147–3154.
- Conforti, F., Wang, Y., Rodriguez, J. A., Alberobello, A. T., Zhang, Y.-W., & Giaccone, G. (2015). Molecular Pathways: Anticancer Activity by Inhibition of Nucleocytoplasmic Shuttling. *Clinical Cancer Research : An Official Journal of the American Association for Cancer Research*, *21*(20), 4508–13. <http://doi.org/10.1158/1078-0432.CCR-15-0408>
- Conti, E., & Kuriyan, J. (2000). Crystallographic analysis of the specific yet versatile recognition of distinct nuclear localization signals by karyopherin ?? *Structure*, *8*(3), 329–338. [http://doi.org/10.1016/S0969-2126\(00\)00107-6](http://doi.org/10.1016/S0969-2126(00)00107-6)
- Conti, Uy, Leighton, Blobel, & Kuriyan. (1998). Crystallographic analysis of the recognition of a nuclear localization signal by the nuclear import factor karyopherin α . *Cell*, *94*(2), 193–204. [http://doi.org/10.1016/S0092-8674\(00\)81419-1](http://doi.org/10.1016/S0092-8674(00)81419-1)
- Cooper, G. M., & Hausman, R. E. (2000). *The Cell: A Molecular Approach* 2nd Edition. *Sinauer Associates*.
- Correia, N. C., G rí o, A., Antunes, I., Martins, L. R., & Barata, J. T. (2014). The multiple layers of non-genetic regulation of PTEN tumour suppressor activity. *European Journal of Cancer*, *50*(1), 216–225. <http://doi.org/10.1016/j.ejca.2013.08.017>
- Cour, L., Kierner, Mølgaard, Gupta, Skriver, & Brunak. (2004). Analysis and prediction of leucine-rich nuclear export signals. *Protein Engineering, Design and Selection*, *17*(6), 527–536. <http://doi.org/10.1093/protein/gzh062>
- Crivellaro, S., Panuzzo, C., Carrà, G., Volpengo, A., Crasto, F., Gottardi, E., ... Guerrasio, A. (2015). Non genomic loss of function of tumor suppressors in CML : BCR-ABL promotes I κ B α mediated p53 nuclear exclusion. *Oncotarget*, *6*(28). <http://doi.org/10.18632/oncotarget.4611>
- Crowell, J. A., Steele, V. E., & Fay, J. R. (2007). Targeting the AKT protein kinase for cancer chemoprevention. *Molecular Cancer Therapeutics*, *6*(8), 2139–2148. <http://doi.org/10.1158/1535-7163.MCT-07-0120>
- Cullen, B. R. (2003). Nuclear mRNA export: Insights from virology. *Trends in Biochemical Sciences*, *28*(8), 419–424. [http://doi.org/10.1016/S0968-0004\(03\)00142-7](http://doi.org/10.1016/S0968-0004(03)00142-7)
- Cyert, M. S. (2001). Regulation of Nuclear Localization during Signaling. *Journal of Biological Chemistry*, *276*(24), 20805–20808. <http://doi.org/10.1074/jbc.R100012200>
- Delaleau, M., & Borden, K. L. B. (2015). Multiple Export Mechanisms for mRNAs. *Cells*, *4*(3), 452–73. <http://doi.org/10.3390/cells4030452>
- Delcuve, G. P., Khan, D. H., & Davie, J. R. (2012). Roles of histone deacetylases in

- epigenetic regulation: emerging paradigms from studies with inhibitors. *Clinical Epigenetics*, 4(1), 5. <http://doi.org/10.1186/1868-7083-4-5>
- Dephoure, N., Zhou, C., Villén, J., Beausoleil, S. A., Bakalarski, C. E., Elledge, S. J., & Gygi, S. P. (2008). A quantitative atlas of mitotic phosphorylation. *Proc Natl Acad Sci U S A*, 105(31), 10762–10767. <http://doi.org/10.1073/pnas.0805139105>
- Dhillon, A. S., Hagan, S., Rath, O., & Kolch, W. (2007). MAP kinase signalling pathways in cancer. *Oncogene*, 26(22), 3279–90. <http://doi.org/10.1038/sj.onc.1210421>
- Ding, Z., Gillespie, L. L., Mercer, F. C., & Paterno, G. D. (2004). The SANT domain of human MI-ER1 interacts with Sp1 to interfere with GC box recognition and repress transcription from its own promoter. *Journal of Biological Chemistry*, 279(27), 28009–28016. <http://doi.org/10.1074/jbc.M403793200>
- Ding, Gillespie, & Paterno. (2003). Human MI-ER1 alpha and beta function as transcriptional repressors by recruitment of histone deacetylase 1 to their conserved ELM2 domain. *Molecular and Cellular Biology*, 23(1), 250–258. <http://doi.org/10.1128/MCB.23.1.250-258.2003>
- Dingwall, & Laskey. (1991). Nuclear targeting sequences - a consensus? *Trends in Biochemical Sciences*, 16(C), 478–481.
- Dingwall, Robbins, Dilworth, Roberts, & Richardson. (1988). The nucleoplasmic nuclear location sequence is larger and more complex than that of SV-40 large T antigen. *Journal of Cell Biology*, 107(3), 841–849. <http://doi.org/10.1083/jcb.107.3.841>
- Dolle, Yazidi-Belkoura, EAdriaenssens, Nurcombe, & Hondermarck. (2003). Nerve growth factor overexpression and autocrine loop in breast cancer cells. *Oncogene*, 22(36), 5592–5601. <http://doi.org/10.1038/sj.onc.1206805>
- Esther Witsch, Michael Sela, and Y. Y. (2010). Roles for Growth Factors in Cancer Progression. *Physiology*, 25: 85–101, 85–101. <http://doi.org/10.1152/physiol.00045.2009>
- Fagotto, F., Gluck, U., & Gumbiner, B. M. (1998). Nuclear localization signal-independent and importin/karyopherin-independent nuclear import of beta-catenin. *Curr Biol*, 8(4), 181–190. [http://doi.org/10.1016/S0960-9822\(98\)70082-X](http://doi.org/10.1016/S0960-9822(98)70082-X)
- Favata, M. F., Horiuchi, K. Y., Manos, E. J., Daulerio, A. J., Stradley, D. A., Feeser, W. S., ... Trzaskos, J. M. (1998). Identification of a Novel Inhibitor of Mitogen-Activated Protein Kinase Kinase. *The Journal of Biological Chemistry*, 273(29), 18623–18632. <http://doi.org/9660836>
- Fischer, U., Sch äuble, N., Sch üt z, S., Altvater, M., Chang, Y., Faza, M. B., & Panse, V. G. (2015). A non-canonical mechanism for Crm1- export cargo complex assembly. *eLife*, 2015(4), 1–20. <http://doi.org/10.7554/eLife.05745>
- Fontes, M. R., Teh, T., & Kobe, B. (2000). Structural basis of recognition of monopartite and bipartite nuclear localization sequences by mammalian importin-alpha. *Journal of Molecular Biology*, 297(5), 1183–94. <http://doi.org/10.1006/jmbi.2000.3642>
- Fowler, T., Sen, R., & Roy, A. L. (2011). Regulation of Primary Response Genes. *Molecular Cell*, 44(3), 348–360. <http://doi.org/10.1016/j.molcel.2011.09.014>
- Freitas, N., & Cunha, C. (2009). Mechanisms and Signals for the Nuclear Import of Proteins, 550–557.
- Fung, H. Y. J., Fu, S. C., Brautigam, C. A., & Chook, Y. M. (2015). Structural determinants of nuclear export signal orientation in binding to exportin CRM1. *eLife*,

- 4(September 2015), 1–19. <http://doi.org/10.7554/eLife.10034>
- Garber, P. M., Vidanes, G. M., & Toczyski, D. P. (2005). Damage in transition. *Trends in Biochemical Sciences*, 30(2), 63–66. <http://doi.org/10.1016/j.tibs.2004.12.004>
- Gardina, P. J., Clark, T. a, Shimada, B., Staples, M. K., Yang, Q., Veitch, J., ... Turpaz, Y. (2006). Alternative splicing and differential gene expression in colon cancer detected by a whole genome exon array. *BMC Genomics*, 7, 325. <http://doi.org/10.1186/1471-2164-7-325>
- Geertz, & Maerkl. (2010). Experimental strategies for studying transcription factor-DNA binding specificities. *Briefings in Functional Genomics*, 9(5–6), 362–373. <http://doi.org/10.1093/bfpg/elq023>
- Gonda, T. J., & Ramsay, R. G. (2015). Directly targeting transcriptional dysregulation in cancer. *Nature Reviews Cancer*, 15(11), 686–694. <http://doi.org/10.1038/nrc4018>
- Gonzalez, F. A., Raden, D. L., & Davis, R. J. (1991). Identification of substrate recognition determinants for human ERK1 and ERK2 protein kinases. *Journal of Biological Chemistry*, 266(33), 22159–22163.
- Goustin, A. S., Leof, E. B., Shipley, G. D., & Moses, H. L. (1986). Growth Factors and Cancer1, 46(March), 1015–1029.
- Gravina, G., Senapedis, W., McCauley, D., Baloglu, E., Shacham, S., & Festuccia, C. (2014). Nucleo-cytoplasmic transport as a therapeutic target of cancer. *Journal of Hematology & Oncology*, 7(1), 85. <http://doi.org/10.1186/s13045-014-0085-1>
- Grazul-Bilska, A. T., Johnson, M. L., Bilski, J. J., Redmer, D. A., Reynolds, L. P., Abdullah, A., & Abdullah, K. M. (2003). Wound healing: the role of growth factors. *Drugs of Today (Barcelona, Spain : 1998)*, 39(10), 787–800. Retrieved from <http://www.ncbi.nlm.nih.gov/pubmed/14668934>
- Greenberg, M. E., Greene, L. A., & Ziff, E. B. (1985). Nerve growth factor and epidermal growth factor induce rapid transient changes in proto-oncogene transcription in PC12 cells. *Journal of Biological Chemistry*, 260(26), 14101–14110.
- Greer, E. L., & Brunet, A. (2005). FOXO transcription factors at the interface between longevity and tumor suppression. *Oncogene*, 24(50), 7410–7425. <http://doi.org/10.1038/sj.onc.1209086>
- Gregoretti, I. V., Lee, Y. M., & Goodson, H. V. (2004). Molecular evolution of the histone deacetylase family: Functional implications of phylogenetic analysis. *Journal of Molecular Biology*, 338(1), 17–31. <http://doi.org/10.1016/j.jmb.2004.02.006>
- Grose, R., & Dickson, C. (2005). Fibroblast growth factor signaling in tumorigenesis. *Cytokine & Growth Factor Reviews*, 16(2), 179–186. <http://doi.org/10.1016/j.cytogfr.2005.01.003>
- Grüne, T., Brzeski, J., Eberharter, A., Clapier, C. R., Corona, D. F. V, Becker, P. B., & Müller, C. W. (2003). Crystal structure and functional analysis of a nucleosome recognition module of the remodeling factor ISWI. *Molecular Cell*, 12(2), 449–460. [http://doi.org/10.1016/S1097-2765\(03\)00273-9](http://doi.org/10.1016/S1097-2765(03)00273-9)
- Grünwald, D., Singer, R. H., & Rout, M. (2011). Nuclear export dynamics of RNA–protein complexes. *Nature*, 475(7356), 333–341. <http://doi.org/10.1038/nature10318>
- Guenther, M. G., Lane, W. S., Fischle, W., Verdin, E., Lazar, M. A., & Shiekhhattar, R. (2000). A core SMRT corepressor complex containing HDAC3 and TBL1, a WD40-repeat protein linked to deafness. *Genes and Development*, 14(9), 1048–1057.

<http://doi.org/10.1101/gad.14.9.1048>

- Haberland, M., Montgomery, R. L., & Olson, E. N. (2009). The many roles of histone deacetylases in development and physiology: implications for disease and therapy. *Nature Reviews. Genetics*, *10*(1), 32–42. <http://doi.org/10.1038/nrg2485>
- Hahn, S. (2005). Machinery, *11*(5), 394–403. <http://doi.org/10.1038/nsmb763>
- Hanahan, D., & Weinberg, R. A. (2000). The Hallmarks of Cancer Review. *Cell*, *100*, 57–70. [http://doi.org/10.1016/S0092-8674\(00\)81683-9](http://doi.org/10.1016/S0092-8674(00)81683-9)
- Hanahan, D., & Weinberg, R. A. (2011). Hallmarks of cancer: The next generation. *Cell*, *144*(5), 646–674. <http://doi.org/10.1016/j.cell.2011.02.013>
- Healy, S., Khan, P., & Davie, J. R. (2012). Immediate early response genes and cell transformation. *Pharmacology & Therapeutics*, *137*(1), 64–77. <http://doi.org/10.1016/j.pharmthera.2012.09.001>
- Heery, D., Kalkhoven, E., Hoare, S., & Parker, M. G. (1997). A signature motif in transcriptional co-activators mediates binding to nuclear receptors. *Nature*, *387*(1990), 733–736. <http://doi.org/10.1038/42750>
- Heery, Hoare, Hussain, Parker, & Sheppard. (2001). Core LXXLL Motif Sequences in CREB-binding Protein, SRC1, and RIP140 Define Affinity and Selectivity for Steroid and Retinoid Receptors. *Journal of Biological Chemistry*, *276*(9), 6695–6702. <http://doi.org/10.1074/jbc.M009404200>
- Hemmings, B. A., & Restuccia, D. F. (2012). PI3K-PKB / Akt Pathway, 1–4. <http://doi.org/10.1101/cshperspect.a011189>
- Hendriks, I. A., Souza, R. C. J. D., Yang, B., Vries, M. V., & Vertegaal, A. C. O. (2015). Europe PMC Funders Group Uncovering Global SUMOylation Signaling Networks in a Site-Specific Manner, *21*(10), 927–936. <http://doi.org/10.1038/nsmb.2890.Uncovering>
- Hettenbach, S., & Herman, M. (1999). The control of cell polarity and cell migration in *C. elegans* by WNT signaling and a protein similar to a metastasis-associated factor. *International C. Elegans Meeting*, *1064*, 1055–1064.
- Hill, R., Cautain, B., de Pedro, N., & Link, W. (2014). Targeting nucleocytoplasmic transport in cancer therapy. *Oncotarget*, *5*(1), 11–28. <http://doi.org/10.18632/oncotarget.1457>
- Ho, J. H., Kallstrom, G., & Johnson, A. W. (2000). Nmd3p is a Crm1p-dependent adapter protein for nuclear export of the large ribosomal subunit. *The Journal of Cell Biology*, *151*(5), 1057–66. <http://doi.org/10.1083/jcb.151.5.1057>
- Hodel, M. R., Corbett, A. H., & Hodel, A. E. (2001). Dissection of a nuclear localization signal. *Journal of Biological Chemistry*, *276*(2), 1317–1325. <http://doi.org/10.1074/jbc.M008522200>
- Huang, W. Y., Yue, L., Qiu, W. S., Wang, L. W., Zhou, X. H., & Sun, Y. J. (2009). Prognostic value of CRM1 in pancreas cancer. *Clinical and Investigative Medicine*, *32*(6), 315–321.
- Hull, K. L., & Harvey, S. (2014). Growth Hormone and Reproduction: A Review of Endocrine and Autocrine/Paracrine Interactions. *International Journal of Endocrinology*, *2014*. <http://doi.org/10.1155/2014/234014>
- Hung, M.-C., & Link, W. (2011). Protein localization in disease and therapy. *Journal of Cell Science*, *124*(Pt 20), 3381–92. <http://doi.org/10.1242/jcs.089110>
- Iwamoto, T., & Pusztai, L. (2010). Predicting prognosis of breast cancer with gene

- signatures: are we lost in a sea of data? *Genome Medicine*, 2(11), 81.
<http://doi.org/10.1186/gm202>
- Jaenisch, & Bird. (2003). Epigenetic regulation of gene expression: How the genome integrates intrinsic and environmental signals. *Nature Genetics*, 33(3S), 245–254.
<http://doi.org/10.1038/ng1089>
- Joshi, P., Greco, T. M., Guise, A. J., Luo, Y., Yu, F., Nesvizhskii, A. I., & Cristea, I. M. (2014). The functional interactome landscape of the human histone deacetylase family. *Molecular Systems Biology*, 9(1), 672–672.
<http://doi.org/10.1038/msb.2013.26>
- Joshi, Greco, Guise, Luo, Yu, Nesvizhskii, & Cristea. (2013). The functional interactome landscape of the human histone deacetylase family. TL - 9. *Molecular Systems Biology*, 9 VN-re(672), 672. <http://doi.org/10.1038/msb.2013.26>
- Jr, J. E. D. (1997). STATs and Gene Regulation, 277(September).
- Juang, Y.-T., Tenbrock, K., Nambiar, M. P., Gourley, M. F., & Tsokos, G. C. (2002). Defective production of functional 98-kDa form of Elf-1 is responsible for the decreased expression of TCR zeta-chain in patients with systemic lupus erythematosus. *Journal of Immunology (Baltimore, Md. : 1950)*, 169(10), 6048–55.
<http://doi.org/10.4049/jimmunol.169.10.6048>
- Kabachinski, G., & Schwartz, T. U. (2015). The nuclear pore complex - structure and function at a glance. *Journal of Cell Science*, 128(3), 423–429.
<http://doi.org/10.1242/jcs.083246>
- Kalderon, Richardson, Markham, & Smith. (1984). Sequence requirements for nuclear location of simian virus 40 large-T antigen. *Nature*, 311, 33–38.
<http://doi.org/10.1038/311033a0>
- Kane, R., Murtagh, J., Finlay, D., Marti, A., Jaggi, R., Blatchford, D., ... Martin, F. (2002). Transcription factor NFIC undergoes N-glycosylation during early mammary gland involution. *Journal of Biological Chemistry*, 277(29), 25893–25903.
<http://doi.org/10.1074/jbc.M202469200>
- Kim, I. S., Kim, D. H., Han, S. M., Chin, M. U., Nam, H. J., Cho, H. P., ... Moon, Y. H. (2000). Truncated form of importin α identified in breast cancer cell inhibits nuclear import of p53. *Journal of Biological Chemistry*, 275(30), 23139–23145.
<http://doi.org/10.1074/jbc.M909256199>
- Knudson, A. G. (1971). Mutation and cancer: statistical study of retinoblastoma. *Proceedings of the National Academy of Sciences of the United States of America*, 68(4), 820–3. <http://doi.org/10.1073/pnas.68.4.820>
- Koyama, M., & Matsuura, Y. (2010). An allosteric mechanism to displace nuclear export cargo from CRM1 and RanGTP by RanBP1. *The EMBO Journal*, 29(12), 2002–2013. <http://doi.org/10.1038/emboj.2010.89>
- Kumar, R., Wang, R.-A., Mazumdar, A., Talukder, A. H., Mandal, M., Yang, Z., ... Vadlamudi, R. K. (2002). A naturally occurring MTA1 variant sequesters oestrogen receptor-alpha in the cytoplasm. *Nature*, 418(6898), 654–7.
<http://doi.org/10.1038/nature00889>
- Kurochkina, & Guha. (2013). SH3 domains: Modules of protein-protein interactions. *Biophysical Reviews*, 5(1), 29–39. <http://doi.org/10.1007/s12551-012-0081-z>
- la Cour, T., Gupta, R., Rapacki, K., Skriver, K., Poulsen, F. M., & Brunak, S. (2003). NESbase version 1.0: A database of nuclear export signals. *Nucleic Acids Research*,

- 31(1), 393–396. <http://doi.org/10.1093/nar/gkg101>
- Lakisic, G., Lebreton, A., Pourpre, R., Wendling, O., Libertini, E., Radford, E. J., ... Bierne, H. (2016). Role of the BAHD1 Chromatin-Repressive Complex in Placental Development and Regulation of Steroid Metabolism. *PLoS Genetics*, 12(3), 1–26. <http://doi.org/10.1371/journal.pgen.1005898>
- Lange, Mills, Lange, Stewart, Devine, & Corbett, A. H. (2007). Classical nuclear localization signals: Definition, function, and interaction with importin α . *Journal of Biological Chemistry*, 282(8), 5101–5105. <http://doi.org/10.1074/jbc.R600026200>
- Lemieux, E., Bergeron, S., Durand, V., Asselin, C., Saucier, C., & Rivard, N. (2009). Constitutively active MEK1 is sufficient to induce epithelial-to-mesenchymal transition in intestinal epithelial cells and to promote tumor invasion and metastasis. *International Journal of Cancer. Journal International Du Cancer*, 125(7), 1575–1586. <http://doi.org/10.1002/ijc.24485>
- Lemmon, M. a, & Schlessinger, J. (2011). NIH Public Access. *Biochemistry*, 141(7), 1117–1134. <http://doi.org/10.1016/j.cell.2010.06.011>.Cell
- Leslie, N. R., & Foti, M. (2011). Non-genomic loss of PTEN function in cancer: Not in my genes. *Trends in Pharmacological Sciences*, 32(3), 131–140. <http://doi.org/10.1016/j.tips.2010.12.005>
- Li, S., Paterno, G. D., & Gillespie, L. L. (2013). Nuclear localization of the transcriptional regulator MIER1a requires interaction with HDAC1/2 in breast cancer cells. *PLoS ONE*, 8(12), 1–11. <http://doi.org/10.1371/journal.pone.0084046>
- Lin, K., Hsin, H., Libina, N., & Kenyon, C. (2001). Regulation of the *Caenorhabditis elegans* longevity protein DAF-16 by insulin/IGF-1 and germline signaling. *Nature Genetics*, 28(2), 139–145. <http://doi.org/10.1038/88850>
- Liu, H., Lee, E., Reyes, A. D. L., Zapf, J. W., & Jordan, V. C. (2001). Silencing and Reactivation of the Selective Estrogen Receptor Modulator-Estrogen Receptor α Complex Silencing and Reactivation of the Selective Estrogen Receptor Modulator-Estrogen, 3632–3639.
- Lopez-Girona, A., Furnari, B., Mondesert, O., & Russell, P. (1999). Nuclear localization of Cdc25 is regulated by DNA damage and a 14-3-3 protein. *Nature*, 397(6715), 172–175. <http://doi.org/10.1038/16488>
- Lott, K., & Cingolani, G. (2011). The importin beta binding domain as a master regulator of nucleocytoplasmic transport. *Biochimica et Biophysica Acta - Molecular Cell Research*, 1813(9), 1578–1592. <http://doi.org/10.1016/j.bbamcr.2010.10.012>
- Lu, Liou, & Zhou. (2002). Pinning down phosphorylation signaling. *Trends in Cell Biology*, 12(4), 164–172.
- Luqmani, Y. a, Graham, M., & Coombes, R. C. (1992). Expression of basic fibroblast growth factor, FGFR1 and FGFR2 in normal and malignant human breast, and comparison with other normal tissues. *British Journal of Cancer*, 66(2), 273–280.
- Mains, P. E., Sulston, I. A., & Wood, W. B. (1990). Dominant maternal-effect mutations causing embryonic lethality in *Caenorhabditis elegans*. *Genetics*, 125(2), 351–369. <http://doi.org/10.1091/mbc.E05>
- Marfori, M., Mynott, A., Ellis, J. J., Mehdi, A. M., Saunders, N. F. W., Curmi, P. M., ... Kobe, B. (2011). Molecular basis for specificity of nuclear import and prediction of nuclear localization. *Biochimica et Biophysica Acta - Molecular Cell Research*, 1813(9), 1562–1577. <http://doi.org/10.1016/j.bbamcr.2010.10.013>

- McCarthy, Mercer, Savicky, Carter, Paterno, & Gillespie. (2008). Changes in subcellular localisation of MI-ER1 alpha, a novel oestrogen receptor-alpha interacting protein, is associated with breast cancer progression. *British Journal of Cancer*, 99(4), 639–46. <http://doi.org/10.1038/sj.bjc.6604518>
- McCarthy, Paterno, & Gillespie. (2013). Protein expression pattern of human MIER1 alpha, a novel estrogen receptor binding protein. *J Mol Histol*. 2013, 17(2), 281–294. <http://doi.org/10.1210/jc.2009-1990>.Glucose
- McInnes, C., & Sykes, B. D. (1997). Growth factor receptors: structure, mechanism, and drug discovery. *Biopolymers*, 43(5), 339–66. [http://doi.org/10.1002/\(SICI\)1097-0282\(1997\)43:5<339::AID-BIP2>3.0.CO;2-W](http://doi.org/10.1002/(SICI)1097-0282(1997)43:5<339::AID-BIP2>3.0.CO;2-W)
- Mendelsohn, J., Mendelsohn, J., Baselga, J., & Baselga, J. (2000). The EGF receptor family as targets for cancer therapy. *Oncogene*, 19(56), 6550–65. <http://doi.org/10.1038/sj.onc.1204082>
- Millard, C. J., Fairall, L., & Schwabe, J. W. R. (2014). Towards an understanding of the structure and function of MTA1. *Cancer and Metastasis Reviews*, 33(4), 857–867. <http://doi.org/10.1007/s10555-014-9513-5>
- Molloy, N. H., Read, D. E., & Gorman, A. M. (2011). Nerve growth factor in cancer cell death and survival. *Cancers*, 3(1), 510–530. <http://doi.org/10.3390/cancers3010510>
- Moriarty, K., Kim, K. H., & Bender, J. R. (2006). Minireview: Estrogen receptor-mediated rapid signaling. *Endocrinology*, 147(12), 5557–5563. <http://doi.org/10.1210/en.2006-0729>
- Mukohara, T., Shimada, H., Ogasawara, N., Wanikawa, R., Shimomura, M., Nakatsura, T., ... Minami, H. (2009). Sensitivity of breast cancer cell lines to the novel insulin-like growth factor-1 receptor (IGF-1R) inhibitor NVP-AEW541 is dependent on the level of IRS-1 expression. *Cancer Letters*, 282(1), 14–24. <http://doi.org/10.1016/j.canlet.2009.02.056>
- Mulligan, P., Westbrook, T. F., Ottinger, M., Pavlova, N., Chang, B., Macia, E., ... Shi, Y. (2008). CDYL Bridges REST and Histone Methyltransferases for Gene Repression and Suppression of Cellular Transformation. *Molecular Cell*, 32(5), 718–726. <http://doi.org/10.1016/j.molcel.2008.10.025>
- Murphy, L. O., MacKeigan, J. P., & Blenis, J. (2004). A network of immediate early gene products propagates subtle differences in mitogen-activated protein kinase signal amplitude and duration. *Molecular and Cellular Biology*, 24(1), 144–53. <http://doi.org/10.1128/MCB.24.1.144>
- Myong, N. H. (2012). Loss of E-cadherin and acquisition of vimentin in epithelial-mesenchymal transition are noble indicators of uterine cervix cancer progression. *Korean Journal of Pathology*, 46(4), 341–348. <http://doi.org/10.4132/KoreanJPathol.2012.46.4.341>
- Nahta, R., Hortobagyi, G. N., & Esteva, F. J. (2003). Growth factor receptors in breast cancer: potential for therapeutic intervention. *Oncologist*, 8, 5–17. <http://doi.org/DOI 10.1634/theoncologist.8-1-5>
- Naim, B., Brumfeld, V., Kapon, R., Kiss, V., Nevo, R., & Reich, Z. (2007). Passive and facilitated transport in nuclear pore complexes is largely uncoupled. *Journal of Biological Chemistry*, 282(6), 3881–3888.
- Nakai, Hung, & Yamaguchi. (2016). A perspective on anti-EGFR therapies targeting triple-negative breast cancer. *American Journal of Cancer Research*, 6(8), 1609–

1623.

- Nardozi, J. D., Lott, K., & Cingolani, G. (2010). Phosphorylation meets nuclear import: a review. *Cell Communication and Signaling : CCS*, 8(1), 32. <http://doi.org/10.1186/1478-811X-8-32>
- Nebert, D. W. (2002). Transcription factors and cancer: an overview. *Toxicology*, 181–182, 131–141.
- Nguyen, D. X., Bos, P. D., & Massagué J. (2009). Metastasis: from dissemination to organ-specific colonization. *Nature Reviews. Cancer*, 9(4), 274–84. <http://doi.org/10.1038/nrc2622>
- Noyes, M. B., Christensen, R. G., Wakabayashi, A., Stormo, G. D., Brodsky, M. H., & Wolfe, S. A. (2008). Analysis of Homeodomain Specificities Allows the Family-wide Prediction of Preferred Recognition Sites. *Cell*, 133(7), 1277–1289. <http://doi.org/10.1016/j.cell.2008.05.023>
- O'Donnell, A., Odrowaz, Z., & Sharrocks, A. D. (2012). Immediate-early gene activation by the MAPK pathways: what do and don't we know? *Biochemical Society Transactions*, 40(1), 58–66. <http://doi.org/10.1042/BST20110636>
- Olivier, M., Hollstein, M., & Hainaut, P. (2010). TP53 mutations in human cancers: origins, consequences, and clinical use. *Cold Spring Harbor Perspectives in Biology*, 2(1), 1–17. <http://doi.org/10.1101/cshperspect.a001008>
- Olsen, J. V., Blagoev, B., Gnad, F., Macek, B., Kumar, C., Mortensen, P., & Mann, M. (2006). Global, In Vivo, and Site-Specific Phosphorylation Dynamics in Signaling Networks. *Cell*, 127(3), 635–648. <http://doi.org/10.1016/j.cell.2006.09.026>
- Ordóñez-Morán, P., & Muñoz, A. (2009). Nuclear receptors: Genomic and non-genomic effects converge. *Cell Cycle*, 8(11), 1675–1680. <http://doi.org/10.4161/cc.8.11.8579>
- Ornitz, D. M., & Itoh, N. (2001). Fibroblast growth factors. *Genome Biology*, 2(3), REVIEWS3005. <http://doi.org/10.1186/gb-2001-2-3-reviews3005>
- Ortega-pe, Cano, Were, Villar, & Redondo. (2005). c-Jun N-terminal Kinase (JNK) Positively Regulates NFATc2 Transactivation through Phosphorylation within the N-terminal Regulatory Domain * □, 280(21), 20867–20878. <http://doi.org/10.1074/jbc.M501898200>
- Ossareh-Nazari, B., Bachelier, F., & Dargemont, C. (1997). Evidence for a role of CRM1 in signal-mediated nuclear protein export. *Science (New York, N.Y.)*, 278(5335), 141–144. <http://doi.org/10.1126/science.278.5335.141>
- Pages, G., Brunet, A., Allemain, G. L., & Pouyssegur, J. (1994). Constitutive mutant and putative regulatory serine phosphorylation site of mammalian MAP kinase kinase kinase . This kinase is in turn activated via Raf-1 and phosphorylation of the TEY motif , suggesting that this. *The EMBO Journal*, 13(13), 3003–3010.
- Park, M., Lee, B. S., Jeon, S. H., Nam, H. J., Lee, G., Kim, C. H., ... Lee, J. H. (2015). A novel isoform of met receptor tyrosine kinase blocks hepatocyte growth factor/met signaling and stimulates skeletal muscle cell differentiation. *Journal of Biological Chemistry*, 290(3), 1804–1817. <http://doi.org/10.1074/jbc.M114.596957>
- Patenaude, A.-M., Orthwein, A., Hu, Y., Campo, V. a, Kavli, B., Buschiazzi, A., & Di Noia, J. M. (2009). Active nuclear import and cytoplasmic retention of activation-induced deaminase. *Nature Structural & Molecular Biology*, 16(5), 517–527. <http://doi.org/10.1038/nsmb.1598>
- Paterno, Ding, Lew, Nash, Mercer, & Gillespie. (2002). Genomic organization of the

- human mi-er1 gene and characterization of alternatively spliced isoforms: Regulated use of a facultative intron determines subcellular localization. *Gene*, 295(1), 79–88. [http://doi.org/10.1016/S0378-1119\(02\)00823-5](http://doi.org/10.1016/S0378-1119(02)00823-5)
- Paterno, Li, Luchman, & Gillespie. (1997). cDNA cloning of a novel, developmentally regulated immediate early gene activated by fibroblast growth factor and encoding a nuclear protein. *The Journal of Biological Chemistry*, 272(41), 25591–25595.
- Paterno, Mercer, Chayter, Yang, Robb, & Gillespie. (1998). Molecular cloning of human er1 cDNA and its differential expression in breast tumours and tumour-derived cell lines. *Gene*, 222(1), 77–82. [http://doi.org/10.1016/S0378-1119\(98\)00473-9](http://doi.org/10.1016/S0378-1119(98)00473-9)
- Pearce, S. T., Liu, H., & Jordan, V. C. (2003). Modulation of estrogen receptor alpha function and stability by tamoxifen and a critical amino acid (Asp-538) in helix 12. *Journal of Biological Chemistry*, 278(9), 7630–7638. <http://doi.org/10.1074/jbc.M211129200>
- Pemberton, L. F., & Paschal, B. M. (2005). Mechanisms of receptor-mediated nuclear import and nuclear export. *Traffic*, 6(3), 187–198. <http://doi.org/10.1111/j.1600-0854.2005.00270.x>
- Podlaha, O., Riester, M., De, S., & Michor, F. (2012). Evolution of the cancer genome. *Trends in Genetics*, 28(4), 155–163. <http://doi.org/10.1016/j.tig.2012.01.003>
- Post, Gillespie, & Paterno. (2001). Nuclear localization signals in the Xenopus FGF embryonic early response 1 protein. *FEBS Letters*, 502(1–2), 41–5. Retrieved from <http://www.ncbi.nlm.nih.gov/pubmed/11478945>
- Powers, C. J., McLeskey, S. W., & Wellstein, A. (2000). Fibroblast growth factors, their receptors and signaling. *Endocrine-Related Cancer*, 7(3), 165–197. <http://doi.org/10.1677/erc.0.0070165>
- Ptashne, M. (2003). A New Class of Yeast Transcriptional Activators, 51, 1–7. Retrieved from http://www.sciencedirect.com/science?_ob=MIimg&_imagekey=B6WSN-4CB6KM2-5B-1&_cdi=7051&_user=4428&_orig=search&_coverDate=10/09/1987&_sk=999489998&view=c&wchp=dGLzVzz-zSkzk&md5=e9a2c8a9ccde3149925aae043bdc83a2&ie=/sdarticle.pdf
- Ray, M., Tang, R., Jiang, Z., & Rotello, V. M. (2015). Quantitative tracking of protein trafficking to the nucleus using cytosolic protein delivery by nanoparticle-stabilized nanocapsules. *Bioconjug Chem*, 26(6), 1004–1007. <http://doi.org/10.1021/acs.bioconjchem.5b00141>
- Rezáková P., Borek, D., Moy, S. F., Joachimiak, A., & Otwinowski, Z. (2008). Crystal structure and putative function of small Toprim domain-containing protein from *Bacillus stearothermophilus*. *Proteins*, 70(2), 311–319. <http://doi.org/10.1002/prot>
- Richter, K. S. (2008). The importance of growth factors for preimplantation embryo development and in-vitro culture. *Current Opinion in Obstetrics & Gynecology*, 20(3), 292–304. <http://doi.org/10.1097/GCO.0b013e3282fe743b>
- Roberts, P., & Der, C. (2007). Targeting the Raf-MEK-ERK mitogen-activated protein kinase cascade for the treatment of cancer. *Oncogene*, 26, 3291–3310. <http://doi.org/10.1038/sj.onc.1210422>
- Rohs, R., Jin, X., West, S. M., Joshi, R., Honig, B., & Mann, R. S. (2010). Origins of specificity in protein-DNA recognition. *Annual Review of Biochemistry*, 79, 233–69. <http://doi.org/10.1146/annurev-biochem-060408-091030>

- Roskoski, R. (2012). ERK1/2 MAP kinases: Structure, function, and regulation. *Pharmacological Research*, 66(2), 105–143. <http://doi.org/10.1016/j.phrs.2012.04.005>
- Roy, S., & Vadlamudi. (2012). Role of estrogen receptor signaling in breast cancer metastasis. *International Journal of Breast Cancer*, 2012, 654698. <http://doi.org/10.1155/2012/654698>
- Ruijter, Gennip, Caron, Kemp, & Kuilenburg. (2003). Histone deacetylases (HDACs): characterization of the classical HDAC family. *The Biochemical Journal*, 370(Pt 3), 737–49. <http://doi.org/10.1042/BJ20021321>
- Ryan, Paula J.; Gillespie, L. L. (1994). Phosphorylation of Phospholipase C γ 1 and Its Association with the FGF Receptor is Developmentally Regulated and Occurs during Mesoderm Induction in *Xenopus laevis*.
- Ryan, Paterno, & Gillespie. (1998). Identification of Phosphorylated Proteins Associated with the Fibroblast Growth Factor Receptor Type I during Early *Xenopus* Development. *Biochemical and Biophysical Research Communications*, 244(3), 763–767. <http://doi.org/10.1006/bbrc.1998.8326>
- Saldaña-Meyer, R., & Recillas-Targa, F. (2011). Transcriptional and epigenetic regulation of the p53 tumor suppressor gene. *Epigenetics*, 6(9), 1068–1077. <http://doi.org/10.4161/epi.6.9.16683>
- Sasaki, T., Hiroki, K., & Yamashita, Y. (2013). The role of epidermal growth factor receptor in cancer metastasis and microenvironment. *Biomed Res Int*, 2013, 546318. <http://doi.org/10.1155/2013/546318>
- Sazer, S., & Dasso, M. (2000). The ran decathlon: multiple roles of Ran. *Journal of Cell Science*, 113 (Pt 7, 1111–1118.
- Scott, M. S., Calafell, S. J., Thomas, D. Y., & Hallett, M. T. (2005). Refining protein subcellular localization. *PLoS Computational Biology*, 1(6), 0518–0528. <http://doi.org/10.1371/journal.pcbi.0010066>
- Sharon, Lubliner, & Segal. (2008). A feature-based approach to modeling protein-DNA interactions. *PLoS Computational Biology*, 4(8). <http://doi.org/10.1371/journal.pcbi.1000154>
- Shen, A., Wang, Y., Zhao, Y., Zou, L., Sun, L., & Cheng, C. (2009). Expression of CRM1 in human gliomas and its significance in p27 expression and clinical prognosis. *Neurosurgery*, 65(1), 153–159. <http://doi.org/10.1227/01.NEU.0000348550.47441.4B>
- Sibly, R., Beverton, R. J. H., Hill, W. G., Contributions, I. S., Casper, B. C., Baudisch, A., ... Scheuerlein, A. (2012). References and Notes 1., 338(November), 619–621. <http://doi.org/10.1126/science.1206034>
- Solari, F., Bateman, A., & Ahringer, J. (1999). The *Caenorhabditis elegans* genes *egl-27* and *egr-1* are similar to MTA1, a member of a chromatin regulatory complex, and are redundantly required for embryonic patterning. *Development (Cambridge, England)*, 126(11), 2483–2494.
- Sprenger, J., Lynn Fink, J., Karunaratne, S., Hanson, K., Hamilton, N. A., & Teasdale, R. D. (2008). LOCATE: A mammalian protein subcellular localization database. *Nucleic Acids Research*, 36(SUPPL. 1), 230–233. <http://doi.org/10.1093/nar/gkm950>
- Stampfel, G., Kazmar, T., Frank, O., Wienerroither, S., Reiter, F., & Stark, A. (2015).

- Transcriptional regulators form diverse groups with context-dependent regulatory functions. *Nature*. <http://doi.org/10.1038/nature15545>
- Statistics Canada. (2014). Canadian Cancer Statistics Special topic : Skin cancers. *Canadian Cancer Society, 2014*, 1–132. <http://doi.org/0835-2976>
- Steidl, S., Tüncher, A., Goda, H., Guder, C., Papadopoulou, N., Kobayashi, T., ... Brakhage, A. A. (2004). A single subunit of a heterotrimeric CCAAT-binding complex carries a nuclear localization signal: Piggy back transport of the pre-assembled complex to the nucleus. *Journal of Molecular Biology*, *342*(2), 515–524. <http://doi.org/10.1016/j.jmb.2004.07.011>
- Sterner, D. E., Wang, X., Bloom, M. H., Simon, G. M., & Berger, S. L. (2002). The SANT domain of Ada2 is required for normal acetylation of histones by the yeast SAGA complex. *Journal of Biological Chemistry*, *277*(10), 8178–8186. <http://doi.org/10.1074/jbc.M108601200>
- Stewart, M. (2007). Molecular mechanism of the nuclear protein import cycle. *Nature Reviews. Molecular Cell Biology*, *8*(3), 195–208. <http://doi.org/10.1038/nrm2114>
- Sun, Q., Carrasco, Y. P., Hu, Y., Guo, X., Mirzaei, H., Macmillan, J., & Chook, Y. M. (2013). Nuclear export inhibition through covalent conjugation and hydrolysis of Leptomycin B by CRM1. *Proceedings of the National Academy of Sciences of the United States of America*, *110*(4), 1303–8. Retrieved from <http://www.pubmedcentral.nih.gov/articlerender.fcgi?artid=3557022&tool=pmcentrez&rendertype=abstract>
- Suntharalingam, M., & Wenthe, S. R. (2003, June 1). Peering through the pore: Nuclear pore complex structure, assembly, and function. *Developmental Cell*.
- Supeno, N. E., Pati, S., Hadi, R. A., Izani, A. R. G., Mustafa, Z., Abdullah, J. M., ... Jaafar, H. (2013). IGF-1 acts as controlling switch for long-term proliferation and maintenance of EGF/FGF-responsive striatal neural stem cells. *International Journal of Medical Sciences*, *10*(5), 522–531. <http://doi.org/10.7150/ijms.5325>
- Suzuki, K., Sako, K., Akiyama, K., Isoda, M., Senoo, C., Nakajo, N., & Sagata, N. (2015). Identification of non-Ser/Thr-Pro consensus motifs for Cdk1 and their roles in mitotic regulation of C2H2 zinc finger proteins and Ect2. *Scientific Reports*, *5*, 7929. <http://doi.org/10.1038/srep07929>
- Tang, P., Wang, J., & Bourne, P. (2008). Molecular classifications of breast carcinoma with similar terminology and different definitions: are they the same? *Human Pathology*, *39*(4), 506–513. <http://doi.org/10.1016/j.humpath.2007.09.005>
- Teplitsky, Paterno, & Gillespie. (2003). Proline365 is a critical residue for the activity of XMI-ER1 in *Xenopus* embryonic development. *Biochemical and Biophysical Research Communications*, *308*(4), 679–683. [http://doi.org/10.1016/S0006-291X\(03\)01461-X](http://doi.org/10.1016/S0006-291X(03)01461-X)
- The Cancer Genome Atlas Network. (2012). Comprehensive molecular portraits of human breast tumours. *Nature*, *490*(7418), 61–70. <http://doi.org/10.1038/nature11412>
- Thompson, M. E. (2010). BRCA1 16 years later: Nuclear import and export processes. *FEBS Journal*, *277*(15), 3072–3078. <http://doi.org/10.1111/j.1742-4658.2010.07733.x>
- Tootle, T. L., & Rebay, I. (2005). Post-translational modifications influence transcription factor activity: A view from the ETS superfamily. *BioEssays*, *27*(3), 285–298.

- <http://doi.org/10.1002/bies.20198>
- Van Der Heide, L. P., Hoekman, M. F. M., & Smidt, M. P. (2004). The ins and outs of FoxO shuttling: mechanisms of FoxO translocation and transcriptional regulation. *The Biochemical Journal*, 380(Pt 2), 297–309. <http://doi.org/10.1042/BJ20040167>
- Venere, M., Lathia, J. D., & Rich, J. N. (2013). Growth Factor Receptors Define Cancer Hierarchies. *Cancer Cell*, 23(2), 135–137. <http://doi.org/10.1016/j.ccr.2013.01.020>
- Vlasova, & Bohjanen. (2016). Post-transcriptional regulation of cytokine and growth factor signaling in cancer. *Cytokine & Growth Factor Reviews*. <http://doi.org/10.1016/j.cytogfr.2016.11.004>
- Vousden, K. H., & Woude, G. F. Vande. (2000). The ins and outs of p53. *Nature Cell Biology*, 2(10), E178–E180. <http://doi.org/10.1038/35036427>
- Wagstaff, K. M., & Jans, D. A. (2009). Importins and beyond: Non-conventional nuclear transport mechanisms. *Traffic*, 10(9), 1188–1198. <http://doi.org/10.1111/j.1600-0854.2009.00937.x>
- Wälde, S., & Kehlenbach, R. H. (2010). The Part and the Whole: Functions of nucleoporins in nucleocytoplasmic transport. *Trends in Cell Biology*, 20(8), 461–469. <http://doi.org/10.1016/j.tcb.2010.05.001>
- Walsh, L. A., & Damjanovski, S. (2011). IGF-1 increases invasive potential of MCF 7 breast cancer cells and induces activation of latent TGF- β 1 resulting in epithelial to mesenchymal transition. *Cell Communication and Signaling : CCS*, 9(1), 10. <http://doi.org/10.1186/1478-811X-9-10>
- Wang, L., Charroux, B., Kerridge, S., & Tsai, C.-C. (2008). Atrophin recruits HDAC1/2 and G9a to modify histone H3K9 and to determine cell fates. *EMBO Reports*, 9(6), 555–562. <http://doi.org/10.1038/embor.2008.67>
- Wang, Han, Bai, Zhou, Li, Jing, ... Zhu. (2013). Dose-dependent effect of tamoxifen in tamoxifen-resistant breast cancer cells via stimulation by the ERK1/2 and AKT signaling pathways. *Oncology Reports*, 29(4), 1563–1569. <http://doi.org/10.3892/or.2013.2245>
- Wang, Lisanti, M. P., & Liao, D. J. (2011). Reviewing once more the c-myc and Ras collaboration: Converging at the cyclin D1-CDK4 complex and challenging basic concepts of cancer biology. *Cell Cycle*, 10(1), 57–67. <http://doi.org/10.4161/cc.10.1.14449>
- Wang, Zhang, Shen, Loggie, Chang, & Deuel. (2006). A variant of estrogen receptor- $\{\alpha\}$, hER- $\{\alpha\}$ 36: transduction of estrogen- and antiestrogen-dependent membrane-initiated mitogenic signaling. *Proceedings of the National Academy of Sciences of the United States of America*, 103(24), 9063–8. <http://doi.org/10.1073/pnas.0603339103>
- Weis, K. (2003). Regulating access to the genome: Nucleocytoplasmic transport throughout the cell cycle. *Cell*, 112(4), 441–451. [http://doi.org/10.1016/S0092-8674\(03\)00082-5](http://doi.org/10.1016/S0092-8674(03)00082-5)
- Wen-ming, Yao, Y., Sun, J., Davie, J. R., & Seto, E. (1997). Isolation and Characterization of cDNAs Corresponding to an Additional Member of the Human Histone Deacetylase Gene Family, 272(44), 28001–28007. <http://doi.org/10.1074/jbc.272.44.28001>
- Wen, Y. D., Perissi, V., Staszewski, L. M., Yang, W. M., Kronen, a, Glass, C. K., ... Seto, E. (2000). The histone deacetylase-3 complex contains nuclear receptor

- corepressors. *Proceedings of the National Academy of Sciences of the United States of America*, 97(13), 7202–7207. <http://doi.org/10.1073/pnas.97.13.7202>
- Wente, S. R., & Rout, M. P. (2017). The Nuclear Pore Complex and Nuclear Transport, 1–20.
- Werner, H., Weinstein, D., & Bentov, I. (2008). Similarities and differences between insulin and IGF-I: structures, receptors, and signalling pathways. *Archives of Physiology and Biochemistry*, 114(1), 17–22. <http://doi.org/10.1080/13813450801900694>
- Whitmarsh, A., Shore, P., Sharrocks, A., & Davis, R. (1995). Integration of MAP kinase signal transduction pathways at the serum response element. *Science*. <http://doi.org/10.1126/science.7618106>
- Witsch, E., Sela, M., & Yarden, Y. (2011). Roles for Growth Factors in Cancer Progression. *Physiology*, 25(2), 85–101. <http://doi.org/10.1152/physiol.00045.2009.Roles>
- Wortzel, I., & Seger, R. (2011). The ERK Cascade: Distinct Functions within Various Subcellular Organelles. *Genes & Cancer*, 2(3), 195–209. <http://doi.org/10.1177/1947601911407328>
- Xing, L., Hung, M., Bonfiglio, T., Hicks, D. G., & Tang, P. (2010). Breast Cancer : Basic and Clinical Research The Expression Patterns of ER , PR , HER2 , CK5 / 6 , EGFR , Ki-67 and AR by Immunohistochemical Analysis in Breast Cancer Cell Lines. *Breast Cancer: Basic and Clinical Research*, 4, 35–41. <http://doi.org/10.4137/BCBCR.S0>
- Yang, X. J., & Seto, E. (2003). Collaborative spirit of histone deacetylases in regulating chromatin structure and gene expression. *Current Opinion in Genetics and Development*, 13(2), 143–153. [http://doi.org/10.1016/S0959-437X\(03\)00015-7](http://doi.org/10.1016/S0959-437X(03)00015-7)
- Yardley, D. a, Ismail-Khan, R. R., Melichar, B., Lichinitser, M., Munster, P. N., Klein, P. M., ... Trepel, J. B. (2013). Randomized phase II, double-blind, placebo-controlled study of exemestane with or without entinostat in postmenopausal women with locally recurrent or metastatic estrogen receptor-positive breast cancer progressing on treatment with a nonsteroidal aromata. *Journal of Clinical Oncology : Official Journal of the American Society of Clinical Oncology*, 31(17), 2128–35. <http://doi.org/10.1200/JCO.2012.43.7251>
- You, a, Tong, J. K., Grozinger, C. M., & Schreiber, S. L. (2001). CoREST is an integral component of the CoREST- human histone deacetylase complex. *Proceedings of the National Academy of Sciences of the United States of America*, 98, 1454–1458. <http://doi.org/10.1073/pnas.98.4.1454>
- Yu, M., Selvaraj, S. K., Liang-Chu, M. M. Y., Aghajani, S., Busse, M., Yuan, J., ... Neve, R. M. (2015). A resource for cell line authentication, annotation and quality control. *Nature*, 520(7547), 307–311. <http://doi.org/10.1038/nature14397>
- Yuh, M. C., & Blobel, G. (2001). Karyopherins and nuclear import. *Current Opinion in Structural Biology*, 11(6), 703–715. [http://doi.org/10.1016/S0959-440X\(01\)00264-0](http://doi.org/10.1016/S0959-440X(01)00264-0)
- Zell, J. A., Tsang, W. Y., Taylor, T. H., Mehta, R. S., & Anton-Culver, H. (2009). Prognostic impact of human epidermal growth factor-like receptor 2 and hormone receptor status in inflammatory breast cancer (IBC): analysis of 2,014 IBC patient cases from the California Cancer Registry. *Breast Cancer Research : BCR*, 11(1), R9. <http://doi.org/10.1186/bcr2225>

- Zermati, Y., Fichelson, S., Valensi, F., Freyssinier, J. M., Rouyer-Fessard, P., Cramer, E., ... Hermine, O. (2000). Transforming growth factor inhibits erythropoiesis by blocking proliferation and accelerating differentiation of erythroid progenitors. *Experimental Hematology*, 28(8), 885–894. [http://doi.org/10.1016/S0301-472X\(00\)00488-4](http://doi.org/10.1016/S0301-472X(00)00488-4)
- Zhang, X., Ibrahimi, O. A., Olsen, S. K., Umemori, H., Mohammadi, M., & Ornitz, D. M. (2006). Receptor specificity of the fibroblast growth factor family: The complete mammalian FGF family. *Journal of Biological Chemistry*, 281(23), 15694–15700. <http://doi.org/10.1074/jbc.M601252200>
- Zhang, Ozawa, Lee, Wen, Tan, Wadzinski, & Seto. (2005). Is Regulated By Interaction With Protein Serine / Threonine Phosphatase 4. *Genes and Development*, 3, 827–839. <http://doi.org/10.1101/gad.1286005.HDAC3>
- Zhou, H., Di Palma, S., Preisinger, C., Peng, M., Polat, A. N., Heck, A. J. R., & Mohammed, S. (2012). Toward a Comprehensive Characterization of a Human Cancer Cell Phosphoproteome. *Journal of Proteome Research*, 12(1), 260–271. <http://doi.org/10.1021/pr300630k>
- Zhou, Shen, Yang, Abe, Horton, Mann, ... Rohs. (2015). Quantitative modeling of transcription factor binding specificities using DNA shape. *Proceedings of the National Academy of Sciences*, 112(15), 4654–4659. <http://doi.org/10.1073/pnas.1422023112>

APPENDICES

Appendix 1: EndoFree® Plasmid Maxi Kit Protocol

1. Harvest overnight LB culture by centrifuging at 6000 x g for 15 min at 4 °C;
2. Completely resuspend the bacterial pellet in 10 ml Buffer P1*;
3. Add 10 ml Buffer P2*, mix thoroughly by inverting 4-6 times, and incubate at room temperature (15-25°C) for 5 min. if using LyseBlue reagent, the solution will turn blue;
4. During the incubation, screw the QIAfilter Cartridge cap onto the outlet nozzle of the QIAfilter Cartridge. Place the QIAfilter Cartridge in a convenient tube or in a QIArack (cat no. 19015);
5. Add 10 ml chilled Buffer P3*, mix thoroughly by inverting 4-6 times. If using LyseBlue reagent, mix the solution until it is completely colorless;
6. Pour the lysate into the barrel of the QIAfilter Cartridge. Incubate at room temperature for 10 min. Do not insert the plunger! Remove the cap from the QIAfilter Cartridge outlet nozzle. Gently insert the plunger into the QIAfilter Cartridge and filter the cell lysate into a 50 ml tube;
7. Add 2.5 ml Buffer ER* to the filtered lysate, mix by inverting the tube approximately 10 times, and incubate on ice for 30 min;
8. Equilibrate a QIAGEN-tip 500 by applying 10 ml Buffer QBT*, and allow the column to empty by gravity flow;
9. Apply the filtered lysate from step 7 to the QIAGEN-tip and allow it to enter the

tip;

10. Wash the QIAGEN-tip with 2 x 30 ml Buffer QC;
11. Elute DNA with 15 ml Buffer QN* into a 30 ml endotoxin-free or pyrogen-free tube;
12. Precipitate DNA by adding 10.5 ml (0.7 volumes) room-temperature isopropanol to the eluted DNA and mix. Centrifuge at $\geq 15,000 \times g$ for 30 min at 4 °C. Carefully decant the supernatant;
13. Wash the DNA pellet with 5 ml of endotoxin-free room-temperature 70% ethanol and centrifuge at $\geq 15,000 \times g$ for 10 min. Carefully decant the supernatant without disturbing the pellet;
14. Air-dry the pellet for 5-10 min and redissolve the DNA in a suitable volume of endotoxin-free Buffer TE*.

*: The buffer P1, P2, P3, QBT, QC, QN & TE is offered in the kit by the company.

Appendix 2: Immunofluorescence

1. Transfected cells were seeded in 8-well chamber slides coated with poly-L-Lysine (Sigma-aldrich, Lot#: SLBG3445V) for 15min. Cells were left to grow in incubator before collection;
2. Cells were then fixed for 10 min with 4% paraformaldehyde and permeabilized with 0.1% Triton X-100/PBS for 10 min;
3. Non-specific sites were blocked with 5% blocking buffer (5% donkey serum/1xPBS) for 1h before overnight incubation with primary antibodies at 4 °C;
4. Add primary antibody 1:200 in 3% BSA/1xPBS and incubate overnight in 4 °C. After the primary antibody aspirated, the slide was then washed with 0.1% triton/PBS and incubated in PBS for 5 minutes.
5. The cells were then incubated with Alexa Fluor-488 labeled donkey anti-mouse secondary antibody and/or with Alexa Fluor-647 labeled donkey-anti-rabbit for 1h at RT. Nuclei were counterstained with 2.5µg/ml 4', 6-diamidino-2-phenylindole (DAPI; Sigma-Aldrich Co.) in the dilution 1:5000 diluted together with secondary antibody;
6. Cells were then washed and incubated in 1xPBS for 5 min. Slides were mounted in 10% glycerol/PBS before sealed with 22x50mm Microscope Coverglasses (VWR, Cat#: 16004-336).

Appendix 3: *In silico* analysis of MIER1 α amino acid sequence by NetNES 1.1

6/13/2017

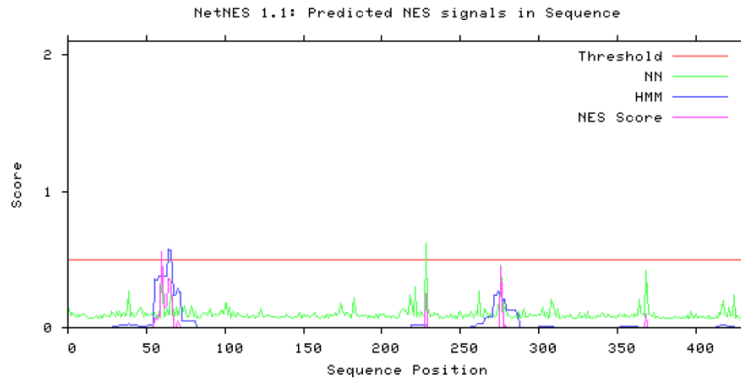
NetNES 1.1 Server - prediction results



NetNES 1.1 Server - prediction results

Technical University of Denmark

>Sequence - NetNES 1.1 prediction



#Seq-Pos-Residue	ANN	HMM	NES	Predicted
#-----				
Sequence-1-M	0.144	0.000	0.000	-
Sequence-2-A	0.093	0.000	0.000	-
Sequence-3-E	0.109	0.000	0.000	-
Sequence-4-P	0.091	0.000	0.000	-
Sequence-5-S	0.080	0.000	0.000	-
Sequence-6-V	0.100	0.000	0.000	-
Sequence-7-E	0.083	0.000	0.000	-
Sequence-8-S	0.090	0.000	0.000	-
Sequence-9-S	0.088	0.000	0.000	-
Sequence-10-S	0.095	0.000	0.000	-
Sequence-11-P	0.085	0.000	0.000	-
Sequence-12-G	0.080	0.000	0.000	-
Sequence-13-G	0.074	0.000	0.000	-
Sequence-14-S	0.073	0.000	0.000	-
Sequence-15-A	0.070	0.000	0.000	-
Sequence-16-T	0.073	0.000	0.000	-
Sequence-17-S	0.081	0.000	0.000	-
Sequence-18-D	0.088	0.000	0.000	-
Sequence-19-D	0.073	0.000	0.000	-
Sequence-20-H	0.072	0.000	0.000	-
Sequence-21-E	0.088	0.000	0.000	-
Sequence-22-F	0.072	0.000	0.000	-
Sequence-23-D	0.095	0.000	0.000	-
Sequence-24-P	0.089	0.000	0.000	-
Sequence-25-S	0.077	0.000	0.000	-
Sequence-26-A	0.091	0.000	0.000	-
Sequence-27-D	0.081	0.000	0.000	-
Sequence-28-M	0.115	0.004	0.000	-
Sequence-29-L	0.098	0.012	0.000	-
Sequence-30-V	0.081	0.014	0.000	-
Sequence-31-H	0.116	0.014	0.000	-
Sequence-32-D	0.091	0.014	0.000	-
Sequence-33-F	0.115	0.023	0.000	-
Sequence-34-D	0.083	0.023	0.000	-
Sequence-35-D	0.113	0.023	0.000	-

<http://www.cbs.dtu.dk/cgi-bin/webface2.fcgi?jobid=593FEB8900018AEB6BDA7B1&wait=20>

1/7

6/13/2017

NetNES 1.1 Server - prediction results

Sequence-36-E	0.087	0.023	0.000	-
Sequence-37-R	0.090	0.023	0.000	-
Sequence-38-T	0.174	0.023	0.000	-
Sequence-39-L	0.273	0.027	0.000	-
Sequence-40-E	0.081	0.021	0.000	-
Sequence-41-E	0.111	0.021	0.000	-
Sequence-42-E	0.083	0.021	0.000	-
Sequence-43-E	0.090	0.021	0.000	-
Sequence-44-M	0.110	0.022	0.000	-
Sequence-45-M	0.134	0.007	0.000	-
Sequence-46-E	0.144	0.007	0.000	-
Sequence-47-G	0.148	0.007	0.000	-
Sequence-48-E	0.078	0.007	0.000	-
Sequence-49-T	0.109	0.008	0.000	-
Sequence-50-N	0.094	0.008	0.000	-
Sequence-51-F	0.096	0.020	0.000	-
Sequence-52-S	0.089	0.020	0.000	-
Sequence-53-S	0.095	0.020	0.000	-
Sequence-54-E	0.100	0.020	0.000	-
Sequence-55-I	0.109	0.354	0.070	-
Sequence-56-E	0.077	0.352	0.065	-
Sequence-57-D	0.077	0.352	0.061	-
Sequence-58-L	0.124	0.380	0.096	-
Sequence-59-A	0.071	0.373	0.085	-
Sequence-60-R	0.449	0.373	0.555	Yes
Sequence-61-E	0.076	0.373	0.148	-
Sequence-62-G	0.099	0.373	0.153	-
Sequence-63-D	0.135	0.373	0.164	-
Sequence-64-M	0.101	0.574	0.360	-
Sequence-65-P	0.102	0.565	0.358	-
Sequence-66-I	0.292	0.566	0.327	-
Sequence-67-H	0.088	0.241	0.004	-
Sequence-68-E	0.091	0.241	0.003	-
Sequence-69-L	0.152	0.257	0.023	-
Sequence-70-L	0.094	0.286	0.050	-
Sequence-71-S	0.102	0.259	0.023	-
Sequence-72-L	0.191	0.259	0.003	-
Sequence-73-Y	0.095	0.053	0.000	-
Sequence-74-G	0.164	0.053	0.000	-
Sequence-75-Y	0.114	0.053	0.000	-
Sequence-76-G	0.079	0.053	0.000	-
Sequence-77-S	0.077	0.053	0.000	-
Sequence-78-T	0.123	0.053	0.000	-
Sequence-79-V	0.157	0.053	0.000	-
Sequence-80-R	0.078	0.047	0.000	-
Sequence-81-L	0.122	0.047	0.000	-
Sequence-82-P	0.072	0.000	0.000	-
Sequence-83-E	0.079	0.000	0.000	-
Sequence-84-E	0.068	0.000	0.000	-
Sequence-85-D	0.085	0.000	0.000	-
Sequence-86-E	0.112	0.000	0.000	-
Sequence-87-E	0.096	0.000	0.000	-
Sequence-88-E	0.107	0.000	0.000	-
Sequence-89-E	0.091	0.000	0.000	-
Sequence-90-E	0.120	0.000	0.000	-
Sequence-91-E	0.138	0.000	0.000	-
Sequence-92-E	0.084	0.000	0.000	-
Sequence-93-E	0.103	0.000	0.000	-
Sequence-94-E	0.101	0.000	0.000	-
Sequence-95-G	0.091	0.000	0.000	-
Sequence-96-E	0.097	0.000	0.000	-
Sequence-97-D	0.095	0.000	0.000	-
Sequence-98-D	0.132	0.000	0.000	-
Sequence-99-E	0.099	0.000	0.000	-
Sequence-100-D	0.182	0.000	0.000	-
Sequence-101-A	0.177	0.000	0.000	-
Sequence-102-D	0.089	0.000	0.000	-
Sequence-103-N	0.148	0.000	0.000	-
Sequence-104-D	0.074	0.000	0.000	-

<http://www.cbs.dtu.dk/cgi-bin/webface2.fcgi?jobid=593FEB89000018AEB6BDA7B1&wait=20>

2/7

6/13/2017

NetNES 1.1 Server - prediction results

Sequence-105-D	0.122	0.000	0.000	-
Sequence-106-N	0.088	0.000	0.000	-
Sequence-107-S	0.080	0.000	0.000	-
Sequence-108-G	0.113	0.000	0.000	-
Sequence-109-C	0.098	0.000	0.000	-
Sequence-110-S	0.088	0.000	0.000	-
Sequence-111-G	0.086	0.000	0.000	-
Sequence-112-E	0.084	0.000	0.000	-
Sequence-113-N	0.081	0.000	0.000	-
Sequence-114-K	0.101	0.000	0.000	-
Sequence-115-E	0.071	0.000	0.000	-
Sequence-116-E	0.083	0.000	0.000	-
Sequence-117-N	0.077	0.000	0.000	-
Sequence-118-I	0.091	0.000	0.000	-
Sequence-119-K	0.070	0.000	0.000	-
Sequence-120-D	0.081	0.000	0.000	-
Sequence-121-S	0.076	0.000	0.000	-
Sequence-122-S	0.089	0.000	0.000	-
Sequence-123-G	0.141	0.000	0.000	-
Sequence-124-Q	0.079	0.000	0.000	-
Sequence-125-E	0.081	0.000	0.000	-
Sequence-126-D	0.088	0.000	0.000	-
Sequence-127-E	0.088	0.000	0.000	-
Sequence-128-T	0.092	0.000	0.000	-
Sequence-129-Q	0.091	0.000	0.000	-
Sequence-130-S	0.076	0.000	0.000	-
Sequence-131-S	0.076	0.000	0.000	-
Sequence-132-N	0.076	0.000	0.000	-
Sequence-133-D	0.073	0.000	0.000	-
Sequence-134-D	0.078	0.000	0.000	-
Sequence-135-P	0.071	0.000	0.000	-
Sequence-136-S	0.078	0.000	0.000	-
Sequence-137-Q	0.080	0.000	0.000	-
Sequence-138-S	0.081	0.000	0.000	-
Sequence-139-V	0.103	0.000	0.000	-
Sequence-140-A	0.088	0.000	0.000	-
Sequence-141-S	0.078	0.000	0.000	-
Sequence-142-Q	0.078	0.000	0.000	-
Sequence-143-D	0.069	0.000	0.000	-
Sequence-144-A	0.083	0.000	0.000	-
Sequence-145-Q	0.082	0.000	0.000	-
Sequence-146-E	0.077	0.000	0.000	-
Sequence-147-I	0.100	0.000	0.000	-
Sequence-148-I	0.113	0.000	0.000	-
Sequence-149-R	0.069	0.000	0.000	-
Sequence-150-P	0.098	0.000	0.000	-
Sequence-151-R	0.083	0.000	0.000	-
Sequence-152-R	0.088	0.000	0.000	-
Sequence-153-C	0.089	0.000	0.000	-
Sequence-154-K	0.080	0.000	0.000	-
Sequence-155-Y	0.082	0.000	0.000	-
Sequence-156-F	0.102	0.000	0.000	-
Sequence-157-D	0.108	0.000	0.000	-
Sequence-158-T	0.083	0.000	0.000	-
Sequence-159-N	0.075	0.000	0.000	-
Sequence-160-S	0.070	0.000	0.000	-
Sequence-161-E	0.073	0.000	0.000	-
Sequence-162-V	0.086	0.000	0.000	-
Sequence-163-E	0.074	0.000	0.000	-
Sequence-164-E	0.086	0.000	0.000	-
Sequence-165-E	0.098	0.000	0.000	-
Sequence-166-S	0.068	0.000	0.000	-
Sequence-167-E	0.104	0.000	0.000	-
Sequence-168-E	0.085	0.000	0.000	-
Sequence-169-D	0.085	0.000	0.000	-
Sequence-170-E	0.105	0.000	0.000	-
Sequence-171-D	0.086	0.000	0.000	-
Sequence-172-Y	0.104	0.000	0.000	-
Sequence-173-I	0.117	0.003	0.000	-

<http://www.cbs.dtu.dk/cgi-bin/webface2.fcgi?jobid=593FEB89000018AEB6BDA7B1&wait=20>

3/7

6/13/2017

NetNES 1.1 Server - prediction results

Sequence-174-P	0.181	0.003	0.000	-
Sequence-175-S	0.114	0.003	0.000	-
Sequence-176-E	0.091	0.003	0.000	-
Sequence-177-D	0.113	0.003	0.000	-
Sequence-178-W	0.105	0.003	0.000	-
Sequence-179-K	0.098	0.003	0.000	-
Sequence-180-K	0.083	0.003	0.000	-
Sequence-181-E	0.071	0.003	0.000	-
Sequence-182-I	0.220	0.003	0.000	-
Sequence-183-M	0.111	0.003	0.000	-
Sequence-184-V	0.090	0.000	0.000	-
Sequence-185-G	0.094	0.000	0.000	-
Sequence-186-S	0.078	0.000	0.000	-
Sequence-187-M	0.092	0.001	0.000	-
Sequence-188-F	0.093	0.001	0.000	-
Sequence-189-Q	0.092	0.001	0.000	-
Sequence-190-A	0.086	0.001	0.000	-
Sequence-191-E	0.071	0.001	0.000	-
Sequence-192-I	0.091	0.001	0.000	-
Sequence-193-P	0.077	0.001	0.000	-
Sequence-194-V	0.078	0.001	0.000	-
Sequence-195-G	0.072	0.001	0.000	-
Sequence-196-I	0.104	0.001	0.000	-
Sequence-197-C	0.079	0.000	0.000	-
Sequence-198-R	0.073	0.000	0.000	-
Sequence-199-Y	0.095	0.000	0.000	-
Sequence-200-K	0.091	0.000	0.000	-
Sequence-201-E	0.097	0.000	0.000	-
Sequence-202-N	0.081	0.000	0.000	-
Sequence-203-E	0.082	0.000	0.000	-
Sequence-204-K	0.081	0.000	0.000	-
Sequence-205-V	0.085	0.000	0.000	-
Sequence-206-Y	0.070	0.000	0.000	-
Sequence-207-E	0.088	0.000	0.000	-
Sequence-208-N	0.077	0.000	0.000	-
Sequence-209-D	0.069	0.000	0.000	-
Sequence-210-D	0.073	0.000	0.000	-
Sequence-211-Q	0.090	0.000	0.000	-
Sequence-212-L	0.117	0.003	0.000	-
Sequence-213-L	0.144	0.003	0.000	-
Sequence-214-W	0.130	0.003	0.000	-
Sequence-215-D	0.126	0.003	0.000	-
Sequence-216-P	0.098	0.003	0.000	-
Sequence-217-E	0.101	0.003	0.000	-
Sequence-218-Y	0.236	0.003	0.000	-
Sequence-219-L	0.187	0.018	0.000	-
Sequence-220-P	0.085	0.016	0.000	-
Sequence-221-E	0.302	0.016	0.000	-
Sequence-222-D	0.079	0.016	0.000	-
Sequence-223-K	0.105	0.016	0.000	-
Sequence-224-V	0.076	0.016	0.000	-
Sequence-225-I	0.124	0.016	0.000	-
Sequence-226-I	0.086	0.017	0.000	-
Sequence-227-F	0.090	0.016	0.000	-
Sequence-228-L	0.616	0.016	0.248	-
Sequence-229-K	0.103	0.002	0.000	-
Sequence-230-D	0.128	0.002	0.000	-
Sequence-231-A	0.079	0.002	0.000	-
Sequence-232-S	0.089	0.002	0.000	-
Sequence-233-R	0.112	0.002	0.000	-
Sequence-234-R	0.098	0.002	0.000	-
Sequence-235-T	0.099	0.002	0.000	-
Sequence-236-G	0.095	0.002	0.000	-
Sequence-237-D	0.071	0.002	0.000	-
Sequence-238-E	0.082	0.002	0.000	-
Sequence-239-K	0.072	0.002	0.000	-
Sequence-240-G	0.077	0.002	0.000	-
Sequence-241-V	0.089	0.003	0.000	-
Sequence-242-E	0.079	0.003	0.000	-

<http://www.cbs.dtu.dk/cgi-bin/webface2.fcgi?jobid=593FEB89000018AEB6BDA7B1&wait=20>

4/7

6/13/2017

NetNES 1.1 Server - prediction results

Sequence-243-A	0.080	0.003	0.000	-
Sequence-244-I	0.096	0.003	0.000	-
Sequence-245-P	0.073	0.000	0.000	-
Sequence-246-E	0.088	0.000	0.000	-
Sequence-247-G	0.074	0.000	0.000	-
Sequence-248-S	0.071	0.000	0.000	-
Sequence-249-H	0.106	0.000	0.000	-
Sequence-250-I	0.121	0.002	0.000	-
Sequence-251-K	0.071	0.001	0.000	-
Sequence-252-D	0.086	0.001	0.000	-
Sequence-253-N	0.101	0.001	0.000	-
Sequence-254-E	0.076	0.001	0.000	-
Sequence-255-Q	0.087	0.001	0.000	-
Sequence-256-A	0.090	0.001	0.000	-
Sequence-257-L	0.115	0.005	0.000	-
Sequence-258-Y	0.069	0.005	0.000	-
Sequence-259-E	0.102	0.005	0.000	-
Sequence-260-L	0.120	0.023	0.000	-
Sequence-261-V	0.093	0.029	0.000	-
Sequence-262-K	0.267	0.028	0.000	-
Sequence-263-C	0.088	0.028	0.000	-
Sequence-264-N	0.075	0.028	0.000	-
Sequence-265-F	0.141	0.068	0.000	-
Sequence-266-D	0.120	0.068	0.000	-
Sequence-267-T	0.114	0.081	0.000	-
Sequence-268-E	0.074	0.081	0.000	-
Sequence-269-E	0.097	0.081	0.000	-
Sequence-270-A	0.099	0.081	0.000	-
Sequence-271-L	0.090	0.239	0.000	-
Sequence-272-R	0.081	0.234	0.000	-
Sequence-273-R	0.092	0.234	0.000	-
Sequence-274-L	0.168	0.272	0.000	-
Sequence-275-R	0.077	0.253	0.000	-
Sequence-276-F	0.458	0.253	0.447	-
Sequence-277-N	0.116	0.203	0.001	-
Sequence-278-V	0.151	0.212	0.024	-
Sequence-279-K	0.126	0.132	0.000	-
Sequence-280-A	0.088	0.132	0.000	-
Sequence-281-A	0.092	0.132	0.000	-
Sequence-282-R	0.075	0.132	0.000	-
Sequence-283-E	0.072	0.132	0.000	-
Sequence-284-E	0.079	0.132	0.000	-
Sequence-285-L	0.090	0.132	0.000	-
Sequence-286-S	0.070	0.103	0.000	-
Sequence-287-V	0.124	0.103	0.000	-
Sequence-288-W	0.080	0.000	0.000	-
Sequence-289-T	0.073	0.000	0.000	-
Sequence-290-E	0.136	0.000	0.000	-
Sequence-291-E	0.076	0.000	0.000	-
Sequence-292-E	0.081	0.000	0.000	-
Sequence-293-C	0.083	0.000	0.000	-
Sequence-294-R	0.096	0.000	0.000	-
Sequence-295-N	0.097	0.000	0.000	-
Sequence-296-F	0.090	0.001	0.000	-
Sequence-297-E	0.092	0.001	0.000	-
Sequence-298-Q	0.086	0.001	0.000	-
Sequence-299-G	0.085	0.001	0.000	-
Sequence-300-L	0.102	0.009	0.000	-
Sequence-301-K	0.091	0.009	0.000	-
Sequence-302-A	0.147	0.009	0.000	-
Sequence-303-Y	0.087	0.009	0.000	-
Sequence-304-G	0.076	0.009	0.000	-
Sequence-305-K	0.106	0.009	0.000	-
Sequence-306-D	0.069	0.009	0.000	-
Sequence-307-F	0.075	0.009	0.000	-
Sequence-308-H	0.211	0.009	0.000	-
Sequence-309-L	0.160	0.009	0.000	-
Sequence-310-I	0.106	0.001	0.000	-
Sequence-311-Q	0.077	0.000	0.000	-

<http://www.cbs.dtu.dk/cgi-bin/webface2.fcgi?jobid=593FEB8900018AEB6BDA7B1&wait=20>

5/7

6/13/2017

NetNES 1.1 Server - prediction results

Sequence-312-A	0.140	0.000	0.000	-
Sequence-313-N	0.074	0.000	0.000	-
Sequence-314-K	0.074	0.000	0.000	-
Sequence-315-V	0.093	0.000	0.000	-
Sequence-316-R	0.071	0.000	0.000	-
Sequence-317-T	0.082	0.000	0.000	-
Sequence-318-R	0.088	0.000	0.000	-
Sequence-319-S	0.082	0.000	0.000	-
Sequence-320-V	0.095	0.001	0.000	-
Sequence-321-G	0.073	0.001	0.000	-
Sequence-322-E	0.071	0.001	0.000	-
Sequence-323-C	0.073	0.001	0.000	-
Sequence-324-V	0.074	0.001	0.000	-
Sequence-325-A	0.085	0.001	0.000	-
Sequence-326-F	0.112	0.001	0.000	-
Sequence-327-Y	0.074	0.000	0.000	-
Sequence-328-Y	0.076	0.000	0.000	-
Sequence-329-M	0.100	0.000	0.000	-
Sequence-330-W	0.072	0.000	0.000	-
Sequence-331-K	0.115	0.000	0.000	-
Sequence-332-K	0.071	0.000	0.000	-
Sequence-333-S	0.082	0.000	0.000	-
Sequence-334-E	0.073	0.000	0.000	-
Sequence-335-R	0.080	0.000	0.000	-
Sequence-336-Y	0.069	0.000	0.000	-
Sequence-337-D	0.094	0.000	0.000	-
Sequence-338-F	0.091	0.000	0.000	-
Sequence-339-F	0.083	0.000	0.000	-
Sequence-340-A	0.111	0.000	0.000	-
Sequence-341-Q	0.089	0.000	0.000	-
Sequence-342-Q	0.076	0.000	0.000	-
Sequence-343-T	0.076	0.000	0.000	-
Sequence-344-R	0.097	0.000	0.000	-
Sequence-345-F	0.093	0.000	0.000	-
Sequence-346-G	0.076	0.000	0.000	-
Sequence-347-K	0.080	0.000	0.000	-
Sequence-348-K	0.079	0.000	0.000	-
Sequence-349-K	0.066	0.000	0.000	-
Sequence-350-Y	0.094	0.000	0.000	-
Sequence-351-N	0.093	0.000	0.000	-
Sequence-352-L	0.102	0.007	0.000	-
Sequence-353-H	0.076	0.007	0.000	-
Sequence-354-P	0.095	0.007	0.000	-
Sequence-355-G	0.082	0.007	0.000	-
Sequence-356-V	0.086	0.008	0.000	-
Sequence-357-T	0.081	0.008	0.000	-
Sequence-358-D	0.075	0.008	0.000	-
Sequence-359-Y	0.100	0.008	0.000	-
Sequence-360-M	0.081	0.008	0.000	-
Sequence-361-D	0.095	0.008	0.000	-
Sequence-362-R	0.093	0.008	0.000	-
Sequence-363-L	0.087	0.008	0.000	-
Sequence-364-L	0.206	0.001	0.000	-
Sequence-365-D	0.111	0.000	0.000	-
Sequence-366-E	0.101	0.000	0.000	-
Sequence-367-S	0.078	0.000	0.000	-
Sequence-368-E	0.414	0.000	0.099	-
Sequence-369-S	0.238	0.000	0.000	-
Sequence-370-A	0.097	0.000	0.000	-
Sequence-371-A	0.100	0.000	0.000	-
Sequence-372-S	0.081	0.000	0.000	-
Sequence-373-S	0.105	0.000	0.000	-
Sequence-374-R	0.070	0.000	0.000	-
Sequence-375-A	0.075	0.000	0.000	-
Sequence-376-P	0.077	0.000	0.000	-
Sequence-377-S	0.072	0.000	0.000	-
Sequence-378-P	0.071	0.000	0.000	-
Sequence-379-P	0.077	0.000	0.000	-
Sequence-380-P	0.066	0.000	0.000	-

<http://www.cbs.dtu.dk/cgi-bin/webface2.fcgi?jobid=593FEB8900018AEB6BDA7B1&wait=20>

6/7

6/13/2017

NetNES 1.1 Server - prediction results

Sequence-381-T	0.069	0.000	0.000	-
Sequence-382-A	0.070	0.000	0.000	-
Sequence-383-S	0.073	0.000	0.000	-
Sequence-384-N	0.073	0.000	0.000	-
Sequence-385-S	0.070	0.000	0.000	-
Sequence-386-S	0.081	0.000	0.000	-
Sequence-387-N	0.078	0.000	0.000	-
Sequence-388-S	0.072	0.000	0.000	-
Sequence-389-Q	0.077	0.000	0.000	-
Sequence-390-S	0.071	0.000	0.000	-
Sequence-391-E	0.067	0.000	0.000	-
Sequence-392-K	0.075	0.000	0.000	-
Sequence-393-E	0.074	0.000	0.000	-
Sequence-394-D	0.085	0.000	0.000	-
Sequence-395-G	0.073	0.000	0.000	-
Sequence-396-T	0.071	0.000	0.000	-
Sequence-397-V	0.121	0.000	0.000	-
Sequence-398-S	0.068	0.000	0.000	-
Sequence-399-T	0.090	0.000	0.000	-
Sequence-400-A	0.104	0.000	0.000	-
Sequence-401-N	0.073	0.000	0.000	-
Sequence-402-Q	0.082	0.000	0.000	-
Sequence-403-N	0.078	0.000	0.000	-
Sequence-404-G	0.081	0.000	0.000	-
Sequence-405-V	0.071	0.001	0.000	-
Sequence-406-S	0.082	0.001	0.000	-
Sequence-407-S	0.067	0.001	0.000	-
Sequence-408-N	0.092	0.001	0.000	-
Sequence-409-G	0.072	0.001	0.000	-
Sequence-410-P	0.067	0.001	0.000	-
Sequence-411-G	0.072	0.001	0.000	-
Sequence-412-I	0.073	0.002	0.000	-
Sequence-413-L	0.090	0.009	0.000	-
Sequence-414-Q	0.071	0.009	0.000	-
Sequence-415-M	0.106	0.014	0.000	-
Sequence-416-L	0.098	0.015	0.000	-
Sequence-417-L	0.199	0.017	0.000	-
Sequence-418-P	0.101	0.017	0.000	-
Sequence-419-V	0.086	0.017	0.000	-
Sequence-420-H	0.075	0.011	0.000	-
Sequence-421-F	0.148	0.011	0.000	-
Sequence-422-S	0.089	0.006	0.000	-
Sequence-423-A	0.086	0.006	0.000	-
Sequence-424-I	0.236	0.006	0.000	-
Sequence-425-S	0.072	0.000	0.000	-
Sequence-426-S	0.092	0.000	0.000	-
Sequence-427-R	0.079	0.000	0.000	-
Sequence-428-A	0.069	0.000	0.000	-
Sequence-429-N	0.071	0.000	0.000	-
Sequence-430-A	0.067	0.000	0.000	-
Sequence-431-F	0.067	0.000	0.000	-
Sequence-432-L	0.096	0.000	0.000	-
Sequence-433-K	0.076	0.000	0.000	-

//

Explain the output. Go **back**.
